New Catanionics as suitable additives for oily formulations, especially lubricants

Dissertation zur Erlangung des Doktorgrades der Naturwissenschaften (Dr. rer. nat.)
an der Fakultät für Chemie und Pharmazie der Universität Regensburg

vorgelegt von
Thomas Myrdek
aus Krefeld
2020

Dissertation submission:	09.07.2020
Dissertation defense:	27.08.2020
Ph. D. Supervisor:	Prof. Dr. Werner Kunz
Ph. D. Committee:	
1st Reviewer:	Prof. Dr. Werner Kunz
2nd Reviewer:	Prof. Dr. Hubert Motschmann
3rd Examiner:	Prof. Dr. Oliver Reiser
Committee Chairman:	Prof. Dr. Jörg Daub

Ich widme diese Arbeit meinen Eltern Christine und Heinrich Myrdek, sowie meiner Frau Magdalena und meiner Tochter Caroline. Ohne euch wäre dies nicht möglich gewesen.

Acknowledgements

Before starting, I wish to express my gratitude to all who helped me and contributed to this work.

First of all, I would like to express my deepest gratitude to my supervisor, Prof. Dr. Werner Kunz for giving me the opportunity to carry out my thesis at his institute, his trust in my capability, the numerous incentive discussions and especially for his patience. He supported me, guided me, and invested time to the realization of this project.

Moreover, I would like to thank Prof. Dr. Hubert Motschmann and Prof. Dr. Oliver Reiser for taking the roles as second and third referee of this thesis.

I would like to thank all colleagues for all the scientific help and especially for the fantastic atmosphere at the institute.

Special thanks to the University of Regensburg's NMR Department, for their willingness to conduct NMR measurements.

I am very grateful to Dr. Reinout van der Veen for his continuous interest in the progress of this work, for the countless scientific discussions as well as for always having some helpful advice.

Also thanks to Dr. Michael Stapels for his innovative ideas, valuable input, helpful scientific discussions and his special kind of humour which keeps me highly motivated to finish this thesis.

I deeply thank Prof. Dr. Crisan Popescu from Kao Germany Darmstadt, for his intensive help, explanations and guidance regarding the TGA and DSC measurements. Many thanks for the interest you gave to my work.

I also would like to express my gratitude to the Kao Corporation for the opportunity to face this project as well as the patience. Thank you for supporting my thesis and for providing the needed equipment.

Admittedly, I am very proud to be part of the KCG R&D group. I cannot imagine a better working atmosphere, including fun, motivation and progress and that is the reason why I want to show my gratitude to the whole group and its members. In particular, I want to mention Kerstin Sonntag, Lea Tekath, Dr. Malgorzata Bohdan, Stefan Dikty and Sarah Peters, as I was convinced and highly motivated to work.

Table of Contents

I Introduction

The lifespan and efficiency of various types of machinery is often limited by the performance of its lubricated interfaces, which are formed by two interacting surfaces and a lubricant. The job of the lubricant is to separate the surfaces and to decrease friction and wear. There is a constant quest for more efficient lubricants.
Ionic Liquids possess many unusual physico-chemical properties compared to molecular liquids including, but not limited to, high polarity, high conductivity, high thermal stability, and a wide liquid range even down to low temperatures. Such properties are essential for formulating lubricants for interfaces in challenging applications like aerospace and wind turbines. Recently, a new family of Ionic Liquid has been deeply investigated. These Ionic Liquids contain surfactants as structural element, therefore they are known as SAILs, Surface Active Ionic Liquids. Due to their unique properties resulting from the combination of an Ionic Liquid and a surfactant, these substances could be interesting for being a high-performance lubricant.

The motivation and concept of this thesis can be summarised by the following ideas.

1. First, the synthesis of different anionic parts based on alkyl ether carboxylic acids. These kinds of molecules are well known as anionic surfactants, with a modular molecule shape. The physico-chemical properties are adjustable by variation of the alkyl chain as well as the alkoxylation type and degree.
   As purity is the key for Ionic Liquids, propylene oxide instead of ethylene oxide has been chosen for the alkoxylation. This relates to a narrower oligomer distribution as well as less remaining non-reacted alcohol and it makes the resulting molecule more oil soluble and less water soluble. A second advantage of the introduction of a certain degree of propylene oxide to the alcohol is the lowered melting point, due to the sterical hindrance of the methyl group in the three-dimensional network. The linking of the acetic acid group to the propoxylated alcohol directly leads to the anionic surfactant. The crucial step of this synthesis is the removal of all by-products as well as the needed high conversion degree to the resulting anionic surfactant. By using a suitable industrial synthesis and purification route, all anionic surfactants could be directly produced in industrial scale.
   As symmetric quaternary ammonium compound, three different molecules have been selected. Tetramethyl, tetraethyl and tetrabutyl, differ in the alkyl chains at the nitrogen atom, therefore also the influence of the molecular shape of the cation could be investigated and the best candidate for the application as lubricant could be defined. These products are also available in large scales from the market.
2. In the second part, the synthesised compounds were characterised with respect to their potential as lubricant or lubricant additive. Typical lubricants or additives have to fulfil different requirements. They should show low electric conductivity and a good handling in terms of liquid flow behaviour, like low viscosity combined with low melting point and high thermal stability. Besides these parameters, also a good solubility in natural oils, like rape-seed oil, as well as low hygroscopic behaviour is preferred for this kind of future application.

Following physico-chemical parameters of the prepared Ionic Liquids have been evaluated: density, viscosity, conductometry, melting, thermal stability, hygroscopy and oil solubility. These factors have then been correlated to the different molecular structures like C-chain lengths, propoxylation-degrees and size of the corresponding cation.

3. In the last part of the thesis, all prepared Ionic Liquids have been tested as neat oil as well as additive in natural oil, rape-seed oil, concerning their potential as lubricant. For this investigation, a modular rheometer has been used. On this rheometer, the film forming properties, the lowest friction coefficient and the resulting lowest sliding speed have been correlated to the molecular structures of different Catanionics.

II Fundamentals

II.1. Tribology

II.1.1 General Aspects

The term “Tribology” is derived from the Greek verb *τρίβειν*, tribein, "rubbing", and the suffix -logy from -*λογία*, "study of".

Tribology refers to the science and technology of friction, lubrication and wear. In 1966, H. Jost published his report, the “Jost-Report“, in which the energy losses caused by friction and wear were highlighted and the word tribology was used for the first time [1–3]. In this report, Lord Peter Jost was able to convince the British government that approximately 515 million pounds sterling per year accrued in wasteful resources were wasted due to the lack of understanding and knowledge of tribological phenomena. It was also estimated that the costs of tribological deficiencies are expected to be 1 % of the gross national product (GNP) of industrialized nations. A more recent analysis reveals that supplying all two gear drives in the United States with a lubricant would allow a relative increase of 5 % in mechanical efficiency compared to conventional mineral oil and would result in savings of approximately $ 1 billion per annum. Therefore, for economic reasons and long term reliability of machinery, the significance of understanding tribological phenomena in terms of friction reduction and wear control cannot be overemphasized. Thus, lubrication is one of the challenges for efficient and durable operation of advanced engineered mechanical systems.
Great effort has been devoted to finding solutions for tribological challenges and to minimize energy losses. Jost defines tribology as science and technology of interacting surfaces in relative motion of associated subjects and practice. This interaction is influenced by many physical and chemical parameters, such as materials, load, temperature, surface roughness and lubricating oil properties etc. The behaviour of a tribo-contact is dependent on all these parameters. Therefore, the thorough understanding of the mechanism needs the consideration of all the above mentioned phenomena. Tribology is an interdisciplinary field ranging from chemistry, physics, material science to engineering and from fundamental research to industrial applications.

Important aspects of tribology have been friction, wear and lubrication since the introduction of this science. Friction is defined as the resistance to motion once two surfaces are moving tangentially to each other. Wear is defined as damage to surfaces due to contact in relative motion. The term lubrication is used for the process or techniques employed to reduce friction. Here a substance called a lubricant is interposing the contacting surfaces in relative motion.

II.1.2 Tribological System

A tribological system, or tribosystem, consists of four components, as described in Figure II-1:

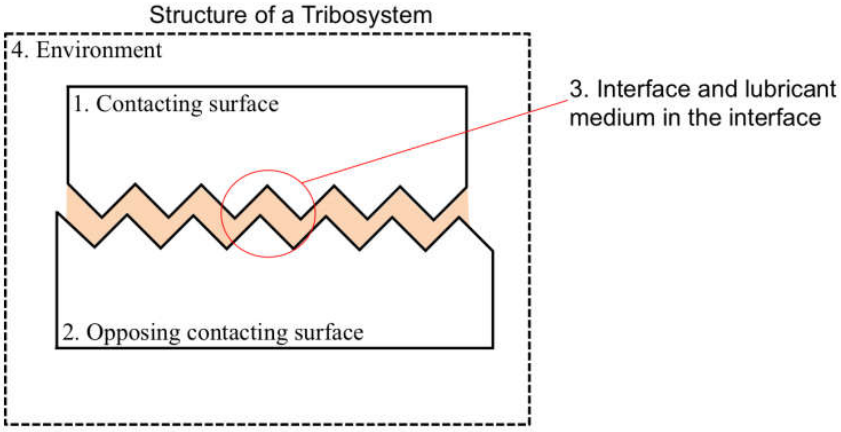

Figure II-1: Structure of a tribosystem [3]

So the tribosystem can be divided in a contacting surface (1); an opposing contacting surface (2); the contacting interface along with the lubricant medium in the interface (3) and the environment and all external properties (4). Tribosystems can consist of numerous components, for example, a plain bearing is a tribosystem. In this example, the material pair is the shaft and bearing shell, with the lubricant located in the annuls gap. Other examples of material pairs that form tribosystems are in combustion engines such as the piston rings and cylinder wall and the camshaft lobes and tappets. In metalworking, the tool and the work piece also constitute a material pair forming a tribosystem. All parts of the tribosystem have an influence in friction, wear and lubrication.

II.1.3 Friction

Friction is one of the most ancient problems in physics/mechanical engineering with major implications on our everyday lives. Friction arises due to forces F transmitted between surfaces, where A is an area on a surface and S is the distance between these surfaces. In continuum mechanical terms, forces F are transmitted as tractions, defined in Equation II-1.

$$t = \lim_{\Delta S \to 0} \Delta F / \Delta A \qquad \textbf{Equation II-1}$$

Oblique tractions can be resolved into normal and tangential tractions. The force along axis x due to a surface traction t can be calculated as in Equation II-2.

$$F = \int_S t \cdot x \, ds \qquad \textbf{Equation II-2}$$

The friction force, F_f, is defined as the interfacial force that opposes the relative motion of two bodies in contact, as shown in Figure II-2. That said, it is important to distinguish between two equally important frictional phenomena [4]: the static friction force, F_s, and the kinetic

friction force, F_k. F_s is defined as the minimal force required to initiate sliding, while F_k is the force required to maintain the sliding process. Depending on the application, friction can be desirable or undesirable. For example, the ability of humans to walk and vehicles to move would not be possible without friction. High friction is also desired in the tightening of screws and bolts as well as in clutch systems. In contrast, friction is undesirable in car engines, moving components of machinery, human joints, turbines, and microelectromechanical systems (MEMS).

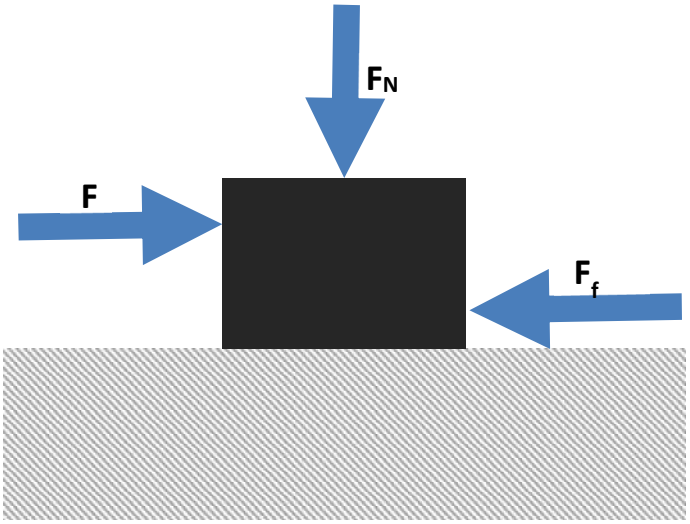

Figure II-2: Schematic illustration of a block subject to a lateral force F and a normal force F_N and an opposing friction force F_f [3]

Leonardo da Vinci is believed to be the first who has studied friction systematically [5]. He concluded that the friction force is proportional to the normal force F_N and independent of the contact area, findings which were rediscovered by Guillaume Amontons, who published the following laws in friction in 1699 [6]. Amontons observed that the friction force F_f is proportional to the normal force F_N (Amontons´ 1st law) and independent of the contact area A (Amontons´ 2nd law), as long as the rolling materials and their weights are equal. Later, Coulomb, another French physicist introduced another law. He observed that the friction force is independent of the sliding velocity (Coulomb's Law) and identified time dependence of static friction, meaning the time varied depending on the materials used [6]. These three laws are summarized in the following enumeration.

1. The friction force is directly proportional to the applied normal force. (Amontons´ 1st law)
2. The force of friction is independent of the apparent area of contact. (Amontons´ 2nd law)
3. Kinetic friction is independent of the sliding velocity. (Coulomb's Law)

The observations of Amontons and Coulomb remained empirical up to the middle of the last century, when Bowden and Tabor finally gave an explanation based on the roughness of the contacting surfaces. They realized that the real contact happens only on the asperities (where atom-atom interaction takes place) and that the actual area of contact is only of the order of 10^{-5} of the visible area. These points of contact are under extreme pressure and with the increase of load, the real contact area grows, due to an increase of the number of contacts

between the asperities [7]. In consequence, the necessary friction force F_f to maintain a certain sliding will also increase. This work was a revolutionary progress in the field of tribology. Bowden and Tabor developed and experimentally demonstrated the model for adhesive friction. They showed that the true contact area, which is based on the linear relationship between electrical conductivity and cross-sectional area, leading to the adhesive model for friction, Equation II-3,

$$\mathrm{F} = \mathrm{I_S} \cdot A_\mathrm{r} \qquad \textbf{Equation II-3}$$

where I_S is the interfacial shear strength and A_r is the true area of contact. They also noted that this mechanism of friction is distinct from energy losses due to deformation of the materials involved in sliding.

According to Hertzian contact mechanics, which had been developed some 50 years before, the contact area between two spherical or spherical and flat elastic contacts should increase with the load to the power of 2/3 [8]. Thus, if their contacts had been elastic, Bowden and Tabor´s results would have appeared at odds with either Hertzian contact mechanics or with Amontons´ first law. They rectified this discrepancy by arguing that deformation in the metals they were working with could be expected to be primarily plastic. The true contact area would then be equal to the load divided by the yield strength of the material. Later models of elastic deformation of a fractal surface and the surface with a random distribution of asperity sizes showed that the deformation should be proportional to load in the case of elastic information as well. Greenwood and Willamson, in what came to be known as GW theory, proposed that the contact area is indeed proportional to the normal load for elastically deformed asperities [9,10]. Many models have proven useful in understanding the elastic behaviour of non-adhesive and adhesive surfaces and their asperities when these are modelled by the Hertz and Johnson-Kendall-Roberts (JKR) theories, respectively [11–13]. Thus Amontons´ first law is generally not due to any physical property of materials, but merely a consequence of stochastic roughness.

Adhesive friction cannot be directly predicted from measurements of adhesion, which usually involve bringing two materials into contact and measuring the force necessary to separate them. An important difference is that sliding friction does not involve separation of materials. Instead, a contact merely moves from one area of the interface between the same pair of materials to another. On an atomic scale, this is linked to the energy required for atoms to move from one local energy minimum to the next [14]. A better predictor of adhesive friction is adhesion hysteresis, the difference between adhesion forces on approach and on separation, as shown by Jacob Israelachvilli´s group in 1991 [15].

II.1.4 Wear

Wear is defined as the progressive loss of substance from the operating surface of a body occurring as a result of relative motion at the surface [16]. Several different mechanisms contribute to wear, most notably adhesive wear, surface fatigue, abrasive wear, corrosion and erosion.

Adhesive wear is the most common mechanism and occurs when the asperities of one surface are strongly adhered to the asperities of another surface resulting in the formation of a junction. When these surfaces are sheared against each other, the softer asperities are separated and material is removed [17]. Fatigue wear occurs when the same volume of asperities are repeatedly sheared against each other. With time, this repetitive sliding will eventually result in the formation of voids and surface cracks that continue to propagate under the shearing action [18]. This type of wear generally occurs in brittle materials [19] and results in the breakup and removal of materials from the surface. Abrasive wear occurs when a hard surface is sheared against a significantly softer one; hence the hard asperities are able to penetrate the softer ones. When these surfaces move relative to one another, grooves and scratches are formed owing to the ploughing action resulting in the removal of material from the softer surface in the form of loose particles [7]. Corrosive wear is material loss due to the combined action of chemical degradation and interfacial sliding. Loss of material properties or material by corrosion often leaves material more susceptible to adhesive and abrasive wear [20]. Erosion occurs when flowing liquid or solid particles remove material from a solid surface as in sandblasting or in a deepening canyon.

It is clear from the definitions above that wear is a complex phenomenon that depends on the materials in contact as well as environmental conditions. Therefore, it is not surprising that no universal equation of wear exists. Models have been developed of rates of adhesive wear [21] and abrasive wear [22], which despite being derived for very different conditions, coincidentally take the same form. In Archard's derivation, Equation II-4, for adhesive wear, K is the probability of each contact forming a wear particle, while in Rabinowicz's derivation for abrasive wear, K is the cotangent of the half angle of the indenter. Practically, the value of K is typically determined by experimentation.

$$\frac{\mathrm{dV}}{\mathrm{dh_s}} = \frac{\mathrm{K \cdot F}}{\mathrm{3H}} \qquad \textbf{Equation II-4}$$

V is the removed volume, h_s is the sliding distance, F is the load, and H is the hardness of the material being worn (the softer of the two surfaces). However, Archard observed that the wear rate (dV/dh_s) is directly proportional to the worn volume and indirectly proportional to the normal load and hardness of the material.

The relationship between friction and wear is far from being straightforward. Wear requires energy and the energy that causes wear comes from friction. Thus, there is a minimum theoretical friction value associated with any given wear rate [23]. Because most friction is generated by mechanisms that do not result in wear, this relationship is not very practical. It is reasonable to conclude that a relationship exists between adhesive friction and adhesive wear and between ploughing friction, which results from a hard asperity pushing through a

softer material and abrasive wear. Surface fatigue would be expected to increase with increasing friction, though not necessarily linear. More research is needed to illuminate the details of these relationships. In practical situations, low friction and high wear is sometimes optimal, as for pencil lead, and high friction and low wear is optimal in other situations, as for brake pads.

II.1.5 Contact and Fluid Lubrication Theory

II.1.5.1 Dry Contact Theory

Based upon some assumptions, Hertz [24] presented the first analytical solution for contact problems. Hertz was attempting to understand how the optical properties of multiple, stacked lenses might change with the force holding them together. Hertzian contact stress refers to the localized stresses that develop as two curved surfaces come into contact and deform slightly under the imposed loads. The amount of deformation is dependent on the modulus of elasticity of the material in contact. It gives the contact stress as a function of the normal contact force, the radii of curvature of both bodies and the modulus of elasticity of both bodies. Hertzian contact stress forms the foundation for the equations of load bearing capabilities and fatigue life in bearings, gears, and any other bodies where two surfaces are in contact. Until now, the Hertz solution has often been used in engineering practice owing to its simple form. Hertz opened the door for a systematic subject called “contact mechanics”. The physical and mathematical formulation of the subject of contact mechanics is based upon the mechanics of materials and continuum mechanics and focuses on computations involving elastic, viscoelastic, and plastic bodies in static or dynamic contact. The central aspects in contact mechanics are the pressures and adhesion acting perpendicular to the contacting bodies surfaces, the normal direction, and the frictional stresses acting tangentially between the surfaces. Since Hertz, the development of contact mechanics mainly focuses on eliminating assumptions made by Hertz, such as removing the friction between interacting surfaces.

Hertz introduced the simplification that, for the calculation of local deformations, each body can be regarded as an elastic half-space loaded over a small region of its plane surface. By this simplification, generally followed in contact stress theory, the highly concentrated contact stresses are treated separately from the general distribution of stress in the two bodies, which arises from their shape and the way, in which they are supported. For this simplification, two conditions should be satisfied: the dimensions of the contact area must be small compared (a) with the dimensions of each body and (b) with the relative radii of curvature of surfaces. The first condition is necessary to ensure that the stress field calculated on the basis of a solid, which is infinite in extent, is not seriously influenced by the proximity of its boundaries to the highly stressed region. The second condition is to ensure firstly that the surfaces just outside the contact region approximate roughly to the plane surface of a half-space, and second that the strains in the contact region are sufficiently small to lie within the scope of the linear theory of elasticity. Hertz also assumed the surfaces to be frictionless so that only the normal pressure is transmitted between two bodies. Hertz was able to give the analytical solution to classical dry contact problems. A line contact problem can be simplified as two cylindrical bodies, lying parallel, pressed in contact by a force per unit length, see Figure II-3. $R_{1,2}$ represents the contact radius of the solids, and $u_{1,2}$ represents the speed of the two solids.

The coordinates are defined as follows: the x direction represents the direction of the rolling speed, for a lubrication case, it also represents the flow direction of the lubricant; the z direction is the direction across the gap between the interacting surfaces, for a lubrication case, it represents the direction across the film. The y direction is vertical to the x z-plane [24].

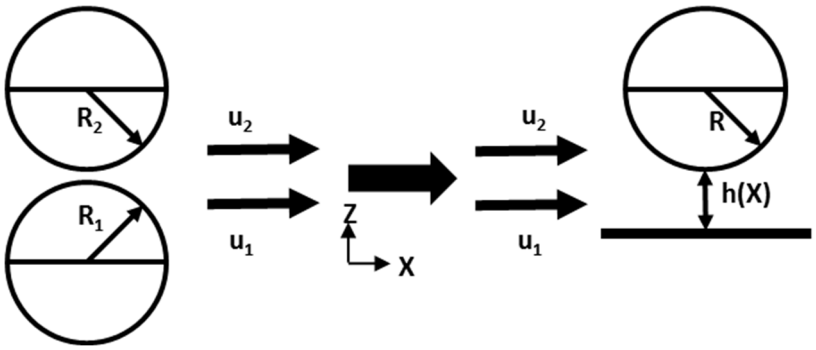

Figure II-3: Simplification of a line contact problem [24]

For line contact problems, the maximum pressure occurs in the nominal contact region, also known as the Hertzian pressure, p_H. It is expressed in Equation II-5:

$$p_H = \sqrt{\frac{E' \cdot F}{R \cdot \pi}} = \frac{4\, p_m}{\pi} = \frac{2\, F}{\pi \cdot b} \qquad \textbf{Equation II-5}$$

where p_m is the mean contact pressure across the contact region. F is the load per unit width, and E' is the equivalent elastic modulus, Young´s modulus, which is derived from:

$$\frac{2}{E'} = \frac{1 - v_1^2}{E_1} + \frac{1 - v_2^2}{E_2} \qquad \textbf{Equation II-6}$$

where v_1 and v_2 are the Poisson ratios of the two subjects and E_1 and E_2 are the elastic moduli of the two subjects. The reduced radius of curvature R, for Equation II-5, is given by Equation II-7:

$$\frac{1}{R} = \frac{1}{R_1} + \frac{1}{R_2} \qquad \textbf{Equation II-7}$$

with R_1 and R_2 as radii of the two subjects. The half contact width b, for Equation II-5, is expressed as:

$$b = \sqrt{\frac{8 \cdot F \cdot R}{\pi \cdot E'}} \qquad \textbf{Equation II-8}$$

The pressure distribution within the Hertzian contact zone can be calculated with Equation II-9:

$$p(x) = \frac{2 \cdot F}{\pi \cdot b^2} \cdot \sqrt{b^2 - x^2} \qquad \textbf{Equation II-9}$$

The pressure falls to zero at the edge of the contact region. By using the elastic mechanics theory, the contact interface stress is:

$$\sigma_x = -p(x) \qquad \textbf{Equation II-10}$$

Outside the contact region, all the stress components at the surface are zero.
Along the z direction, the principal stresses are given by:

$$u_s = u_1 - u_2 < 0 \qquad \textbf{Equation II-11}$$

$$\sigma_z = -\frac{p_H}{b} \cdot \frac{1}{\sqrt{(b^2 + z^2)}} \qquad \textbf{Equation II-12}$$

For plane strain, the third principal stress is:

$$\sigma_y = v\,(\sigma_x + \sigma_z), \qquad \textbf{Equation II-13}$$

where σ_x, σ_y and σ_z are stresses along x , y and z direction, respectively. The principal shear stress τ_1 therefore can be calculated by Equation II-14.

$$\tau_1 = -\frac{p_H}{b} \cdot [z - z^2 \frac{1}{\sqrt{(b^2 + z^2)}}] \qquad \textbf{Equation II-14}$$

The Hertz contact theory is introduced here, because the theory is still the basis for surface contact strength standard for gears, bearings, etc. Bowden and Tabor [25] were the first to study the effects of surface roughness on bodies in contact. Through the investigation of the surface roughness, the true contact area between friction partners is found to be less than the apparent contact area. Such understanding also drastically changed the direction of tribology. The works of Bowden and Tabor yielded several theories in contact mechanics of rough surfaces. Archard's work [9] should also be mentioned, because he concluded that even for rough elastic surfaces, the contact area is approximately proportional to the normal force. This work was followed by Greenwood and Williamson [10] and others. In the 1970s, Johnson et al. [26], among others, proposed their adhesive elastic contact model. The work by Greenwood and co-workers [27] is used as reference for Elastohydrodynamic Lubrication (EHL) researchers studying statistical rough surface EHL models, which will be mentioned later. In the early days, owing to the limit of computation ability, researchers used statistical models [28,29] as the main tool to study rough surface contact problems. However, statistical models ignore the interaction between neighbouring asperity micro-contacts, which becomes prominent at high contact loads [30].

Additionally, those models cannot represent the essentially multiscale nature of surface roughness [31]. It is fair to argue that if the real surface topography is explicitly considered in the model, the problem occurring in statistical models would disappear. As the development of computer technology progressed, more work focused on the deterministic models, such as work done by Lai and Cheng [32]. Among those numerical methods, two advanced algorithms should be emphasized: the multi-level multi-integration (MLMI) method [33], and the FFT-based (Fast-Fourier-Transformation) method, [34,35]. The MLMI and FFT-based methods have their own advantages and both of them could reduce computation time significantly compared with the direct summation method.

II.1.5.2 Fluid Lubrication Theory

Lubrication is an ancient technology that dates back to the days of the Egyptian Pharaohs, who used animal fats and water in their building of the pyramids [36]. The idea is to reduce the intimate contact between surfaces through the introduction of a lubricant between them. There are two common types of lubrication: a) fluid lubrication, where a fluid is introduced between the mating surfaces and b) surface film lubrication, where a film is physically or chemically bound to the surface. While solids, liquids, and gases can be used as lubricants, the main focus of this thesis will be on lubrication through Ionic Liquids.
The well-known Stribeck curve [37], illustrated in Figure II-4, has been widely employed in determining the lubrication regime. It describes the variation of the friction coefficient, μ, in connection to the dynamic viscosity, η, of the lubricant, the sliding velocity, V, and the applied load, P. This function, ηV/P, of the friction coefficient, μ, represents the dimensionless number, usually named the Hersey number, Hs, given by Equation II-15 [23,38].

$$\mathrm{Hs} = \mu = \frac{\eta V}{P} \qquad \textbf{Equation II-15}$$

From Figure II-4, one can clearly distinguish between three lubrication regimes: Hydrodynamic Lubrication, Mixed Lubrication or Elastohydrodynamic Lubrication and Boundary Lubrication. Each of these three regimes will be discussed in detail in the following sections.

The main difference in the three lubrication regimes is the thickness of the lubricating film, h_{min}. The film thickness parameter, λ decides the lubrication regime with Boundary Lubrication characterized by a value of λ less than 1; mixed or Elastohydrodynamic Lubrication (EHL) described as $1 \leq \lambda \leq 3$ and Hydrodynamic Lubrication characterized by a value of λ greater than 3 [38–41]. Equation II-16 combines minimum film thickness, h_{min}, and roughness of the two contacting surfaces r_a and r_b.

$$\lambda = \frac{h_{min}}{\sqrt{r_a{}^2 + r_b{}^2}} \qquad \textbf{Equation II-16}$$

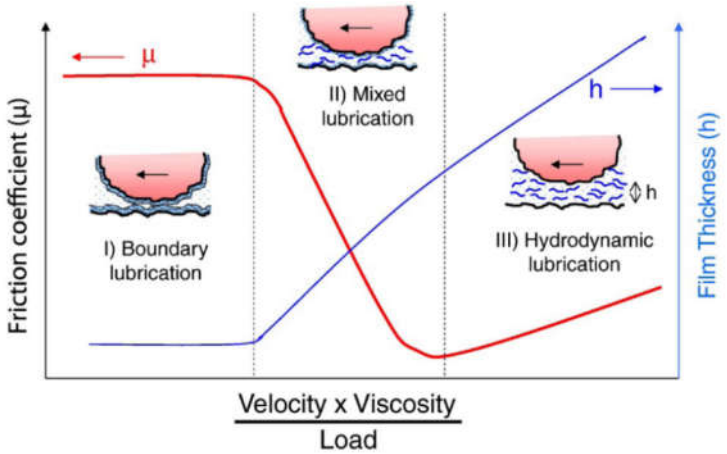

Figure II-4: Stribeck curve illustrating the different lubrication regimes for different fluid film thickness [37]

II.1.5.3 Boundary Lubrication

There are many practical situations, where the lubricant film thickness is not large enough to prevent direct contact between asperities, resulting in high friction and wear rates. In this regime, the typical film thickness ranges from 0.005 to 0.1 µm resulting in friction coefficients of the order of 0.03-0.2. This mode of lubrication is commonly referred to in the literature as boundary lubrication, Figure II-5.

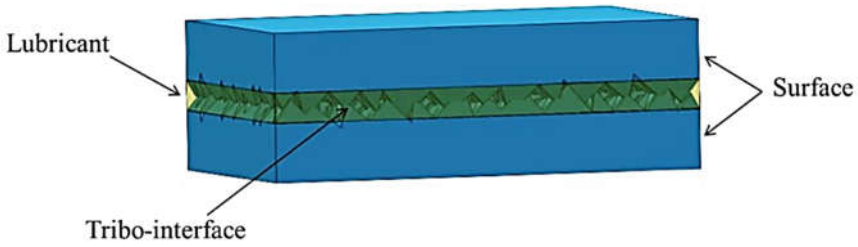

Figure II-5: Boundary lubrication at the interface of a tribosystem; full contact of the asperities, and lubrication occurs through surface interactions [3]

Knowledge of boundary lubrication is attributed to Hardy and Doubleday [42,43] and later deeply investigated by Bowden and Tabor [7]. This lubrication regime occurs, when the load increases or the speed decreases as well as when the fluid viscosity decreases, giving rise to a sharp increase of the friction coefficient, which reaches very high values. These circumstances make it difficult to maintain a thin film between the contacting surfaces, i.e. the film is squeezed out of the contact area. So the lubricant in boundary lubrication serves as the last defence line, it is critical to select the appropriate materials as the boundary lubricant. Under these conditions, the contact is dominated by the interaction between the thin lubricant film and the solid asperities. Therefore, the physical and chemical properties of the film as well as those of the surface determine the behaviour of the contact, whereas influence of lubricant viscosity is almost negligible.

The boundary lubrication can be divided in four categories. Here, the sliding speed and the load are the variable dimensions. These four classes are described in Table II-1.

Sliding speed	Load	Lubrication mechanisms
low	low	Viscosity enhancement close to contacting surface, not specific to lubricant
	high	Friction minimization by coverage of contacting surfaces with adsorbed monomolecular layers of surfactants
high	medium	Irreversible formation of soap layers and other viscous materials on worn surface by chemical reaction between lubricant additives and metal surface Surface-localised viscosity enhancement specific to lubricant additive and base stock oil Formation of amorphous layers of finely divided debris from reaction between additives and substrate metal surface
	high	Reaction between lubricant additives and metal surface Formation of sacrificial films of inorganic material on the worn surface, preventing metallic contact and severe wear

Table II-1: Four different categories of boundary lubrication as a function of the sliding speed and the applied load [3]

Boundary lubrication is a complex process and is controlled by additives in the oil that form a thin molecular layer (monolayer) of fluid film [7,44]. The ideal lubricant should have both load-carrying, i.e., solid-like, and self-healing, i.e., liquid-like, capability. High load-carrying capability prevents the lubricant from being squeezed out of the interface and is usually achieved by the strong adsorption of the lubricant onto the solid surface. Good self-healing allows the lubricant to flow back to the original spot after it is removed and is promoted by the high mobility of the lubricant. A long-lasting dilemma here is the trade-off between load-carrying and self-healing capability. The idea is that molecules that adsorb on the contacting surfaces are able to provide a protective layer, which prevents direct contact between the asperities. This protective layer is characterized by low shear strength and results in significant reduction in the friction coefficient. To better understand this effect, consider an alternative expression for the friction coefficient given by Equation II-17 [19]:

$$\mu = \frac{\tau}{\sigma_y}, \qquad \textbf{Equation II-17}$$

where τ is the effective shear stress and σ_y is the plastic flow stress of the material. From this equation, it can be easily seen that with low shear stress and high plastic flow stress, i.e. high hardness, low friction coefficients can be obtained.

This protective layer, see Figure II-6, can be obtained through physical adsorption, chemisorption, and tribochemical reactions on the contacting surfaces. Physisorption, or physical adsorption, occurs, when molecules are attached to the surface via bonds resulting from Van der Waals forces [45]. Therefore, these molecules are weakly bound to the surface and very sensitive to temperature, and can desorb, when the temperature is sufficiently high.

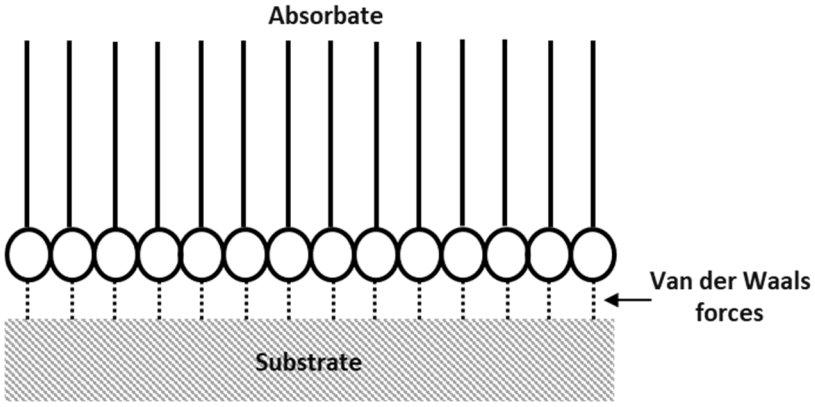

Figure II-6: Schematic illustration of physisorption [3]

However, as long as they remain bound to the surface, they can provide a protective layer. One of the more common boundary lubrication additives, based on physisorption, is fatty acids, which adhere to the metallic surfaces and form a tightly packed monolayer [7,46,47], illustrated in Figure II-7. Besides the strong polar fatty acids, also other organic compounds like fatty alcohols and fatty amines, have sufficient polarity to be of practical use.

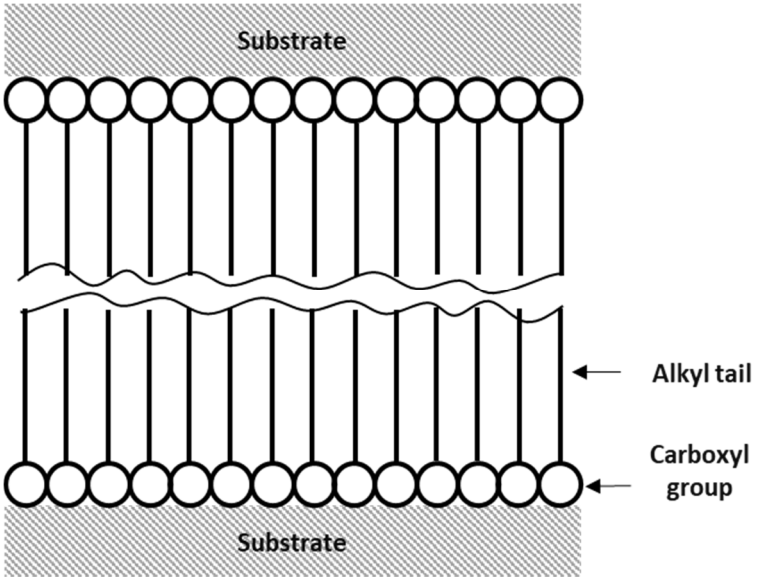

Figure II-7: Monomolecular layer of adsorbed organic polar molecules on metallic surfaces [3]

The molecular structure or shape of the adsorbate has a very strong influence on the effectiveness of lubrication. In addition to the basic requirement that the adsorbing molecules are polar, preferably with an acidic end group for attracting to a metallic surface, the shape of the molecule must also facilitate the formation of close-packed monolayers. This latter requirement virtually ensures that only linear molecules are suitable for this purpose. Also the size of the molecules is critical. It was found that the friction transition temperature for fatty acids increased, when the molecular weight was raised [7,46]. More importantly, there is a critical minimum chain length of fatty acids required in order to provide effective lubrication. Bowden and Tabor found that the minimum chain length for effective lubrication is C_9, nonanoic acid [7,46–49]. An increase in chain length from C_9 to C_{18} raises the friction transition temperature by about 40°C. Short-chain fatty acids with chain lengths shorter than C_9 do not show any useful lubricating properties. This effect may be explained in terms of relatively weak bonding between the C-chains of adjacent fatty acid molecules compared to the bonding at the base of the film. It seems that sufficiently large numbers of methylene groups are required to ensure the strength of the adsorbed monolayer. The effect of chain length is quite strong. For example, octadecanol provides a lower coefficient of friction, when used with steel than dodecanoic acid, despite the far stronger attraction fatty acids have to metals [7,46–50].

Deviations from the ideal linear molecular shape can severely degrade the lubricating properties of an adsorbate. The differences in friction characteristics become clearly visible for various isomers of octadecanic acid which include linear and branched molecular configurations. This effect is illustrated in Figure II-8, where the friction coefficient is shown for a steel ball on a steel plate lubricated by varying concentrations of fatty acid in paraffinic oil [7,46–49].

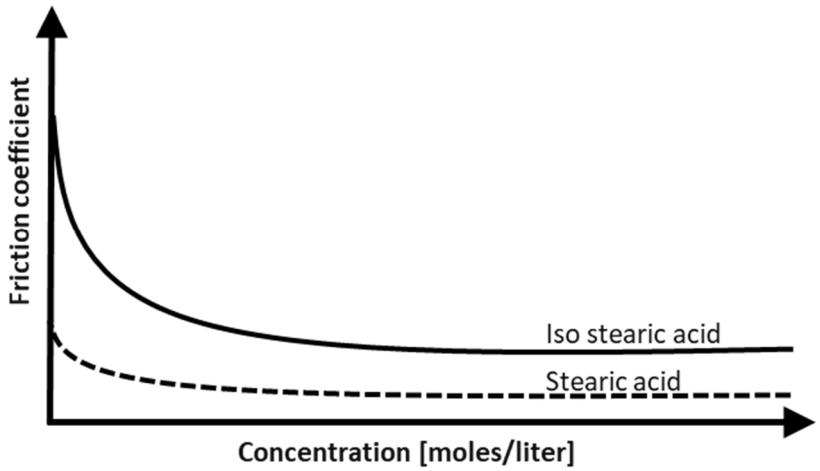

Figure II-8: Effect of different concentrations of octadecanoic acid and iso-octadecanoic acid in paraffinic oil on the coefficient of friction [3]

The difference between the molecular shape of octadecanic acid and iso-octadecanic acid is that in the latter there are 17 main chain carbon atoms with one branching to the side, as opposed to 18 main chain carbon atoms in the former. As can be seen from Figure II-8, this difference causes the coefficient of friction between the surfaces to almost triple. The possible effect of the branched isomerism is illustrated in Figure II-9.

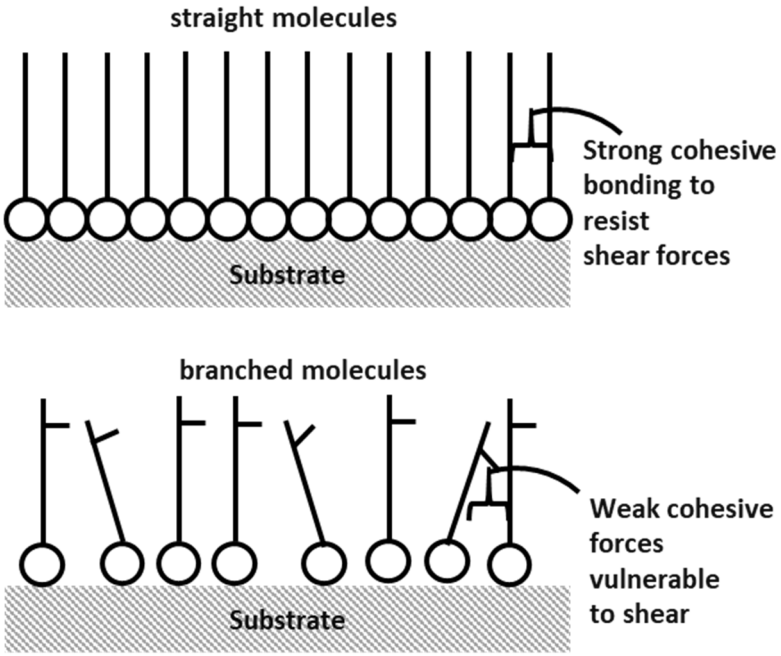

Figure II-9: Disruption of adsorbate film structure consisting of branched molecules [3]

The branched molecular shape results in two detrimental effects:

- complete surface coverage is difficult to achieve so that the probability of metallic contact is increased
- there is a deeper interactions zone between opposing adsorbate surfaces, allowing stronger bonding between adsorbate films, resulting in higher coefficients of friction

On the other hand, chemisorption, or chemical adsorption, occurs when molecules of the adsorbate, i.e. lubricant, and those of the substrate are held together via chemical bonds, shown in Figure II-10. A chemically attached protective layer is effective under moderate loads and temperatures and typically contains reactive elements such as sulphur, chlorine and phosphorus [51].

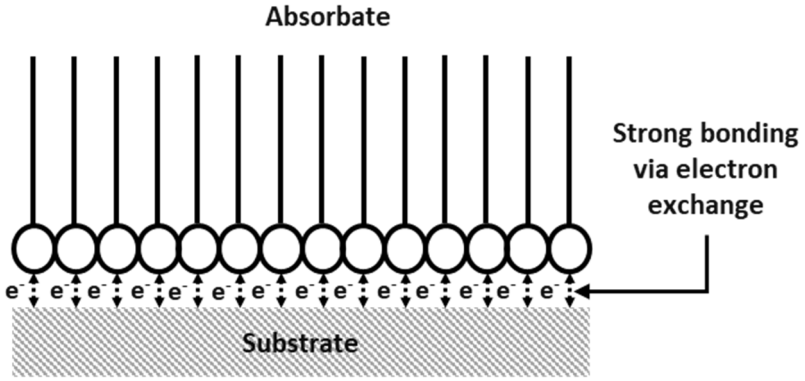

Figure II-10: Mechanism of Chemisorption [3]

II.1.5.4 Mixed and Elastohydrodynamic Lubrication

Mixed film lubrication is the combination of full film hydrodynamic lubrication and boundary lubrication. In this lubrication regime, the surfaces are transitioning away from boundary lubrication into hydrodynamic lubrication, where there may be frequent asperity contacts, but at least a portion of the bearing surface remains supported partially by a hydrodynamic film [52], as shown in Figure II-11. In mixed lubrication, the effects of monolayers formed by physical absorption, chemisorption, and chemical reaction remain critical to prevent unwanted adhesion during the asperity contacts [53].

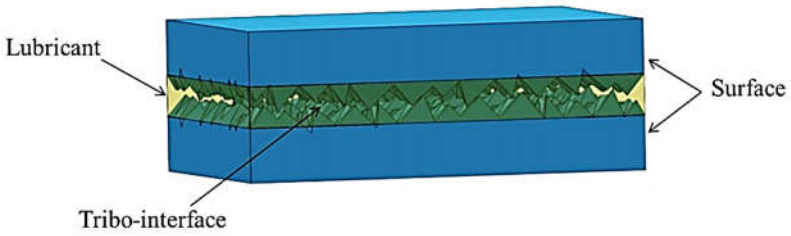

Figure II-11: Mixed lubrication/elastohydrodynamic lubrication at the interface of a tribosystem partial asperity; contact where fluid film is of the order of the surface roughness [3]

Elastohydrodynamic (EHL) lubrication is a subset of hydrodynamic lubrication, in which the elastic deformation of the contacting solids plays a significant role in the hydrodynamic lubrication process. The viscosity-pressure effect cannot be neglected either in this lubrication regime. This kind of lubrication may occur in gears, bearings, cam drives, etc. The film thickness in EHL lubrication is thinner (typically 0.5-5 µm) than that in hydrodynamic lubrication and the load is still primarily supported by the EHL film [52]. In this transitional region, there is less asperity contact than that of mixed lubrication with more of the contacting surfaces being supported by the hydrodynamic fluid film. In EHL regime, the load is high enough that the contact zone elastically deforms. Also, liquid lubricant in contact zone is subjected to such a high pressure that the viscosity of lubricant can increase by several orders of magnitude due to pressure effect. This approximately exponential increase of viscosity, as the pressure goes up, is one dominant effect accounting for the film formation in nominal Hertz contact regions. The thermal effect on viscosity is sometimes neglected in part of investigations on EHL. In this case, the most widely used viscosity-pressure relation is introduced, the exponential isothermal Barus equation (Equation II-18).

$$\eta\,(p) = \eta_0 \cdot e^{\alpha \cdot p} \qquad \textbf{Equation II-18}$$

where η_0 is the viscosity under ambient pressure, and α is the pressure-viscosity coefficient. Typically its value is in the range $1 \times 10^{-8}\ Pa^{-1} < \alpha < 3 \times 10^{-8}\ Pa^{-1}$. The Barus equation is applied extensively in early days, owing to its simplicity.
Generally, the compressibility of the lubricant under high pressures should not be neglected. One of the most cited relations is the one proposed by Dowson and Higginson [54], which reads:

$$\rho\,(p) = \rho_0 \cdot \frac{0.59 \cdot 10^9 + 1.34 \cdot p}{0.59 \cdot 10^9 + p} \qquad \textbf{Equation II-19}$$

where ρ_0 is the density at ambient pressure. This density-pressure relation is depicted in Figure II-12. The figure shows that the compressibility of the lubricant is less than approximately 30%, which indicates that the effect of the compressibility of the lubricant on the film formation is much smaller than the effect of the elastic deformation and the effect of the viscosity.

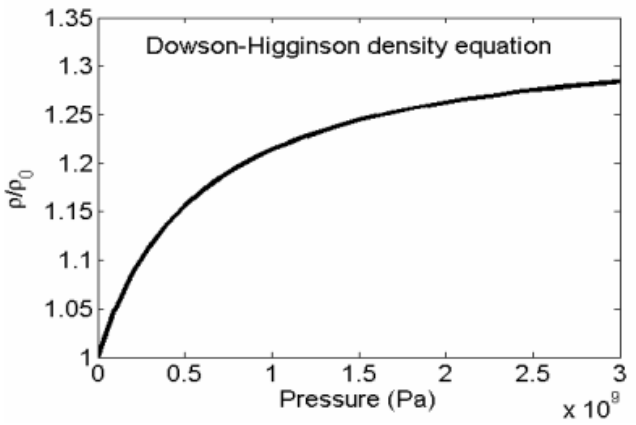

Figure II-12: Dowson-Higginson density-pressure relation [54]

With the further increase of bearing load, some contact between asperities of both surfaces takes place. The main variables in this regime are pressure distribution and film thickness. Based on the exact analysis of the Elastohydrodynamic Lubrication by Hamrock and Dowson [55,56], it is now possible to calculate the minimum film thickness in EHL contacts, see Equation II-20. This formula applies to any contact, such as point, linear or elliptical, and is now routinely used in film thickness calculations. It can be used with confidence for many material combinations, even up to maximum pressures of 3-4 GPa [57]. The numerically derived formula for the minimum film thickness is in the following form [55]:

$$\frac{h_0}{R'} = 3.63 \cdot \left(\frac{U \cdot \eta_0}{E' \cdot R'}\right)^{0.68} \cdot \left(\alpha \cdot E'\right)^{0.49} \cdot \left(\frac{W}{E' \cdot R'^2}\right)^{-0.073} \cdot \left(1 - e^{-0.68k}\right) \qquad \textbf{Equation II-20}$$

h_0 is the minimum film thickness, U is the entraining surface velocity of the bodies, η_0 is the viscosity of the lubricant at atmospheric pressure, E´ is the reduced Young´s modulus, R´ is the reduced radius of curvature in the direction of rolling, α is the pressure-viscosity coefficient, W is the contact load and k is the ellipticity parameter.

In the literature, the equation for minimum film thickness is frequently given with the non-dimensional groups:

- non-dimensional film parameter $H = \frac{h_0}{R'}$
- non-dimensional speed parameter $U = \left(\frac{U \cdot \eta_0}{E' \cdot R'}\right)$
- non-dimensional material parameter $G = \left(\alpha \cdot E'\right)$
- non-dimensional load parameter $W = \left(\frac{W}{E' \cdot R'^2}\right)$
- non-dimensional ellipticity parameter $k = \frac{a}{b}$

So the formula is often described as

$$H = 3.63 \cdot U^{0.68} \cdot G^{0.49} \cdot W^{-0.073} \cdot \left(1 - e^{-0.68k}\right) \qquad \textbf{Equation II-21}$$

II.1.5.5 Hydrodynamic Lubrication

Hydrodynamic lubrication is the ideal state of lubrication. It is also referred as “full-film” lubrication, the moving surfaces are separated by a viscous and thick lubricant film. Generally speaking, the film thickness is usually much thicker than the height of asperity of the moving surfaces, see Figure II-13.

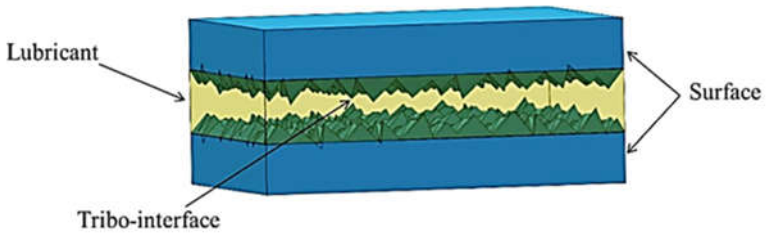

Figure II-13: Hydrodynamic lubrication at the interface of a tribosystem; full separation of the two surfaces by the lubricant occurs [3]

This will result in friction coefficients of the order of 0.001-0.01 [58,59]. Moreover, hydrodynamic lubrication requires that one of the surfaces be tilted forward in the direction of the motion. This converging configuration will result in the dragging of the fluid to the narrowing gap, while at the same time, developing a positive pressure that will support the load in the gap, and keep the surfaces apart [23]. The differential equation that governs the generation of pressure in lubricating films is known as the Reynolds equation, a special kind of Navier-Stokes equation. Reynolds first derived the equation, and it forms the foundation of hydrodynamic lubrication analysis [53]. Reynolds’ classical paper contained not only the basic differential equation of fluid film lubrication, but also a direct comparison between his theoretical predictions and the experimental results, obtained by Tower. The Reynolds equation relates the pressure in the lubricant film to the geometry of the gap and the velocities of the moving surfaces. In order to obtain the Reynolds equation, several assumptions are made:

- the flow is considered to be laminar;
- side-leakage is neglected;
- inertial forces are neglected;
- no external forces act on the fluid;
- there is no slip at the boundaries; and
- there is no pressure variation across the fluid film.

The Reynolds equation can be derived in two different ways, from the Navier-Stokes and continuity equations and directly from the principle of mass conservation.
It is clear from the quantity of the Hersey Number (Equation II-15) that this type of lubrication is governed by the viscosity of the fluid and the speed of moving surfaces. Therefore, a relatively viscous fluid and high speed conditions will prevent asperity-asperity contact and result in low friction coefficients.

II.2. Lubricants

II.2.1 General properties and common types of industrial lubricants

In order to reduce friction and minimise wear between two contacting materials, a lubricant is applied to the contacting surfaces. A lubricant reduces the friction by providing a low shear strength layer between both surfaces which is less than the material shear strength [3].

However, it is essential that the lubricant also has other functional properties to ensure its efficient application. These are good oxidation- and thermal stability, corrosion protection property, compatibility with different materials, low foaming and the ability to release air, good detergent-dispersant properties and good de-emulsification properties.
Based on the molecular structure of the lubricant material as well as its shear strength, lubricants are classified as follows:

- Solid Lubricants

A solid lubricant is a solid material such as graphite, molybdenum disulfide (MoS_2), silicone, or polytetrafluoroethylene (PTFE), which is applied or inserted between two moving surfaces or bearing surfaces. At the molecular level, these particles are super slippery, so they reduce the friction between surfaces. It is common to find these lubricants in spray form, where they are mixed with water, alcohol, or some other solvent that will evaporate away after application, leaving behind a thin film.

- Semi-Solid Lubricants

A semi-solid lubricant or grease is made by using oil, e.g. mineral oil, and mixing it with thickeners, like metal based soaps or clay. They may also contain additional solid lubricating particles, such as graphite, molybdenum disulfide (MoS_2) or polytetrafluoroethylene (PTFE). Greases combine the lubricating properties of oils with added stickiness, allowing the lubricant to adhere to the surfaces. Greases can even act as a barrier, protecting the surfaces from contaminants that can corrode or damage them. Like oils, greases have a range of consistencies, from ketchup-thin to cheddar cheese thick like.

- Liquid Lubricants

Liquid lubricants or oils are liquids made of long polymer chains, with additives for various extra properties. Common additives include antioxidants to keep the oil from oxidizing, corrosion inhibitors to prevent parts from corroding, and detergents to keep deposits from forming. These long chains are hard to squeeze out, making oils useful as a slippery barrier between them. There are three types of oils, mineral, synthetic and natural oil.
Mineral oil based lubricants are extracted from crude oil. These lubricants can be divided in additional two types. The first type is paraffinic oil. It has good resistance to oxidation and a good thermal stability. Also it is less volatile, and has a high flash point.
The second type is naphthenic oil. This type of lubricant is good for low-temperature applications, but it has a lower flash point than paraffinic oil. Nevertheless, when naphthenic oil is burnt, soft deposits are formed, which lower the abrasive wear.
Synthetic oil is another type of lubricant. These lubricants are artificially made. Synthetic lubricants can be manufactured using chemically modified petroleum components, but can

also be synthesised from other raw materials. Some commonly used synthetic oils are esters, poly-alpha-olefines (PAO), silicon oils, polyglycols, and perfluoropolyethers (PFPE).
Natural oil based lubricants are made from vegetable or animal fats. Oil refined from rape-seed or castor is used as raw material for vegetable oil lubricants. The sources of animal oils are fish and other animals. In both cases, the crude oil has to be refined before usage as lubricant. Due to their chemical structure, these oils contain more natural boundary lubricant than mineral oils. Especially the high polar ester group of the triglyceride is responsible for the good adsorption on metal surfaces. Besides this, the good biodegradability of natural oils is essential for several applications, like marine lubricants.
However, natural oils are less stable than mineral oils at high temperatures and they could be easily oxidized.

- Gas Lubricants

Gases like nitrogen and helium are used as lubricants in applications, where film thickness between the contacting surfaces is ultra-small. The advantages of using gases as lubricant are large temperature range, no sealing required for lubrication, very low friction due to low viscosity, no vaporization, no solidification, and no decomposition.
The drawback for gas lubricants are low load capacity and lower tolerance for any errors in load estimation.

II.2.2 The history of lubricants, a brief overview

The use of lubricating oils can be traced back to ancient Egypt. At that time, people have been aware that certain products between surfaces in relative motion could reduce friction.
On wall painting of Egyptian murals from 2000-1700 B.C.E., people are depicted standing in front of a wooden sledge and wetting the sand. Dry sand forms a heap in front of the sled hindering its movement and relatively high force was needed. Adding a lubricant, e.g. olive oil, made the sand more rigid, and the heaps decreased in size until no heap formed in front of the moving sled and therefore a lower applied force was needed to reach a steady state, see Figure II-14.

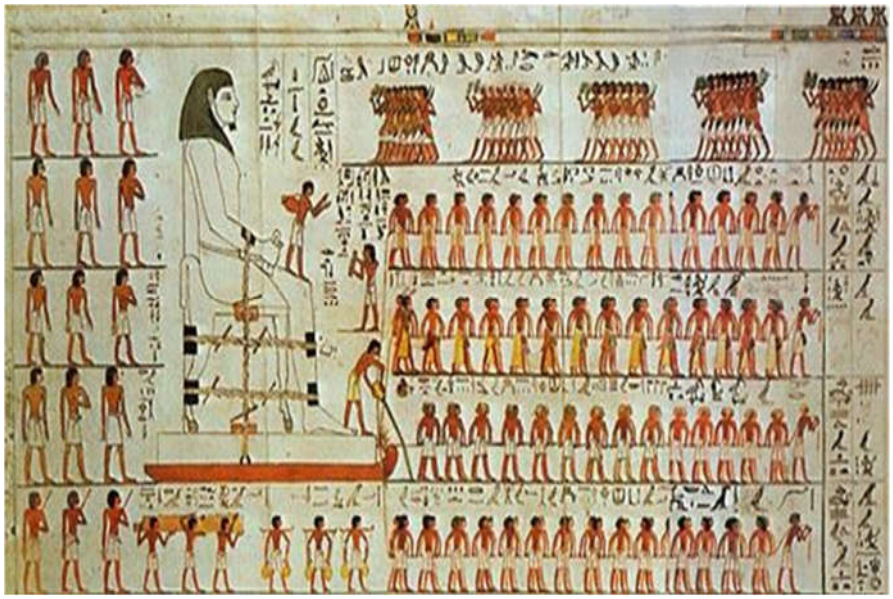

Figure II-14: Wall painting from the tomb of Djehutihotep. Large statue is being transported by sledge and a person on the front of the sledge wets the sand [36]

In the tombs of Yuaa and Thuiu in ancient Egypt, dated around 1400 B.C.E., examples of early chariots were discovered. They were believed to have used tallow along with lime powder and calcium soaps to lubricate chariot axles [36].

Until the industrial revolution in the 18th and 19th century, animal fats and vegetable oils are the mainly used lubricants worldwide. This has changed in the middle of the 19th century, with the discovery of petroleum and the petroleum-based lubricants. However, with the development of rocket motors and space vehicles, as well as the discovery of the gas turbine in World War II, people found that at condition of extreme temperature, mineral oil lubricants were not suitable for applications in the harsh condition. For example, mineral oil lubricants were easy to oxidize at temperatures above 100 °C and it would become very viscous or gelatinous at temperatures below -20 °C. Because of the disadvantages of mineral oil lubricants, synthetic lubricants and lubrication additives intended for extreme conditions, such as higher loads, extreme temperature and vacuum, became also available. The most common examples of synthetic lubricants are poly-alpha-olefines (PAO), silicon oils, polyglycols, and perfluoropolyethers (PFPE) [3].

II.3. Ionic Liquids

II.3.1 General Aspects

About 20 years ago, research on Ionic Liquids was a relatively unknown field of chemistry. In the years between 1986 and 1997 there were less than 25 papers on Ionic Liquids published each year. Since then, this field grows exponentially. There were more than 4000 papers on the topic published in 2009 and over 2000 in the first six months in 2010 [60].

Nowadays the generally accepted definition of an Ionic Liquid is a salt with a low melting point, normally below the boiling point of water, typically close to room temperature. For the classical salts, the melting points are much higher, e.g. for NaCl, which melts at 801 °C. So, the Ionic Liquids are "molten salts", but there are many other synonyms used for Ionic Liquids, such as liquid organic salts, ionic melts, ionic fluids, fused salts, liquid salts and ionic glasses. Usually, they exist as a large organic cation, shown in Figure II-15, paired with a smaller organic or inorganic anion, Figure II-16. It has been estimated that the number of cation-anion combinations could produce up to one trillion (10^{12}) different Ionic Liquids [60–62]. Research on the chemical and physical properties of these compounds has expanded greatly in the last few years [62,63]. The large number of combinations promotes the implementation of "design-specific" compounds.

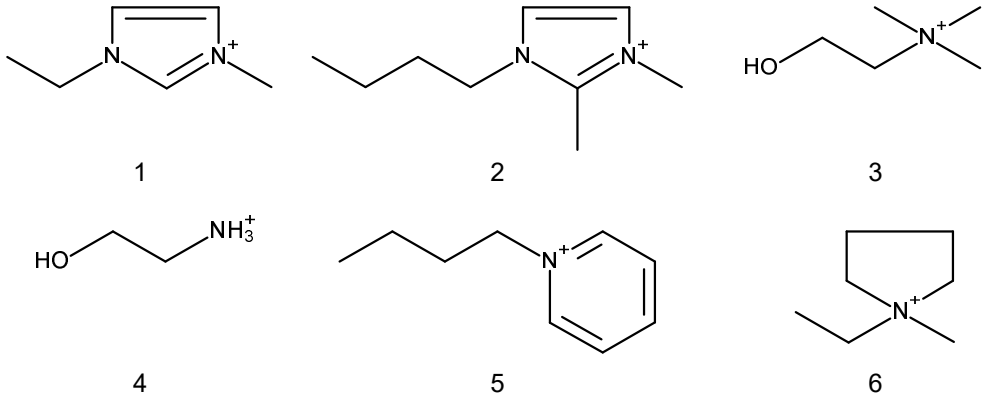

Figure II-15: Common cations of Ionic Liquids: (1) 1-ethyl-3-methyl imidazolium, (2) 1-butyl-3-methylimidazolium, (3) choline, (4) 2-hydroxyethylammonium, (5) 1-butylpyridinium, (6) 1-ethyl-1-methylpyrrolidinium [60]

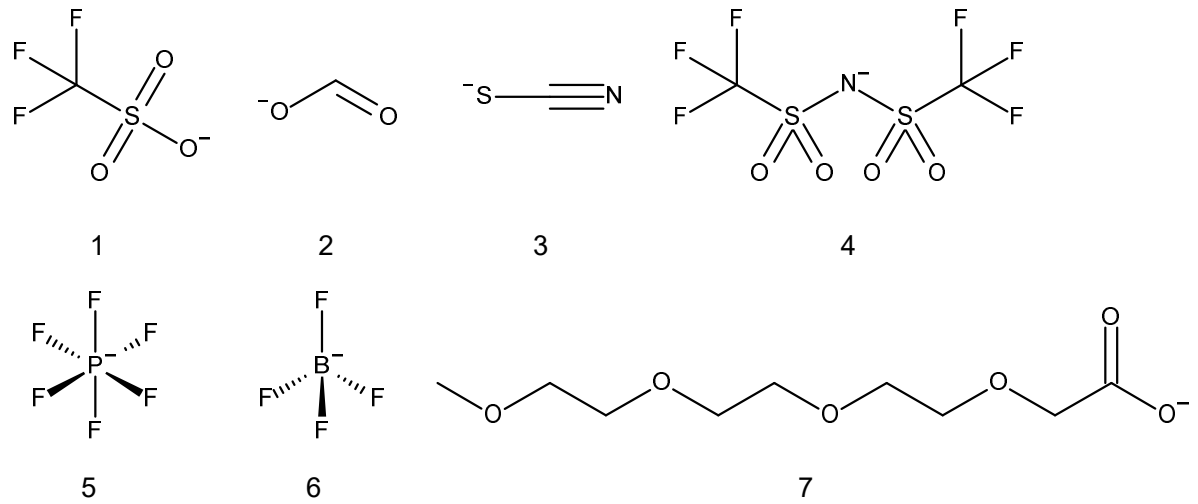

Figure II-16: Common anions of Ionic Liquids: (1) triflate, (2) formate, (3) thiocyanate, (4) bis(trifluoromethylsulfonyl)imide, (5) hexafluorophosphate, (6) tetrafluoroborate, (7) 2,5,8,11-tetraoxatridecan-13-oic acid (TOTO) [60]

Ionic Liquids made their first appearance in the scientific literature in 1914 by the report of Walden about the physical properties of ethyl ammonium nitrate $[EtNH_3][NO_3]$, which has a melting point of 12 °C [64–66]. Aluminium chloride based molten salts were used for high temperature electroplating during the 1940s. In 1951 Hurley et al. reported the synthesis of an Ionic Liquid by warming a mixture of 1-ethylpyridinium chloride with aluminium chloride for low temperature electroplating of aluminium [67,68]. In the 1970s and 1980s, a thorough investigation on organic chloride-aluminium chloride ambient temperature Ionic Liquids was carried out by Robinson et al. [69,70] and Hussey et al. [71–73] In the 1970s, Wilkes et al. developed electrolytes with lower melting temperature to tackle the temperature related problems associated with the molten salt electrolytes [74]. In 1983, Hussey wrote the first major review on room-temperature Ionic Liquids [75]. In the mid-1980s, low melting point Ionic Liquids were used as solvents for organic synthesis [76,77]. Following their work, Ionic Liquids became one of the most important classes of solvent systems. Initially, the applications of aluminium chloride based Ionic Liquids were limited, because of their highly hygroscopic nature. Moreover, they were not inert towards various organic compounds [78]. The first report on air and water stable Ionic Liquids based on the 1-ethyl-3-methylimidazolium cation and different anions such as tetrafluoroborate and hexafluorophosphate appeared in 1992 [79]. After this report, the number of air and water stable Ionic Liquids started to increase rapidly. In 1998, a new class of Ionic Liquids called "functionalised Ionic Liquids" were prepared by Davis and co-workers [60,80], based on cations derived from the antifungal drug miconazole, Figure II-17.

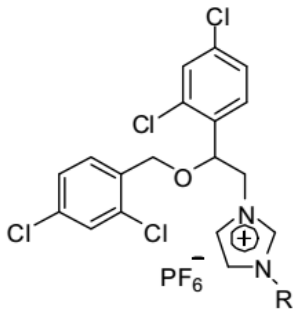

Figure II-17: First "task specific Ionic Liquid" based on the miconazole cation [60,80]

II.3.2 Physico-chemical properties of Ionic Liquids

Properties of Ionic Liquids are strongly affected by different factors, such as chemical structure, chemical composition of the ionic moieties, intermolecular and interionic interactions and the Ionic Liquids purity. As they are made up of at least two ions, which can be varied independently (the anion and cation), Ionic Liquids can be designed with a particular end use in mind, possessing a particular set of properties. Hence, the term "task-specific solvents" have come into common use [81]. Their properties can be adjusted to suit the requirements of a particular process. Properties such as melting point, viscosity, density, and hydrophobicity can be varied by simple changes to the structure of the ions. Therefore, designing an Ionic Liquid for a specific application requires a detailed understanding of the relationship between Ionic Liquid structure and its properties.

II.3.2.1 Melting point

The melting point is one of the key parameters for the applicability of a lubricant. It defines the low operation temperature level of the mechanical system. With lower temperature the viscosity of the lubricant increases, until first crystals occur. This crystallisation eventually forming a flow-preventing network, which leads to a fatal machine error, due to the missing lubrication. Therefore, the melting point should be the first parameter which has to be checked for a new lubricant or lubricant additive.

Ionic liquids are commonly defined as salts with a melting point below 100 °C. The structure of Ionic Liquids has an impact on their physical properties. Both cations and anions contribute to the melting point of Ionic Liquids. Large organic cations with less symmetry will lower the melting point, because they disturb the efficient packing of ions in the crystal lattice [82–84]. This can be observed in the melting point diagram of the Ionic Liquids based on 1,3-dialkylimidazolium cations with different alkyl chain lengths and hexafluorophosphate as the anion, shown in Figure II-18 [85,86]. The melting point decreases when the size and asymmetry of the cation increases up to a certain point. After that, an increase in the alkyl chain length increases the melting point.

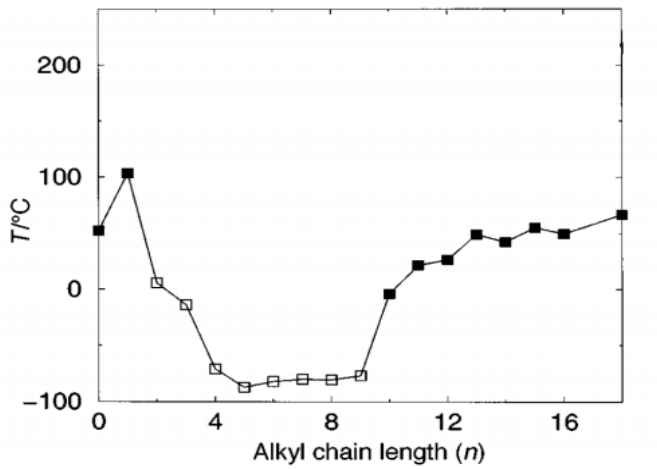

Figure II-18: Melting point diagram for 1,3-dialkylimidazolium and hexafluorophosphate [PF_6] Ionic Liquids as a function of alkyl chain length showing the melting transitions from crystalline (closed square) and glassy (open square) materials [85,86]

MacFarlane et al. showed the effect of symmetry on the melting points of Ionic Liquids derived from ammonium and pyrrolidinium cations, see Table II-2 [84]. If the substitution on the cation makes it more symmetric, the Ionic Liquids formed will tend to be solid at room temperature. If the substitution renders the cation asymmetric, the Ionic Liquids will be liquid at room temperature.

Structure	Melting Point [°C]
Tetramethylammonium bis(trifluoromethylsulfonyl)imide ($[N_{1111}][Tf_2N]$)	133
Dimethylethylbutylammonium bis(trifluoromethylsulfonyl)imide ($[N_{1124}][Tf_2N]$)	-8
N,N-dimethylpyrrolidinium bis(trifluoromethylsulfonyl)imide ($[C_1mpyr][Tf_2N]$)	132
N,N-butyl-methylpyrrolidinium bis(trifluoromethylsulfonyl)imide ($[C_4mpyr][Tf_2N]$)	-18

Table II-2: Melting points of selected ammonium and pyrrolidinium bis(triflimide) (NTf_2) Ionic Liquids [84]

Similar effects can also be observed in phosphonium Ionic Liquids, Figure II-19. In the series of $[P_{666n}][PF_6]$ Ionic Liquids, the highest melting point was observed for those with a highly symmetric cation tetrahexylphosphonium $(C_6H_{13})_4P^+$. The melting point decreased when any of the chains got longer or shorter [87].

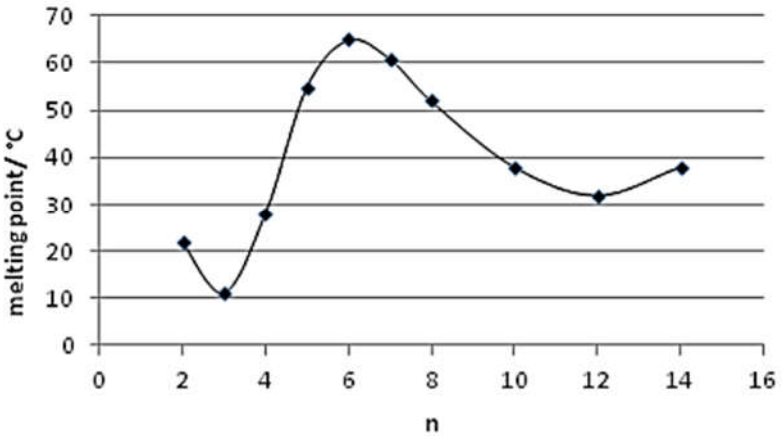

Figure II-19: Melting points of tetraalkylphosphonium $[P_{666n}]$ hexafluorophosphate $[PF_6]$ as a function of different C-chain length n [87]

The effect of anions on the melting point is more difficult to rationalize. Anions with large charge delocalization will reduce the Coulombic force of attraction between the ions and result in a lower melting point. The presence of hydrogen bonding in the lattice is a major factor in increasing the melting point. Ionic liquids with strongly coordinating anions such as halides have higher melting points than their tetrafluoroborate or hexafluorophosphate analogues, because of the formers' ability to form hydrogen bonding [85,88]. A special class of Ionic Liquids will be discussed in chapter II.4.2.3 Catanionics and Surface Active Ionic Liquids (SAILs).

II.3.2.2 Density

Density is one of the most often measured properties of Ionic Liquids. It is another key parameter for the application as lubricants. If lubricants are less dense than water, this let them float on the water surface. If there is a moisture problem in the lube system the water settles to the bottom of the sump. This can lead to a fatal machine error, if other additives are washed out or the lubricant loss lubrication efficiency due to the solubilised water.
In general, Ionic Liquids are denser than water. The molar mass of the anions has a significant effect on the density of the Ionic Liquids. For instance, the pyrrolidinium Ionic Liquids with bis(methanesulfonyl)amide anion have lower density than the bis(trifluoromethanesulfonyl)amide anion [71]. This is in agreement with the fact that the molecular volume of these anions is similar, but the mass of fluorine is higher. The densities of Ionic Liquids decrease with the increase in the length of the alkyl chains in the cations, Figure II-20 [89–91].

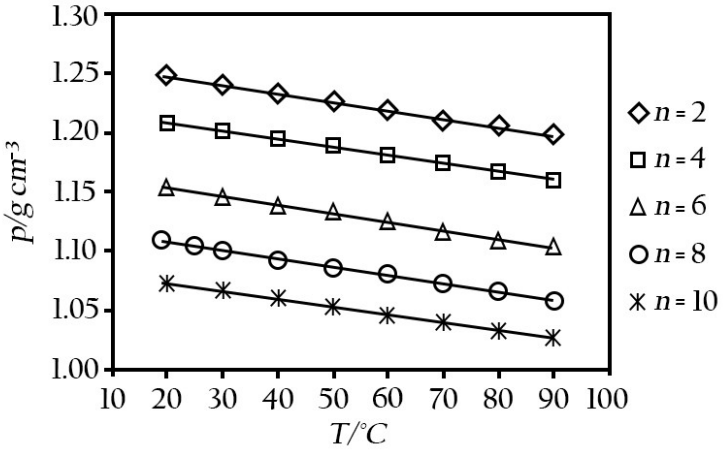

Figure II-20: Density of different 1-alkyl-3-methylimidazole tetrafluoroborate [$C_n$mim][BF_4] Ionic Liquids as a function of temperature [89–91]

The bulkiness of the longer alkyl chains prevents them from efficiently close packing, leading to a decrease in the density, whereas the shorter ones pack more effectively. Earlier, it has been reported that generally the density of Ionic Liquids is higher than that of water. However Wilkes et al. reported that the density of some of the phosphonium based Ionic Liquids with different anions is lower than that of water, Figure II-21 [92]. This also shows the effect of anions on the density of Ionic Liquids.

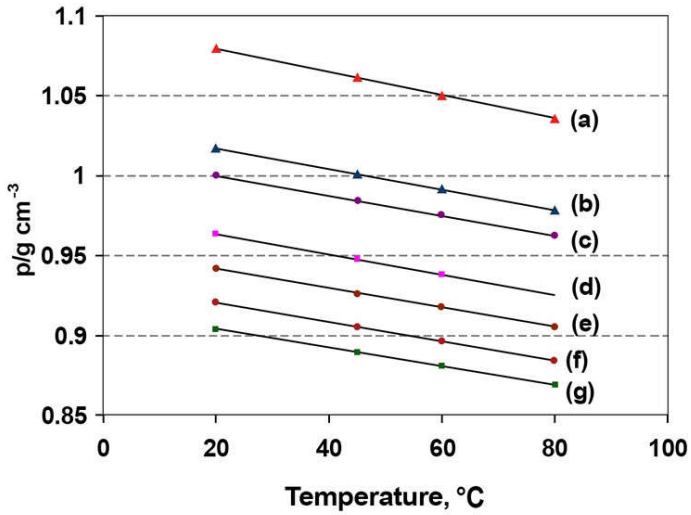

Figure II-21: Densities of [P_{66614}] Room Temperature Ionic Liquids with anions: (a) pyrrolidinium bis(triflimide) (NTf_2), (b) tetraselenocyanatocobaltate [$Co(NCSe)_4$], (c) bis-dicarbollylcobalt(III) , (d) tetrathiocyanatocobaltate [$Co(NCS)_4$], (e) dithiomaleonitrile, (f) methylxanthate, and (g) dicyanamide [$N(CN)_2$] [92]

Rogers and co-workers reported that for both hydrophobic and hydrophilic Ionic Liquids, an increase in the water content would decrease their density [93]. Seddon et al. reported that the halide impurities in the Ionic Liquids lead to a decrease of their density, as shown in Figure II-22 [94].

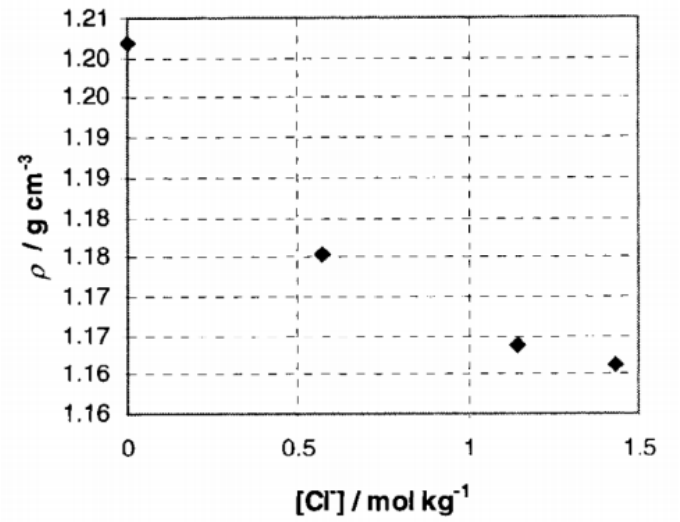

Figure II-22: Density of 1-n-butyl-3-methylimidazolium tetrafluoroborate at 30 °C vs. molar concentration of chloride [94]

II.3.2.3 Viscosity

The understanding of the viscosity of Ionic Liquids is of prime importance, because it plays a major role in stirring, mixing, pumping operations. Furthermore, viscosity is the most important parameter in the context of lubrication. The viscosity will determine how easily the oil is pumped to the working components, how easily it passes through the filters and how quickly it drains back. But more important is that the viscosity is directly related to the load-carrying capabilities. The greater a fluid´s viscosity, the greater the load it can withstand. In general, viscosities of Ionic Liquids are higher than water and common organic solvents, ranging from 20 to 30000 cP [62,95]. The choice of cations and anions has a strong influence on the viscosity of Ionic Liquids. Toduka et al. studied the effect of alkyl chain length and the nature of the anion on the viscosity of imidazolium-based Ionic Liquids [96,97]. The symmetry of the anion and its ability to form hydrogen bonds will influence the viscosity of Ionic Liquids. The fluorinated anions such as [BF_4] and [PF_6] form viscous Ionic Liquids, because of the formation of complexes with hydrogen bonding donors [98]. The viscosity of Ionic Liquids also depends on the alkyl chain length of the cations. The viscosity of the [$C_n$mim] [BF_4] series with increasing temperature is shown in Figure II-23. Alkyl groups with modest chain lengths will lower the viscosity. Longer alkyl chains will increase the viscosity, because of the increase in the van der Waals forces between the cations, which in turn increase the energy needed for the molecular motions.

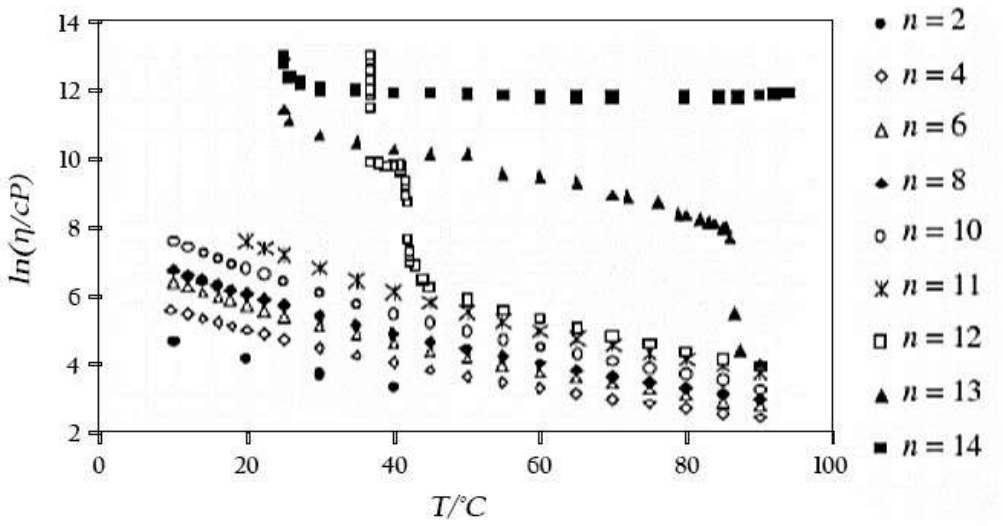

Figure II-23: Viscosities of different [$C_n$mim][BF_4] Ionic Liquids as a function of the temperature [96,97]

As for density, the impurities also play a key role in the determination of the viscosity of Ionic Liquids. Marsh et al. studied the effect of impurities on the measured physicochemical properties of Ionic Liquids. Seddon and co-workers performed a detailed investigation about the influence of halides and water on the physicochemical properties of Ionic Liquids [94]. As can be seen in the Table II-3 and Figure II-24, a low concentration of halide (chloride) can raise the viscosity.

Ionic Liquid	[Cl]/mol kg^{-1}	η/mPa s
1-ethyl-3-methylimidazolium tetrafluoroborate ($[C_2mim][BF_4]$)	0.01 1.8	66.5 92.4
1-butyl-3-methylimidazolium tetrafluoroborate ($[C_4mim][BF_4]$)	0.01 0.5	154 201
1-butyl-3-methylimidazolium nitrate ($[C_4mim][NO_3]$)	0.02 1.7	67 222.7
1-octyl-3-methylimidazolium nitrate ($[C_8mim][NO_3]$)	0.01 2.2	1238 8465

Table II-3: Comparison of viscosities of chloride contaminated Ionic Liquids and low chloride content batches of Ionic Liquids at 20 °C [94]

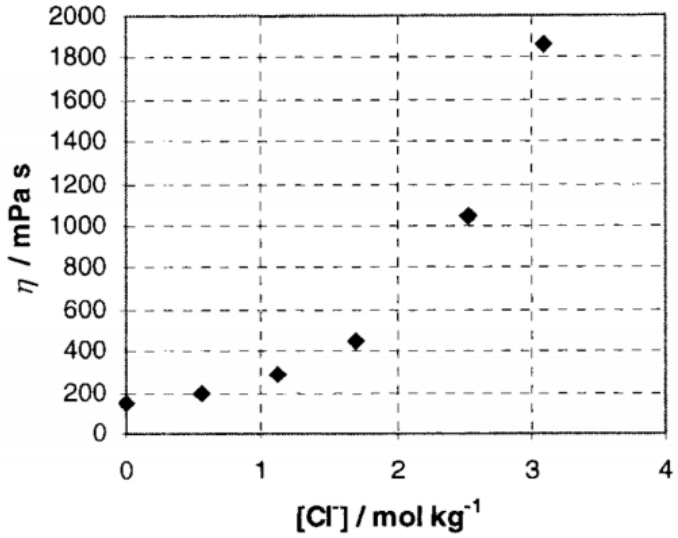

Figure II-24: Viscosity at 20 °C of 1-n-butyl-3-methylimidazolium tetrafluoroborate as a function of the molar concentration of chloride [94]

The viscosity of Ionic Liquids is found to be very high, which will affect its applications. This drawback can be overcome by adding some organic solvents, which reduces their viscosity dramatically, Figure II-25 [94].

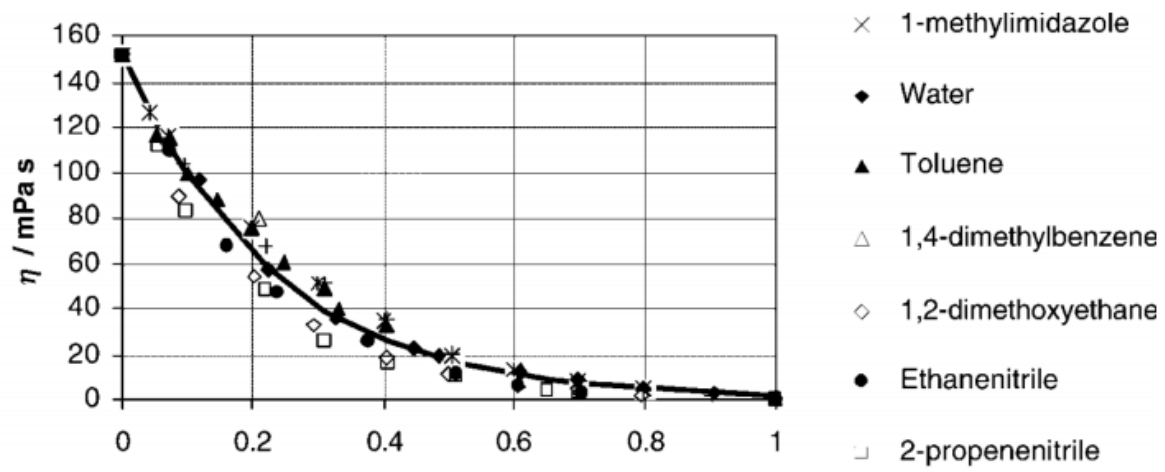

Figure II-25: Viscosity at 20 °C of co-solvents and 1-n-butyl-3-methylimidazolium tetrafluoroborate mixtures as function of the mole fraction of co-solvent [94]

The temperature dependence of the viscosity can often be expressed by the empiric Vogel-Fulcher-Tammann Equation, Equation II-22, which describes the viscosity decrease of a liquid, fundamentally, of a glass forming liquid, with increasing temperature [99].

$$\eta = \eta_0 \cdot e^{\left(\frac{B}{T-T_0}\right)} \qquad \textbf{Equation II-22}$$

In this equation, η is the viscosity at a given temperature T, η_0, B and T_0 are fitting parameters, depending on the investigated system.
Only a few Ionic Liquids reach viscosities as low as that of water or the most common organic solvents. Usually, their values can be compared with those of paraffin oils [100].
It should be noted that present impurities remaining from the synthesis influence viscosity drastically. A viscosity reduction in the case of remaining solvents is observed, whereas a viscosity increase in the case of halide impurities by 30 to 600 %, depending on the concentration, is found [94,101].

II.3.2.4 Conductivity

The conductivity of Ionic Liquids is of vital importance for their applications in electro-chemistry. A large conductivity was expected for Ionic Liquids, because they consist entirely of charge carrier ions. However, the conductivity of Ionic Liquids was found to be relatively low at room temperature [73]. The conductivity of any solution depends on the number of charge carriers and their mobility. The large constituent ions of the Ionic Liquids reduce the ion mobility, which in turn reduces the conductivity [102]. The conductivity of Ionic Liquids is comparable to those of organic solvents with added inorganic salt (Table II-4) [103].

Solvent	Viscosity [mPa s]	Conductivity [mS cm^{-1}]
N,N-Dimethylformamide	0.794	4.0[a]
Acetonitrile	0.345	7.6[a]
Ethanol	1.074	0.6[a]
Dimethylsulfoxide	1.987	2.7[a]
1-ethyl-3-methylimidazolium bis(trifluoromethylsulfonyl)imide ($[C_2mim][Tf_2N]$)	28	8.4
1-butyl-3-methylimidazolium bis(trifluoromethylsulfonyl)imide ($[C_4mim][Tf_2N]$)	44	3.9
1-ethyl-3-methylimidazolium tetrafluoroborate ($[C_2mim][BF_4]$)	43	13
1-butyl-3-methylimidazolium hexafluorophosphate ($[C_4mim][PF_6]$)	275	1.5
Triethylhexylammonium bis(trifluoromethylsulfonyl)imide ($[N_{6222}][Tf_2N]$)	167	0.67
Tributylhexylammonium bis(trifluoromethylsulfonyl)imide ($[N_{6444}][Tf_2N]$)	595	0.16

Table II-4: Comparison of viscosity and conductivity for a representative selection of molecular solvents and non-haloaluminate Room Temperature Ionic Liquids.
a) Conductivity for organic solvent containing 0.1M tetrabutylammonium perchlorate at 22 °C [103]

Although the conductivity of Ionic Liquids is not much higher than that of conventional non-aqueous solvents, Ionic Liquids do offer the advantage that this property is intrinsic to the pure Ionic Liquids and thus the addition of any separate salt is avoided. The conductivity of Ionic Liquids having the same anions with different cations is found to decrease in the order 1-alkyl-3-methylimidazolium > N,N-dialkylpyrrolidinium > tetraalkylammonium. This can be explained by the decrease in the planarity of the cation. The flat imidazolium cation has a higher conductivity than the tetrahedral tetraalkylammonium cation. The pyrrolidinium-based Ionic Liquids, adopting an intermediate geometry, have an intermediate conductivity. An increase in temperature will lead to an increase in the conductivity of Ionic Liquids [104,105].

It is clear that the molar conductivity is related to the viscosity of an electrolyte. This is reflected by an empirical relation, proposed by Walden in his paper published in 1906 [106]. According to the classical Walden's rule, the molar conductivity (Λ) of many small molecule electrolytes is inversely proportional to its fluidity = $1/\eta$. The Walden rule is typically obeyed,

when solutions consist large and only weakly coordinating ions in solvents with almost no ion solvent interaction. Therefore, the Walden rule can be used as quantitative approach to the ionicity of an Ionic Liquid [107–109].

The ideal line in the Walden plot is set by using data for a dilute aqueous solution of KCl (0.01M KCl aq. solution), where ions are fully dissociated showing equal mobilities. The Walden rule has been used in our laboratory to classify Ionic Liquids into ”non”, “poor”, and “good” Ionic Liquids, see Figure II-26.

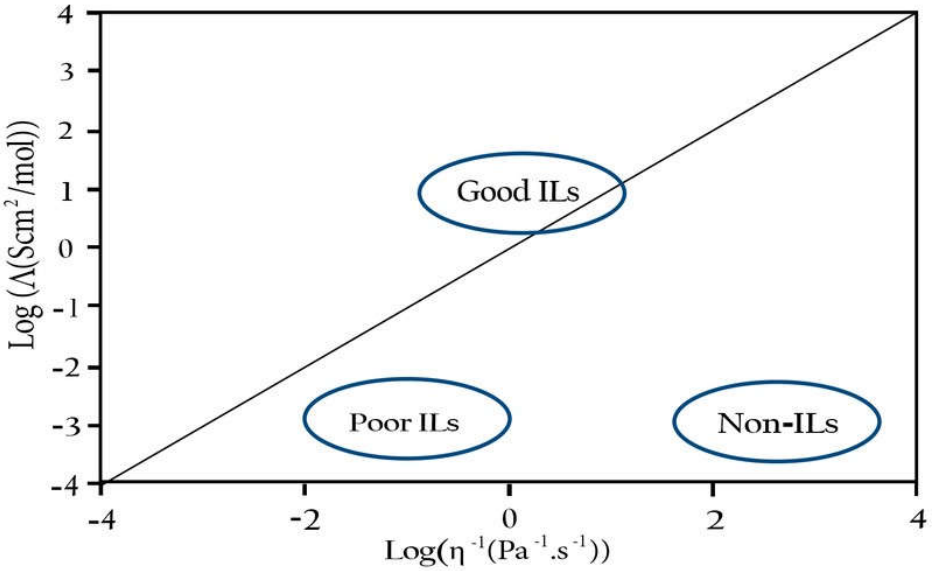

Figure II-26: Application of the Walden plot to classify Ionic Liquids by relating their equivalent conductivity to their fluidity [109]

The charge distribution in “poor” Ionic Liquids is not spherically symmetric around each ion throughout the liquid; therefore, they appear below the ideal line in the Walden plot. “Good” Ionic Liquids have exceptionally low vapour pressure due to the dipole-dipole interactions among ions.

II.3.2.5 Thermal Stability & Flammability

Like the melting point determine the low operation temperature level of the mechanical system, the thermal stability limits the upper range. High-temperature conditions can disrupt the stability of the used lubricant, due to oxidation reactions or thermal decompositions. Therefore, it is essential to check the thermal stability of a new lubricant or additive to prevent this kind of effects. Many Ionic Liquids are reported to be resistant to thermal decomposition and thus suitable for high temperature applications [110,111]. The thermal stability of Ionic Liquids is directly linked to the nature of the anions. Ionic liquids containing more nucleophilic and coordinating anions such as halides decompose at lower temperature. Ionic liquids with poor proton abstracting anions such as bis(trifluoromethylsulfonyl)amide are more stable against high-temperature decomposition [112–115]. The decomposition temperature of Ionic Liquids also depends on the type of cations. Most studies have been performed on imidazolium-based Ionic Liquids [116]. They are thermally more stable than pyridinium [101,117] and tetraalkylammonium-based Ionic Liquids [116,118]. The methyl substitution on the C-2 position of the imidazolium cation increases the thermal stability due to the replacement of the acidic hydrogen [97,114,119,120]. It was also reported that the chain length of the alkyl group on the cation has not much influence on the thermal stability of the Ionic Liquids [101]. Ammonium-based Ionic Liquids have lower stability compared to imidazolium-based Ionic Liquids, whereas the thermal stability of phosphonium based Ionic Liquids is better than that of the ammonium-based Ionic Liquids [97,118]. Two important thermal decomposition mechanisms of Ionic Liquids are Hofmann elimination and reverse Menschutkin reaction. A schematic representation of Hofmann elimination is given in the Figure II-27.

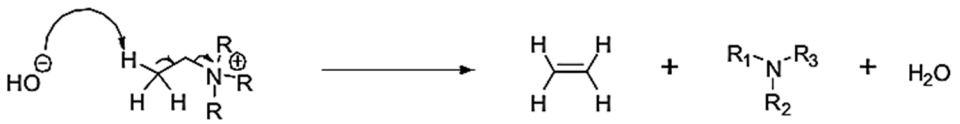

Figure II-27: Schematic representation of Hofmann elimination [115]

A quaternary ammonium salt with a β-hydrogen atom will undergo Hofmann elimination in the presence of a base, at elevated temperature. It has been reported that the imidazolium cations with strongly nucleophilic anions, such as halides, decompose by dealkylation of the cation via an SN_2 reaction of the most easily accessible alkyl group [115,116,121–124], see Figure II-28.

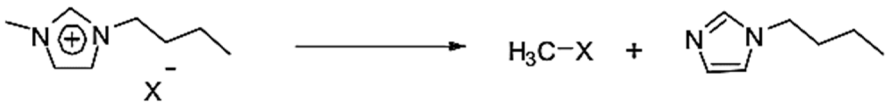

Figure II-28: Thermal decomposition of [C_4mim][X] [116]

Wilkes et al. reported that imidazolium-based Ionic Liquids are stable up to 450 °C [125]. However, most of the Ionic Liquids can tolerate such a high temperature only for a short time. Most of the investigations overestimate the thermal stability of Ionic Liquids, because the values are obtained by thermogravimetric analysis. Since the heat transfer in Ionic Liquids is slow, the sample temperature lags behind the measured temperature by between 75 and 150 °C, at the high heating rates (between 10 and 20 °C/min) that are used. Under these

conditions, the decomposition reaction does not reach equilibrium before the end of the experiment. More accurate data require isothermal conditions.

Ionic liquids are considered as green solvents, because of their non-flammability. This is considered as a safety advantage over volatile organic compounds (VOCs). However, Smiglak et al. questioned the non-flammability of Ionic Liquids [126]. They reported that a large number of Ionic Liquids are combustible due to their positive heats of formation. They tested the flammability of twenty Ionic Liquids based on protonated imidazolium nitrates and picrates, protonated C-nitro-substituted imidazolium nitrates and picrates, 1-butyl-3-methylimidazolium azolates, 2-hydroxyethylhydrazinium nitrate and commercially available trihexyltetradecylphosphonium chloride ([P_{66614}][Cl]). The combustibility was determined by heating 40 mg of each sample by a small flame torch no longer than 5-7 seconds in a small aluminum pan. All of the tested Ionic Liquids ignite under these conditions. The rate of combustion depends on the nitrogen and oxygen content. While some of the Ionic Liquids burned for a short period of time and went out, others, after first ignition, burned quickly to complete or nearly complete combustion. The most rapid combustion was recorded for the [C_4mim][4,5-di-NO_2-imidazolate]. In the literature, there are many publications, which describe the design of Ionic Liquids as energetic materials [126–130]. Those Ionic Liquids were prepared by the incorporation of energetic functionalities such as NO_2, CN, N_3 etc.

II.3.2.6 Hydrophobicity

A remarkable example for the modulation of Ionic Liquids is represented by the commonly used dialkyl-substituted imidazolium salts, in which the nature of both the anion and the cation determines the degree of hydrophilicity-hydrophobicity [108].
Anions such as halides, nitrate, methyl sulfonate or formate facilitate water miscibility, whereas anions such as hexafluorophosphate and bis(trifluoromethylsulfonyl)imide prevent mixing with water. The cation contributes to the solubility: the elongation of the cation alkyl chain reduces water solubility, whereas the introduction of specific functional groups (hydroxyl, ethers, and amines) increases solubility. In addition, the central cation group also influences water solubility: pyridinium and pyrrolidinium cations disfavour water absorption, if compared to imidazolium salts [109].
However, independently of their miscibility with water, all Ionic Liquids are hygroscopic to a certain extent and can adsorb significant amounts of water from the atmosphere.
The water content of a substance is a limiting factor for many applications. Several fields of use, like electrochemistry or lubricants, are completely inaccessible, if the water content is too high or the water uptake cannot be controlled without complex methods. In addition, it is well-known that water is almost inevitable in Ionic Liquids. Even those Ionic Liquids classified as hydrophobic ones can be saturated with about 1.4 wt% of water, which is a significant molar amount. For more hydrophilic Ionic Liquids, water uptake from air is even more pronounced. This means that all commercial products contain a certain amount of water, which depends on the production conditions and the logistics, since the Ionic Liquids can reasonably be expected to come into contact with traces of water. Depending on the application, this water content can cause enormous problems. The presence of water generally has significant influence on the physicochemical properties of Ionic Liquids. It has been demonstrated that a simple 0.1 molar fraction of water content (which means about 1 wt% of water in the sample) decreases viscosity by about 20 % and it increases the electrical conductivity by about 30 % [131].

Especially in the field of lubrication, the water content plays a major role. If an additive contains a lot of water or attracts water from the atmosphere, the lubricant mixture could be disturbed or the lubricating properties are not available anymore.
As mentioned above, the content of water within an Ionic Liquid is of main interest, from the practical point of few. Ionic Liquids can generally be divided into two groups, according to their solubility in water. Hydrophobicity can often be modified by a suitable choice of anion, e.g. 1-butyl-3-methylimidazolium tetrafluoroborate [C_4mim][BF_4] is completely miscible with water while the corresponding hexafluorophosphate [PF_6] salt is not, which make them each suitable for different applications. Fluorinated anions such as bis(trifluormethylsulfonyl)imide [TFSI] usually form hydrophobic Ionic Liquids. For example, the water immiscible (hydrophobic) Ionic Liquids such as 1-butyl-3-methylimidazolium hexafluorophosphate [C_4mim][PF_6] and 1-decyl-3-methylimidazolium bis(trifluoromethanesulfonyl)imide [C_{10}mim][TFSI] were used in glassy carbon electrodes as films and on carbon ceramics, because of their hydrophobicity [132,133].
Matsumoto et al. reported a new family of hydrophobic Ionic Liquids, by combining large 1,3-dialkylimidazolium and small quaternary ammonium cations with the perfluoroalkyltrifluoroborates, [$RfBF_3$], Rf = CF_3, C_2F_5, n-C_3F_7, n-C_4F_9, where they described the anion as weakly coordinating and more resistant to hydrolysis than their [BF_4] analogues, due to their hydrophobicity [134].
A new asymmetric fluorinated anion has also been introduced by Liu et al., the (fluorosulfonyl) (pentafluoroethanesulfonyl)imide [FPFSI] that resulted in hydrophobic Room Temperature Ionic Liquids, when combined with quaternary ammonium, imidazolium, pyrrolidinium and pyridinium cations [135].
The other type of Ionic Liquid is water-miscible (hydrophilic) Ionic Liquid such as [C_4mim][BF_4], which can also form electrochemically active films on glassy carbon that can be used in aqueous media [136].
Papaiconomou et al. reported that the pyridinium-based Ionic Liquids show lower miscibility in water than their imidazolium analogues and as the alkyl chain length on the anion increases, hydrophobicity of the Ionic Liquid increases [137].
Asymmetric phosphonium Ionic Liquids, which are highly fluorinated, have been reported to be suitable for developing new super-hydrophobic coatings [138].
Interestingly, some Ionic Liquids showed switchable hydrophilicity. Jessop et al. reported that N,N,N`-tributylpentanamidine had reversible miscibility with water, Figure II-29, in air this Ionic Liquid had low solubility in water, but was completely miscible with water under a CO_2 atmosphere (1 bar) [139].

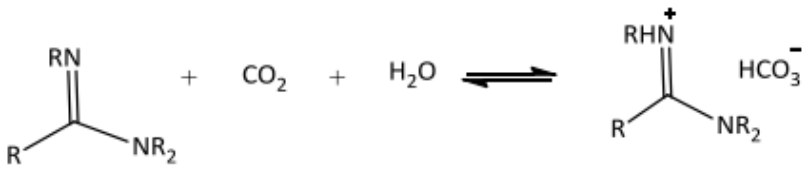

Figure II-29: Protonation of an amidine by carbonic acid [139]

The authors utilised these solvents for the extraction of organic materials, such as soya bean oil, without the need for distilling the solvent from the product. In the presence of both water and carbon dioxide, the amidine is protonated by carbonic acid, forming water soluble bicarbonate salt, see Figure II-30.

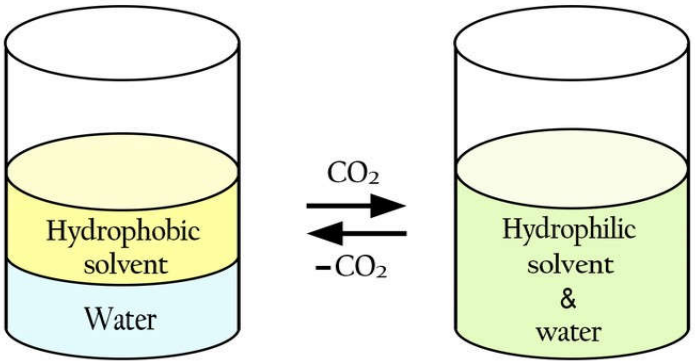

Figure II-30: The phase behaviour of a mixture of water and a switchable hydrophilicity solvent (SHS) [139]

High purity hydrophobic Room Temperature Ionic Liquids composed of N-methyl-N-alkylpyrrolidinium cations and perfluoroalkylsulfonylimide anions were synthesised by Giovanni et al., suitable for electrochemical applications such as high-voltage super capacitors and lithium batteries [140], photochemistry, catalysis [141], and electrosynthesis.

II.3.3 Ionic Liquids in Tribology

In the last decade, Ionic Liquids have been considered as promising candidates for tribological applications, since the first proposal in 2001 by Liu et al. [142–145]. Their remarkable properties suitable for lubrication include negligible vapour pressure, non-flammability, high thermal-oxidative stability and reasonable viscosity-temperature behaviour. The reason why these properties are so important for lubrication is that at the surfaces' contact points the temperature will increase, due to friction, therefore the thermo-oxidative stability of the lubricant is essential to minimize its degradation during sliding. For the same reason and also for storage purposes, the non-volatility and non-flammability are very important properties, when choosing a lubricant oil. The viscosity behaviour of the Ionic Liquid is also an important property, since it determines the load-carrying capacity of the fluid and the film formation at the sliding surfaces. In addition, the polar structure of Ionic Liquids will contribute to the formation of an adsorbed layer at the sliding surfaces, which can potentially reduce friction and wear [146]. Designing a lubricant oil with suitable physical and chemical properties and appropriate tribological behaviour is a complicated task, hence Ionic Liquids are highly promising candidates.

Generally, Ionic Liquids can be used as net lubricants or additives for common lubricant oils. This last possibility has been largely explored in the last few years, since the presence of Ionic Liquids as additives can enhance the anti-wear behaviour of the lubricant oil by preventing some tribochemical reactions at the surface like corrosion and oxidation [147,148]. Among the possible cationic moieties, imidazoliums are by far the most studied structures, followed by ammoniums, aromatic amines and phosphoniums. The works of Liu and co-workers showed the excellent tribological performance of several imidazolium-based Ionic Liquids [149] and their anti-wear/anticorrosion properties, when used as additives for poly (ethylene glycol) and poly urea grease [150–152].

Due to the large number of possible ionic structures suitable for lubrication, structure-property relations need to be established in order to obtain insights about lubricant performance. In the first paper to investigate Ionic Liquids as lubricants, Ye et al. proposed that they could be used as a universal lubricant for various systems [142]. Since this report, research has focused on more specific systems, for example, the steel-on-steel system has had the majority of the interest [152–163]. The more challenging systems in terms of efficient lubrication, including steel/aluminium and titanium/steel, have also received attention [148,164–178].

Early publications concerning lubricant testing of Ionic Liquids evaluated the performance of imidazolium cations with hexafluorophosphate (PF_6) and tetrafluoroborate anions (BF_4). They were readily available, and the chemistry of the imidazolium cation was well known, such that the effect of increasing the alkyl chain length or addition of functional groups would be relatively easy to investigate [142,148,158,159,173]. Generally, friction and wear volume decreases with an increase of the chain length of the alkyl group in the cation, as a consequence of the increased viscosity [179], see Figure II-31.

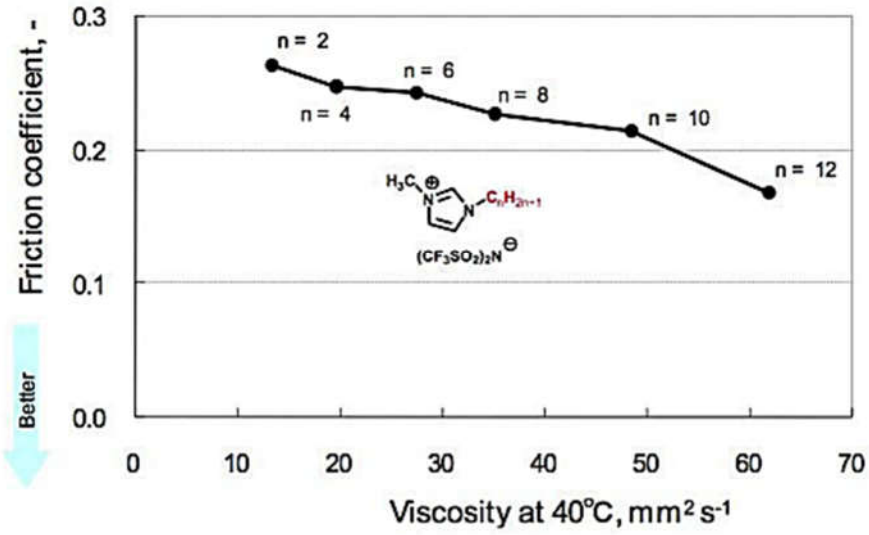

Figure II-31: Effect of alkyl chain length n in the imidazolium cation on the friction coefficient [179]

The anions can have an equally important influence in the tribological performance of the Ionic Liquids. Anions can change the viscosity of the Ionic Liquid and affect the formation of a boundary film, either by physisorption or chemical reaction. For example, it was observed that PF_6 and BF_4 anions formed protective tribofilms, when present in an Ionic Liquid. But it is known that BF_4 and PF_6 can corrode steel under humid condition due to the formation of the species HF, by hydrolysis. So, subsequent work began to investigate other fluorine containing anions, such as triflate (CF_3SO_3), bis (trifluoromethylsulfonyl)imide (NTf_2) and perfluoroalkylphosphate (FAP) [142,154,160,180]. The Ionic Liquid containing the anion bis (trifluoromethylsulfonyl)imide (NTf_2) presents better anti-wear properties than BF_4 or PF_6. The reason for this is a tribochemical reaction which takes place between NTf_2 and steel with the formation of a surface protective film composed of organic fluoride, inorganic fluoride and FeS, that helps to prevent friction and wear [160]. Other non-fluorinated anions that include known useful elements, such as phosphorus (e.g., dibutylphosphate, DBP) and boron (e.g., bis (oxalato) borate, BOB) have also been studied. In the wear environment, all of these anions were assumed to undergo favourable reactions to result in protective tribofilms [154,163,165–167]. In fact, compounds that are formed by chemical reaction between the anion and the material's contact points, where temperatures are high, are of crucial importance in preventing seizure in freshly generated metal surfaces. This is probably one of the basic reasons why Ionic Liquids have superior tribological performance than conventional lubricant oils. As mentioned above, the imidazolium cation was initially investigated, and the alkyl chain length has been varied to investigate its effect on friction and wear [148,158,159,163]. Imidazolium has also been functionalised to incorporate groups that may more readily adsorb onto a surface, such as phosphonyls and esters [149,161]. As the cation chemistry available has expanded, so too has the type of cations being investigated in Ionic Liquids lubricants. In subsequent work, Ionic Liquids with an ammonium cation were investigated as an alternative to imidazoliums [142,148,154], followed by the quaternary phosphonium cation [188; 191; 205; 206]. Interestingly, the pyrrolidinium family of cations has only received a little attention thus far, even though they have shown some promising wear performance results [154,167].

When comparing the results between different research groups in the existing literature, it can be difficult to determine, which Ionic Liquids perform best, due to the different tests used, and due to the differences in how wear is actually presented and lack of a common reference point [154]. The diversity of test conditions for three of the major Ionic Liquid lubricant research facilities testing steel on aluminium can be seen in Table II-5.

Facility	State Key Laboratory, Lanzhou, China	Polytechnic University of Cartagena, Spain	Oak Ridge National Laboratory, USA
Wear Test Type	Optimol SRV Pin-on-flat Reciprocating	Microtest Pin-on-disk Rotating	Phoenix Ltd. Pin-on-disk Reciprocating & rotating
Ball Diameter	10 mm	0.8 mm	9.525 mm
Ball Type	ASTM 52100	ASTM 52100	ASTM 52100
Load	50 - 300 N	2.45 - 4.45 N	38.3 - 100 N
Velocity	1 mm strike, 25 Hz, 0.1 m/s	0.06 - 0.20 m/s	0.02 - 1.0 m/s
Distance	180 m	850 - 2500 m	400 - 500 m
Aluminium alloy	2024	2011	6061, 1100, 319
Lubricant amount	2 drops	2 ml	5 drops
Standard	Phosphazene (X1-P)	Mineral oil Propylene glycol dioleate	Mineral oil 15W40 engine oil

Table II-5: Wear test conditions at various test facilities [180]

Whilst this variation in test methods and lack of a universal standard makes it difficult to identify specific Ionic Liquids with optimal wear performance, it is possible to identify trends in structure that lead to improved behaviour [180].

In order for traditional lubricant systems to be replaced by other more efficient and/or more environmentally friendly alternatives, the cost of the new lubricants is a significant consideration. Currently, Ionic Liquids are expensive in comparison to mineral base oils and synthetic base oils, such as poly alpha olefins, and they are not yet made in large volumes. Therefore, their use as neat lubricants may be limited to critical applications, such as low-pressure environments or micro-electro mechanical machines. On the other hand, there is much more scope for their use as a lubricant additive, in which a small amount of Ionic Liquid in a base oil could make a large difference to the friction and wear. As mentioned in the introduction, there is always a need to improve existing additives in order to further improve the friction coefficient and wear rates for common combinations, such as steel/steel. Of even greater interest is the development of new technology that will facilitate new applications for systems difficult to lubricate, such as aluminium/steel. There is also a drive for additives that are low in or free from sulphated ash, phosphorus and sulphur (SAPS). Given the breadth of chemistries available for Ionic Liquids, these offer significant possibilities. Ionic liquids have been added to a number of base oils, such as hydrocarbons, polyethylene glycol (PEG), poly alpha olefins (PAO) propylene glycol dioleate (PGDO) and glycerol [148,152,172,174,181–189]. The amount of Ionic Liquid added to base oils has varied from 0.3 wt% to 10 wt%, with the

proportion depending on the solubility and the amount required to give the best performance. It has been found that Ionic Liquids usually have low solubility in non-polar base oils, such as mineral oils and PAO, and this has been attributed to the Ionic Liquids polar nature [186]. Some researchers have improved the solubility by using more polar base oils, such as PEG and PGDO [152,174], while others have tested the Ionic Liquid / base oil as an emulsion [148,174,184]. Mistry et al. used a succinimide dispersant and sulphonate detergent to increase the solubility of an imidazolium Ionic Liquid in a naphthenic base oil, but otherwise little work has been done on improving the solubility of Ionic Liquids in base oils [185]. As an additive, the Ionic Liquids that performed well in neat form did not always perform well, when blended into a base oil. In fact, Jiminez et al. tested a series of imidazolium Ionic Liquids and found two ones that caused tribo-corrosion in the neat state, resulting in high wear and friction, and led to the lowest wear as an additive in mineral oil [148,174]. They found that the short alkyl chain Ionic Liquids that caused tribo-corrosion in the neat state had better miscibility in the mineral oil than the longer alkyl chain Ionic Liquids. It was suggested that this low miscibility may prevent the formation of a lubricating adsorbed layer. Recently, two phosphonium Ionic Liquids, trihexyl (tetradecyl) phosphonium bis (2-ethylhexyl) phosphate and trihexyl (tetradecyl) phosphonium bis (2,4,4-trimethylpentyl) phosphinate, were found to be fully miscible in a mineral oil and PAO. The solubility was attributed to the long alkyl chains on both the anions and cations. Both of the Ionic Liquid additives resulted in reduced friction and wear for a simulated engine wear test, as compared to traditional additives [186,187].

II.4. Surfactants

II.4.1 General Aspects

The word surfactant is an abbreviation of SURFace ACTive AgeNT. Surfactants possess both a hydrophilic and a hydrophobic part; therefore they are called amphiphilic molecules. The term amphiphilic is composed of the two Greek words, *ἀμφί*, amphi, "both sides" and *φῐλῐ́ᾱ*, philia, "love".

The hydrophobic part, commonly referred to as the tail group, is generally a linear or branched hydrocarbon group. The tail group region is generally oil soluble and its presence in bulk water is not energetically favoured, as it tends to disrupt the water molecule network.

The hydrophilic part, or head group, consists of a polar group. Different degrees of hydration can be observed depending on the nature of the head group, but this part of the surfactant is generally water soluble. However, some degree of solubility in oil could be observed, particularly for non-ionic surfactants. The size of the head group can vary from a few atoms to very complex structures and its nature extensively influences the surfactant's behaviour. The schematic structure of a surfactant is shown in Figure II-32, with Sodium Dodecylsulfate as example.

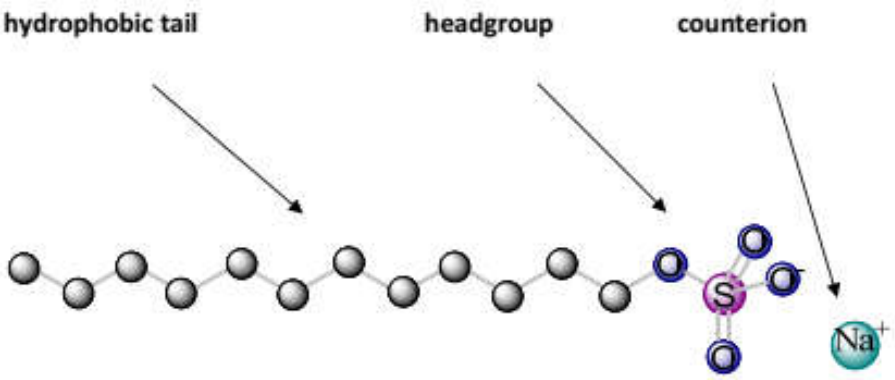

Figure II-32: Schematic structure of an ionic surfactant [190]

II.4.2 Classification of Surfactants

In fact, surfactants are generally classified depending on the nature of the head group, i.e. presence or absence of charges. There are three main surfactant categories: they are schematically shown in Figure II-33 and briefly presented here. Each class can be further divided in sub-categories.

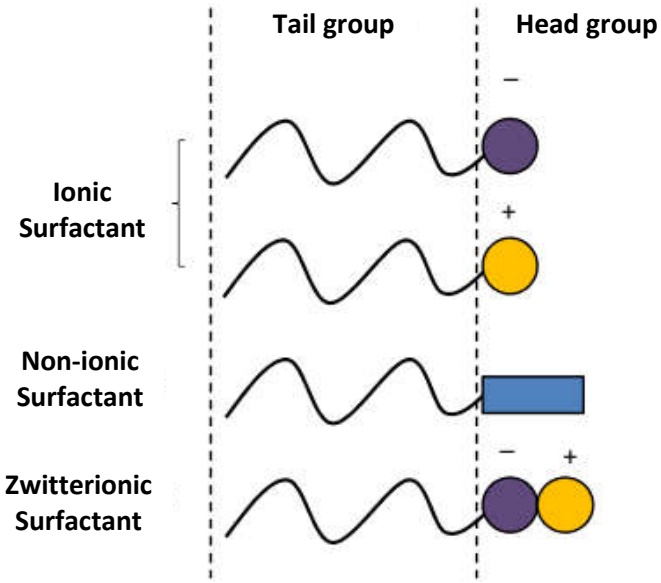

Figure II-33: General representation of the three surfactant categories: ionic, non-ionic and zwitterionic [190]

II.4.2.1 Alkyl ether carboxylic acid surfactants

Although known for a long time, the alkylether carboxylic acids turned interesting for industrial applications only in the 1980s [191], when environmental features of surfactants became important along with other properties of ether carboxylates, such as anti-corrosiveness, electrolyte stability or alkaline stability, foam-enhancing ability, dispersabilty of e.g. silicone oils [191]. At the same time, in cosmetics more and more emphasis was made on mildness. Thus, the use of ether carboxylates in products such as shampoos, foam baths, and shower baths began to develop. Besides the application in cosmetics, alkyl ether carboxylates are used in the field of technical application. Here, their potential for dispersing calcium and magnesium is demanded. Besides this property, the good compatibility with other additives is important. According to pK_a studies reported by Aalbers, an internal neutralization of the ether carboxylate micelles can result in a less anionic character than that of alkyl sulfates [192,193]. Ether carboxylate surfactants are weakly dissociated acids with a pronounced non-ionic behaviour at low pH (neutral acid form) and with anionic properties in neutralized or alkaline solutions (ionized form). Besides the mentioned polyethylene glycol chain, it is possible to implement a polypropylene glycol chain. This change in the molecular structure leads to completely different physicochemical properties.

The alkyl ether carboxylates are the starting material of this thesis. Therefore, the detailed industrial synthesis will be explained in the following paragraph.
Alkyl ether carboxylic acids can be divided into two parts:

1. non-ionic part
2. anionic part

The starting material for every alkyl ether carboxylic acid is always a non-ionic compound. These molecules do not carry any charges in the head group. Their chemical structure is relatively simple and the majority of them are only composed of hydrogen, carbon and oxygen atoms. Fatty alcohols and alkyl ethoxylates or propoxylates are amongst the most used non-ionic surfactants, but the structure of both the head and tail group can vary significantly.
The propoxylation is a polyaddition reaction of propylene oxide with a hydroxyl group. The mechanism depends mainly on the used catalyst. The general reaction is described in Figure II-34.

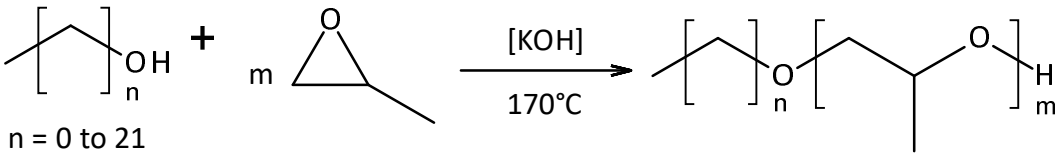

n = 0 to 21
m = 0 to 50

Figure II-34: General synthesis of alkyl ether alcohols

In the absence of catalyst, pure propylene oxide polymerizes only at temperatures exceeding 200°C [194]. This temperature is clearly lowered by the presence of water or alcohols. However, the resulting reaction speed is too slow for technical applications, therefore different catalysts are used for acceleration. Mostly strong bases, like potassium hydroxide or potassium methoxide, are used as homogeneous catalysts in industrial production. The benefits of these catalysts are the low costs, the small amount of produced by-products and the ability to remove the catalyst at the end of the reaction by neutralisation. However, a relatively broad homologue distribution is obtained, because of the relatively high amount of not-reacted fatty alcohol.

In principle, this reaction can also be acid-catalysed. Here, first propylene oxide is activated, by protonation of the Brønsted acids or by electron transfer with Lewis acids, before attacking the alcohol or another propylene oxide molecule. The resulting homologue distribution is much narrower, but the amount of unwanted by-products like polypropylene glycole is significantly higher. Various catalysts have been developed for a narrower distribution and a lower amount of by-products [195–198]. In addition to homogeneous catalysts, also heterogeneous catalysts have been tested: like metal halides, e.g. KF as well as metal oxides such as CaO, but also ion exchange resins and hydrotalcites show catalytical activity [199–201].

In this work, only potassium hydroxide was used as a catalyst. This is why only the alkaline-catalysed reaction is described in detail. The addition of propylene oxide is carried out with an activated alkoxide, i.e. an alcoholate group. This anion attacks the ethylene oxide molecule nucleophilically and opens the ring. The reaction can be divided in following steps:

1. Preparation of catalyst: Figure II-35
2. Propagation reaction: Figure II-36
3. Proton transfer: Figure II-37

The active species in the basic catalysed ethoxylation is the alcoholate anion R-O^-. This has to be produced before the polymerisation reaction by dissolving potassium hydroxide in the fatty alcohol. The resulting water is removed via vacuum and high temperatures. Thus, the equilibrium can be shifted to the side of the alcoholate, see Figure II-35.

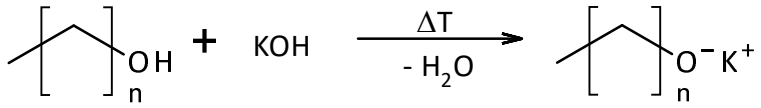

n = 0 to 21

Figure II-35: Preparation of catalyst

The actual propoxylation is a polyaddition of propylene oxide to the alkoxide [202]. Both fatty alcohol and ethoxylate alcoholate anions react in the same way, see Figure II-36.

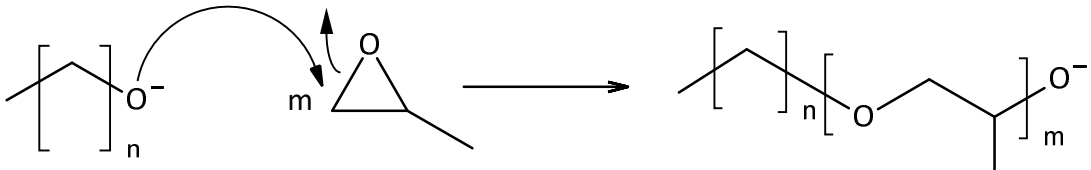

n = 0 to 21
m = 3 to 50

Figure II-36: Propagation reaction

Since there is no chain termination reaction, propoxylation reactions can be seen as a special case of the "Living Anionic Polymerisation ".
The proton transfer reaction ensures that the chain growth is continued by activating an inert alcohol molecule. Thus, a catalytic amount of the alkaline catalyst is sufficient to ensure the reactivity even to a larger amount of alcohol. This transfer step and the reservoir of unreacted alcohol is the main difference between the propoxylation reaction and the “classical Living Anionic Polymerisation”. In the “classical Living Anionic Polymerisation”, the chains are activated by an initiator at the beginning of the reaction and only these activated chains can react with the monomers, see Figure II-37. In the literature, it is usually assumed that the proton transfer is very fast, in comparison with the propagation reaction, so that a balance is established between the different alcohol and alcoholate species:

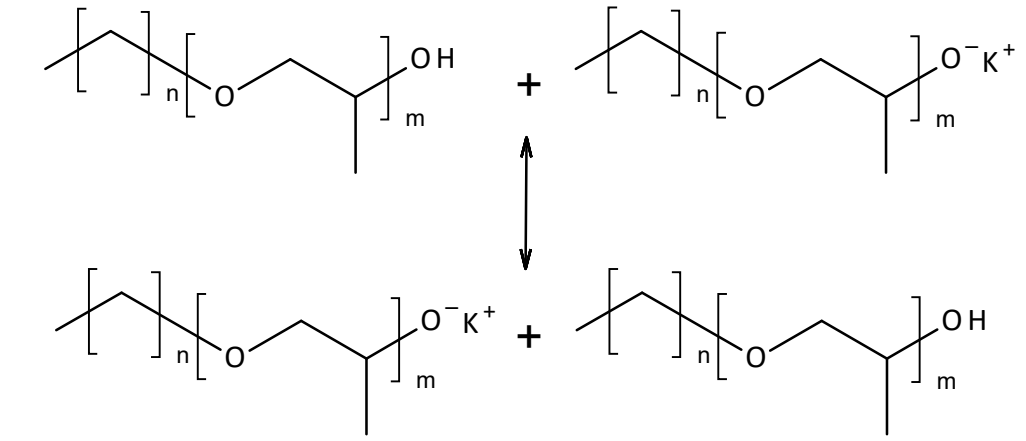

Figure II-37: Proton transfer

During the propoxylation, the propagation reaction can be carried out in two different ways. Due to the two different possibilities for a nucleophilic attack at the propylene oxide, constitutional isomers can be formed. This phenomenon is shown in Figure II-38.

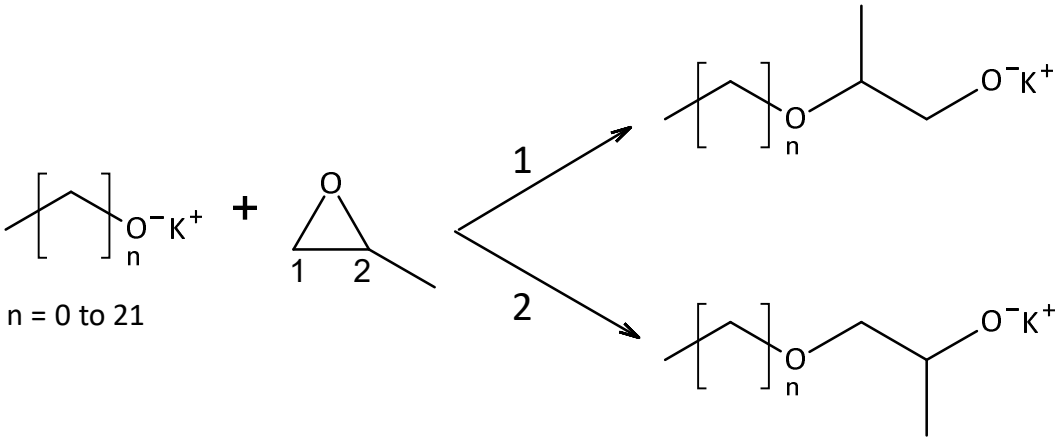

Figure II-38: Formation of primary and secondary alcohols during the alkaline-catalysed propoxylation of primary fatty alcohols

The propylene oxide ring can be attacked in position 1 and position 2. Position 1 is preferred, due to the sterically hindrance of the methylene group at position 2 [203,204]. So, the reaction of the fatty alcohol and the corresponding polypropylation products is different from the reaction of fatty alcohol and ethylene oxide. After the addition of the first propylene oxide, stereo isomers can be formed. Following three isomer types are possible:

- Constitutional isomers: Figure II-39
- Conformational isomers: Figure II-40
- Enantiomers: Figure II-41

The formation of the constitutional isomers continues by increasing the polymerisation degree. After the addition of two moles propylene oxide, four different isomers are formed, see Figure II-39:

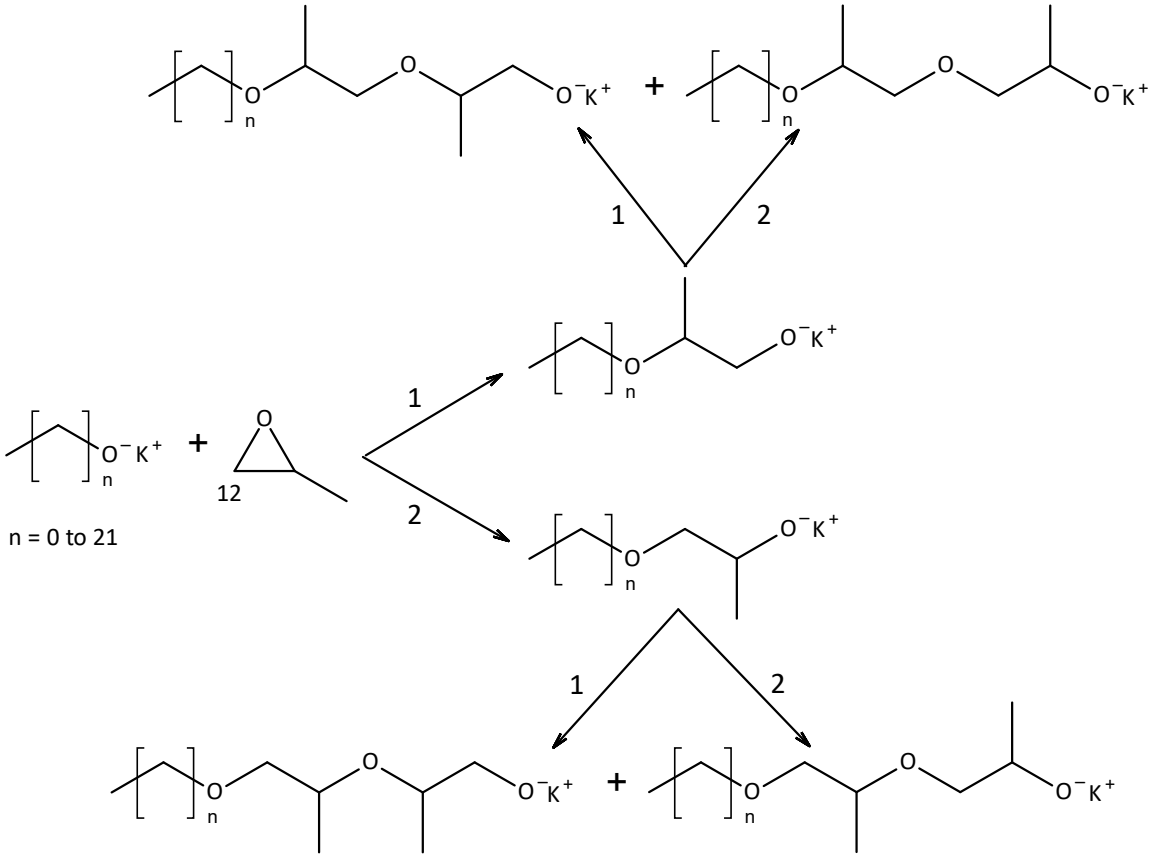

Figure II-39: Continuous formation of constitutional isomers with enlarged polymerisation degree

Di Serio et al. already described the formation of this constitutional isomers [203,204]. They also said that the amount of primary or secondary alcohols cannot be influenced during the alkaline catalysed propoxylation.
Due to the rotation at the single bond, several conformational isomers could be formed by enlarging the polymerisation degree. These types of isomers are exemplarily described in Figure II-40.

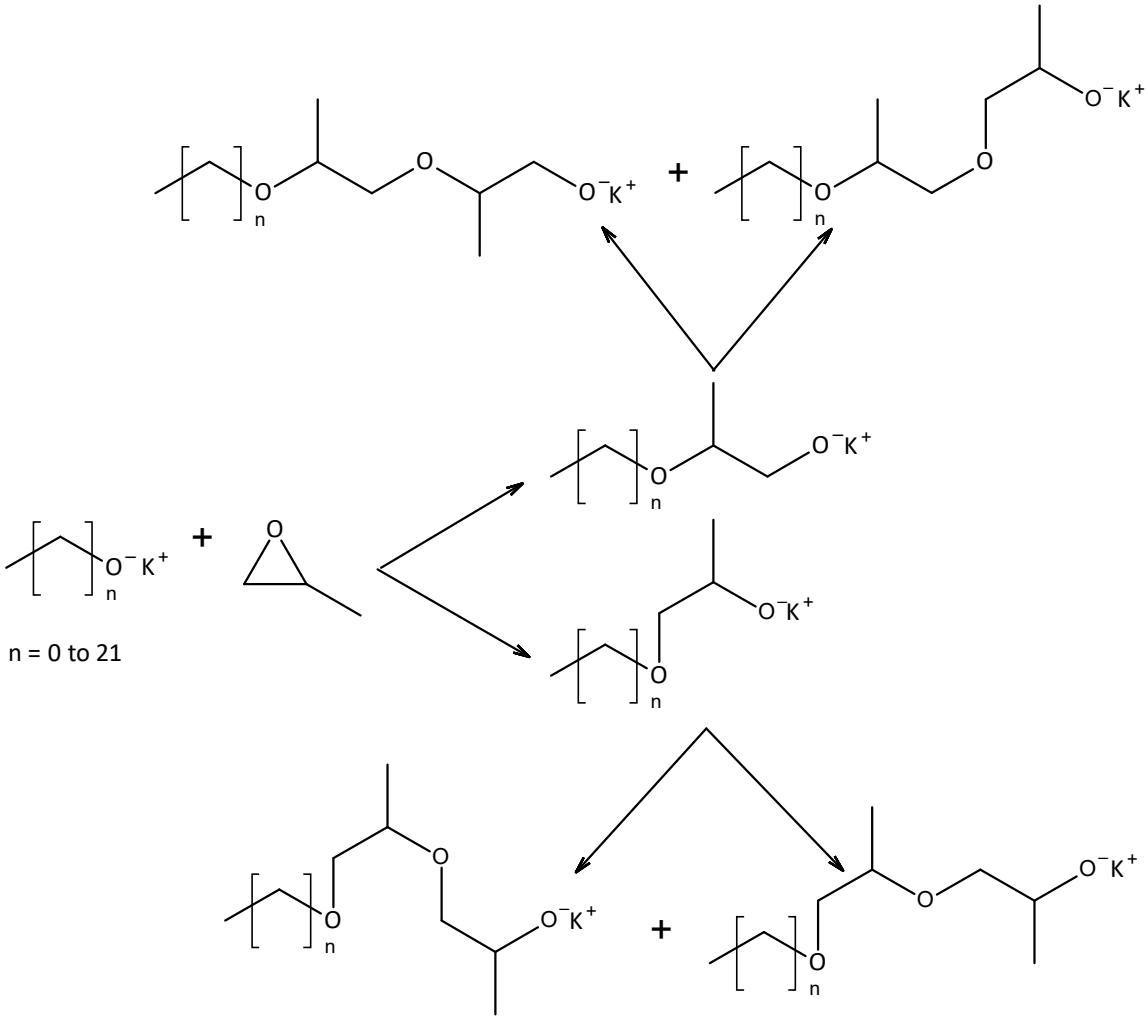

Figure II-40: Formation of conformational isomers during the propoxylation

The addition of propylene oxide to a fatty alcohol also forms two different enantiomeric structures. In Figure II-41, the chiral centre of the mono propoxylate is shown.

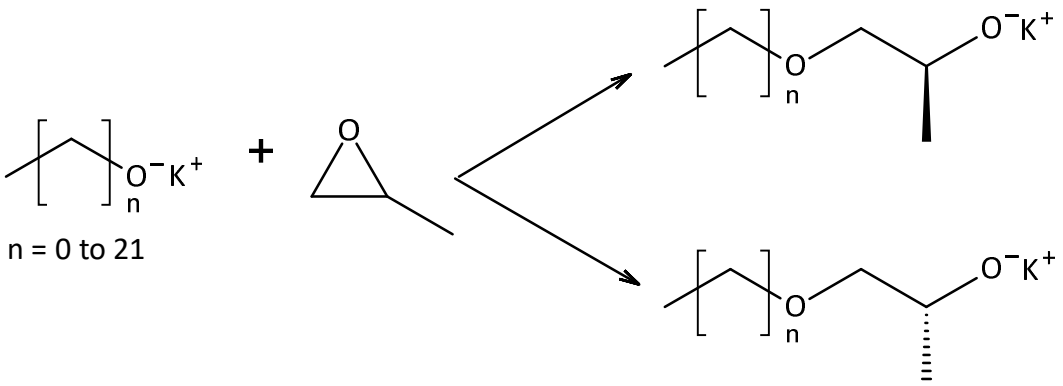

Figure II-41: Formation of enantiomers during the propoxylation of primary fatty alcohols

Besides the described main reaction, also different by-products could be formed during the propoxylation reaction. In the industrial production of alkoxylates, one important side reaction, is the formation of poly glycols. These molecules are formed, if water is not properly removed, that means the reaction mixture is not well dried. Water or glycols could also be formed due to decomposition reactions of already formed alkoxylate molecules.
The OH-groups of alkoxy glycols or water are reacting analogously to fatty alcohol, see Figure II-42.

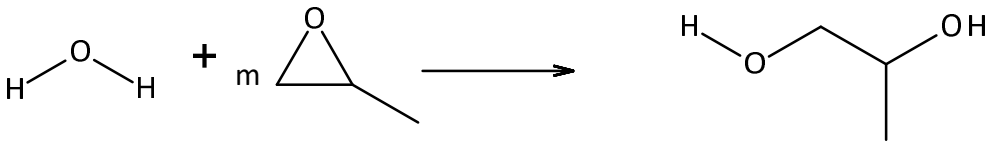

Figure II-42: Formation of poly propylene glycols

The mechanism of the alkoxylation reaction described in the previous paragraphs implies that the receiving products have a statistical distribution of alkoxylates with different chain lengths.
For example, in Figure II-43 different homologues are shown, based on broad range alkaline catalysed and narrow range acid catalysed ethoxylation, in batch reaction.

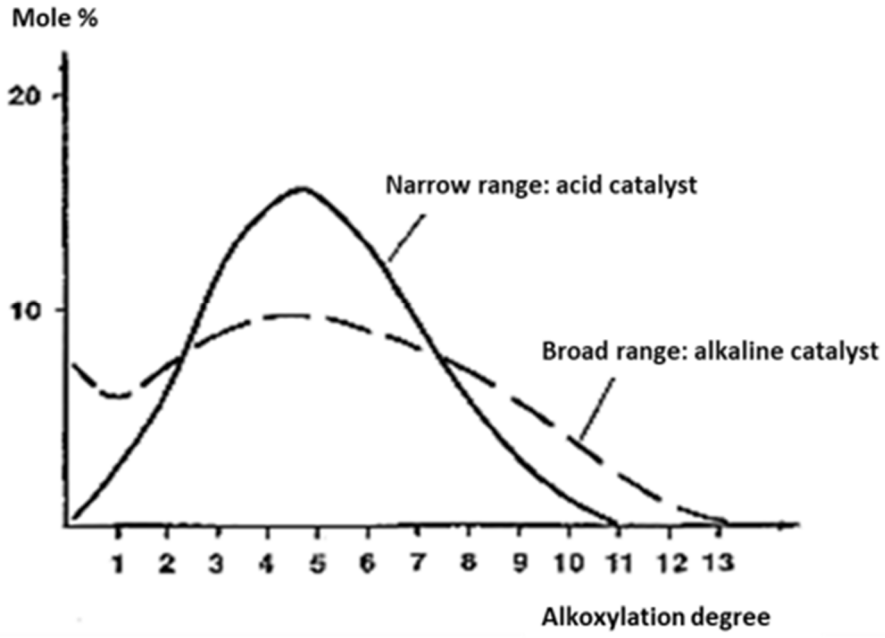

Figure II-43: Different alkoxylation distributions of the used catalyst [205]

The shape of the distribution curve depends on the used catalyst system. The acid-catalysed reaction results in a Poisson distribution in good approximation, while the alkaline-catalysed products have a significantly flatter or broader distribution curve (Figure II-43).
The KOH-catalysed products have a very wide distribution with a large proportion of unreacted starting alcohol. Especially, if ethylene oxide is used, the amount of free fatty alcohol is significantly higher compared to propylene oxide. This phenomenon could be explained by the formation of the constitutional isomers. After the formation of a secondary

alcoholate, the reactivity drops, and therefore a primary one is preferred. So, the amount of primary alcohol decreases, consequently also the free fatty alcohol amount.

After finishing the non-ionic part, this will be converted into the anionic alkylethercarboxylic acid by an additional synthesis.

Anionic surfactants carry a negative charge on the head group. Carboxylates, sulphates, sulphonates and phosphates are among the most common anionic surfactants. All these compounds carry a permanent charge on the head group. Anionic surfactants are extensively used as cleaning products because of their marked detergency properties.
The previously synthesised propoxylated non-ionic compounds are converted via carboxymethylation into the corresponding alkylethercarboxylic acids (Figure II-44). This conversion can be divided into three separate synthesis steps.

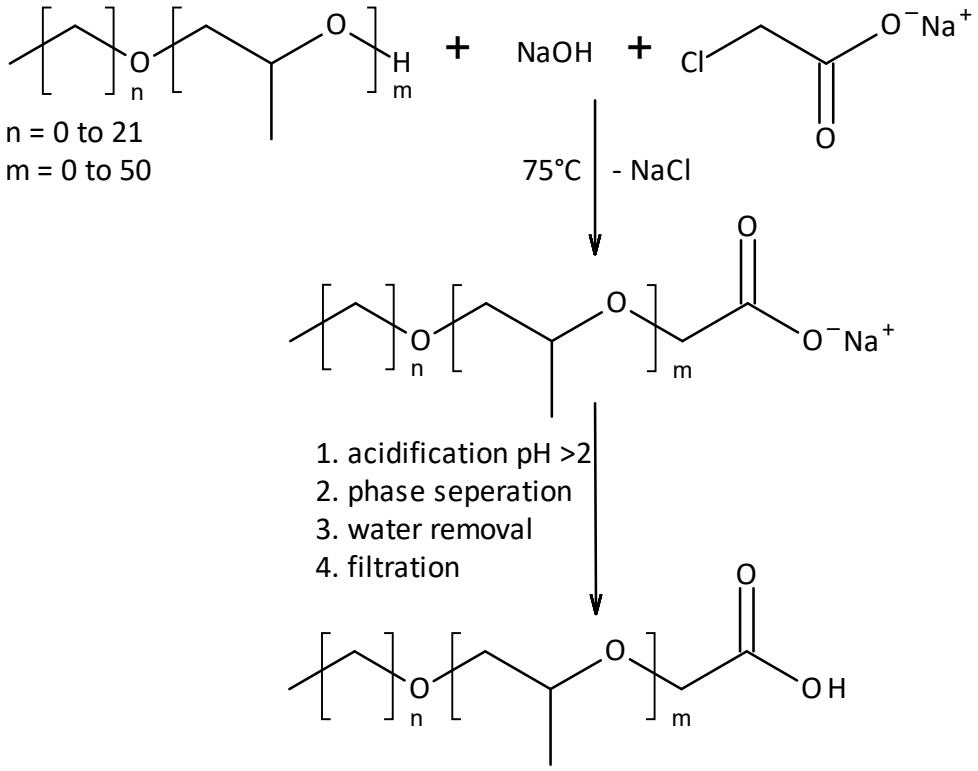

Figure II-44: General synthesis of alkyl ether carboxylic acids

The so-called carboxymethylation is formally a Williamson-Ether synthesis. The secondary alcohol formed in the propoxylation reaction reacts with sodium hydroxide and forms the alcoholate. The produced water is removed and the equilibrium is shifted to the product side, see Figure II-45.

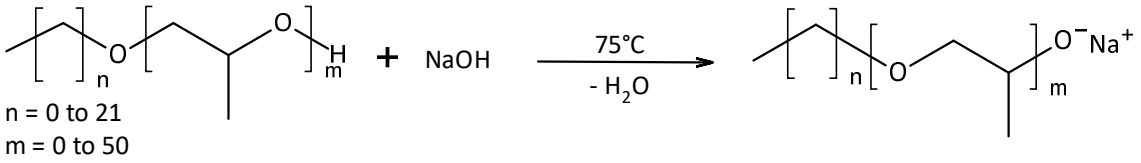

Figure II-45: Formation of the alkoholate anion

The negatively charged oxygen atom of the alcoholate attacks the α-C atom of sodium monochloroacetate in an SN_2 reaction and forms the sodium salt of the corresponding alkyl propoxylate, Figure II-46.

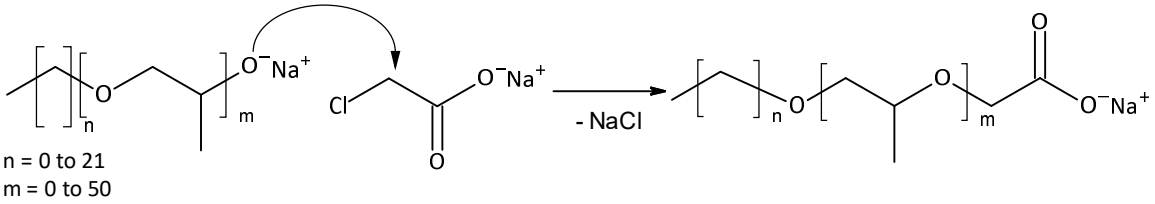

Figure II-46: Nucleophilic substitution of sodium monochloroacetate and the alcoholate

The obtained sodium salt is acidified with a small excess of hydrochloric acid solution,

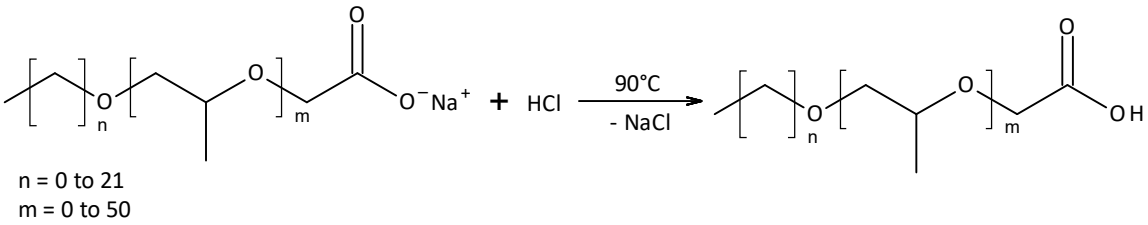

Figure II-47: Formation of the alkylethercarboxylic acid

II.4.2.2 Symmetric Quaternary Ammonium Compounds

Cationic surfactants mostly consist of amines. These compounds can also carry a permanent or a pH-dependent charge. Quaternary ammonium compounds, for example, carry a permanent charge, while other amines can be charged or neutral, depending on the pH-value. Due to this, they adsorb strongly onto most solid surfaces, which are usually negatively charged, and can impart special characteristics to the substrate. Some examples are softeners, anti-static agents, corrosion inhibitors, hair conditioners, lubricants and flotation agents [206–208]. The adsorption of surfactant ions from aqueous solutions onto hydrophilic negatively charged surfaces is based on two main interactions: electrostatic and hydrophobic [209–211]. The electrostatic interaction is involved in the first step of a two-step adsorption mechanism and its contribution to adsorption depends largely on the charge of the surfactant ions, surface charge density of the adsorbent, electrolyte concentration and pH. Hydrophobic interactions are involved in the second step of the two-step adsorption mechanism, where additional surfactants are associated with electrostatically anchored surfactants. This interaction is mainly influenced by the surfactant structure and particularly by the size of the hydrophobic part [212–215]. The hydrophobic interaction acts between the non-polar parts of the surfactant ions (hydrocarbon chain) and it is due to release of water molecules forming a dynamic cage around the non-polar moiety [214]. Van der Waals forces also contribute to the association, but this contribution is small compared to the hydrophobic interaction. For a deeper discussion on hydrophobic interactions see for instance the book by Tanford [213,214]. The corresponding attractive forces cause aggregation into micelles in the bulk phase.

The reaction chart for a typical synthesis of a symmetric quaternary ammonium compound is described in Figure II-48. The reaction mechanism follows the Menshutkin reaction for the alkylation of tertiary amines [216,217].

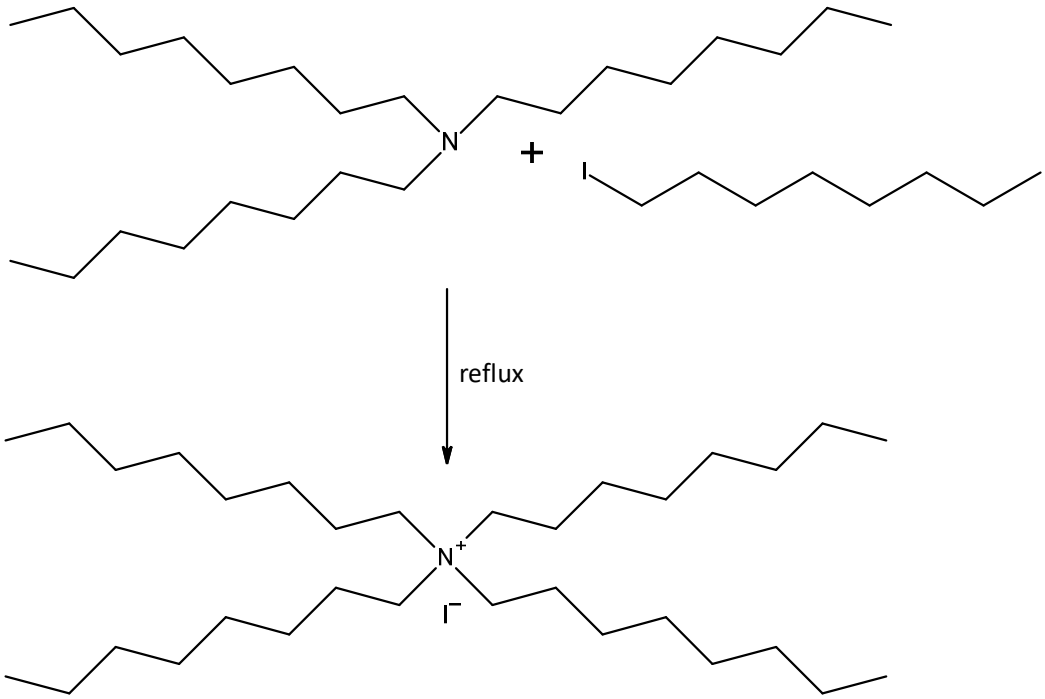

Figure II-48: Reaction chart for the synthesis of Tetraoctylammonium Iodide

II.4.2.3 Catanionics and Surface Active Ionic Liquids (SAILs)

Many biologically relevant structures consist of amphiphilic bilayers, like the cell membranes. All types of natural bilayer structures, mainly vesicles, consist of double chained amphiphiles like phospholipids. However, in the past years, lots of research projects proved that bilayers can also be formed from single chain surfactants, under special conditions. For instance, this is the case for mixtures of anionic and cationic surfactants, whose association through their interactions can mimic the type of structures originated by phospholipids.

The term 'Catanionic' consists of the words cationic and anionic, and describes the spontaneous self-assembly that occurs by mixing both types of surfactants. It is now commonly accepted to term such structures, which were already mentioned in the literature, before this term was introduced [218]. In the case of equimolar amounts of both types of surfactants due to strong Van der Waals interactions between their chains and the intense electrostatic attraction of their heads, the surfactants commonly arrange pair-wise by removal of hydration water at the mixed aggregate/solution interface. That association leads to a strong reduction of the surface per head, which induces the formation of bilayers. This pair-wise aggregation of two single chained amphiphiles results in a type of surfactant, which can be considered as pseudo- double-chained zwitter-ionics, see Figure II-49, as the two alkyl chains are not attached to the same head group [219].

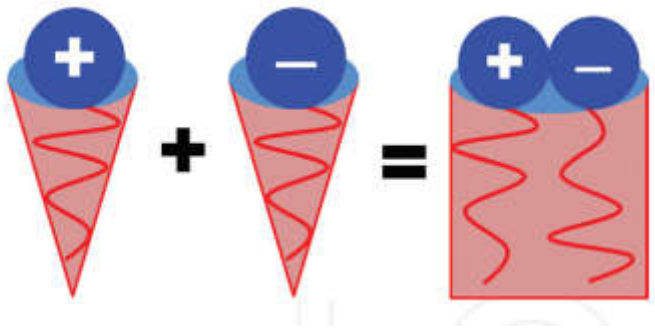

Figure II-49: A schematic representation of ion pair formation in catanionic mixtures [219]

A typical phase diagram for Catanionic mixtures is schematically illustrated in Figure II-50. However, there are numerous variations in the appearance of the Catanionic phase diagram. The concentration regions in which vesicles form are represented by the lobes on both sides of the equimolar line. This indicates that vesicles are stabilized by the presence of excess surfactants. Catanionic vesicles usually have high degree of polydispersity, and their stability can be tailored by the choice of surfactant molecular structure, that is branched surfactants, and/ or those containing a bulky group in alkyl tail usually form more stable vesicles [219]. Likewise, in asymmetric surfactant mixtures, in terms of different alkyl chain numbers or length as well as different chain morphology, the vesicle phase is often considerably enlarged and found in a broad concentration range [220–222]. The size, surface charge density and permeability of Catanionic vesicles can be tailored by varying temperature, concentration and molar ratio, as well as chain length of surfactants [223].

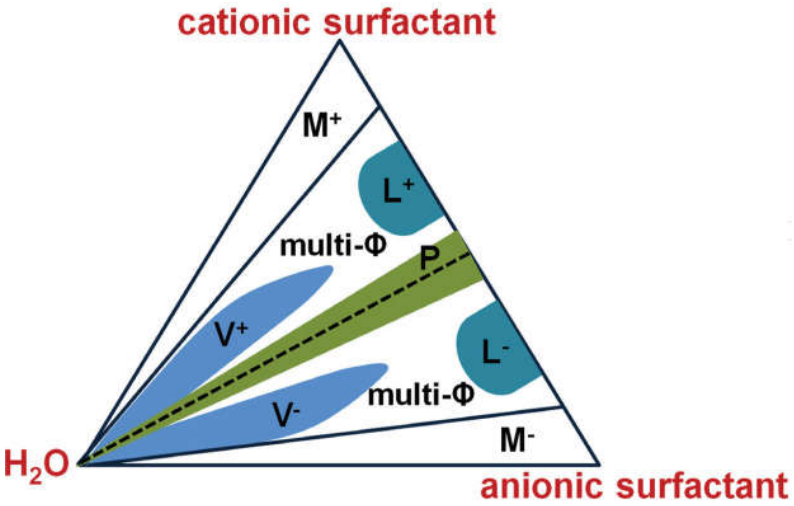

Figure II-50: A schematic triangular phase diagram of symmetric Catanionic mixture at constant temperature and pressure. The dashed line denotes the equimolar line dividing the diagram into the cationic-rich and the anionic-rich region. Close to the charge neutrality line, a solid precipitate (P) is usually formed, but excess charge in the system usually leads to vesicle stabilization (denoted as V^+ and V^-). Mixed micelles (denoted as M^+ and M^-) are usually formed at the highest excess of the mixture components. Multiphase regions (multi-Φ) often involve a lamellar phase occurring at higher concentrations (denoted as L^+ and L^-) [223]

The important difference to the classical zwitter-ionic surfactant type is the tune-ability of the properties of the Catanionic system. By slightly varying factors like the mixing ratio of anionic and cationic component, the chain length of the surfactants or the degree of saturation of the alkyl chains, the properties of the system can be shifted immensely.

For instance, the critical micelle concentration (cmc) of the mixture of two contrarily charged surfactants can differ a lot from the cmc of the pure surfactants [224]. If no net interaction between the amphiphiles exists, the cmc of a mixture of surfactants generally is the average of the cmc of the pure surfactants. Yet, between anionic and cationic amphiphiles, a strong interaction, about 5 to 10 times higher than for non-ionic and anionic type ones, is present, which leads to the result of strongly reduced cmc values, compared to the ideal mixing case without interactions, see Figure II-51.

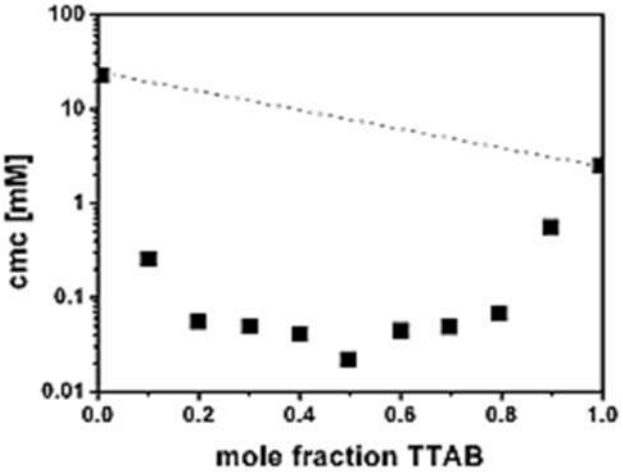

Figure II-51: Cmc of the mixture tetradecyltrimethylammonium bromide (TTAB) and sodium laurate versus the mole fraction of TTAB at 25 °C [225]

The investigation of long-chain Catanionic Ionic Liquids attracted rather recent scientific interest. Long-chain Ionic Liquids are composed of a charged hydrophilic head group and one or more hydrophobic tails. Due to their structure and their amphiphilic nature, they can self-assemble, like conventional surfactants and can form aggregates [190]. Ionic Liquids containing the 1-alkyl-3-methylimidazolium ion, [$C_n$mim], have been extensively studied in the field of colloid and interface science. Such kinds of combinations are nowadays widely known as SAILs, Surface Active Ionic Liquids.

Brown et al. have investigated anionics, based on dodecylsulfate and bis(2-ethyl-1-hexyl) sulfosuccinate, mixed with various trimethylalkyl ammonium compounds, trimethyl butyl-; trimethyl hexyl-; trimethyl octyl- and trimethyl dodecyl ammonium. They have found that especially the melting point of the Ionic Liquids based on dodecylsulfate does not change with enlarging cation molecule. The linear chain of the anions and cation can pack efficiently [226].
Iglesias and co-workers reported on the synthesis and determination of thermophysical properties of new protic Catanionics based on long-chain Ionic Liquids with oleate as anion- and ethanol or diethanolamine as cation [227,228]. They determined the physical chemical properties of several aprotic Ionic Liquids, based on fatty acids and symmetric and asymmetric quaternary ammonium compounds.

Kunz, Buchner and co-workers have presented oligo-ether based short-chain carboxylates as efficient counter ion to form Ionic Liquids. As anionic part they used 2,5,8,11-tetraoxatridecan-13-oic acid (TOTOA), see Figure II-52.

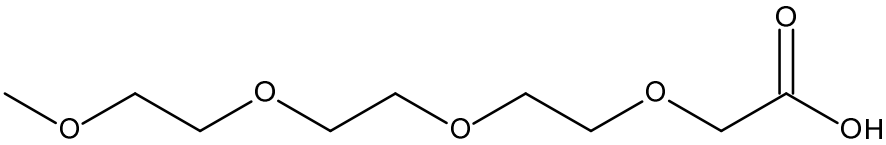

Figure II-52: 2,5,8,11-tetraoxatridecan-13-oic acid (TOTOA)

In their investigations, they used various cations, starting with sodium, quaternary ammonium compounds and primary amines [229–231]. Kunz et al. could prove that the low melting point of the Ionic Liquids containing TOTO as anionic part is not a result of the bulkiness of the cation. The high conformational flexibility of the ether groups is the reason for this phenomenon and leads to the **CO**ncept of **M**elting **P**oint **L**owering due to **E**thoxylation (COMPLETE) [231]. Using 2,5,8,11-tetraoxatridecan-13-oate (TOTO) as anion with small alkali ions such as lithium and sodium, Ionic Liquids of high electrochemical and thermal stability are gained. Dielectric relaxation and polarity measurements showed that Na-TOTO forms a cross-linked structure, crown ether-like complex, with strong $–COO^{-}\cdots Na^{+}$ interactions. These strong ionic interactions cause low ionicities of the alkali TOTO salts and viscosities as high as for example ~95.000 mPa s at 30 °C with sodium as cation. The ion interactions are influenced by the size of the alkali cation. With increasing size ($Li^{+} > Na^{+} > K^{+} > Cs^{+}$) the fluidity and ion mobility of Ionic Liquids are increased [229]. If quaternary ammonium ions are used as cations, the resulting TOTO salts change their behaviour completely. The resulting Ionic Liquids show up to 600 times lower viscosities, e.g. tetrabutylammonium-TOTO (TBA-TOTO) η = 575 mPa s at 30 °C and increased conductivities up to a factor of 1000. The Walden plot further revealed

that Ionic Liquids based on quaternary ammonium ions and TOTO belong to the class of "good" Ionic Liquids. Remarkably, ionic liquids formed by TOTO and the per se highly polar sodium ion are in fact less polar than those comprising quaternary ammonium ions [230]. If the quaternary ammonium compounds are exchange against primary amines, again Room Temperature Ionic Liquids are obtained. Replacing sodium by ammonium ions, the three-dimensional cross-linked structure seems to be broken, therefore the resulting viscosity of e.g. C8-TOTO (octyl amine-TOTO) is ~200 mPa s at 30 °C. But the conductivity stays in the same order of magnitude as Na-TOTO. The primary amine-TOTO Ionic Liquids are located far from the ideal line in the Walden Plot, resulting in "poor" Ionic Liquids. So, the vertical deviation ΔW becomes large. This phenomenon is in contrast to the quaternary ammonium-TOTO Ionic Liquids. These molecules seem to have a "loose" three-dimensional organisation. The primary amine-TOTO Ionic Liquids form strong hydrogen bonds to the carboxylate group, which resembles a metal cation complexed by a crown ether [231]. Besides the TOTO-anion, E. Müller also investigated different commercially available alkyl ether carboxylic acids combined with primary amines. She could also synthesise Room Temperature Ionic Liquids with low viscosities combined with low conductivity values [232]. In contrast to the TOTO-anion, these Ionics Liquids could be considered as SAILs (Surface Active Ionic Liquids). The COMPLETE-concept (**CO**ncept of **M**elting **P**oint **L**owering due to **E**thoxylation) opens a new possibility of combining Surface Active Ionic Liquids (SAILs). Now commercially available surfactants, containing an alkoxylation distribution, could be used as anionic raw material for Ionic Liquids. It is not necessary to use bulky and environmentally unfriendly cations, like imidazolium or pyridinium, to form Room Temperature Ionic Liquids with tuneable properties.

As already mentioned in chapter II.3.3, especially the lubrication industry shows high interest in this kind of novel technology. Many investigations have been started to check the performances of Ionic Liquids as base oils or additives for fully formulated lubricants. However, even though there are 10^9 possible anion/cation combinations that may lead to Ionic Liquids, almost all studies focussed on imidazolium based moieties with halide counter ions. This has significant practical implications such as relative expense, unknown toxicity, environmentally hazardous starting materials, incompatibility with active metals and strong bases due to the acidity of the C_2-proton of the imidazolium. For example, Gausain et al. studied the influence of surfactant like Catanionics based on fatty acid and quaternary ammonium Ionic Liquids. In their study, the property of the Catanionics as lubricant additives have been investigated [233].

Based on these previous investigations, new carboxylates based on different fatty alcohols have been synthesised and the ethylene glycol has been changed to propylene glycol (methyl-ethylene glycol). These anions are then mixed with different symmetric quaternary ammonium compounds to form new Catanionics.

III Experimental

III.1. Chemicals

All fatty alcohols (C_8 till C_{18}) have been provided by Kao Chemicals (purity ≥ 99 %). These materials were not purified before use.

Docosanol (C_{22}) has been provided by Sasol with a purity ≥ 99 %. This material has not been purified before use.

Methanol (Fluka, purity ≥ 99 %) and Butanol (Fluka, purity ≥ 99 %) have been stored over molecular sieves before usage.

Propylene oxide has been purchased at Chemogas B.V. with a purity ≥ 99 %.

Sodium monochloroacetate has been provided by Akzo Nobel (purity ≥ 99.5 %) and sodium hydroxide powder has been purchased from Merck (purity ≥ 99.5 %). Amberlyst A26 has been purchased at Sigma Aldrich.

Tetramethylammonium hydroxide, 25 % in methanol, tetraethyammonium hydroxide, 30 % in water and tetrabutylammonium hydroxide, 45 % in methanol, have been delivered by SACHEM B.V. All products have been used without further purification and the purity grades have been ≥ 99 %.

Acetonitrile, methanol, isopropanol, dichloromethane and potassium hydroxide solution in ethanol (0.5 mol/l) have been purchased at Merck, purity ≥ 99 %.

The used rape-seed oil has been provided by O. & L. SELS GmbH (Neuss). The used oil was a refined quality and it was not purified before use.

III.2. Synthesis

The possible usage as lubricants of combinations of alkyl ether carboxylates and quaternary ammonium compounds are investigated during this study. It has been carried out in close cooperation with Kao Chemicals.

The main focus of this investigation was to check the influence of the chain length of the fatty alcohol and the degree of propoxylation, as well as the chain length of the quaternary ammonium compound on the friction coefficient on the steel/steel tribo pair. The investigated ion-combinations with corresponding abbreviations are given in Table III-1.

Cations	Anions
	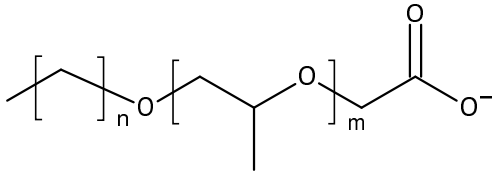
 [TMAH; N_{1111}]	n = 0 m = 6 C1 PO6 COO^- MeP6
	n = 3 m = 6 C4 PO6 COO^- BuP6
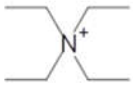 [TEAH; N_{2222}]	n = 7 m = 6 C8 PO6 COO^- OcP6
	n = 11 m = 6 C12 PO6 COO^- LP6
	n = 17 m = 6 C18 PO6 COO^- SP6
	n = 21 m = 6 C22 PO6 COO^- BP6
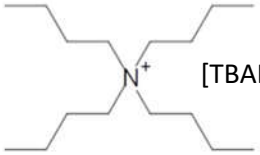 [TBAH; N_{4444}]	n = 17 m = 0 C18 COO^- Stearyl
	n = 17 m = 3 C18 PO3 COO^- SP3
	n = 17 m = 9 C18 PO9 COO^- SP9
	n = 17 m = 12 C18 PO12 COO^- SP12
	n = 17 m = 15 C18 PO15 COO^- SP15
	n = 17 m = 25 C18 PO25 COO^- SP25
	n = 17 m = 50 C18 PO50 COO^- SP50

Table III-1: Prepared Cat-Anion combination

Based on these three cations and thirteen anions, a total of thirty-nine new Ionic Liquids has been synthesised.

III.2.1 Synthesis of the alkyl ether alcohols

The alkyl ether carboxylic acids have been synthesised at Kao Chemicals. First the corresponding non-ionic surfactant based on different fatty alcohols, which differs in different C-chain lengths with purity grades ≥ 99%, are reacted with various polyoxopropylene degrees (PO-degree).

When carrying out the propoxylation, fatty alcohol is introduced into the stainless-steel reactor. Also a certain amount of solid catalyst (2.5 mole%, based on the molar amount of fatty alcohol), in our case potassium hydroxide, is added. After the reactor has been closed, the autoclave is heated to 313-373 K, depending on the fatty alcohol boiling point. The formed water has to be removed by full vacuum to supress the formation of by-products, like polypropylene glycol. After reaching the reaction temperature (443 K), propylene oxide is gravimetrically dosed into the reactor. The dosing speed is dependent on the exothermic reaction of the propoxylation that means it is important to find a balance between dosing speed and cooling capacity of the system. After the complete addition of the desired amount, the postreaction is carried out.

III.2.2 Synthesis of the alkyl ether carboxylic acids

For the synthesis of the corresponding alkyl ether carboxylic acids, a certain amount of previously prepared alkyl ether alcohol is introduced into a double wall glass reactor. The PO-alcohol is heated to 348 K. The one and a half molar excess, based on the molar amount of PO-alcohol, of sodium monochloracetate (150 mol%) is charged at once. Then 152.5 mol% of solid sodium hydroxide powder is dosed manually in 15 times. After complete addition, an aging step of two hours is carried out. After checking the complete conversion of sodium monochloroacetate by argentometric titration, the sodium salt of the alkyl ether carboxylic acid is charged into hydrochloric acid and water for neutralisation. The pH of the mixture has to be lower than 2. To accelerate the phase separation, small amounts of isopropanol is charged. Then, again 1.5 times water based on the amount of alkyl ether carboxylic acid is charged and a second phase separation is proceeded. Again, small traces of isopropanol are added to accelerate the separation.
After this step, the excess of water and solvent is removed by heating (383 K) and reduced pressure (20 mbar). The participated inorganic and organic salts are removed via filtration. The remained non-reacted PO-alcohol as well as esters, which are formed as by-products are removed by using Amberlyst A26. Here the reaction mixture is dissolved in isopropanol and then elutriated on the ion-exchange resin (Amberlyst A26). To remove the alkylethercarboxylic acid from the resin, it is rinsed with potassium hydroxide in ethanol. Than this alkaline solution is neutralised with hydrochloric acid. Afterwards the solvent and water are removed via distillation (383 K) under reduced pressure (20 mbar). Precipitations are removed by filtration. The conversion degree of the alkyl ether carboxylic acids has been ≥ 98 % and determined by titrimetric analysis. The requirement for further tests of the Ionic Liquids has been, that the water content was below 1000 ppm and the halogenate content below 10 ppm.

III.2.3 Synthesis of the Ionic Liquids

Equimolar amounts of alkyl ether carboxylic acid molar mass is calculated via saponification value and quaternary ammonium compound (TMAH; TEAH and TBAH) were dissolved in dichloromethane. The amine was added to the acid dropwise and the solution was stirred at room temperature for 120 minutes. The solvent was evaporated under heating (383 K) and reduced pressure (10 mbar).

The purity was analysed via NMR. If not explicitly mentioned, all Ionic Liquids were featured by water- and halogenate contents below 100 and 10 ppm prior to physicochemical investigation. The ion combinations are summarized in Table III-1.

III.3. Experimental methods

III.3.1 Analytical Methods

All Ionic Liquids as well as the intermediates have been analysed to check the purity and the by-product content.

The polymerisation degree of the alkyl ethercarboxylic acids has been determined by using ASTM D2959 (Standard Test Method for Ethylene Oxide Content of Polyethoxylated Nonionic Surfactants). Here, the polyether chains have been cracked using hydrogen iodide. The formed fragments, alkyl halides and alkyl dihalides, have been determined via gas chromatography, with a HP 6890 analyser equipped with an auto sampler and a FID detector. The calculation for the corresponding polymerisation degree is described in ASTM D2959.

The conversion degree of the anionic, as well of the cationic surfactant has been determined by using a two-phase titration based on DIN EN 14480. Here the amount of surfactant is measured by using benzethoniumchloride (Hyamine 1622) for anionics and sodium dodecylsulfate for cationics as titrant. The equivalent point is potentiometrically determined and the measurement has been performed on a fully automated titration platform from Metrohm.

The purity was ascertained by ^{1}H- and ^{13}C- NMR ($CDCl_3$). NMR spectra were recorded on a Bruker Avance 300 spectrometer at 300 MHz with tetramethylsilane (TMS) as internal standard.

The water content determination has been performed by using a fully automated titration platform by Metrohm. Here the potentiometric Karl Fischer method has been used.
The halogenate content has also been determined using the potentiometric argentometric platform of Metrohm.

III.3.2 Densities

Densities ρ were measured using a U-shaped vibrating tube density meter DM40 (Mettler Toledo) operating in a static mode from 298.15 to 363.15 K. The temperature was maintained constant to 0.01 K. Measurements were viscosity-corrected and carried out under atmospheric conditions. The instrument was calibrated using ultrapure water. The uncertainty of ρ was estimated to be less than 0.1 kg/m³.

III.3.3 Viscosities

For the measurement of the viscosity, a rotational rheometer from Anton Paar (MCR 301) has been used for all tests. The instrument was fitted with the platinum cone (0.5 ° / 60 mm) and plate and the sample was located in a 0.056 mm gap between the cone and the plate. For the temperature control, a Peltier temperature control system was employed. It consists of a Peltier-controlled bottom plate and an additional Peltier-controlled hood. The accurate temperature is therefore ensured by a combination of conduction and convection heating. The additional use of a Peltier-controlled hood ensures a uniform temperature distribution

within the sample over the whole measurement range. This is crucial, since the temperature gradient within the sample will induce misleading results, when only the lower plate will be temperature controlled. The accuracy in temperature was estimated to be better than ± 0.1 K.

The viscosity is determined between 273.15 and 373.15 K. First, repeat scans of viscosity as a function of shear stress at 298.15 K were carried out to ensure the material has given linear responses with no shear history. Once Newton behaviour has been verified, plots of viscosity against temperature were recorded at constant shear stress (50 sec^{-1}) and different temperature, 273.15; 293.15; 313.15; 333.15; 353.15; 373.15 K.

The same Peltier-controlled hood was used in combination with the tribology cell, as will be described later.

III.3.4 Electrical conductivity

Conductivities of the pure substances were determined at ambient temperature (293.15 K) as well as in steps of 10 K between 293.15 and 393.15 K. The measuring cell was connected to a water bath to guarantee the temperature in the sample. The accuracy of this bath has been ± 0.1 K.

Measurements were carried out with an 856 conductivity module (Methrom), connected to a conductivity measuring cell (stainless steel) with a cell constant of c = 0.1 cm^{-1}. The cell constants were derived by measuring aqueous KCl solution. The dependence of temperature to the cell constants was not taken into account, since the changes in the conductivities, when correcting for this effect, were marginal and within the given limits of error.

III.3.5 Thermal stabilities

Thermal stability was studied using a thermogravimetric analyser STARe System TGA/DSC 3+ BASIC from Mettler Toledo. Samples were measured at a heating rate of 10 K per minute, applying a continuous nitrogen flow. Decomposition temperatures were determined using onset points of mass loss, being defined as the intersection of the baseline before decomposition and the tangent to the mass loss versus temperature.

III.3.6 Differential scanning calorimetry

Melting points of the substances were determined by a DSC 3+ BASIC from Mettler Toledo. The instrument was connected to a cooling thermostat working at 273.15 K. To avoid steam condensation in the calorimetric wall, especially at low temperatures, a constant purge of dry nitrogen was circulated through the sample holders during the measurements. A standard batch vessel, made of Hastelloy C276 steel, was used throughout the present experiments. The samples were held at 293.15 K below their melting point for 30 minutes and subsequently heated with 1 K per minute. The onset of the resulting peaks in the detected heat flow was taken as the melting point.

III.3.7 Hygroscopicity

For the hygroscopicity test, 1 g ± 0.1 µg of the Ionic Liquid is placed in an aluminium sample holder, size 63 mm ± 1 mm. To have a better comparability and to increase the reproducibility, it is important that all tested Ionic Liquids cover the same area of the bottom at the sample holder and the surface of the tested substances should be as thin as possible. The samples are stored in a room under stable conditions (298.15 K and 60% humidity) for max. 120 hours. The humidity and temperature is adjusted by an air conditions system. The increase of weight, due to the hygroscopic behaviour, is monitored after 2, 3, 4, 8, 12, 24 and 120 hours. The reported values are average values of three measurements.

III.3.8 Oil solubility

The oil solubility test has been carried out by preparing a 1, 2.5, 5, 10 and 25 % solution of the Ionic Liquid in rape-seed oil. These solutions have been stored at room temperature (298.15 K) in a glass vessel under a nitrogen blanket. After 1 and 7 days, the solutions have been checked visually. If precipitation (turbid solution) and or solidification occurred, the stability of the substance was negative.

III.3.9 Tribological measurements

Tribological measurements were carried out in a special cell of the MCR301 rheometer (Anton Paar). A schematic diagram and a picture of the set-up is shown in Figure III-1.

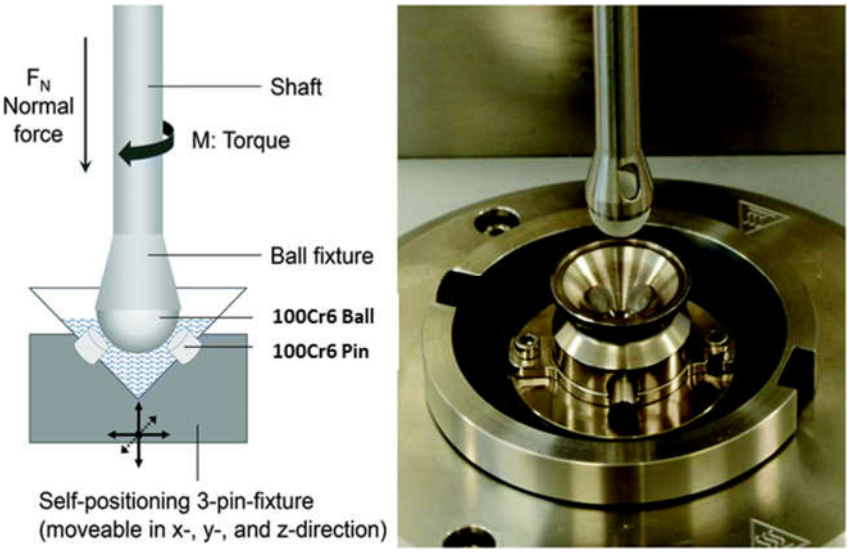

Figure III-1: Tribology cell for the Anton Paar Rheometer

In this set up, a ball, with a radius R, is pressed at a given normal force F_N against three pins that are mounted in an angle of $\alpha = 45°$ on a moveable stage. As a result, the load is distributed evenly on all three frictional pairs and the ball has 3 contact points.
Next, the ball is commanded to rotate with a rotation, n, at an increasing sliding speed, V, while the pins are held stationary. This generates three sliding point contacts. The sliding speed, V, is related to the angular velocity, ω, through Equation III-1.

$$V = \frac{2\pi}{60} \cdot R \cdot n \cdot \sin\alpha \qquad \textbf{Equation III-1}$$

The sliding distance, d, can be derived by Equation III-2.

$$d = \omega \cdot R \cdot \sin \alpha \qquad \textbf{Equation III-2}$$

The resulting torque, M, can be correlated with the friction force, F_f, by employing simple geometric calculations, see Equation III-3.

$$F_f = \frac{M}{3 \cdot R \cdot \sin \alpha} \qquad \textbf{Equation III-3}$$

The normal force, F_N, of the rheometer can be transferred into a tribological normal force, $F_{N;tribo}$, by simple geometrical arguments, see Figure III-2.

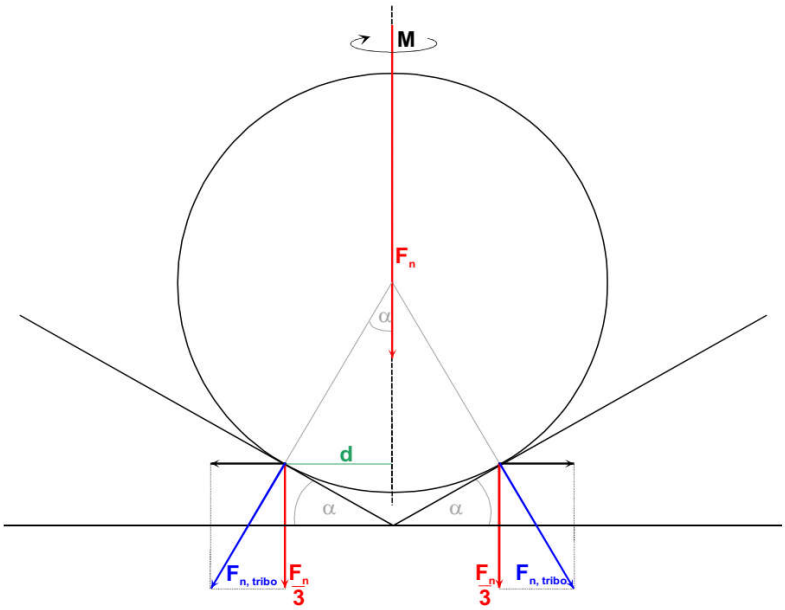

Figure III-2: Schematics of the tribology measuring cell

This force is decisive for the force acting perpendicular to the bottom pins at the contact points.

The relations between the normal force, F_N and tribological normal force, $F_{N;tribo}$, is given by Equation III-4.

$$F_{N,tribo} = \frac{F_N}{3 \cdot \sin \alpha} \qquad \textbf{Equation III-4}$$

The resulting friction coefficient, μ, is the ratio between tribological normal force, $F_{N;tribo}$ to the friction force, F_f, Equation III-5.

$$\mu = \frac{F_f}{F_{N,tribo}} \qquad \textbf{Equation III-5}$$

Therefore the friction coefficient, μ, is directly related to the normal force, F_N, the radius of the used ball, R, and the resulting torque, M, see Equation III-6.

$$\mu = \frac{M}{F_N \cdot R} \qquad \textbf{Equation III-6}$$

The experimental protocol was as follows. First, the tribo pair, pins and ball, characteristics see Table III-2, were ultrasonically cleaned using acetone and dried prior to the test.

	Ball	**Pin**
Material	bearing steel 100Cr6	bearing steel 100Cr6
Material number	1.3505	1.3505
Diameter [mm]	12.7	6
Elastic Modulus [GPa]	210	210
Poisson's Ratio	0.3	0.3
Hardness [HCR]	64	64
Mean Roughness depth (R_z)	0.2	0.11
Average Roughness (R_a)	1.43	1.23

Table III-2: Characteristics of the specimen

The test rig was then assembled and approximately 5 mL of lubricant was added to fully immerse the three point contacts. Temperature was stabilised to 298.15 K. The same Peltier-controlled hood, like already described in the viscosity measurements, is used to ensure the same at the bottom pins and the upper ball. The ball was loaded against the pins. Next, the ball is made to slide over the plates at a controlled speed. The experiments were performed under pure sliding conditions, by keeping the pins stationary. The speed V is increased logarithmically from 10^{-3} to 1.44 m/sec. The resulting torque, M, by the ball is monitored and using Equation III-5 the friction coefficient is calculated.
The normal force F_N was fixed at 50 N, this results in a tribological force $F_{N,tribo}$ to 23.5 N, see Equation III-4, this results in a contact pressure of 950 MPa, using the Hertz equation, see Equation II-6.
From the resulting Stribeck curve, the minimum friction coefficient is determined. This point is the transition from boundary to hydrodynamic lubrication. Besides this, also the average value of friction from the first one hundred points is evaluated. This shows characteristics for the first monolayer, which is formed.
To confirm the reproducibility of the tribo test system, the rheometer has to be calibrated. This was done automatically before each measurement. By this calibration the mass and shape deviation of the ball is determined by the rheometer. Nevertheless a commercially available engine oil 10W40 has been chosen as internal standard. Here, the friction curves of 10W40 were measured with the above mentioned parameters after ten times usage. If the friction coefficient of the 10W40 differ more than 1 %, the complete system, rheometer, motor and air bearing are calibrated again. It is important to use a new ball and new pins for each experiment. The Ionic Liquid or rape-seed Ionic Liquid mixture has been also replaced for each measurement. All measured curves are average of at least three measurements.

IV Results and discussion

IV.1. Results of the synthesis of the different Catanionics

IV.1.1 Results and discussion of the synthesis results

IV.1.1.1 Anionic Part

As mentioned in Table III-1, thirty-nine different Ionic Liquids have been synthesised.
In the following chapter, all synthesis and purification steps are described more in detail.

After the polymerisation of propylene oxide to the corresponding alcohol, as described in Chapter III.2.1, the different alkoxylation degrees are analysed, the corresponding method is described in Chapter III.3.1. The results can be seen in Table IV-1.

	MeP 6	**BuP 6**	**OcP 6**	**LP 6**	**SP 6**	**BP 6**
C-chain	1	4	8	12	18	22
intended PO-degree	6	6	6	6	6	6
achieved PO-degree	5.9	6.1	6.1	6.1	5.9	5.9

	SP 3	**SP 9**	**SP 12**	**SP 15**	**SP 25**	**SP 50**
C-chain	18	18	18	18	18	18
intended PO-degree	3	9	12	15	25	50
achieved PO-degree	3.3	8.7	11.8	14.9	24.7	49.5

Table IV-1: Analytical data of the achieved polymerisation degrees

It can be clearly concluded that, based on the analytical data, the polymerisation of propylene oxide and the alcohol was very selective. All intended PO-degrees have been achieved, with slight variations. These variations occur, due to the gravimetrical dosing of propylene oxide. Using the mentioned fully automatized dosing, slight overdosing or under-dosing of the gaseous raw material (PO) could happen. This mass deviation is clearly observable in higher or lower PO-degrees.

In Figure IV-1, the distribution of the propoxylation degree of octanol, dodecanol and octadecanol is shown exemplarily.

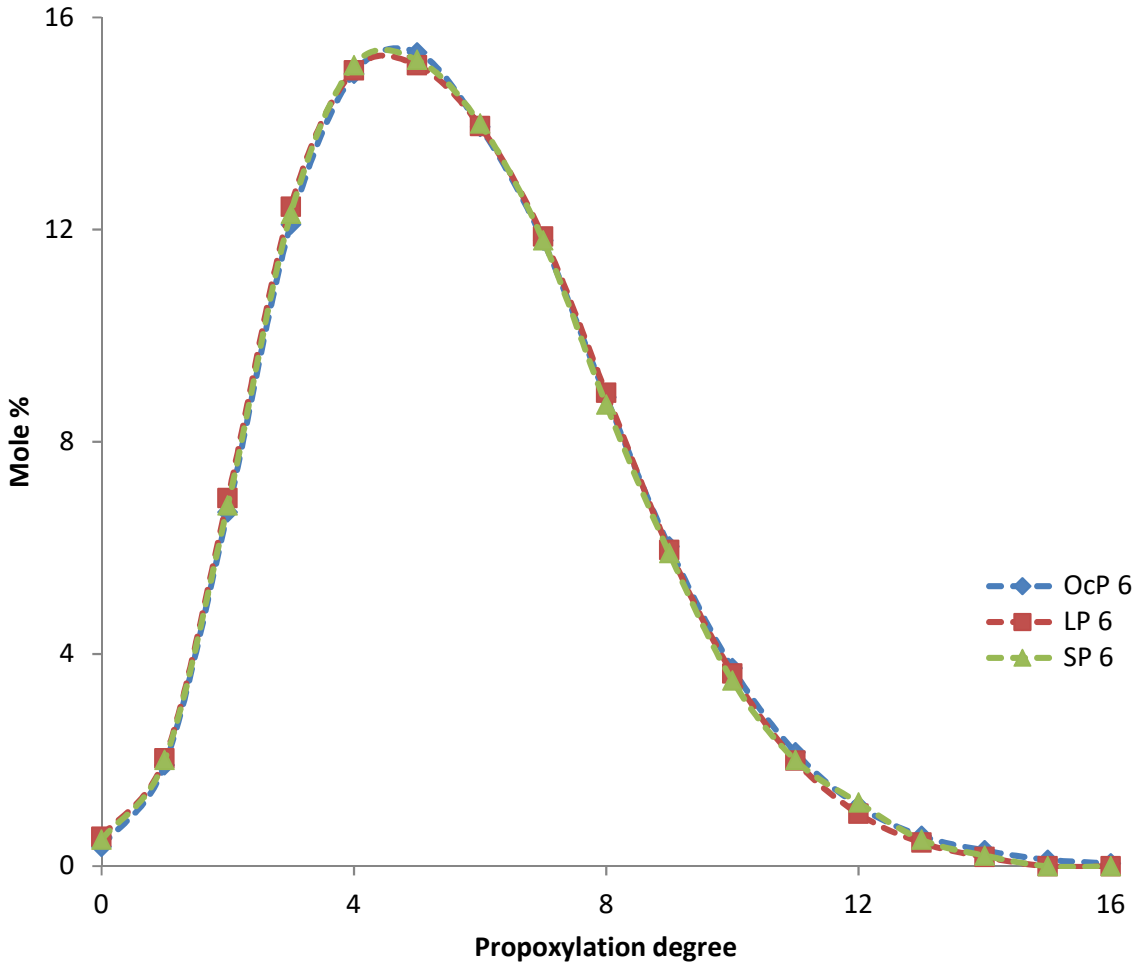

Figure IV-1: Distribution of the propoxylation degree of three different alcohols (octanol; dodecanol and octadecanol)

Out of Figure IV-1 it can be concluded that the molar mass distribution is not influenced by the used alcohol. All three distributions are very similar, therefore also the lengths of the different glycol units are also similar in this example.

Due to the constant reaction conditions for the propoxylation, it can be considered that the addition and the reaction rate of propylene oxide are also almost the same.

In Figure IV-2, three different propoxylation degrees of octadecanol are shown.

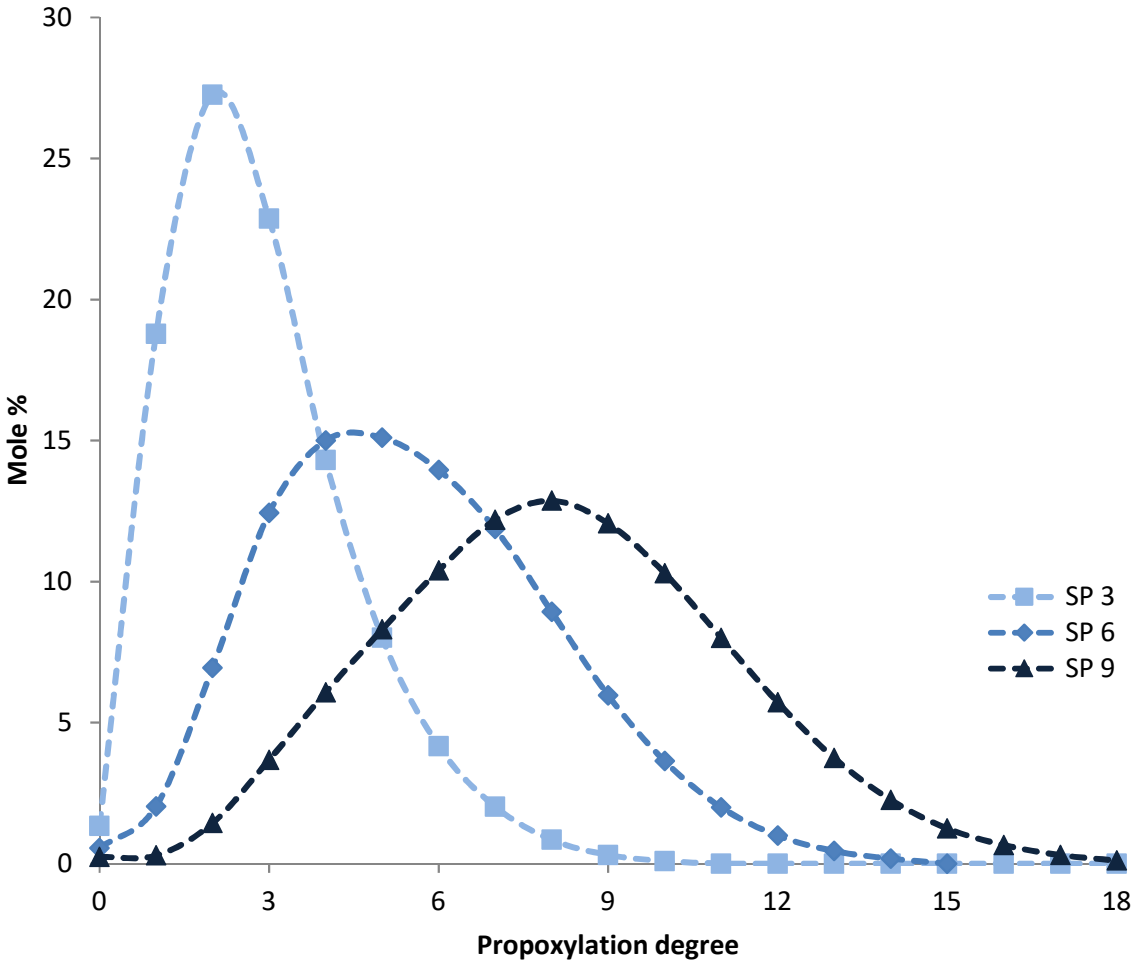

Figure IV-2: Three different propoxylation degrees (3, 6, and 9) of octadecanol

The shift of the distribution to higher oligomerisation degrees is clearly observable.

The propoxylation is characterised by the low amount of free alcohol and the narrow molar mass distribution. With higher PO-degrees, the amount of free alcohol equals zero. This is a clear contrast to ethoxylation. Figure IV-3 shows two different distributions of alkoxylations, ethoxylation and propoxylation.

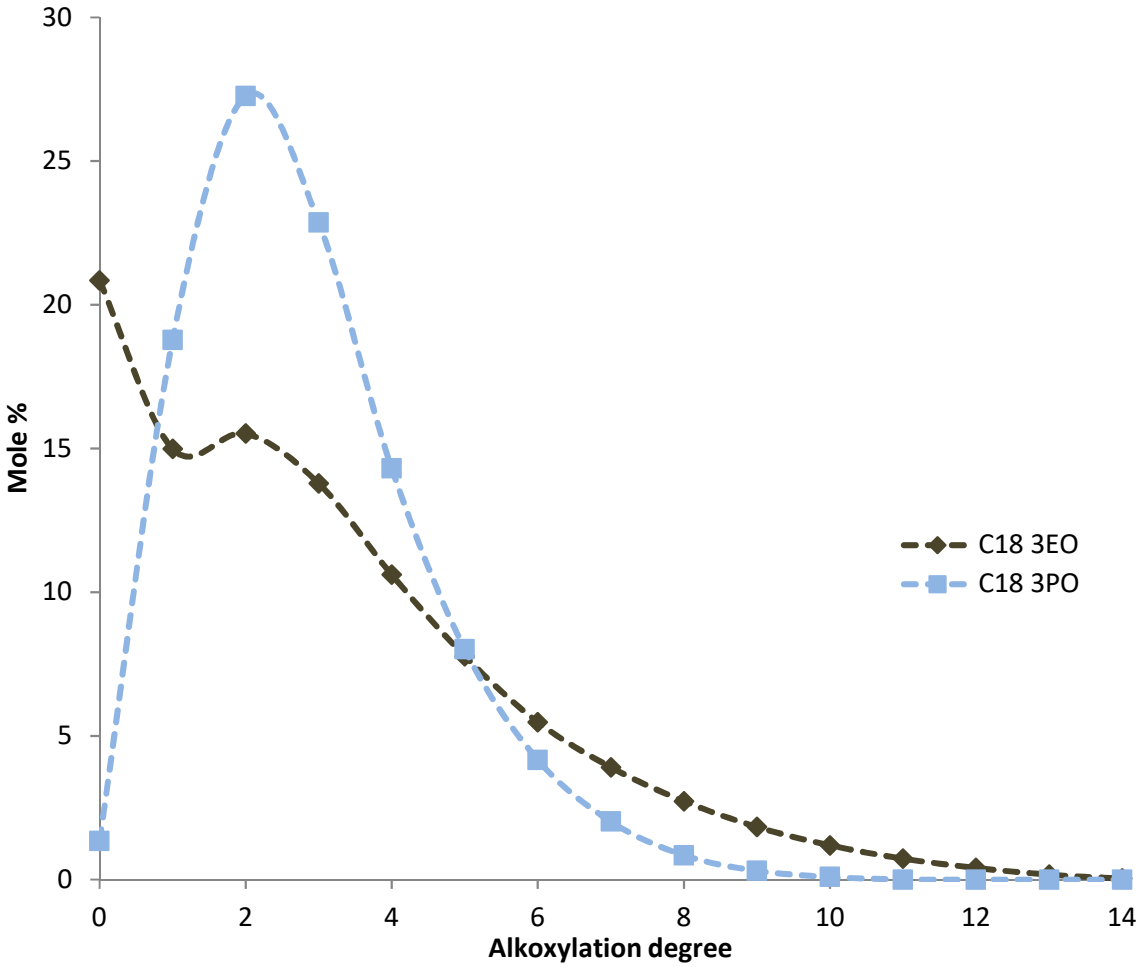

Figure IV-3: Comparison of ethoxylation and propoxylation

Figure IV-3 shows clearly the difference of the two different alkoxylations. The ethoxylation leads to much higher free alcohol amounts and broader distributions than the propoxylation, even with equal process circumstances.

The different selectivity of propylene oxide compared to ethylene oxide leads to this different molar mass distributions. As described in III.2.3, the addition of one mole propylene oxide leads to a primary and secondary alcohol, see Figure II-38. This secondary alcohol is less reactive than the primary one, so the second addition again leads to primary and secondary alcohol, see Figure II-39. With longer propylene oxide chains, the amount of primary alcohol equals zero. The result of this addition is a much narrower distribution than the ethoxylation. Here, only primary alcohols are formed, this results in a broader molar mass distribution and a much higher free alcohol content.

After the propoxylation, the conversion to the corresponding ethercarboxylic acid is followed. As mentioned in III.2.3, a high conversion degree is wanted, therefore the carboxymethylation is performed with a huge excess of sodium monochloroacetate and sodium hydroxide, 0.5 and 0.55 mol% excess based, on the moles of propoxylate. This leads to high conversions and a higher production of by-products, like glycolic and diglycolic acid. Besides this, the amount

of water and sodium chloride is still very high, directly after the neutralisation followed by phase separation, see Table IV-2.

	MeP 6	BuP 6	OcP 6	LP 6	SP 6	BP 6
C-chain	1	4	8	12	18	22
PO-degree	5.9	6.1	6.1	6.1	5.9	5.9
Water [ppm]	42298	32895	25841	18412	14289	13111
NaCl [ppm]	23985	19845	11128	10998	9541	6521
Glycolic acid [ppm]	12136	11896	10112	9745	9021	8412
Diglycolic acid [ppm]	42398	39874	25698	20368	18452	12365
Σ Impurities [ppm]	120817	104510	72779	59523	51303	40409

	SP 3	SP 9	SP 12	SP 15	SP 25	SP 50
C-chain	18	18	18	18	18	18
PO-degree	3.2	8.9	11.8	14.9	24.7	49.5
Water [ppm]	16235	12356	11025	10009	9263	8142
NaCl [ppm]	9993	9412	9025	8947	8145	7458
Glycolic acid [ppm]	9526	8587	8023	7825	7741	7152
Diglycolic acid [ppm]	20006	18256	17845	17214	16925	16596
Σ Impurities [ppm]	55760	48611	45918	43995	42074	39348

Table IV-2: Composition of the alkyl ether carboxylic acids, directly after synthesis, without any purification step

Both main side products, glycolic and diglycolic acid, are formed from the excess sodium monochloroacetate, Figure IV-4 and Figure IV-5.

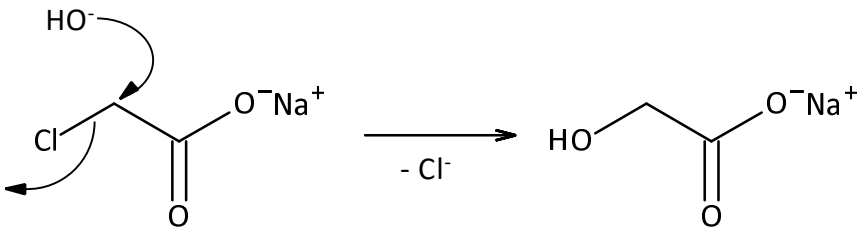

Figure IV-4: Formation of glycolic acid, caused by the hydrolysis of sodium monochloroacetate

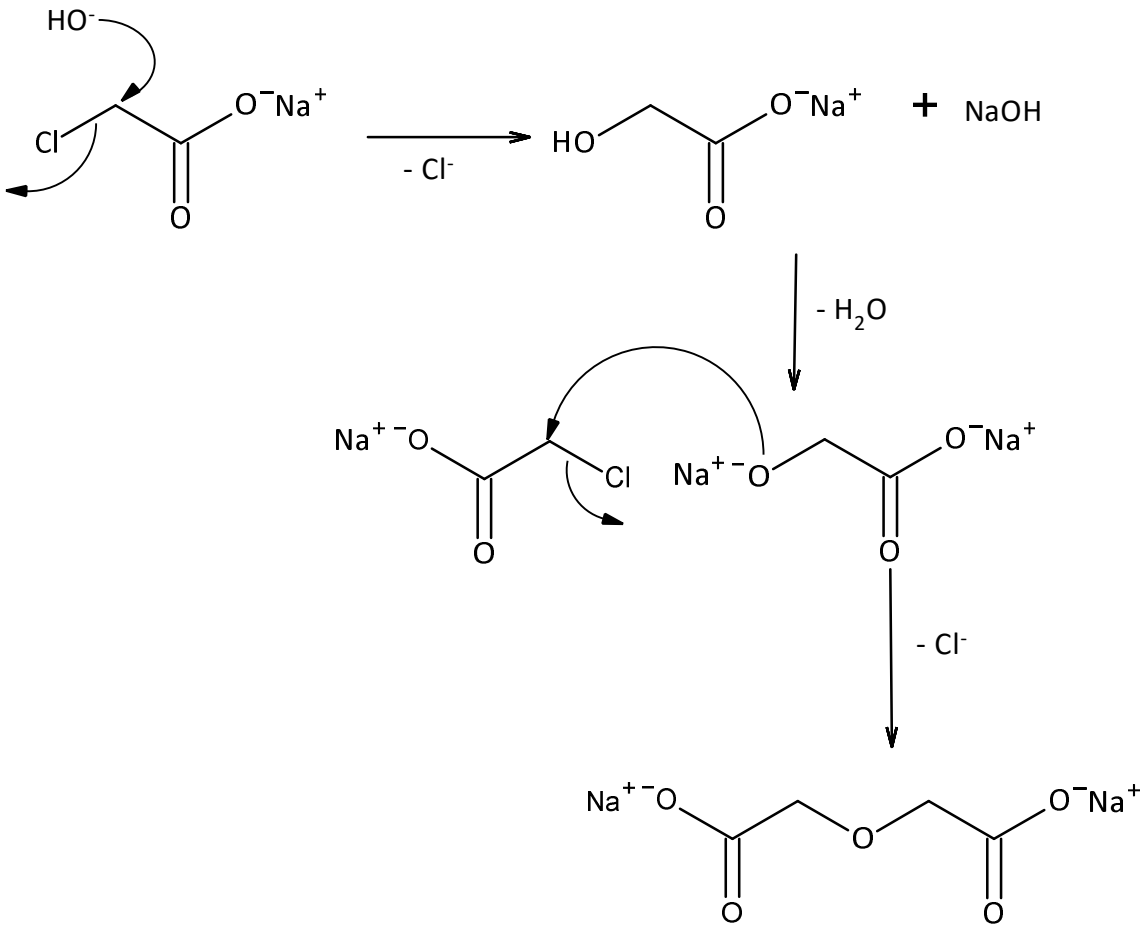

Figure IV-5: Formation of diglycolic acid, induced by condensation of glycolic acid and monochloroacetate

The higher amounts of water and sodium chloride are the consequence of the bad phase separation conditions.
After the second extraction step, using 1.5 times deionised water, based on the amount of the alkylether carboxylic acid, almost all impurities, sodium chloride, glycolic acid and diglycolic acid are removed. But the water content increases significantly, see Table IV-3.

	MeP 6	BuP 6	OcP 6	LP 6	SP 6	BP 6
C-chain	1	4	8	12	18	22
PO-degree	5.9	6.1	6.1	6.1	5.9	5.9
Water [ppm]	93269	52698	42159	32587	28895	23015
NaCl [ppm]	84	89	98	74	65	55
Glycolic acid [ppm]	22	31	29	38	29	22
Diglycolic acid [ppm]	42	45	39	35	39	46
Σ Impurities [ppm]	93417	52863	42325	32734	29028	23138

	SP 3	SP 9	SP 12	SP 15	SP 25	SP 50
C-chain	18	18	18	18	18	18
PO-degree	3.2	8.9	11.8	14.9	24.3	49.5
Water [ppm]	32320	29993	26519	23695	19002	15988
NaCl [ppm]	96	92	85	83	81	72
Glycolic acid [ppm]	20	16	26	31	19	21
Diglycolic acid [ppm]	29	36	43	39	27	26
Σ Impurities [ppm]	32465	30137	26673	23848	19129	16107

Table IV-3: Composition of the alkylether carboxylic acids after synthesis, directly after the second phase separation

To remove the residual by-products and water, all alkylether carboxylic acids are dehydrated via vacuum distillation at 15 mbar and 393.15 K.
The now dried remaining salts are precipitating and removed via filtration. The effectivity of this method can be seen in the analytical data in Table IV-4.

	MeP 6	BuP 6	OcP 6	LP 6	SP 6	BP 6
C-chain	1	4	8	12	18	22
PO-degree	5.9	6.1	6.1	6.1	5.9	5.9
Water [ppm]	1788	1986	2001	1846	1565	1018
NaCl [ppm]	75	86	76	56	53	41
Glycolic acid [ppm]	2	7	3	3	2	8
Diglycolic acid [ppm]	25	21	15	16	19	21
Σ Impurities [ppm]	1890	2100	2095	1921	1639	1088

	SP 3	SP 9	SP 12	SP 15	SP 25	SP 50
C-chain	18	18	18	18	18	18
PO-degree	3.2	8.9	11.8	14.9	24.3	49.5
Water [ppm]	1113	1478	1654	1521	1296	1034
NaCl [ppm]	56	52	49	41	36	26
Glycolic acid [ppm]	2	9	7	6	4	9
Diglycolic acid [ppm]	20	21	23	19	17	15
Σ Impurities [ppm]	1191	1560	1733	1587	1353	1084

Table IV-4: Composition of the alkylether carboxylic acids after the purification step

Besides the by-products included in the alkylether carboxylic acids, also esters and non-reacted PO-alcohol have to be taken into account. Esters are produced during the neutralisation and phase-separation step. Table IV-5 show the amount of esters and non-reacted PO-alcohol in the final products.

	MeP 6	BuP 6	OcP 6	LP 6	SP 6	BP 6
C-chain	1	4	8	12	18	22
PO-degree	5.9	6.1	6.1	6.1	5.9	5.9
Esters [%]	0.5	0.6	0.6	0.7	0.8	0.8
Free R-PO-OH [%]	2.4	1.8	1.2	0.9	2.1	1.1

	SP 3	SP 9	SP 12	SP 15	SP 25	SP 50
C-chain	18	18	18	18	18	18
PO-degree	3.2	8.9	11.8	14.9	24.3	49.5
Esters [%]	0.6	0.8	0.8	0.9	0.9	1.1
Free R-PO-OH [%]	1.7	2.1	1.1	0.7	0.5	2.3

Table IV-5: Amount of esters in the alkylether carboxylic acids

As described in III.2.2, the alkylether carboxylic acid was further purified using an ion exchange resin (Amberlyst A26). This treatment removes all neutral compounds, like esters and non-reacted PO alcohol. Besides this, also the amount of NaCl and water is lowered due to the additional distillation step, 15 mbar and 393.15 K, followed by filtration.
After all samples have been purified, the conversion degree to the alkyl ether carboxylic acid has been determined. Here, the already mentioned Epton (III.3.1) titration has been used. The conversions are listed in Table IV-6.

	MeP 6	BuP 6	OcP 6	LP 6	SP 6	BP 6
C-chain	1	4	8	12	18	22
PO-degree	5.9	6.1	6.1	6.1	5.9	5.9
Water [ppm]	1068	1125	1621	1387	1145	818
NaCl [ppm]	32	21	16	39	16	28
Glycolic acid [ppm]	5	11	9	6	7	11
Diglycolic acid [ppm]	29	27	19	23	24	25
Esters [%]	< 0.01	< 0.01	< 0.01	< 0.01	< 0.01	< 0.01
Free R-PO-OH [%]	< 0.01	< 0.01	< 0.01	< 0.01	< 0.01	< 0.01
R-PO-CH_2-COOH [%]	> 99.5	> 99.5	> 99.5	> 99.5	> 99.5	> 99.5

	SP 3	SP 9	SP 12	SP 15	SP 25	SP 50
C-chain	18	18	18	18	18	18
PO-degree	3.2	8.9	11.8	14.9	24.3	49.5
Water [ppm]	903	1023	1147	1092	977	824
NaCl [ppm]	28	31	25	23	19	15
Glycolic acid [ppm]	4	11	9	9	7	10
Diglycolic acid [ppm]	31	28	29	22	19	18
Esters [%]	< 0.01	< 0.01	< 0.01	< 0.01	< 0.01	< 0.01
Free R-PO-OH [%]	< 0.01	< 0.01	< 0.01	< 0.01	< 0.01	< 0.01
R-PO-CH_2-COOH [%]	> 99.5	> 99.5	> 99.5	> 99.5	> 99.5	> 99.5

Table IV-6: Compositions, remaining impurities and conversion degrees of the alkyl ether carboxylic acids

IV.1.1.2 Cationic Part

The second part of the Catanionics are the symmetric quaternary ammonium compounds. As mentioned in III.1, all three used components, TMAH [N_{1111}], TEAH [N_{2222}] and TBAH [N_{4444}], have been supplied by an external company (SACHEM B.V.) and can be used without further purification. The conversion degrees of the ammonium compounds have been checked and are listed in Table IV-7.

	TMAH [N_{1111}]	**TEAH [N_{2222}]**	**TBAH [N_{4444}]**
Conversion degree [%]	99.8	99.8	99.8

Table IV-7: Conversion degrees of the corresponding symmetric quaternary ammonium compounds

After finishing the preparation of the cationics and anionics, the actual synthesis of the Ionic Liquids is done, as described in III.2.3.

IV.1.1.3 Catanionic Part

For the calculation of the equimolar amounts, an accurate molar mass is needed. The cationic part is easy to calculate, due to the high purity, see Table IV-8.

	TMAH [N_{1111}]	**TEAH [N_{2222}]**	**TBAH [N_{4444}]**
Theoretical Mw [g/mol]	91.15	147.30	249.48
Achieved Mw [g/mol]	90.99	147.09	249.15
Deviation [%]	0.18	0.14	0.13

Table IV-8: Theoretical and calculated molar masses of the symmetric quaternary ammonium compounds

For the anionic part, alkyl ether carboxylic acid, the molar mass deviates more. This can be seen in Table IV-9.

	MeP 6	**BuP 6**	**OcP 6**	**LP 6**	**SP 6**	**BP 6**
Theoretical Mw [g/mol]	438.57	480.65	536.76	592.87	677.02	733.13
Achieved Mw [g/mol]	441.38	481.49	539.59	593.29	675.25	737.34
Deviation [%]	0.64	0.17	0.53	0.07	0.26	0.58

	SP 3	**SP 9**	**SP 12**	**SP 15**	**SP 25**	**SP 50**
Theoretical Mw [g/mol]	502.78	851.26	1025.50	1199.74	1780.54	3232.54
Achieved Mw [g/mol]	505.65	857.70	1022.73	1195.57	1779.89	3229.82
Deviation [%]	0.56	0.76	0.27	0.35	0.04	0.08

Table IV-9: Theoretical and calculated molar masses of the alkyl ether carboxylic acids

Table IV-9 shows that the deviation of the theoretical and the achieved molar mass can be up to 0.76 %. This deviation has to be taken into account for the calculation of the equimolar mixture for the Ionic Liquids.

The Ionic Liquids have been synthesised according to the method described in III.2.3. All water and NaCl amounts of the obtained Catanionics are below 1000 ppm.

All Ionic Liquids have water and sodium chloride contents lower than 1000 ppm, see Table IV-10.

Anionic	Cationic	H2O [ppm]	NaCl [ppm]
MeP 6	TMAH	975	22
	TEAH	955	19
	TBAH	941	18
BuP 6	TMAH	972	20
	TEAH	921	16
	TBAH	900	15
OcP 6	TMAH	868	13
	TEAH	869	10
	TBAH	888	11
LP 6	TMAH	855	20
	TEAH	841	26
	TBAH	891	24
SP 6	TMAH	860	15
	TEAH	851	14
	TBAH	799	13
BP 6	TMAH	805	23
	TEAH	812	20
	TBAH	803	18
Stearyl	TMAH	560	-
	TEAH	621	-
	TBAH	452	-
SP 3	TMAH	721	19
	TEAH	714	22
	TBAH	700	23
SP 9	TMAH	851	28
	TEAH	826	25
	TBAH	786	21
SP 12	TMAH	836	25
	TEAH	814	21
	TBAH	741	20
SP 15	TMAH	799	20
	TEAH	784	15
	TBAH	752	13
SP 25	TMAH	803	13
	TEAH	771	12
	TBAH	711	13
SP 50	TMAH	775	14
	TEAH	749	13
	TBAH	699	14

Table IV-10: Water and sodium chloride content of the synthesised Ionic Liquids

The detailed NMR-data are shown in the appendix.

IV.2. Properties of new Catanionics based on alkyl ether carboxylic acids and symmetric quaternary ammonium compounds

IV.2.1 Results and discussion of the physico-chemical properties

IV.2.1.1 Density

Density is one of the most often measured parameters for Ionic Liquids. It is needed for many calculations in the field of lubricants, e.g. construction of bearings etc.
In this investigation, the density is correlated to the different molecular structures of the synthesised Ionic Liquids. All data concerning the molar volumes can be found in the Appendix.
Besides the different cations, i.e. quaternary ammonium compounds, also the anions have been modified in various ways, C-chain lengths and PO-degree.
The following Figure IV-6, show the temperature dependence of the densities of the Ionic Liquids, where the anions consist of different C-chain lengths, constant PO-degree (PO = 6) and different cationics.

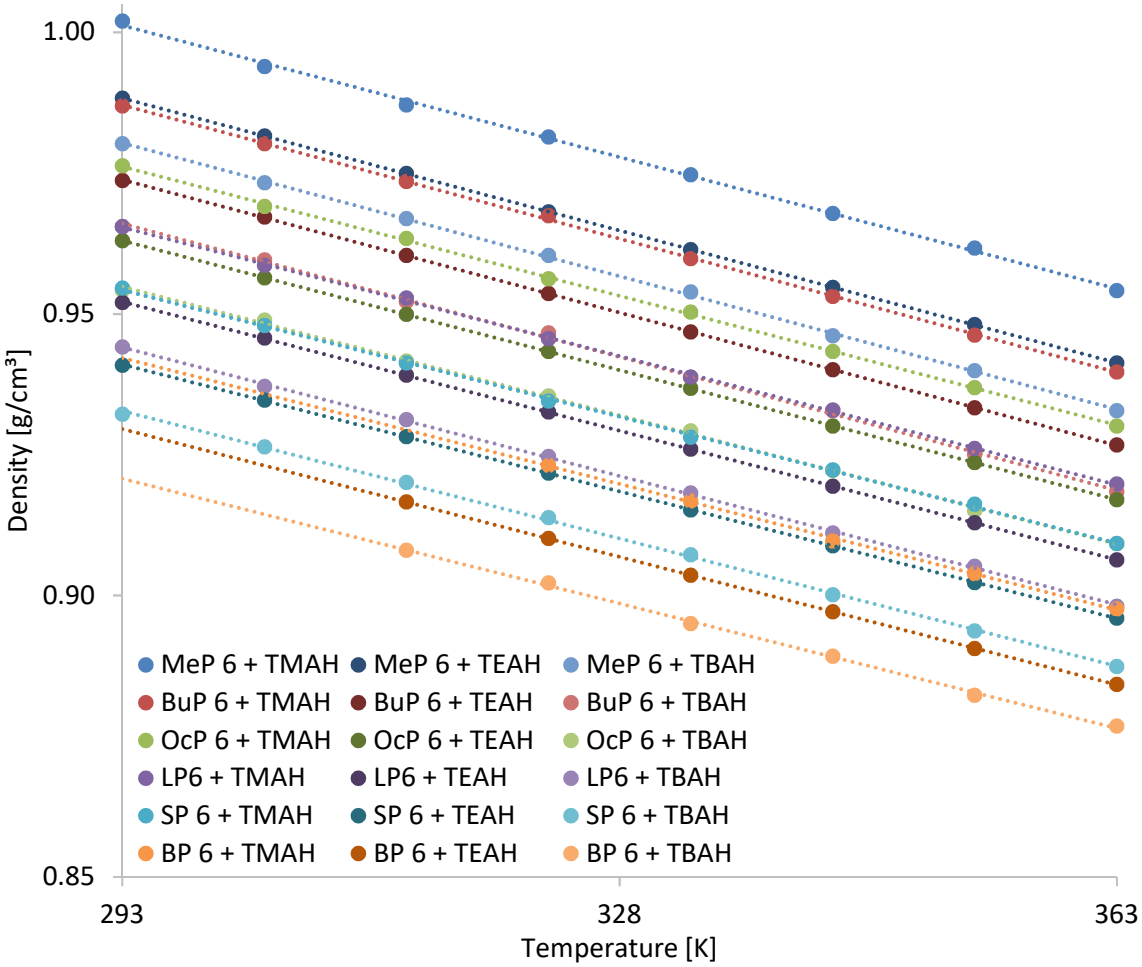

Figure IV-6: Effect of the alkyl chain lengths in the anion and the cation on the density at different temperatures

Out of this figure, it can be clearly seen that the density is linearly dependent on the temperature that means with higher temperature, the density decreases.

After set up linear equations, see Appendix, for each temperature dependence of the density of each Ionic Liquid, it can be concluded that the slope of each equation is -0.0007. So, the decrease is independent of the molecular structure.

Plotting the y-interception of the equations against the C-chain lengths of the anions, again a linear dependence can be seen, see Figure IV-7.

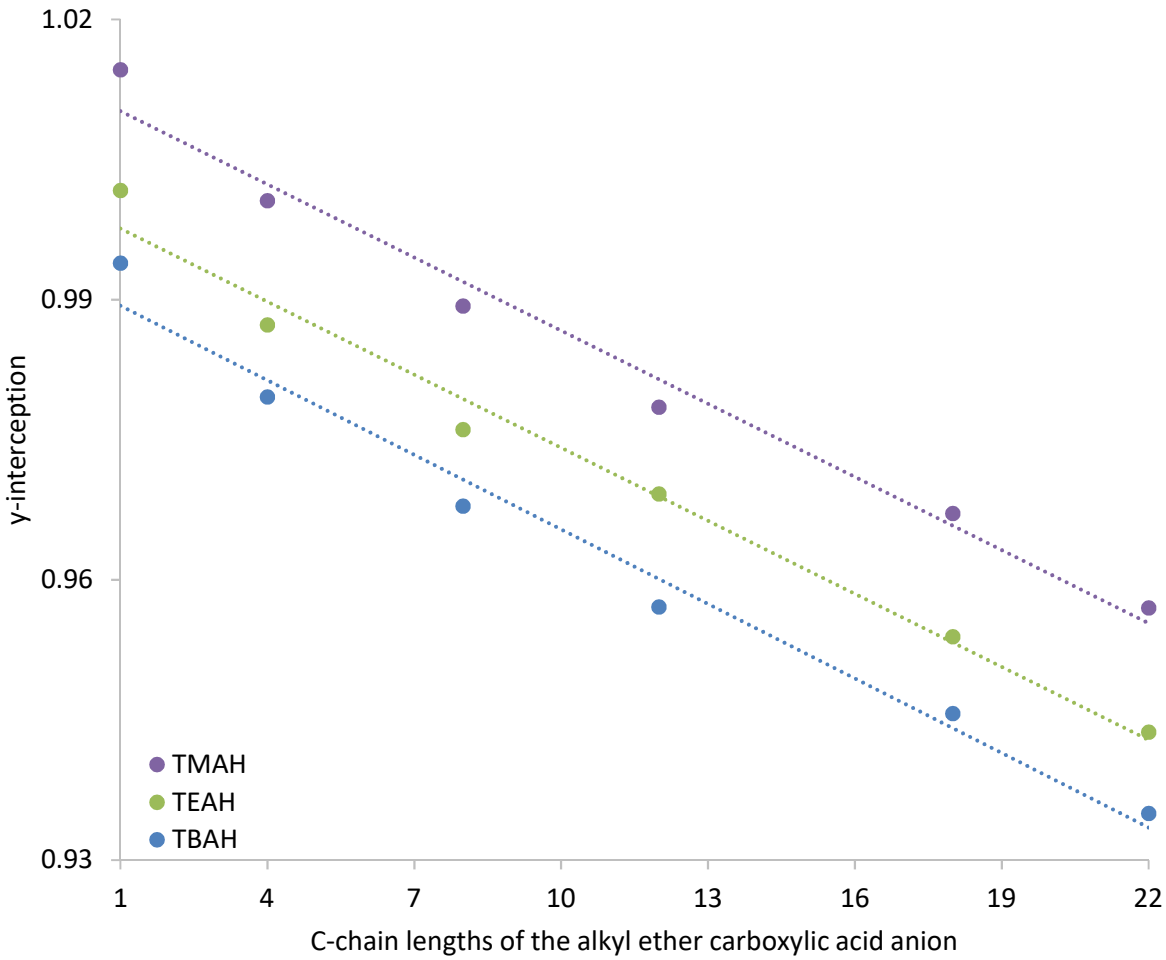

Figure IV-7: Plot of the different y-interceptions with different C-chain length of the anions

It can be concluded that the density is affected by the molecular weight of the Ionic Liquid. With higher weights, the density is lower. Also, the cations influence the density. Smaller cations, like TMAH or TEAH, still have a huge influence on the density. In contrast Ionic Liquids based on TBAH, show not such significant dependence. This dependence of the cation is already described in the article of Klein et al., they also found lower densities for following sequence: $[N_{4444}]$-TOTO < $[N_{3333}]$-TOTO < $[N_{2222}]$-TOTO [230]. From Figure IV-7, it can also be concluded that with longer C-chains the density decreases. This phenomenon has also been reported for different non-ionics based on EO [234].

Next, the molecular shape has been changed to constant C-chain (C_{18}) and different PO-degrees. Figure IV-8 shows the determined densities versus temperature.

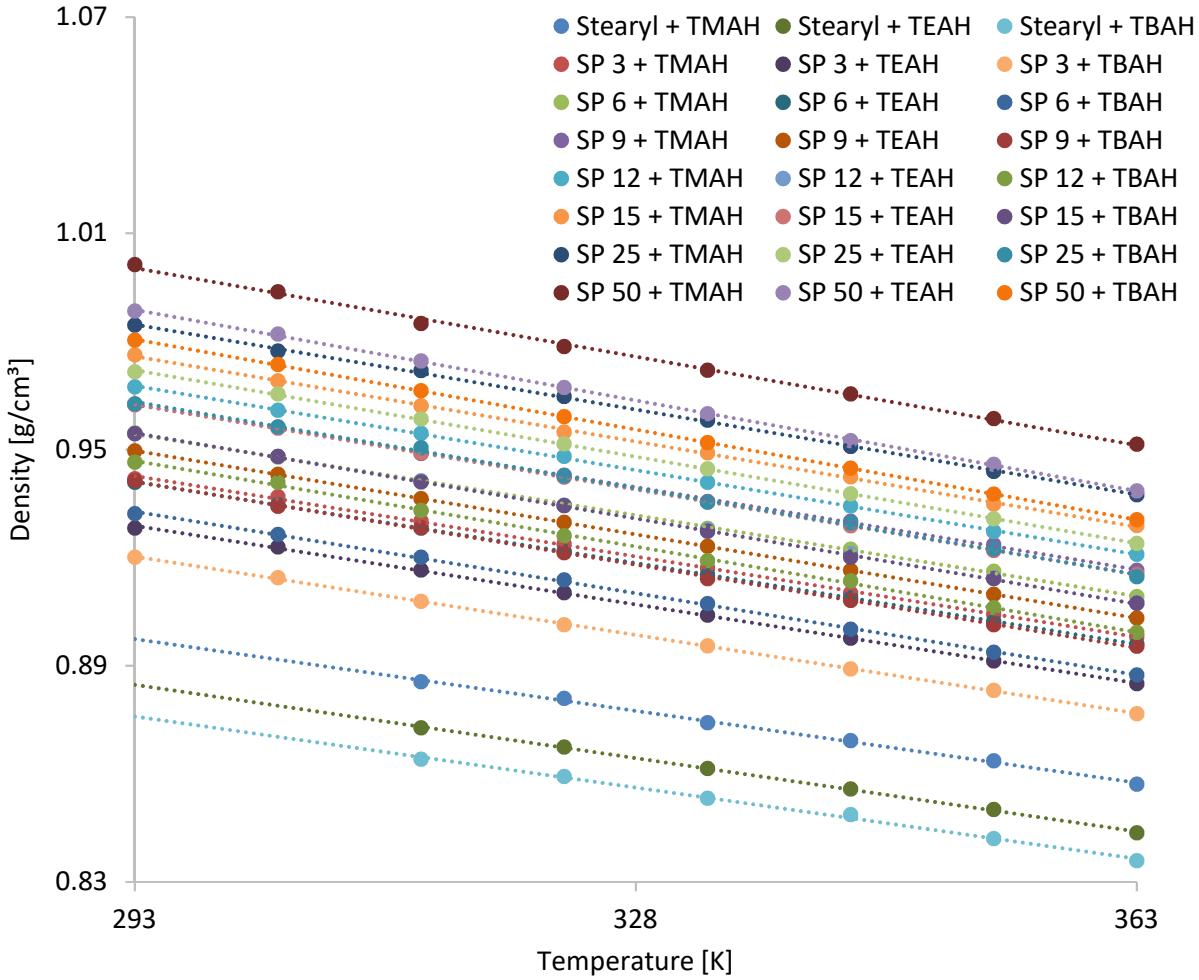

Figure IV-8: Effect of the PO-degree in the anion and of the cation on the density at different temperatures

Again, the linearity of the density as a function of temperature can be observed. In this case, the lower molar weight Ionic Liquids show lower density values than the higher molecular weight ones. The high flexibility of the polypropylene glycol chain in the molecule causes a denser arrangement in a specific volume. Therefore, more molecules are available in a constant volume, causing higher density values [234]. Also, the cations again are an important factor. With bigger cations the density becomes smaller.

If we again take the linear equations into account and we plot the y-interception against the PO-degrees, Figure IV-9 is obtained. Here, it can be concluded that the effect of the cation on the density is again decreasing with increasing cation and it also can be concluded that the PO-degree increases the density, but even with very high PO-degrees, like 25 or 50, the effect is not so high.

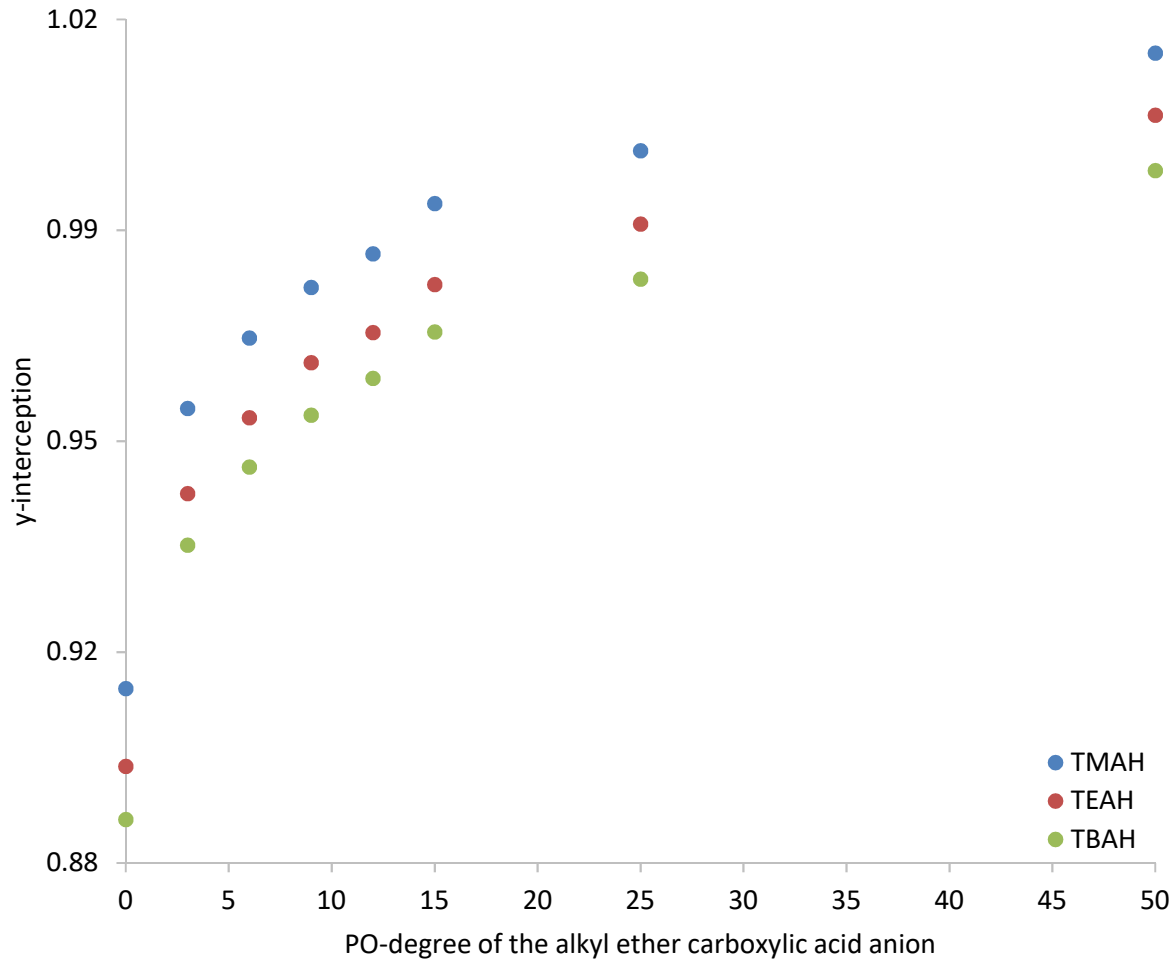

Figure IV-9: Plot of the different y-interceptions as a function of the different PO-degrees of the anions

With the determined density data, it is now possible to calculate the molar volume of the Ionic Liquids. The molar volume is necessary to calculate the molar conductivities ($10^4\ \Lambda_m$ / S m^2 mol^{-1}) which are needed for the Walden Plot in IV.2.1.2. All data concerning the molar volumes can be found in the Appendix. In the following table, Table IV-11, the molar weight, density and the molar volumes of the different Catanionics are depicted at 323 K. This temperature has been chosen, because density of all data Ionic Liquids are available.

Anionic	Cationic	Molar Weight [g/mol]	Density [g/cm³]	Molar Volume [cm³/mol]
MeP 6	TMAH	514.35	0.9814	524
	TEAH	570.45	0.9681	589
	TBAH	672.51	0.9604	700
BuP 6	TMAH	554.46	0.9674	573
	TEAH	610.56	0.9536	640
	TBAH	712.62	0.9466	753
OcP 6	TMAH	612.56	0.9562	641
	TEAH	668.66	0.9433	709
	TBAH	770.72	0.9354	824
LP 6	TMAH	666.26	0.9456	705
	TEAH	722.36	0.9326	775
	TBAH	824.42	0.9247	892
SP 6	TMAH	748.22	0.9345	801
	TEAH	804.32	0.9217	873
	TBAH	906.38	0.9138	992
BP 6	TMAH	810.31	0.9231	878
	TEAH	866.41	0.9101	952
	TBAH	968.47	0.9080	1073
Stearyl	TMAH	357.45	0.8809	406
	TEAH	413.55	0.8674	477
	TBAH	515.61	0.8593	600
SP 3	TMAH	578.62	0.9238	626
	TEAH	634.72	0.9103	697
	TBAH	736.78	0.9014	817
SP 9	TMAH	930.67	0.9429	987
	TEAH	986.77	0.9298	1061
	TBAH	1088.83	0.9214	1182
SP 12	TMAH	1095.70	0.9481	1156
	TEAH	1151.80	0.9345	1233
	TBAH	1253.86	0.9261	1354
SP 15	TMAH	1268.54	0.9549	1328
	TEAH	1324.64	0.9423	1406
	TBAH	1426.70	0.9344	1527
SP 25	TMAH	1852.86	0.9647	1921
	TEAH	1908.96	0.9516	2006
	TBAH	2011.02	0.9427	2133
SP 50	TMAH	3302.79	0.9786	3375
	TEAH	3358.89	0.9672	3473
	TBAH	3460.95	0.9591	3608

Table IV-11: Molar weights, densities and molar volumes at 323 K of the different Catanionics

IV.2.1.2 Viscosity and conductivity

For many applications, like dissolution or lubrication, which are classical applications of Ionic Liquids, the viscosity is a crucial factor. The range of viscosity of common Ionic Liquids varies from almost water to honey-like.

In the following part, the viscosity is determined and compared to the different molecular structures. The influences of C-chain, propoxylation degree as well of the different cations on the viscosity have been determined. The detailed values of the viscosity can be found in the Apendix.

In Figure IV-10, the viscosities of the Ionic Liquids with constant PO-degree and different C-chains are presented.

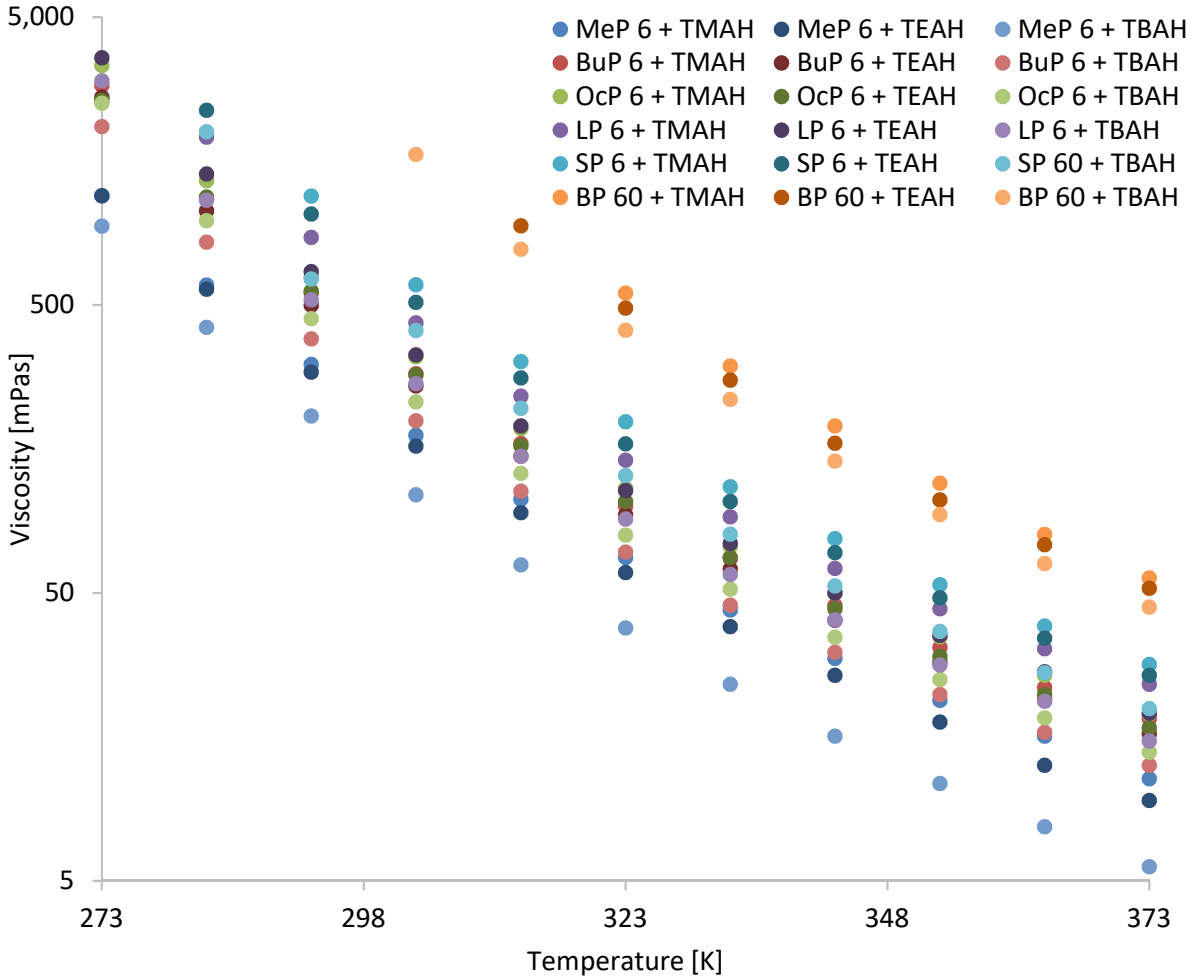

Figure IV-10: Temperature dependence of the viscosity of the different Ionic Liquids with a constant PO-degree (PO = 6)

In Figure IV-11, the viscosities of the different molecules with constant C-chain (C_{18}) and different PO-degrees as well as different cations are shown.

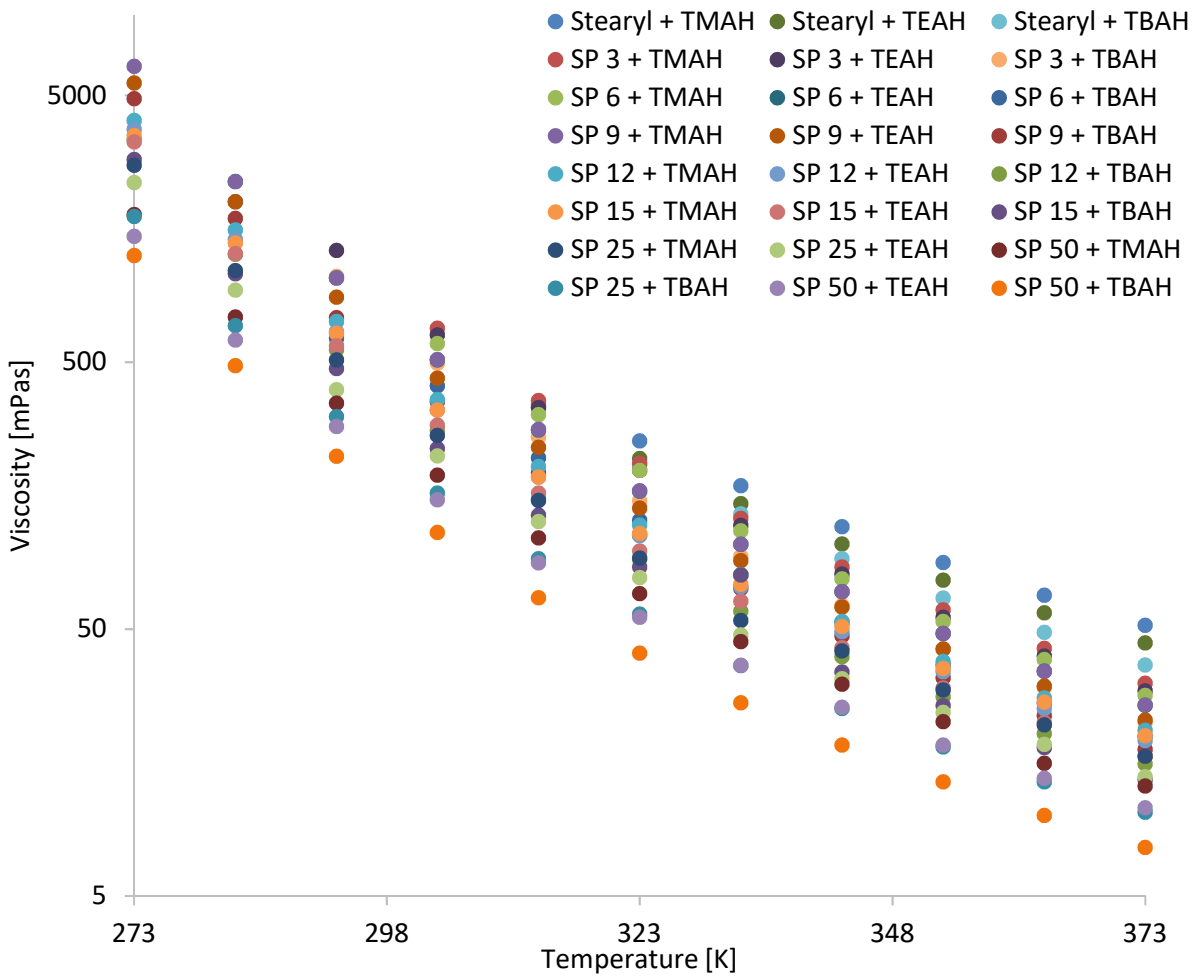

Figure IV-11: Viscosities of the different Ionic Liquids with a constant C-chain (C_{18}) and different PO-degrees and the cations

In general, the number of PO units, the chain length of the anion and the size of the cation have a significant influence on the viscosity. Three trends can be inferred: the shorter the C-chain of the anion or the more POs as well as the bigger the symmetric cation, the less viscous are the Ionic Liquids.

The higher viscosities of the longer C-chains are a result of the stronger intermolecular Van der Waals forces. With longer C-chains, the intermolecular friction is increased and this results in a higher viscosity. Especially the molecules based on MeP 6 show low viscosities, due to their reduced intermolecular friction between the single C-chain, see Figure IV-12.

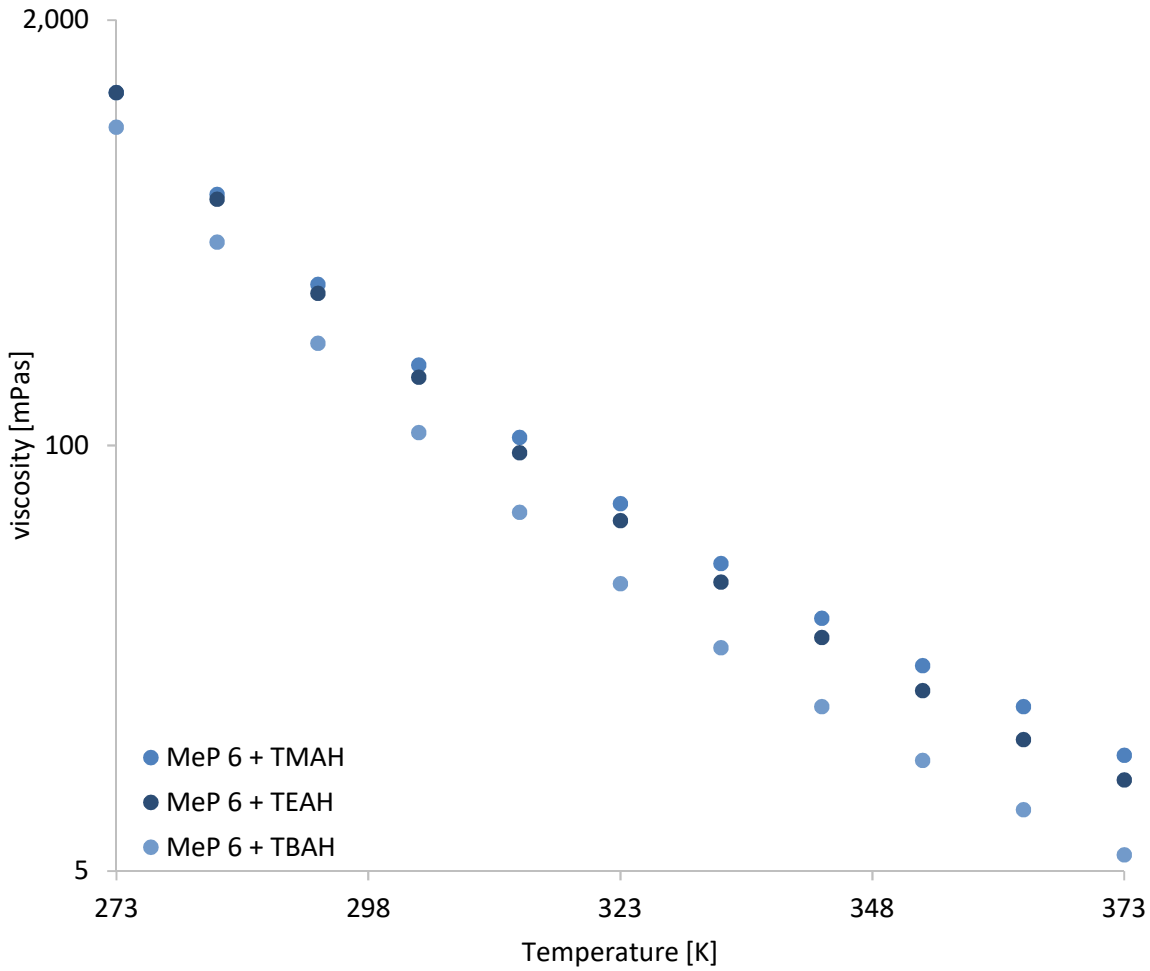

Figure IV-12: Viscosities of the Ionic Liquids based on C_1 6PO (MeP 6) with the three different symmetric cations

Particularly, the MeP 6 + TBAH shows very low values over the complete temperature range, 940 mPa s at 273.15 K, 205 mPa s at 293.15 K and 6 mPa s at 373.15 K.

The viscosity data of the Ionic Liquids could be described with the Vogel-Fulcher-Tamann equation, see Equation II-22. In the following Table IV-12, the corresponding three different constants are shown for the molecules based on constant propoxylation degree, PO = 6, various alkyl chains and different quaternary compounds.

Anionic	Cationic	η_0 [mPa s]	B	T_0 [K]
MeP 6	TMAH	0.007	1903.47	114.9
	TEAH	0.006	1887.76	119.4
	TBAH	0.003	1814.41	128.3
BuP 6	TMAH	0.087	1095.43	167.9
	TEAH	0.084	1079.01	168.9
	TBAH	0.071	1039.31	172.1
OcP 6	TMAH	0.091	1106.41	168.0
	TEAH	0.086	1089.67	168.9
	TBAH	0.073	1055.67	172.1
LP 6	TMAH	0.093	1128.64	169.5
	TEAH	0.087	1107.39	169.0
	TBAH	0.075	1070.37	172.1
SP 6	TMAH	0.095	1152.71	171.1
	TEAH	0.092	1139.91	170.9
	TBAH	0.076	1099.37	175.1
BP 6	TMAH	0.099	1193.95	184.6
	TEAH	0.097	1191.53	183.4
	TBAH	0.082	1080.80	183.0

Table IV-12: VFT parameters obtained from fits of temperature-dependent viscosity data, according to Equation II-22 for the Ionic Liquids with constant propoxylation degree, PO = 6, various alkyl chains and different quaternary compounds

The low intermolecular Van der Waals forces of the Ionic Liquids based on MeP 6 are reflected by the very different VFT-parameters. The η_0 and T_0 value are much lower, in contrast, the B value is up to two times higher.

It has been shown that three-dimensional networking in sodium alkyl ether carboxylates generates very high viscosities [229,235]. Especially in the case of alkali cations the resulting viscosities are high, e.g. Na-TOTO is ~95.000 mPa s at 303 K [229]. If quaternary ammonium compounds are used together with TOTO, the viscosity decreases significantly [230]. In the investigation of Klein et al., it was found that smaller quaternary ammonium compounds in combination with TOTO are leading to lower viscosities, in following sequence $[N_{2222}]$-TOTO < $[N_{3333}]$-TOTO < $[N_{4444}]$-TOTO. This sequence has not been found within this investigation.
Figure IV-13, the viscosity of SP 50 (C_{18} 50 PO) with the different symmetric cations is plotted against temperature.

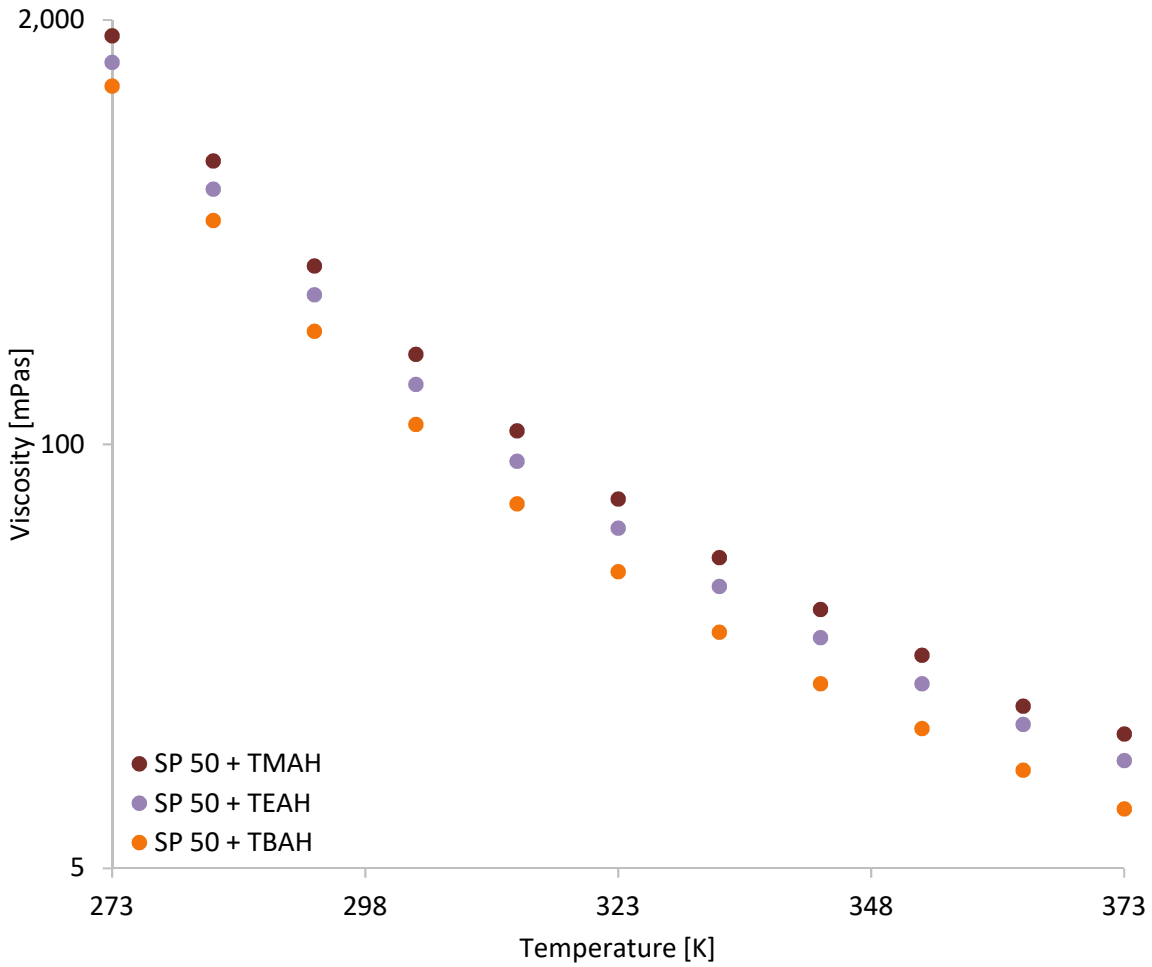

Figure IV-13: Viscosities of the Ionic Liquids based on C_{18} 50 PO (SP 50) with the three different symmetric cations

Particularly, the SP 50 + TBAH shows very low values over the complete temperature range, 1250 mPa s at 273.15 K, 220 mPa s at 298.15 K and 8 mPa s at 373.15 K.

The comparatively smaller TMAH and TEAH cations may fit in the meshes, in which TBAH with the four hydrophobic chains is prone to destroy these networks. In consequence, the relative displacement of molecules in the mixture is facilitated, resulting in low viscosities. TBAH has, in contrast to, e.g. tetraethanolamine, no OH-groups, therefore no intermolecular interactions, like H-bonds, are possible. Hence, the cohesive energy of the system is lowered, implicating lower viscosities.

The impact of the PO-chain can be easily explained by their high flexibility and mobility. This phenomenon is described in the **CO**ncept of **M**elting **P**oint **L**owering due to **E**thoxylation (COMPLETE) [231]. The effect of propylene oxide might be even higher compared to ethylene oxide, due to the additional methyl group. This part increases the steric hindrance, resulting in even higher flexibility and mobility. The intermolecular orientation might be disturbed and the formation of H-bonds are hindered. As a result, with increased PO-degree, the entropy of the system is increased. An evidence for this statement is the decrease of viscosity with longer PO-degrees, see Figure IV-14.

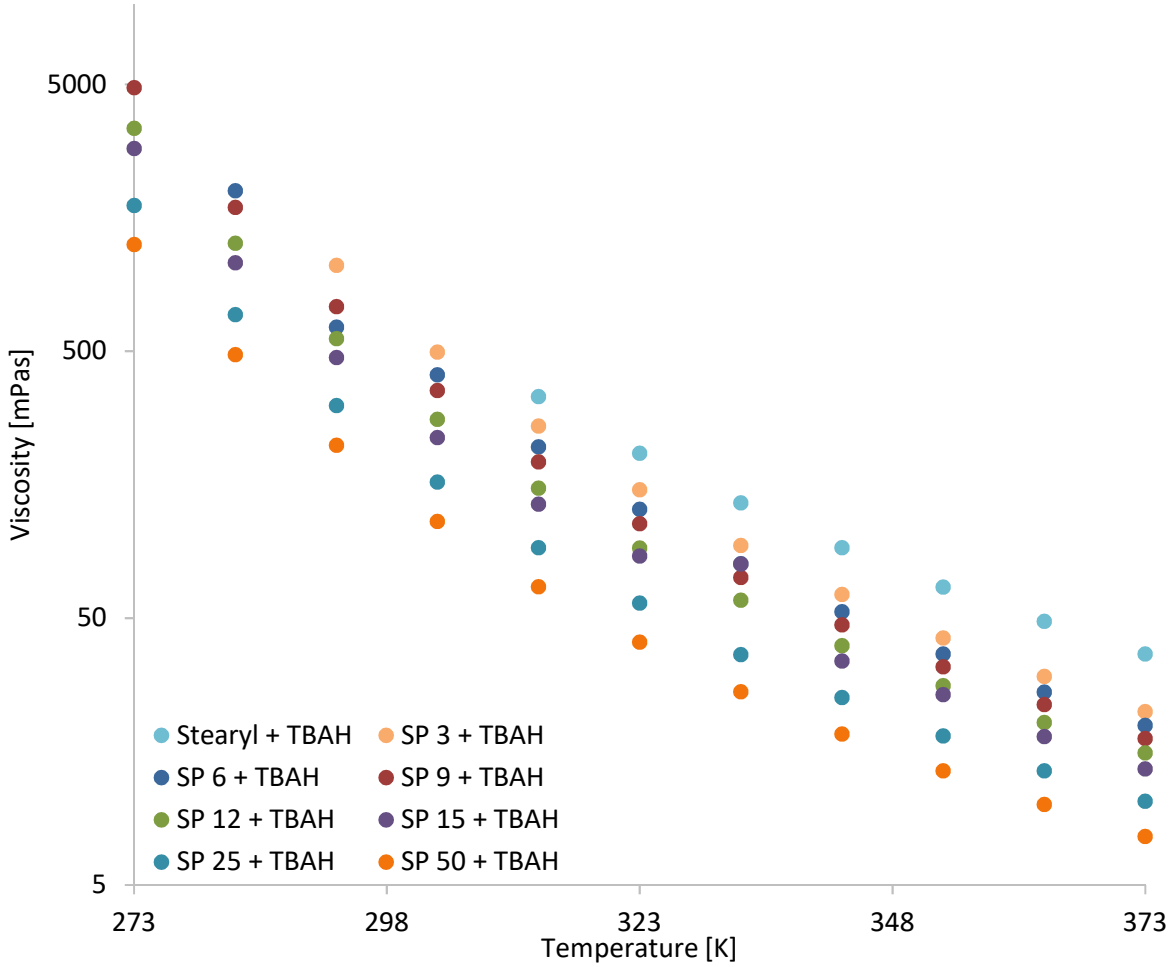

Figure IV-14: Viscosities of the Ionic Liquids based on TBAH as cation and alkylether carboxylic acids based on C_{18} with various PO-degrees

In the next table, Table IV-13, also the VFT parameter are given for the molecules with constant alkyl chain (C_{18}) with different PO-degrees and quaternary ammonium compounds.

Anionic	Cationic	η_0 [mPa s]	B	T_0 [K]
Stearyl	TMAH	0.227	905.82	202.7
	TEAH	0.192	889.56	204.8
	TBAH	0.182	841.14	209.4
SP 3	TMAH	0.097	1164.64	171.4
	TEAH	0.095	1151.25	172.4
	TBAH	0.082	1108.27	176.3
SP 6	TMAH	0.095	1152.71	171.1
	TEAH	0.092	1139.91	170.9
	TBAH	0.076	1099.37	175.1
SP 9	TMAH	0.092	1139.51	170.9
	TEAH	0.089	1119.59	171.4
	TBAH	0.075	1076.89	175.9
SP 12	TMAH	0.090	1105.43	169.9
	TEAH	0.087	1089.65	171.0
	TBAH	0.074	1055.26	174.9
SP 15	TMAH	0.089	1099.99	169.2
	TEAH	0.085	1057.11	173.3
	TBAH	0.073	1029.99	175.8
SP 25	TMAH	0.085	1074.21	169.7
	TEAH	0.080	1034.99	172.6
	TBAH	0.068	991.31	175.6
SP 50	TMAH	0.078	1038.71	169.7
	TEAH	0.073	1001.27	172.3
	TBAH	0.062	936.46	178.7

Table IV-13: VFT parameters, calculated according to Equation II-27 for the Ionic Liquids with constant alkyl chain (C_{18}) with different PO-degrees and quaternary ammonium cations

Again, the molecule without PO, stearic acid, shows different η_0, B and T_0 values. Due to the higher viscosities of the molecules based on stearic acid, η_0 and T_0 have much higher values than the Ionic Liquids based on PO. In contrast, the B values are lower.

Further to the viscosities, also the conductivity of the Ionic Liquids has been determined. In Figure IV-15 the conductivities of the different Ionic Liquids based on different C-chains with constant PO-degree (PO = 6) are shown. The detailed values are given in the Appendix.

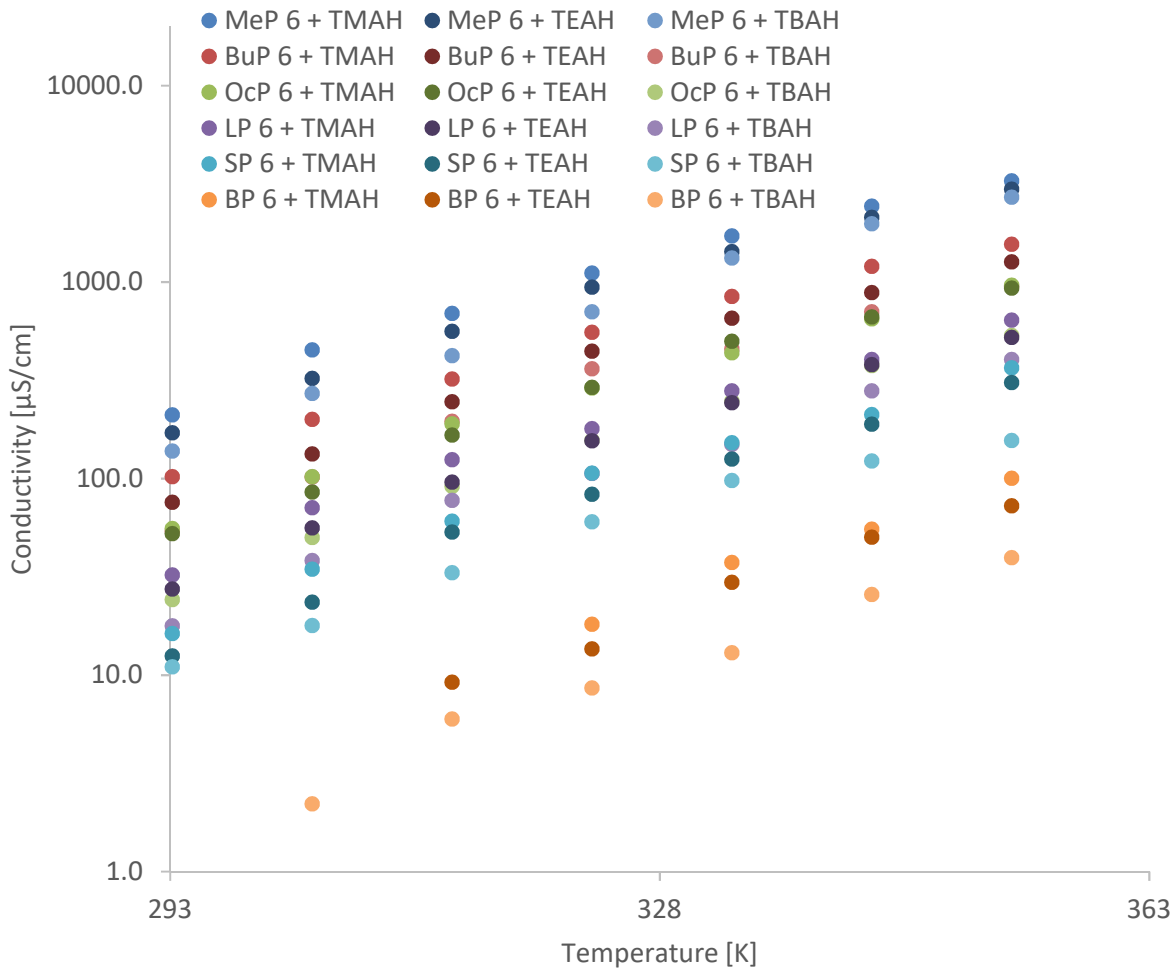

Figure IV-15: Temperature dependence of the conductivity of the different Ionic Liquids with a constant PO-degree (PO = 6) and different C-chains

Out of both figures, it can be concluded that the conductivities of the present Ionic Liquids are in the range of 1 to 3000 µS / cm. Typical values of imidazolium based Ionic Liquids are around 1000 µS / cm, meaning thousand or three orders of magnitude higher. This leads to the conclusion that the conductivity is strongly affected by the C-chain. The Ionic Liquids based on Methanol (C_1) show again different behaviour, compared to the other Ionic Liquids. The three Ionic Liquids exhibit remarkably higher conductivity values, compared to the molecules based on a longer alkyl chain. The C_{18} based Ionic Liquid has a conductivity of 11 µS / cm at 298 K, but the C_1 based Ionic Liquid 211 µS / cm, so around 20 times higher.

Also the influence of the different quaternary ammonium molecules can be deduced. It is found that with increasing quaternary ammonium molecule, the conductivity decreases. This phenomenon has also been found in the investigation of Klein et al [230]. In this article the conductivity has been shown to follow the series of $[N_{2222}]$-TOTO >> $[N_{3333}]$-TOTO > $[N_{4444}]$-TOTO. The here investigated Ionic Liquids show the same behaviour, TMAH > TEAH >> TBAH. The smaller quaternary ammonium molecules seem not to form three-dimensional networks, i.e. Na-TOTO [229]. As already mentioned, the propylene oxide units are strongly disturbing the formation of a three-dimensional network.

In Figure IV-16 the conductivities of the Ionic Liquids with constant C-chain (C_{18}) and different PO-degrees are shown as a function of temperature.

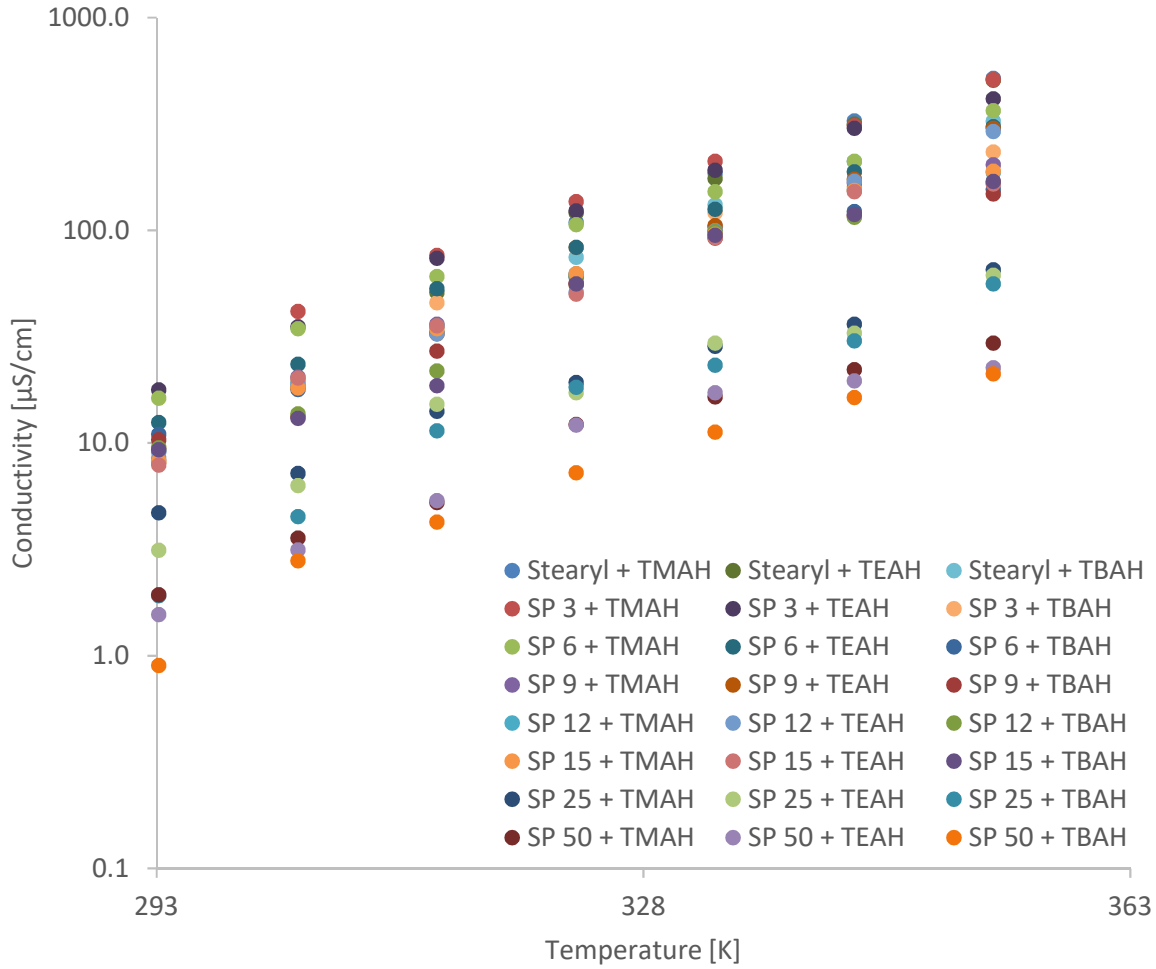

Figure IV-16: Temperature dependence of the conductivity of the different Ionic Liquids with a constant C-chain (C_{18}) and different PO-degrees

Also from this figure it can be concluded that the conductivity is influenced by the PO-degree of the Ionic Liquids. The higher the PO-degree, the lower the conductivity. This effect is smaller until PO = 15 is reached, and with PO = 25 and 50, the conductivity is significantly lower.

As for the viscosity, also for the conductivities, the Vogel-Fulcher-Tamann equation can be used for the fitting of the data, see Equation IV-1.

$$\kappa = \kappa_0 \cdot e^{\left(\frac{B}{T-T_0}\right)} \qquad \textbf{Equation IV-1}$$

The VFT-parameters for the different Ionic Liquids are presented in Table IV-14 and Table IV-15. In Table IV-14, the molecules based on different alcohols with a constant PO-degree (PO = 6) are presented.

Anionic	Cationic	κ_0 [µS/cm]	B	T_0 [K]
MeP 6	TMAH	10321755.32	1905.45	115.8
	TEAH	9668420.21	1862.76	121.1
	TBAH	8095000.21	1805.35	127.5
BuP 6	TMAH	651434.24	1087.44	169.4
	TEAH	505302.96	1079.44	170.4
	TBAH	459488.21	1038.44	178.4
OcP 6	TMAH	390305.24	1109.44	167.5
	TEAH	358914.13	1086.53	170.0
	TBAH	204623.43	1044.64	177.6
LP 6	TMAH	245120.21	1127.43	166.4
	TEAH	223461.53	1109.46	170.0
	TBAH	140441.26	1059.43	174.3
SP 6	TMAH	160565.56	1145.76	165.0
	TEAH	117950.13	1127.76	167.4
	TBAH	80319.24	1083.45	172.0
BP 6	TMAH	34753.98	1167.66	163.0
	TEAH	25399.32	1146.54	168.4
	TBAH	15379.12	1109.41	175.9

Table IV-14: VFT-parameter of the different Ionic Liquids based on different alcohols with constant PO-degree (PO = 6)

In Table IV-15, the VFT-parameters for the Ionic Liquids with constant C-chain (C_{18}) and different PO-degrees are depicted.

Anionic	Cationic	κ_0 [µS/cm]	B	T_0 [K]
Stearyl	TMAH	804517.28	1941.26	96.7
	TEAH	694393.26	1911.70	102.0
	TBAH	520242.36	1897.55	107.4
SP 3	TMAH	192025.23	1125.23	166.0
	TEAH	159479.65	1107.65	170.0
	TBAH	92450.36	1075.00	174.4
SP 6	TMAH	160565.56	1145.76	165.0
	TEAH	117950.13	1127.76	167.4
	TBAH	80319.24	1083.45	172.0
SP 9	TMAH	110472.94	1164.97	162.7
	TEAH	88436.18	1149.92	165.0
	TBAH	73199.99	1107.17	169.9
SP 12	TMAH	90454.00	1182.20	160.3
	TEAH	80414.99	1156.16	163.2
	TBAH	70362.92	1111.23	168.0
SP 15	TMAH	72232.61	1206.17	158.2
	TEAH	79391.49	1168.49	161.2
	TBAH	68333.16	1138.49	166.0
SP 25	TMAH	33143.89	1241.26	155.1
	TEAH	31333.49	1204.68	158.9
	TBAH	21287.16	1179.16	162.7
SP 50	TMAH	16341.22	1271.16	152.8
	TEAH	12062.16	1221.62	155.0
	TBAH	9139.16	1202.93	162.0

Table IV-15: VFT-parameters of the different Ionic Liquids based on constant C-chain (C_{18}) and different PO-degrees

In case of the viscosity and the conductivity, it could be concluded that the present Ionic Liquids show a very weak three dimensional network, resulting in low viscosities and lower conductivities. The Walden plot can be used, here the association of cations with anions can be quantified, as suggested by Angell and co-workers [235,236].

The Walden rule relates the ionic mobility, represented by the molar conductivity Λ, to the fluidity, 1/η, of the medium. If the ions could move independently from their next neighbours, i.e. the salt is fully dissociated, the plot would give a line, such as for dilute aqueous potassium chloride solutions. In turn, if ion-pairs are formed, the movement of the distinct ions will be correlated. Consequently, a negative deviation of the ideal line should be detected.

The resulting Walden plots for the present Ionic Liquids are given in Figure IV-17 for the molecules based on different alcohols with constant PO-degree (PO = 6), and in Figure IV-18, for the molecules with constant C-chain (C_{18}) and different PO-degrees.

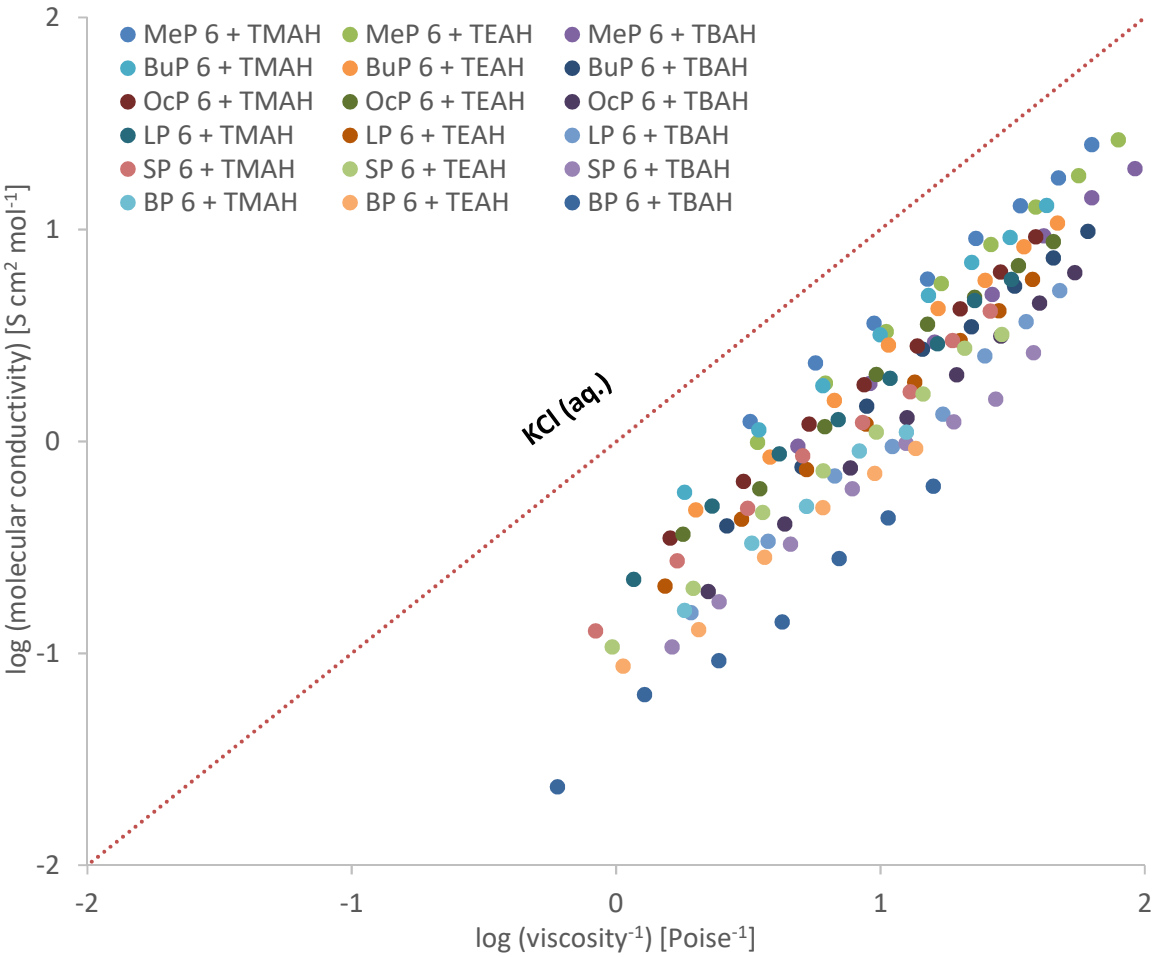

Figure IV-17: Walden plot for the molecules based on different alcohols with constant PO-degree (PO = 6)

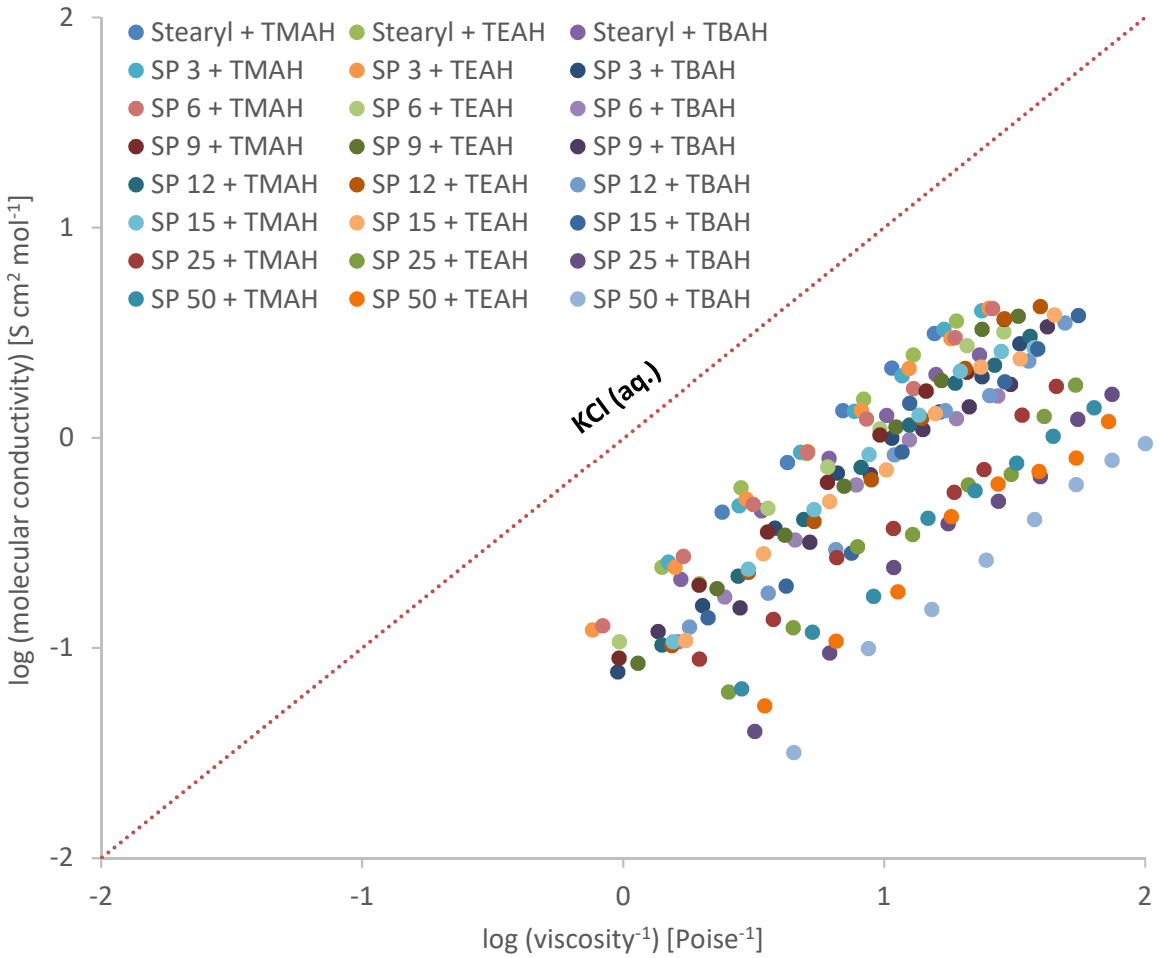

Figure IV-18: Walden plot for the molecules with constant C-chain (C_{18}) and different PO-degrees

Besides the Walden plots, also the ΔW values have been calculated, see Table IV-16 and Table IV-17. Angell and co-workers classified Ionic Liquids as "good" and "poor", according to a small or large vertical deviation, ΔW, of the ideal KCl line, respectively. ΔW denotes the vertical distance to the KCl line, and it is used to define the extent, to which a fluid is ionic. Ionic Liquids with small ΔW (ΔW < 1), close to the KCl line, combine high fluidities with high conductivities and are therefore referred to as "good" Ionic Liquids. Such molecules are additionally featured by low vapour pressures [235,236].

			T [K]							
	Anionic	**Cationic**	**293.15**	**303.15**	**313.15**	**323.15**	**333.15**	**343.15**	**353.15**	**363.15**
ΔW	MeP 6	TMAH	0.41	0.38	0.42	0.41	0.40	0.42	0.43	0.40
		TEAH	0.54	0.52	0.50	0.49	0.49	0.48	0.50	0.48
		TBAH	0.71	0.69	0.74	0.73	0.65	0.65	0.68	0.66
	BuP 6	TMAH	0.50	0.49	0.52	0.50	0.49	0.50	0.52	0.53
		TEAH	0.63	0.66	0.63	0.58	0.59	0.64	0.62	0.64
		TBAH	0.82	0.83	0.78	0.72	0.80	0.78	0.79	0.80
	OcP 6	TMAH	0.66	0.67	0.65	0.67	0.68	0.69	0.65	0.62
		TEAH	0.69	0.77	0.72	0.67	0.63	0.68	0.69	0.71
		TBAH	1.06	1.03	1.01	0.99	0.98	0.96	0.95	0.94
	LP 6	TMAH	0.72	0.67	0.68	0.74	0.74	0.76	0.69	0.73
		TEAH	0.87	0.84	0.85	0.86	0.85	0.83	0.83	0.81
		TBAH	1.09	1.05	0.99	1.07	1.11	0.99	0.99	0.97
	SP 6	TMAH	0.82	0.79	0.81	0.78	0.84	0.88	0.80	0.80
		TEAH	0.96	0.99	0.89	0.92	0.94	0.94	0.88	0.95
		TBAH	1.18	1.15	1.15	1.12	1.11	1.19	1.24	1.16
	BP 6	TMAH	-	-	-	1.06	0.99	1.03	0.97	1.05
		TEAH	-	-	1.09	1.20	1.11	1.10	1.13	1.17
		TBAH	-	1.41	1.30	1.42	1.48	1.40	1.39	1.41

Table IV-16: ΔW values for the Ionic Liquids based on different alcohols and constant PO-degree (PO = 6)

			T [K]							
	Anionic	**Cationic**	**293.15**	**303.15**	**313.15**	**323.15**	**333.15**	**343.15**	**353.15**	**363.15**
ΔW	Stearyl	TMAH	-	-	-	0.73	0.75	0.71	0.70	0.70
		TEAH	-	-	0.76	0.69	0.78	0.74	0.72	0.72
		TBAH	-	-	0.89	0.88	0.89	0.90	0.90	0.97
	SP 3	TMAH	-	0.76	0.77	0.75	0.76	0.77	0.71	0.77
		TEAH	0.80	0.81	0.76	0.77	0.78	0.77	0.78	0.79
		TBAH	1.09	1.10	1.01	0.99	1.03	1.09	1.08	1.07
	SP 6	TMAH	0.82	0.79	0.81	0.78	0.84	0.88	0.80	0.80
		TEAH	0.96	0.99	0.89	0.92	0.94	0.94	0.88	0.95
		TBAH	1.18	1.15	1.15	1.12	1.11	1.19	1.24	1.16
	SP 9	TMAH	1.03	0.99	1.00	0.99	0.97	0.94	1.00	0.90
		TEAH	1.13	1.08	1.08	1.08	0.99	0.95	0.86	0.94
		TBAH	1.06	1.26	1.21	1.12	1.11	1.18	1.23	1.10
	SP 12	TMAH	1.13	1.10	1.08	1.05	1.04	1.01	1.08	1.08
		TEAH	1.18	1.12	1.13	1.15	1.05	0.98	0.90	0.97
		TBAH	1.15	1.29	1.35	1.12	1.10	1.20	1.19	1.15
	SP 15	TMAH	1.16	1.10	1.07	1.02	1.03	0.97	1.04	1.15
		TEAH	1.20	1.09	1.10	1.16	1.08	1.03	1.15	1.07
		TBAH	1.18	1.32	1.42	1.14	0.93	1.20	1.17	1.16
	SP 25	TMAH	1.34	1.44	1.39	1.47	1.53	1.53	1.42	1.41
		TEAH	1.61	1.56	1.42	1.57	1.55	1.66	1.51	1.48
		TBAH	1.90	1.81	1.65	1.65	1.74	1.78	1.65	1.67
	SP 50	TMAH	1.65	1.65	1.71	1.55	1.60	1.63	1.64	1.66
		TEAH	1.82	1.78	1.76	1.63	1.66	1.75	1.83	1.78
		TBAH	2.15	1.94	2.00	1.97	1.96	1.96	1.98	2.03

Table IV-17: ΔW values for the Ionic Liquids based on different PO-degrees with constant C-chain (C_{18})

In line with the trend indicated by the viscosity and conductivity data, ΔW increases with rising number of carbons in the aliphatic chain of the ether carboxylic acid, see Figure IV-19.

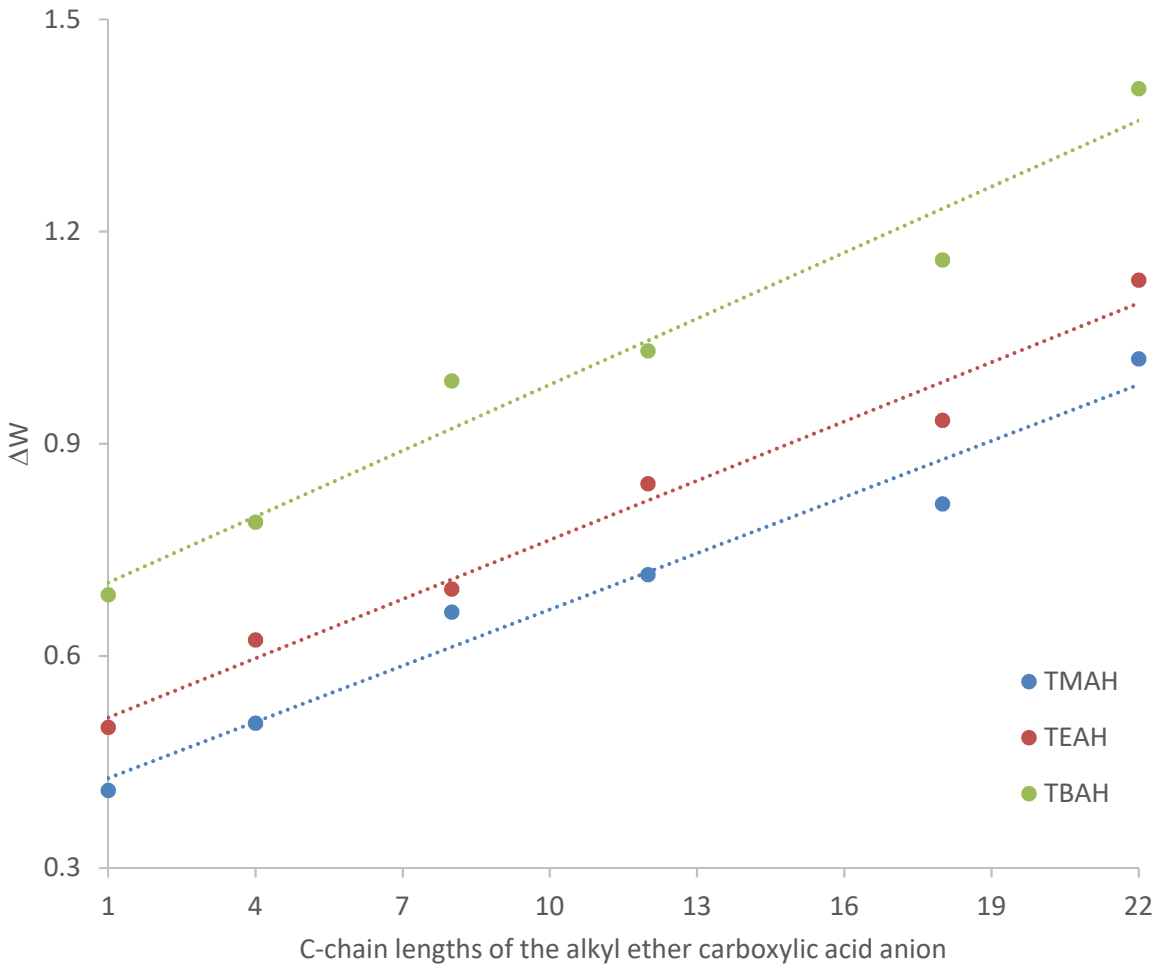

Figure IV-19: ΔW of the different Ionic Liquids based on different alcohols with constant PO-degree (PO = 6) as a function of temperature

It can be concluded from Figure IV-19 that the ΔW increases linearly with increasing C-chain lengths. Further, it can be seen that with bigger quaternary ammonium molecules, the ΔW also increases.
Additionally, the propoxylation degree has a significant influence on ΔW. The value increases with longer PO-chains and larger cations, see Figure IV-20.

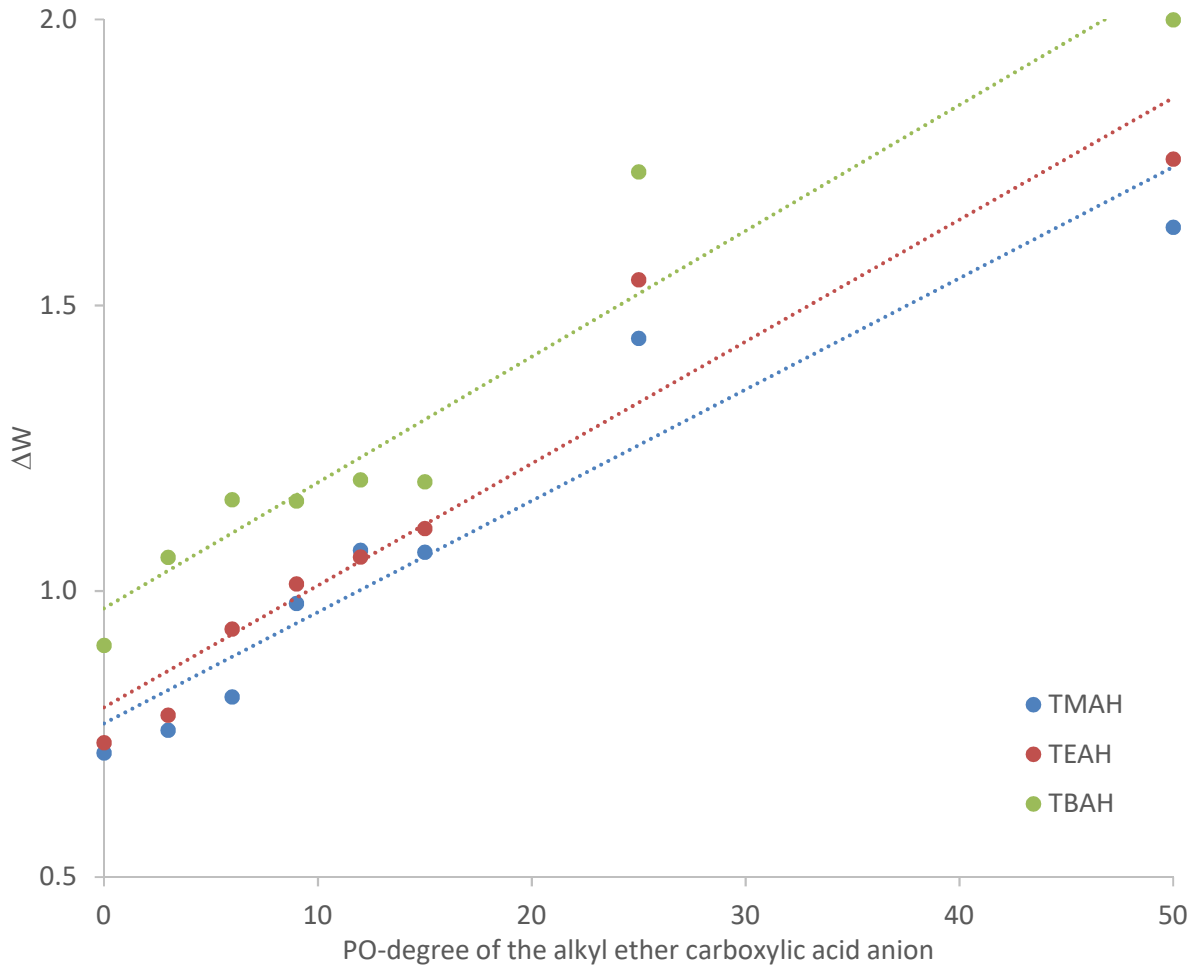

Figure IV-20: ΔW of the different Ionic Liquids based on different PO-degrees and constant C-chain (C_{18}) of the temperature

With longer PO-degree, the ΔW values also increases. Especially for long PO-degrees PO > 15, the ΔW value increases significantly. The ΔW values for the Ionic Liquids for PO < 15 are almost lower than 1, which means "good" Ionic Liquids according to the investigation of Angell et al.

Based on this result, it can be concluded that especially smaller C-chain Ionic Liquids with short PO-degree and small quaternary ammonium cations are fully dissociated. With increasing molar weight, e.g. longer C-chain, longer PO-degree and larger cations, this dissociation is incomplete and ΔW values larger than 1 are achieved.

IV.2.1.3 Melting Points and Thermal stability

Ionic Liquids are prone to be applied at high temperature, due to their high stability and low vapour pressure. Just like the decomposition temperature, the point determining the lower limit of the range of liquid state is of high interest. In case of room-temperature Ionic Liquids, melting points or glass transitions occur at quite low temperatures, likewise enabling applications below 273 K or lower. The thermal stability is an important feature of Ionic Liquids. Since Ionic Liquids only have a very low vapour pressure, they can be applied in liquid state up to the temperature of thermal destruction [237].

In the present chapter, the melting points and the thermal stability of the Ionic Liquids will be given. Especially, the influence of the structural changes of the Ionic Liquids will be shown and discussed.

In the following Table IV-17, the onset temperatures of the DSC measurements on the present Ionic Liquids are shown.

Anionic	Cationic	m.p. [K]
MeP 6	TMAH	< 193.15
	TEAH	< 193.15
	TBAH	< 193.15
BuP 6	TMAH	< 193.15
	TEAH	< 193.15
	TBAH	< 193.15

Anionic	Cationic	m.p. [K]
OcP 6	TMAH	231.05
	TEAH	221.52
	TBAH	210.83
LP 6	TMAH	260.32
	TEAH	255.32
	TBAH	237.98

Anionic	Cationic	m.p. [K]
SP 6	TMAH	297.65
	TEAH	290.51
	TBAH	274.88
BP 6	TMAH	328.48
	TEAH	320.04
	TBAH	305.32

Table IV-18: Melting Points (m.p.) of the Ionic Liquids, based on different alcohols with constant PO-degree (PO = 6)

It can be concluded that especially the Ionic Liquids based on short-chain alcohols show melting points below 193.15 K. Due to the used DSC equipment, this is the minimum temperature that can be measured.
Due to the oligomer distribution and the very short C-chain, these molecules have a low tendency to form aggregates. The influence of the bulkiness of the cation and the different C-chains on the melting point is shown in Figure IV-21.

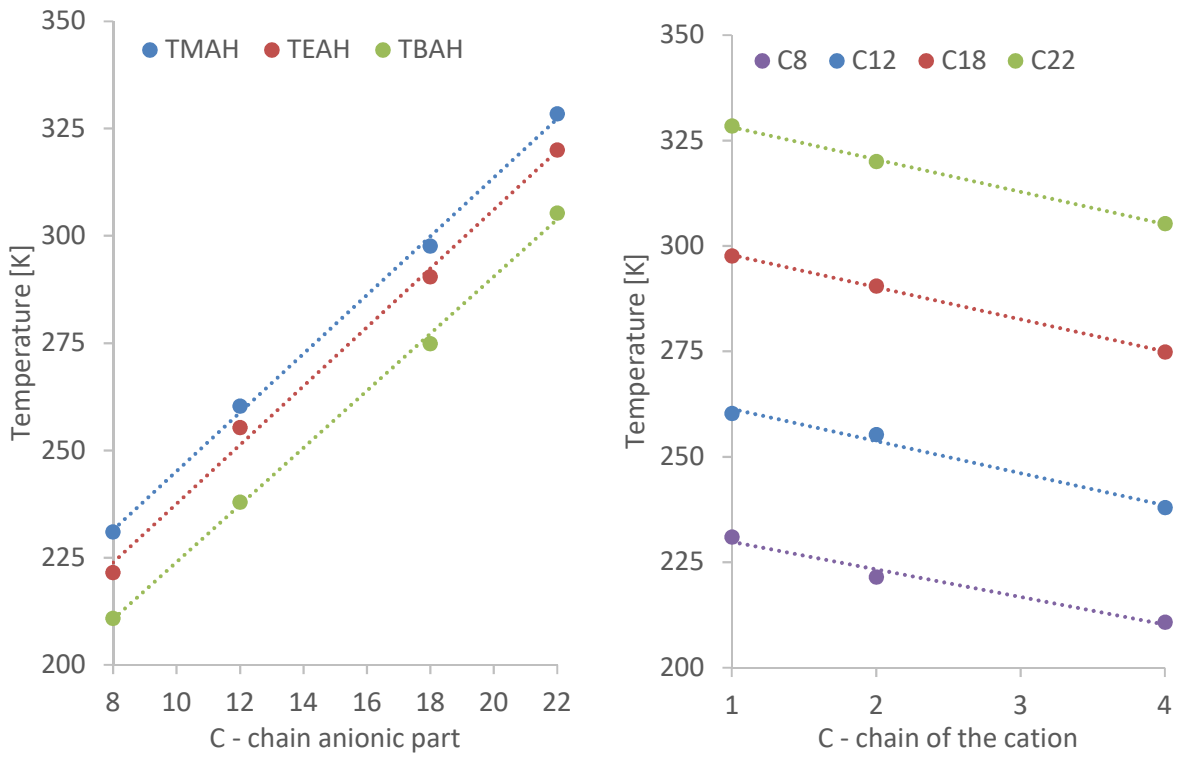

Figure IV-21: Melting points of the different Ionic Liquids with different alcohol bases and with constant PO-degree (PO = 6)

It can be clearly seen in Figure IV-21, left side, that with longer C-chains the melting point also increases. This is because of the high intermolecular attraction forces of the alkyl chains from the used alcohols.
But bulky cations disturb the packaging, and the melting point decreases, see Figure IV-21, right side. The dependence on the bulkiness can also be seen in Figure IV-21, left side. The blue line (TMAH) and the red line (TEAH) are quite close, the green line of the TBAH Ionic Liquids is much lower. The bulky cations and the oligomer distribution of the propylene oxide disturb the formation of uniformly packed crystals.

Besides the C-chain length of the different alcohols, also the PO-degree combined with the bulky cations has significant influence on the melting point. In Table IV-19, all melting points of the Ionic Liquids based on different PO-degrees and constant C-chain (C_{18}) are listed.

Anionic	Cationic	m.p. [K]
Stearyl	TMAH	337.48
	TEAH	331.48
	TBAH	316.95
SP 3	TMAH	321.12
	TEAH	315.36
	TBAH	303.21
SP 6	TMAH	297.65
	TEAH	290.51
	TBAH	274.88
SP 9	TMAH	270.25
	TEAH	266.32
	TBAH	261.74
SP 12	TMAH	262.15
	TEAH	260.48
	TBAH	257.42
SP 15	TMAH	259.98
	TEAH	257.01
	TBAH	255.01
SP 25	TMAH	255.20
	TEAH	253.00
	TBAH	250.89
SP 50	TMAH	245.02
	TEAH	243.22
	TBAH	240.01

Table IV-19: Melting points (m.p.) of the different Ionic Liquids based on different PO-degrees and constant C-chain (C_{18})

The determined melting points are summarised and depicted in Figure IV-22, left side. On the right side of Figure IV-22, the influence of the PO-degree and bulkiness of the cation on the melting point is given. On the left side, the trend of the melting point for the different cations is shown.

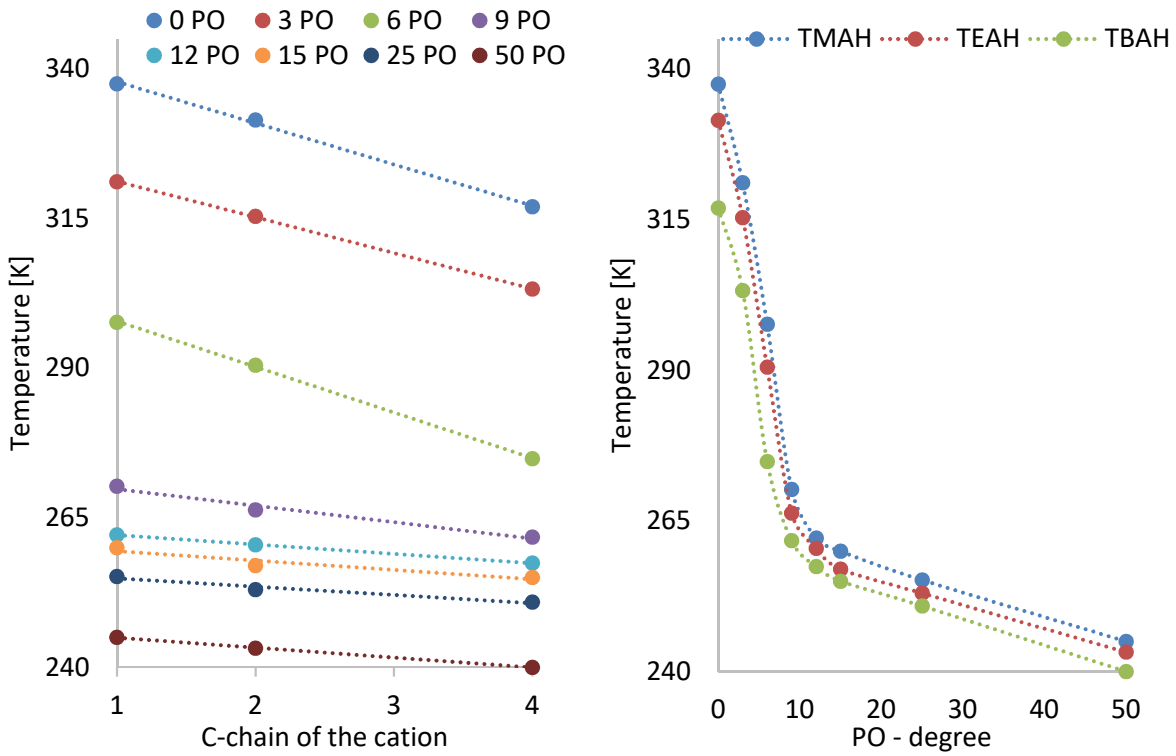

Figure IV-22: Left side shows the melting point of the Ionic Liquids for different cation bulkiness; right side shows the melting point dependence of cation type and PO-degree

Again, Figure IV-22 shows that the bulky cation decreases the melting point, due to its disturbance of the formation of aggregates.
Besides this, especially the PO-degree plays an important role for the lowering of the melting point. The distribution and the flexibility of the polyalkylene group disturb the intermolecular attraction. Also, the methyl group of the polypropylene group interrupts this aggregation, resulting in low melting points.
Figure IV-22, right side, shows that this effect is very strong, mainly for the small oligomer groups. With higher degrees, PO > 6, this effect is smaller. Here, the effect of the bulky cation outweighs this behaviour.
This phenomenon of strongly lowering the melting point by introduction of polyalkylene groups was already published by Kunz et al. in their **CO**ncept of **M**elting **P**oint **L**owering due to **E**thoxylation (COMPLET) [231]. This investigation has shown that the flexibility of an EO-chain is lowering the melting point significantly.
In this investigation, PO-groups with an oligomer distribution has been used, this might lead to even a stronger influence on the melting point.

Further the melting point, also the thermal stability of the Ionic Liquids has been determined. Here, also the influence of the C-chains; PO-degree and of the different bulky cations has been determined. In the following, in Figure IV-23 to Figure IV-28, the temperature-dependent mass loss curves are shown.

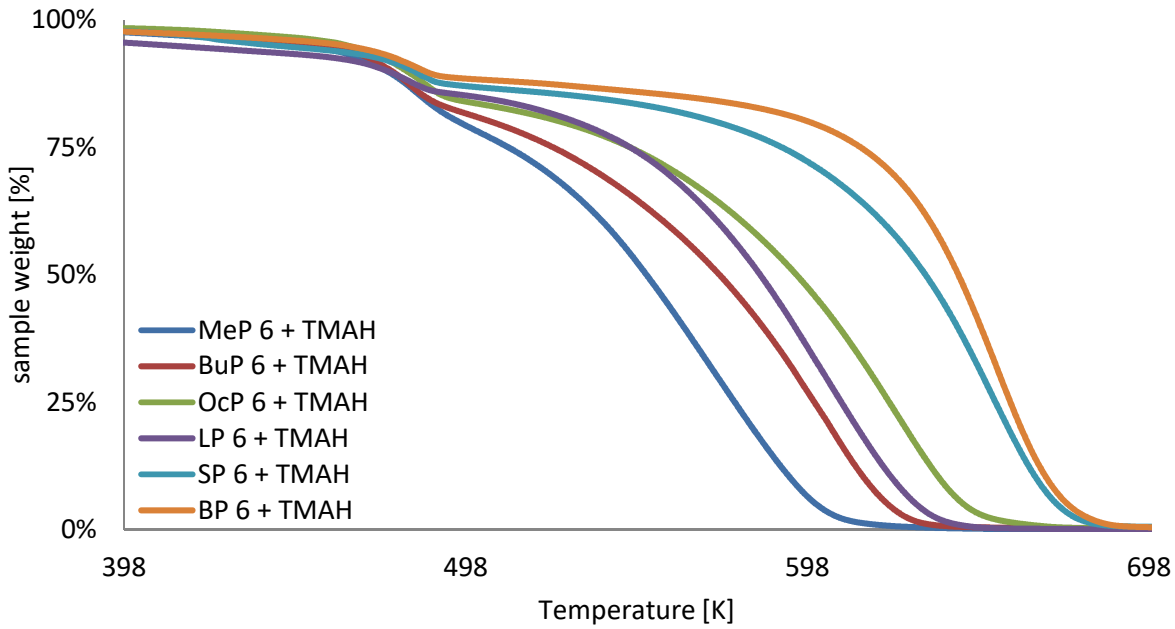

Figure IV-23: Temperature-dependent mass loss curves of the Ionic Liquids based on different alcohol bases with the same PO-degree (PO = 6) and TMAH as cationic part

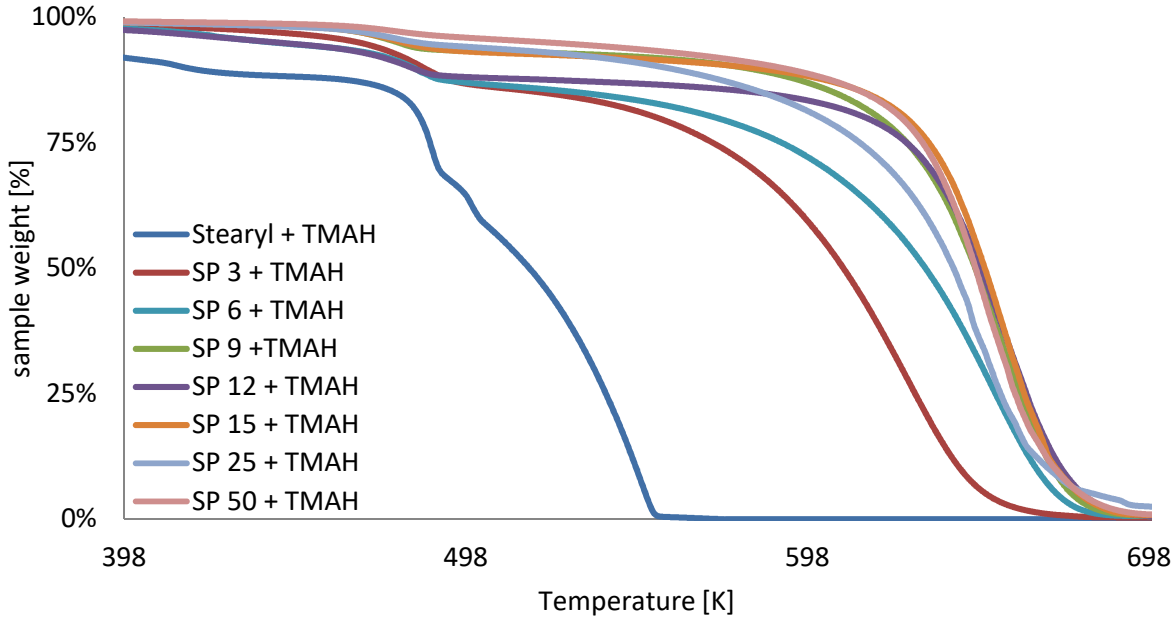

Figure IV-24: Temperature-dependent mass loss curves of the Ionic Liquids, based on different PO-degrees and same C-chain (C_{18}) and TMAH as cationic part

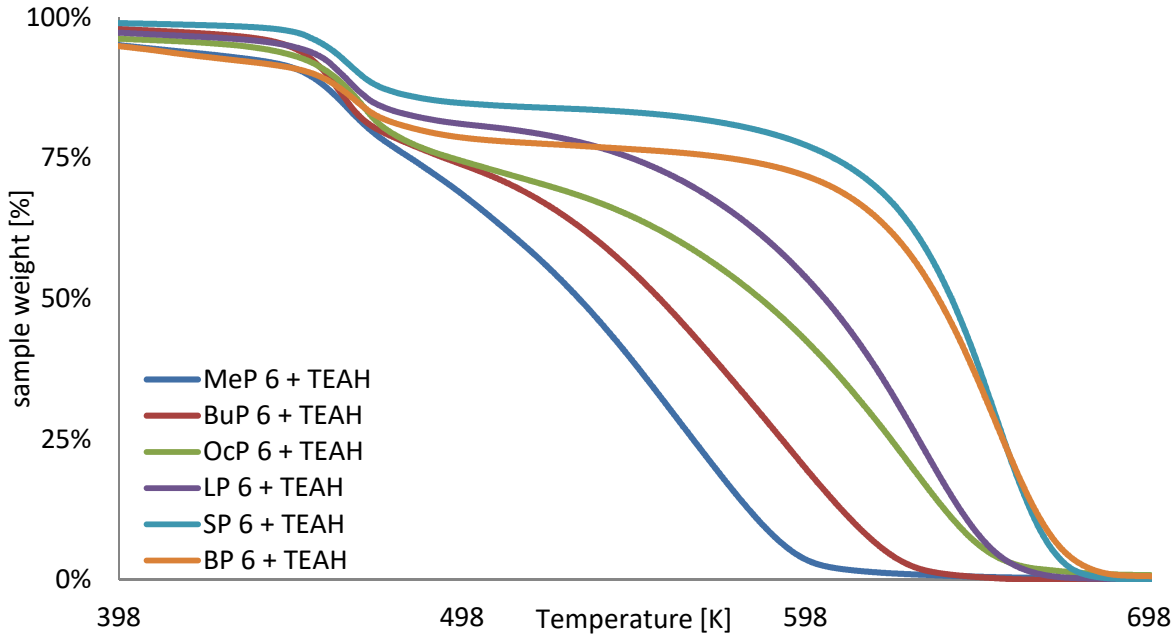

Figure IV-25: Temperature-dependent mass loss curves of the Ionic Liquids based on different alcohol bases with the same PO-degree (PO = 6) and TEAH as cationic part

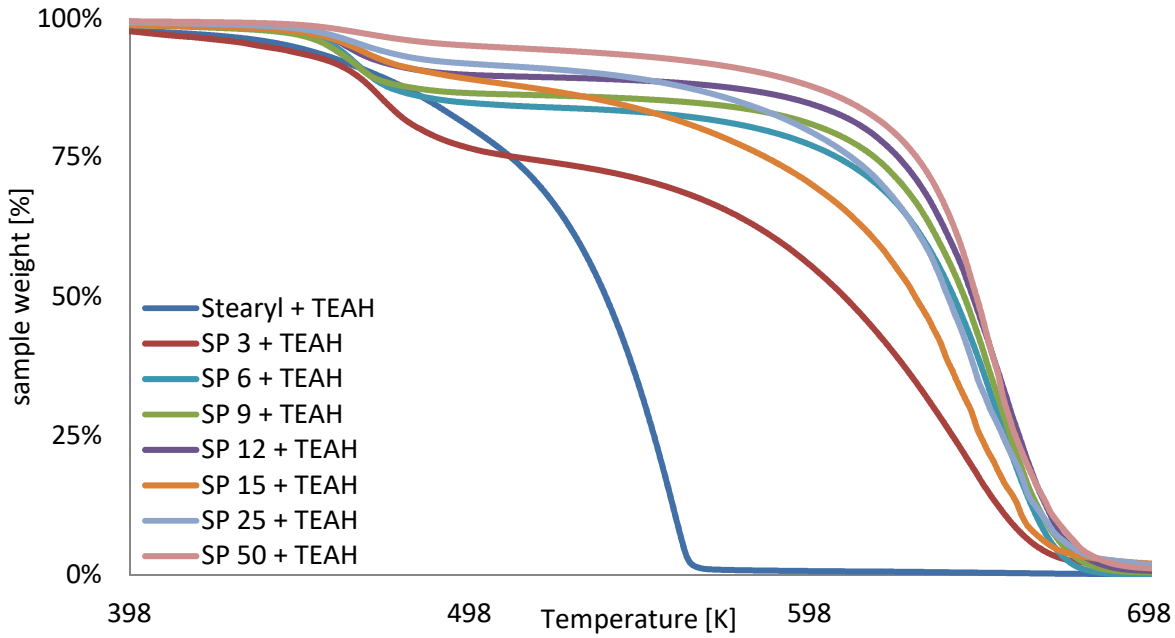

Figure IV-26: Temperature-dependent mass loss curves of the Ionic Liquids based on different PO-degrees and same C-chain (C_{18}) and TEAH as cationic part

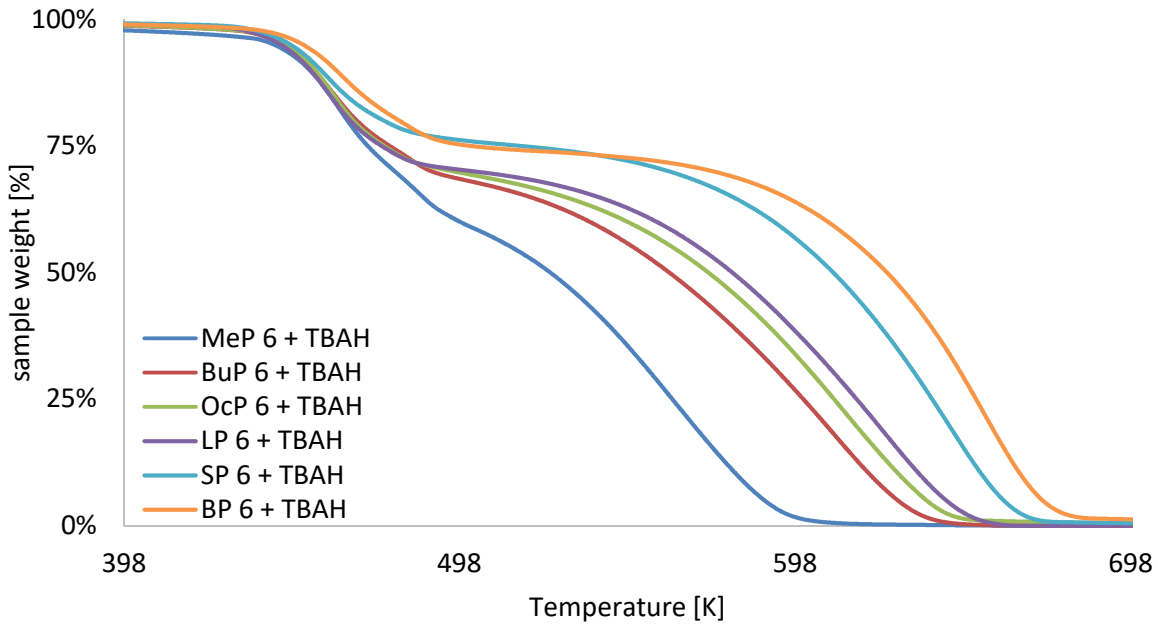

Figure IV-27: Temperature-dependent mass loss curves of the Ionic Liquids based on different alcohol bases with the same PO-degree (PO = 6) and TBAH as cationic part

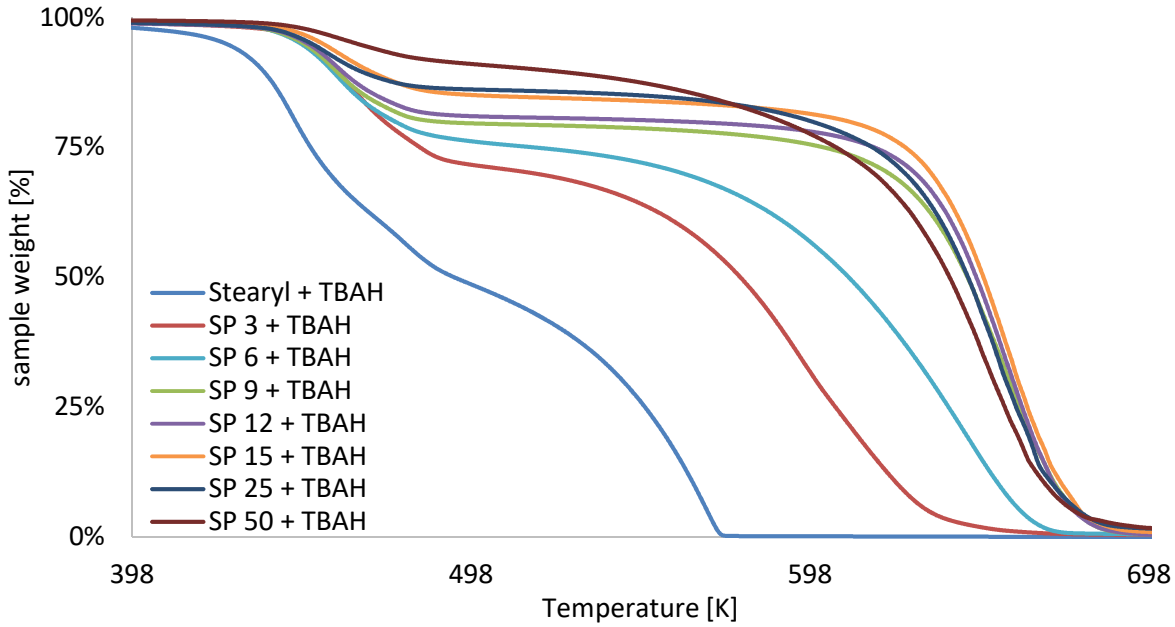

Figure IV-28: Temperature-dependent mass loss curves of the Ionic Liquids based on different PO-degrees and same C-chain (C_{18}) and TBAH as cationic part

All of the tested compounds showed decomposition only above 473 K. Decomposition temperatures of common Ionic Liquids can be found in the same range [119].
Obviously, all tested Ionic Liquids decomposed by a two-step mechanism. Accordingly, two decomposition temperatures are determined, see Table IV-20.

Anionic	Cationic	$T_{dec\,1}$ [K]	$T_{dec\,2}$ [K]
MeP 6	TMAH	481.20	569.11
	TEAH	465.23	565.69
	TBAH	460.36	566.78
BuP 6	TMAH	482.32	604.65
	TEAH	470.32	622.59
	TBAH	462.31	602.36
OcP 6	TMAH	483.36	624.59
	TEAH	468.87	629.96
	TBAH	459.84	615.99
LP 6	TMAH	479.99	602.32
	TEAH	465.84	635.95
	TBAH	458.74	624.69
SP 6	TMAH	482.45	648.95
	TEAH	465.98	644.99
	TBAH	459.15	644.26
BP 6	TMAH	483.26	650.21
	TEAH	467.85	654.82
	TBAH	462.98	656.19

Anionic	Cationic	$T_{dec\,1}$ [K]	$T_{dec\,2}$ [K]
Stearyl	TMAH	487.24	547.50
	TEAH	465.24	556.98
	TBAH	454.26	566.78
SP 3	TMAH	486.69	627.81
	TEAH	470.21	647.26
	TBAH	463.66	594.95
SP 6	TMAH	482.48	648.52
	TEAH	465.84	644.14
	TBAH	459.29	644.59
SP 9	TMAH	479.52	649.26
	TEAH	465.21	647.92
	TBAH	456.99	656.98
SP 12	TMAH	482.32	651.29
	TEAH	465.32	654.87
	TBAH	457.89	652.36
SP 15	TMAH	475.69	655.13
	TEAH	466.23	646.33
	TBAH	458.69	657.48
SP 25	TMAH	477.84	644.92
	TEAH	465.49	645.95
	TBAH	458.95	653.29
SP 50	TMAH	474.56	655.66
	TEAH	468.74	652.99
	TBAH	457.96	647.96

Table IV-20: Decomposition temperatures T_{dec} of the investigated substances

From Table IV-20, it can be concluded that especially T_{dec1} seems to be similar for all three cation types. In case of TMAH, the T_{dec1} is in average 481 K, for TEAH 467 K and for TBAH 459 K. Prasad et al. studied the onset temperatures of thermal decomposition of different quaternary ammonium Ionic Liquids and showed that, as the size of the substituted alkyl group increases, the thermal stability of these compounds decreases [238]. It is well accepted that quaternary ammonium compounds of the type $R_4N^+X^-$ decompose thermally to yield an amine, R_3N, and the corresponding alkyl compound, R.

It can be also seen that with increased C-chain, the thermal stability becomes higher. Especially the Ionic Liquids based on C_{18} show a higher thermal stability. The implementation of PO-units increases the thermal stability, e.g. the thermal stability of the Ionic Liquid based on stearic acid is comparable to MeP 6 (C_1 6PO). But the overall impact of the degree of propoxylation is small. The covalent bonds just like the hydrogen bond formation potential are in the same order of magnitude, independently of the number of oxygens present. This becomes evident, when comparing the decomposition temperatures of the different C_{18} compounds with different PO-degrees. The measured values are within the same order of magnitude, within the uncertainty of the measurement.

The second decomposition temperature T_{dec2} seems to have a direct connection to the anionic part, too. In all cases, T_{dec2} seems to be independent of the cationic part. In Table IV-21, the calculated anionic / cationic w/w ratio is compared with the decomposed amount, inferred from the temperature-dependent mass loss curve from each step.

		MeP 6 + TMAH	**BuP 6 + TMAH**	**OcP 6 + TMAH**	**LP 6 + TMAH**	**SP 6 + TMAH**	**BP 6 + TMAH**
calculated ratio [%]	cationic	15	13	12	11	10	9
	anionic	85	87	88	89	90	91
mass loss from TGA-curve [%]	Step 1	15	14	38	11	11	9
	Step 2	85	86	88	89	89	91
		MeP 6 + TEAH	**BuP 6 + TEAH**	**OcP 6 + TEAH**	**LP 6 + TEAH**	**SP 6 + TEAH**	**BP 6 + TEAH**
calculated ratio [%]	cationic	21	19	17	16	14	13
	anionic	79	81	83	84	86	87
mass loss from TGA-curve [%]	Step 1	22	20	38	15	15	12
	Step 2	78	80	82	85	85	88
		MeP 6 + TBAH	**BuP 6 + TBAH**	**OcP 6 + TBAH**	**LP 6 + TBAH**	**SP 6 + TBAH**	**BP 6 + TBAH**
calculated ratio [%]	cationic	36	33	31	29	26	25
	anionic	64	67	69	71	74	75
mass loss from TGA-curve [%]	Step 1	36	33	38	30	26	25
	Step 2	64	67	69	70	74	75

		Stearyl + TMAH	**SP 3 + TMAH**	**SP 9 + TMAH**	**SP 12 + TMAH**	**SP 15 + TMAH**	**SP25 + TMAH**	**SP 50 + TMAH**
calculated ratio [%]	cationic	20	13	8	7	6	4	2
	anionic	80	87	92	93	94	96	98
mass loss from TGA-curve [%]	Step 1	21	12	38	7	6	4	3
	Step 2	79	88	93	93	94	96	97
		Stearyl + TEAH	**SP 3 + TEAH**	**SP 9 + TEAH**	**SP 12 + TEAH**	**SP 15 + TEAH**	**SP 25 + TEAH**	**SP 50 + TEAH**
calculated ratio [%]	cationic	28	18	12	10	9	6	3
	anionic	72	82	88	90	91	94	97
mass loss from TGA-curve [%]	Step 1	28	18	38	11	9	6	2
	Step 2	72	82	88	89	91	94	98
		Stearyl + TBAH	**SP 3 + TBAH**	**SP 9 + TBAH**	**SP 12 + TBAH**	**SP 15 + TBAH**	**SP 25 + TBAH**	**SP 50 + TBAH**
calculated ratio [%]	cationic	46	32	23	19	17	12	7
	anionic	54	68	77	81	83	88	93
mass loss from TGA-curve [%]	Step 1	47	31	38	20	18	14	8
	Step 2	53	69	78	80	82	86	92

Table IV-21: calculated cationic / anionic ratio of the investigated Ionic Liquids against the mass loss, determined by TGA measurements for each decomposition step

From the values of Table IV-21, it can be concluded that, in the first step, at T_{dec1}, always the cationic part, TMAH, TEAH and TBAH, of the Ionic Liquid is decomposed. In the second step, at T_{dec2}, the anionic part, fatty acid or alkyl ether carboxylic acid, will undergo a thermal decay. Despite the strong Coloumb attraction in the aprotic Ionic Liquid, the components decompose separately.

IV.2.1.4 Hygroscopy

As discussed before, most of the Ionic Liquids are hygroscopic. On the one hand, the presence of water is inevitable during the synthesis, storage, and application procedures of Ionic Liquids. On the other hand, Ionic Liquids absorb water from the atmosphere or wet surfaces [239–241]. The water content of a substance is a limiting factor for many applications. Several fields of use are completely inaccessible, if the water content is too high or the water uptake cannot be controlled without complex methods. In addition, it is well-known that water is almost inevitable in Ionic Liquids. Even these Ionic Liquids, classified as hydrophobic ones, can absorb up to 1.4 wt% of water, which is a significant molar amount. For more hydrophilic Ionic Liquids, water uptake from air is even more pronounced. This means that all commercial products contain a certain amount of water, which depends on the production conditions and the logistics, since the Ionic Liquids can reasonably be expected to come into contact with traces of water. Depending on the application, this water content can cause enormous problems. The presence of water generally has significant influence on the physico-chemical properties of Ionic Liquids.

Water contamination is one possible explanation for the high variability of results obtained by different authors measuring the same Ionic Liquid property. Absorbed water can also influence reactions and processes occurring in Ionic Liquids. Such an impurity is difficult to remove from hydrophilic Ionic Liquids, because of their high hygroscopicity.

By excessive drying of the samples, it was ensured that their water content was well below 1000 ppm before starting the measurement, see
Table **IV-10**.

In the following Figure IV-29, the increase of weight by water uptake is depicted for the Ionic Liquids based on different alcohols and constant PO-degree (PO = 6).

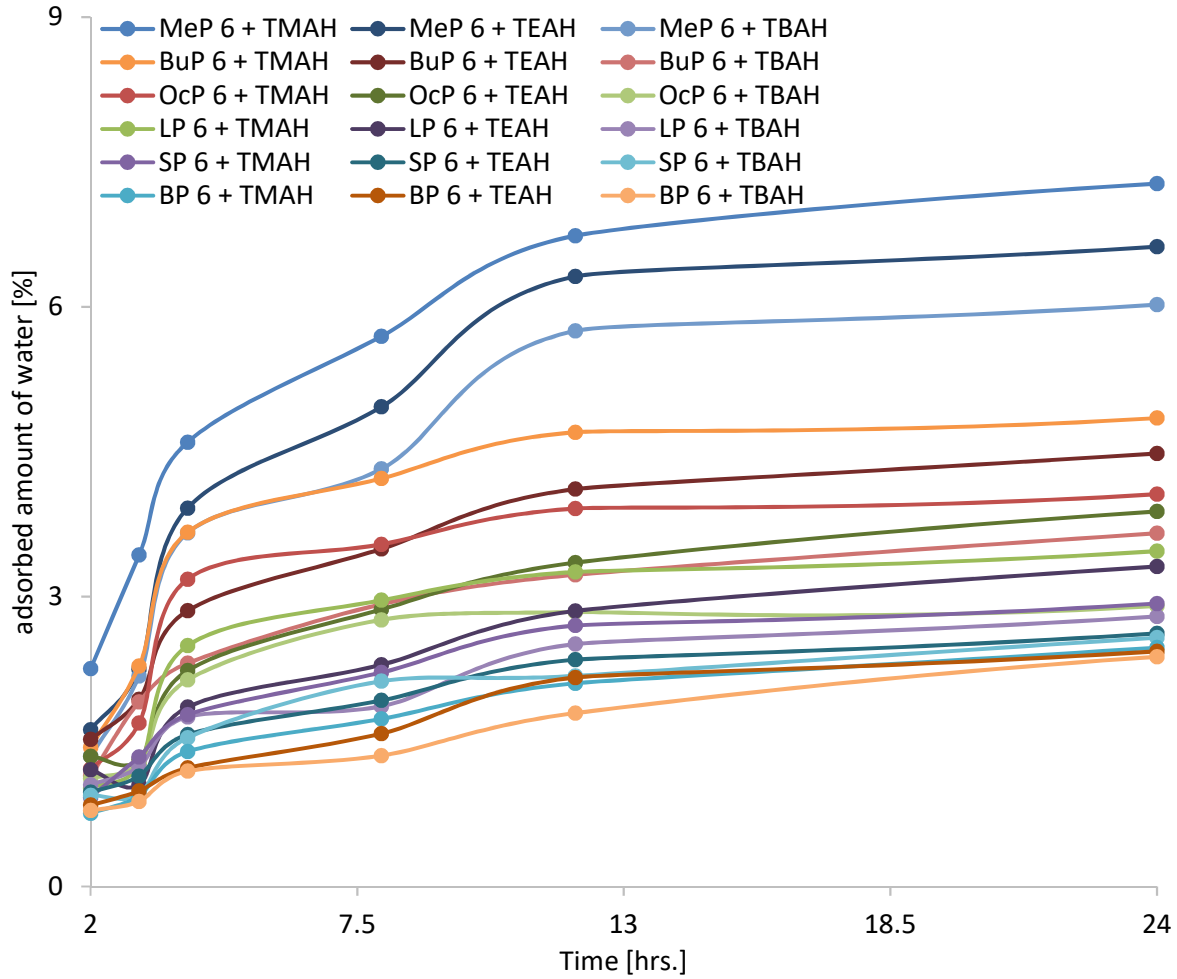

Figure IV-29: Hygroscopicity behaviour of the different Ionic Liquids, based on different alcohols with same PO-degree (PO = 6)

Based on the data from Figure IV-29, it can be concluded that especially the Ionic Liquids based on short C-chains show a rather high tendency to adsorb water from the environment. Besides this, also the cationic part seems to have an influence. Ionic Liquids based on TMAH are more hygroscopic than TEAH and TBAH. Particularly, the Catanionics based on methanol, MeP 6, absorb already after 24 hours around 7% water. Figure IV-29 show also that longer C-chains do not absorb so much water. Due to the higher lipophilicity of the long alkyl chain, less water from the atmosphere is absorbed by the Ionic Liquid. Following trend concerning the water absorption can be concluded, $C_1 >> C_4 > C_8 > C_{12} > C_{18} > C_{22}$.

In Figure IV-30, the hygroscopic behaviour of the Ionic Liquids with constant C-chain (C_{18}) and different PO-degree is depicted.

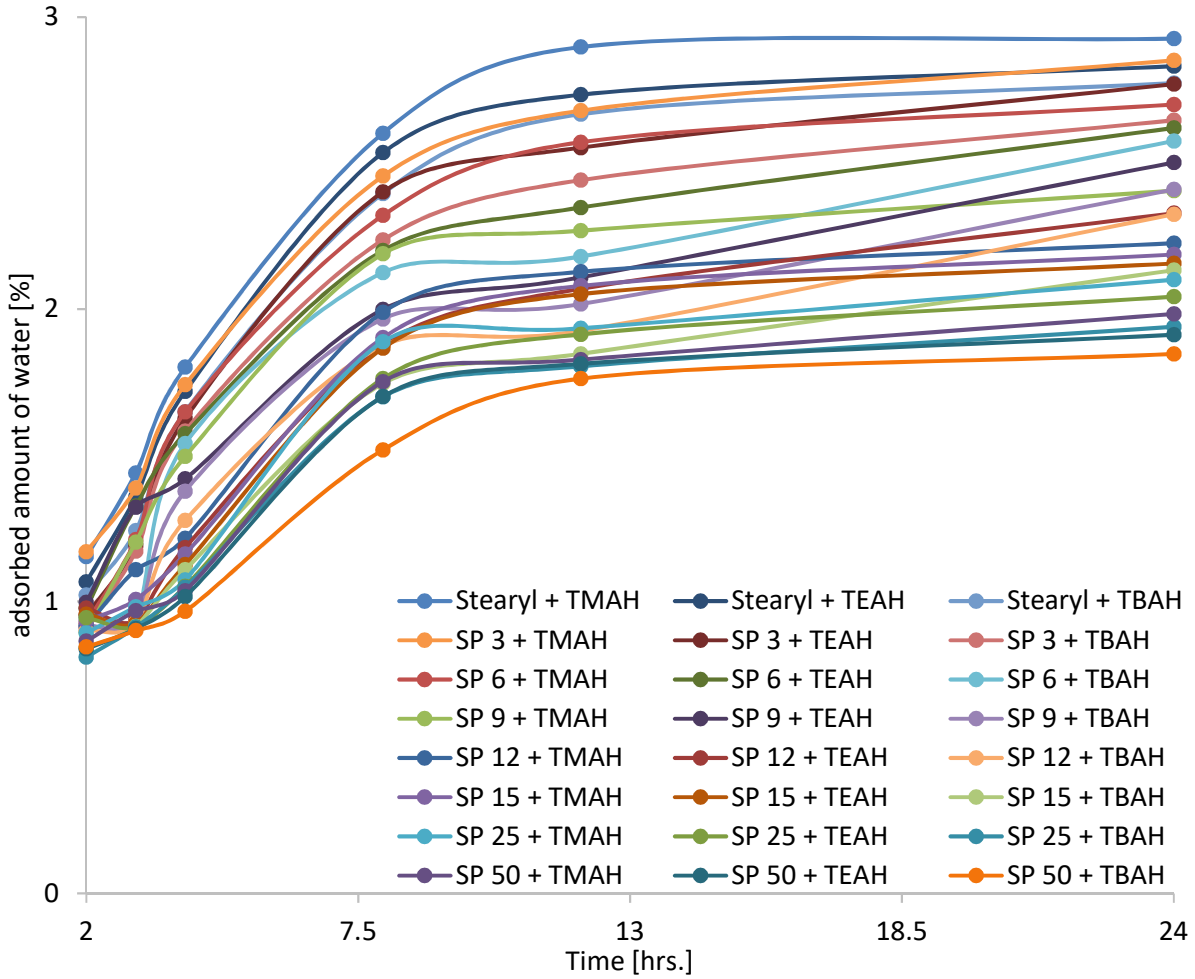

Figure IV-30: Hygroscopycity behaviour of the different Ionic Liquids, based on different PO-degrees and constant C-chain (C_{18})

The values gathered from Figure IV-30 show a similar trend. Ionic Liquids based on TBAH are much less hygroscopic than TMAH or TEAH. Also, longer PO-degrees seem to decrease the tendency to absorb water from the environment. The methyl group in the polypropylene glycol group seems to interrupt the formation of hydrogen bounds, this directly leads to lower adsorbed amounts of water. Nevertheless, the obtained data in Figure IV-30 show also that the maximum amount of water is around 3% after 24 hours. This is rather low and a good value for the application as lubricant or lubricant additive.

Cuadrado-Prado et al. have measured the quantity of mass adsorbed by six Ionic Liquids according to the humidity grade of the atmosphere [242]. Their results showed that the water adsorbs to the surface of the Ionic Liquid, generating a film on it. The quantity of adsorbed water strongly depended on the chemical nature of the Ionic Liquid. However, they also found that for the same family of compounds, the increase in alkyl chain length decreased the adsorbed quantity of water. It was concluded that, if the alkyl chain length was diminished, the number of anchorage sites for water molecules to be adsorbed was increased.

For the present Ionic Liquids, the same observations are made. The amount of water strongly depends on the molecular structure of the Ionic Liquids, meaning the longer the alkyl-chain

in the anionic part and the bigger the quaternary ammonium compound, the lower the hygroscopic behaviour of the Ionic Liquid, see Figure IV-29 and Figure IV-30.

These results need to be handled with care, because the quantity of adsorbed water also depends strongly on the area of open surface to the atmosphere, as Cuadrado-Prado et al. have shown. The detectable amount of water will rise with the surface of the Ionic Liquid; however. All measurements were carried out in equal sample holders with similar masses and comparable surface area covered by the Ionic Liquid. Furthermore, relative humidity profoundly influences the total water content, like Fabio et al. have shown [243].

Also, the water adsorption after 5 days (120 hours) has been determined and compared to the start value of H_2O and after 1 day (24 hours).

Figure IV-31 shows the long term hygroscopicity of the Ionic Liquids, based on same PO-degree (PO = 6) with different alcohols.

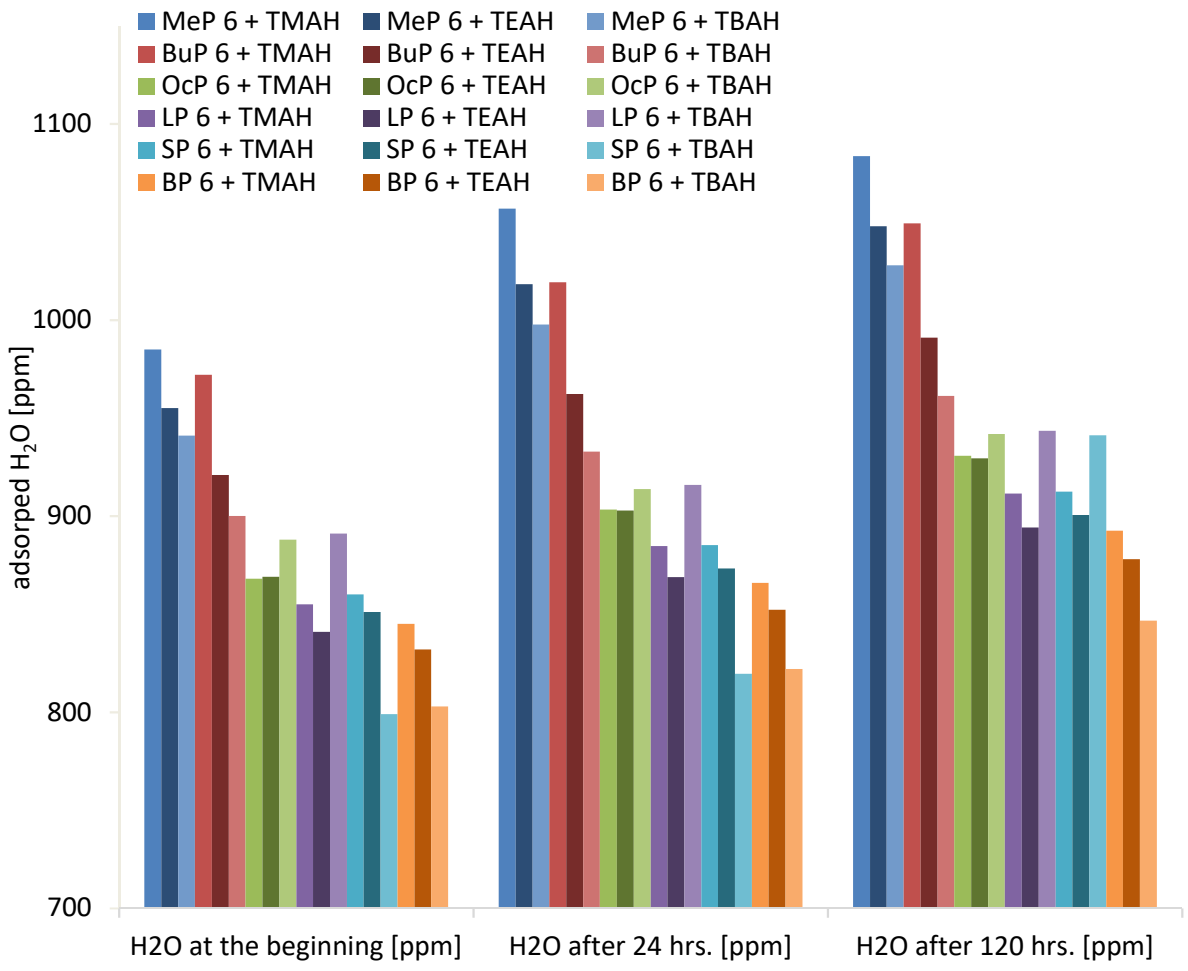

Figure IV-31: Long term hygroscopicity test of the different Ionic Liquids with same PO-degree (PO = 6) and different alcohols

The previously made conclusions, short alcohols combined with small quaternary ammonium compound tend to high hygroscopic behaviour, are again approved. Even after 120 hours, the Ionic Liquids seem to absorb constantly water from the surrounding.

Figure IV-32 shows the long-term hygroscopicity test of the Catanionics, based on same C-chain (C_{18}) and different PO-degrees.

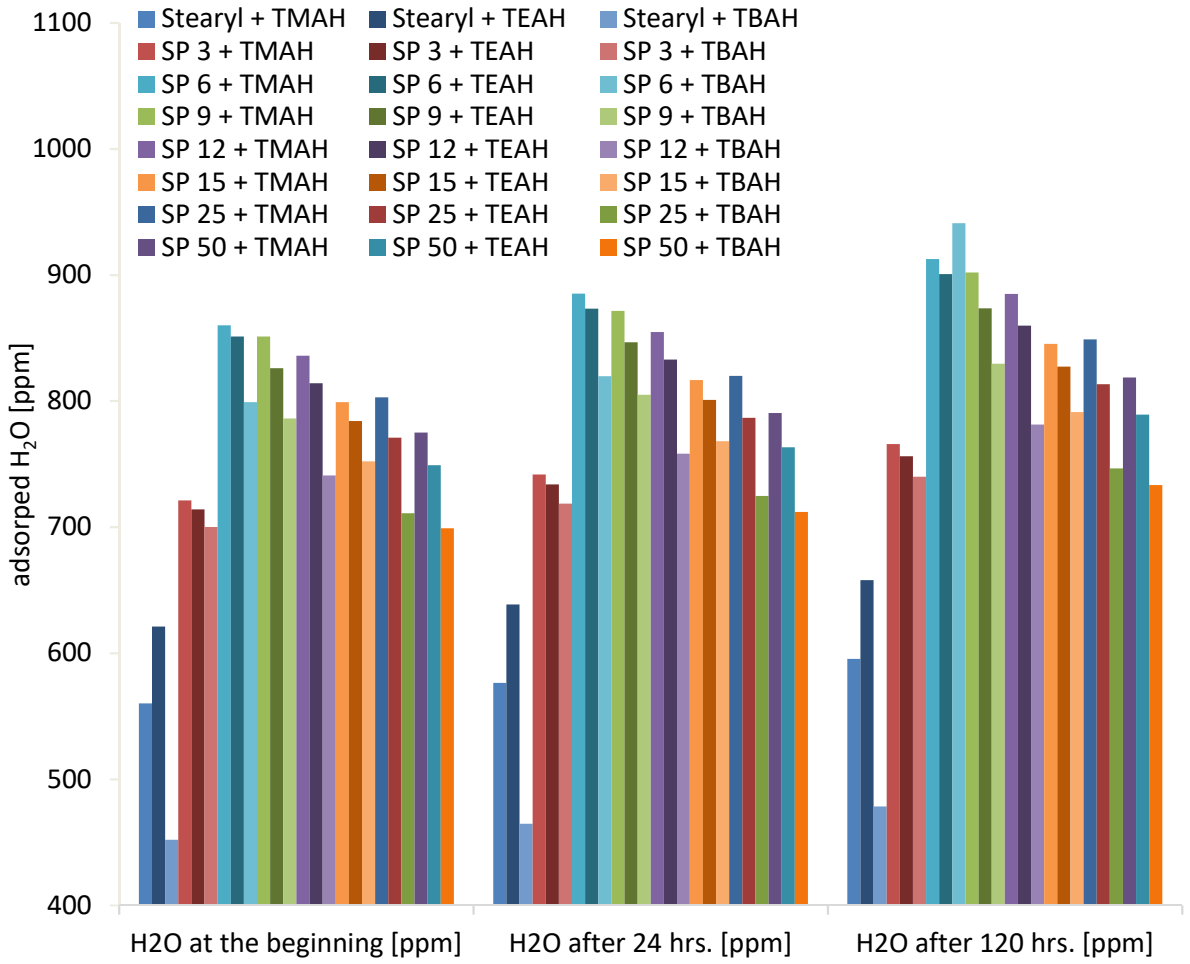

Figure IV-32: Long term hygroscopicity test of the different Ionic Liquids with same alcohol (C_{18}) and different PO-degrees

Here, the previously made conclusions, long PO combined with bulky cation gives less water absorption, cannot be seen directly. Particularly, the Ionic Liquids based on stearic acid seem to be of quite low hygroscopicity. After 5 days, the molecules based on C_{18} acid adsorb around 6% water, the alkyl ethercarboxylic acids only 5%. But due to the very low amount of water at the starting point, these stearic acid based Catanionics, seem to have a higher hygroscopic tendency. Nevertheless, also here, the Ionic Liquids seem to still adsorb water from the environment.

Fabio et al. [243] have used a special construction to stabilise the humidity in the test chamber. To verify the made observations, such kind of testing chamber has to be used.

The detailed values concerning the hygroscopy test can be found in the Appendix.

IV.2.1.5 Oil solubility

Ionic liquids were used as base oil with good results in most of the above-cited papers. However, in some cases the utilization of the Ionic Liquids as neat lubricants is not feasible, from the economical point of view right now, because of their high prices. Therefore, they would be more likely used as additives in the lubricant industry. Some papers have reported the lubricating ability of a series of Ionic Liquids, in particular imidazolium derivatives, as mineral oil additives.

As mentioned above, Ionic Liquids could play a significant role in the lubricant industry as additive. Typical additives are present between 0.1 to 5 weight%. In the present chapter, the oil miscibility of the prepared Ionic Liquids will be presented. As already mentioned in Chapter II.3.3, typical base oils for Ionic Liquids are hydrocarbons, polyethylene glycol (PEG), poly-alpha olefins (PAO) propylene glycol dioleate (PGDO) and glycerol. Due to their polar character, Ionic Liquids tend to be better soluble in more polar oils than in non-polar oils, like PAO or mineral oil. For this reason, natural based rape-seed oil has been chosen as base oil. The test procedure is described in III.3.8.

The oil solubility has been divided in three different classes, see Figure IV-33.

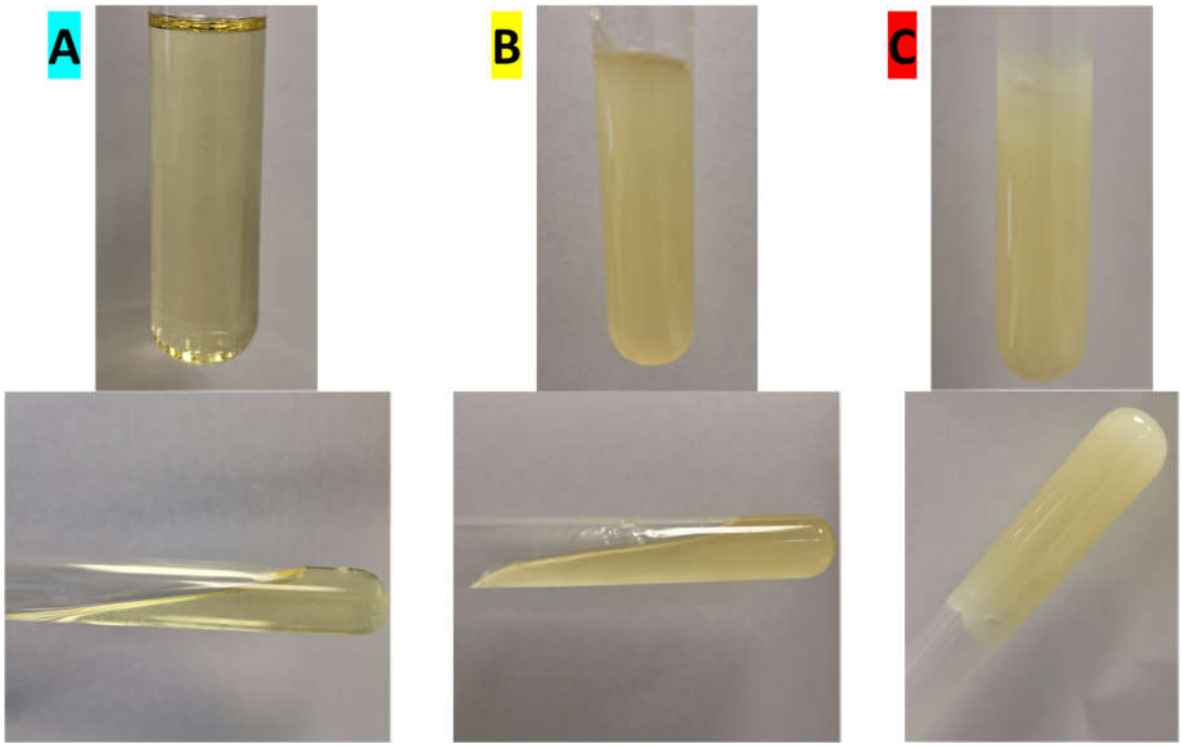

Figure IV-33: Definition of the different solubility classes; clear and fluent (blue), turbid and fluent (yellow) and turbid and solid (red)

Table IV-23 and Table IV-23 show the solubility of the different Ionic Liquids in rape-seed oil as a function of the concentration and the storage time.

		Solubilisation stability after 1 day					Solubilisation stability after 7 days				
		Amount of Ionic Liquid in base oil [w/w %]									
Anionic	**Cationic**	**1**	**2**	**5**	**10**	**25**	**1**	**2**	**5**	**10**	**25**
MeP 6	TMAH	clear & fluent	clear & fluent	turbid & fluent	turbid & fluent	turbid & fluent	clear & fluent	turbid & fluent	turbid & fluent	turbid & fluent	turbid & fluent
	TEAH	clear & fluent	clear & fluent	clear & fluent	turbid & fluent	turbid & fluent	clear & fluent	clear & fluent	turbid & fluent	turbid & fluent	turbid & fluent
	TBAH	clear & fluent	clear & fluent	clear & fluent	turbid & fluent	turbid & fluent	clear & fluent	clear & fluent	turbid & fluent	turbid & fluent	turbid & fluent
BuP 6	TMAH	clear & fluent	clear & fluent	turbid & fluent	turbid & fluent	turbid & fluent	clear & fluent	clear & fluent	turbid & fluent	turbid & fluent	turbid & fluent
	TEAH	clear & fluent	clear & fluent	clear & fluent	turbid & fluent	turbid & fluent	clear & fluent	clear & fluent	clear & fluent	turbid & fluent	turbid & fluent
	TBAH	clear & fluent	clear & fluent	clear & fluent	turbid & fluent	turbid & fluent	clear & fluent	clear & fluent	clear & fluent	turbid & fluent	turbid & fluent
OcP 6	TMAH	clear & fluent	clear & fluent	clear & fluent	clear & fluent	turbid & fluent	clear & fluent	clear & fluent	turbid & fluent	turbid & fluent	turbid & fluent
	TEAH	clear & fluent	clear & fluent	clear & fluent	clear & fluent	turbid & fluent	clear & fluent	clear & fluent	clear & fluent	turbid & fluent	turbid & fluent
	TBAH	clear & fluent	clear & fluent	clear & fluent	clear & fluent	turbid & fluent	clear & fluent	clear & fluent	clear & fluent	turbid & fluent	turbid & fluent
LP 6	TMAH	clear & fluent	clear & fluent	clear & fluent	clear & fluent	turbid & fluent	clear & fluent	clear & fluent	turbid & fluent	turbid & fluent	turbid & fluent
	TEAH	clear & fluent	clear & fluent	clear & fluent	clear & fluent	turbid & fluent	clear & fluent	clear & fluent	clear & fluent	turbid & fluent	turbid & fluent
	TBAH	clear & fluent	clear & fluent	clear & fluent	clear & fluent	turbid & fluent	clear & fluent	clear & fluent	clear & fluent	turbid & fluent	turbid & fluent
SP 6	TMAH	clear & fluent	clear & fluent	clear & fluent	clear & fluent	turbid & fluent	clear & fluent	clear & fluent	turbid & fluent	turbid & fluent	turbid & fluent
	TEAH	clear & fluent	clear & fluent	clear & fluent	clear & fluent	turbid & fluent	clear & fluent	clear & fluent	clear & fluent	turbid & fluent	turbid & fluent
	TBAH	clear & fluent	clear & fluent	clear & fluent	clear & fluent	turbid & fluent	clear & fluent	clear & fluent	clear & fluent	turbid & fluent	turbid & fluent
BP 6	TMAH	clear & fluent	turbid & solid	turbid & solid	turbid & solid	turbid & solid	turbid & solid	turbid & solid	turbid & solid	turbid & solid	turbid & solid
	TEAH	clear & fluent	turbid & fluent	turbid & solid	turbid & solid	turbid & solid	turbid & solid	turbid & solid	turbid & solid	turbid & solid	turbid & solid
	TBAH	clear & fluent	turbid & fluent	turbid & solid	turbid & solid	turbid & solid	turbid & fluent	turbid & solid	turbid & solid	turbid & solid	turbid & solid

clear & fluent
turbid & fluent
turbid & solid

Table IV-22: Solubility of the different Ionic Liquids based on different alcohols with constant PO-degree (PO = 6) in rape-seed oil, at room temperature as a function of correlation to the concentration and storage time

		Solubilisation stability after 1 day						Solubilisation stability after 7 days				
		Amount of Ionic Liquid in base oil [w/w %]										
Anionic	**Cationic**	**1**	**2**	**5**	**10**	**25**		**1**	**2**	**5**	**10**	**25**
Stearyl	TMAH											
	TEAH											
	TBAH											
SP 3	TMAH											
	TEAH											
	TBAH											
SP 6	TMAH											
	TEAH											
	TBAH											
SP 9	TMAH											
	TEAH											
	TBAH											
SP 12	TMAH											
	TEAH											
	TBAH											
SP 15	TMAH											
	TEAH											
	TBAH											
SP 25	TMAH											
	TEAH											
	TBAH											
SP 50	TMAH											
	TEAH											
	TBAH											

clear & fluent
turbid & fluent
turbid & solid

Table IV-23: Solubility of the different Ionic Liquids with constant C-chain (C_{18}) and different PO–degrees in rape-seed oil, at room temperature as a function of concentration and storage time

The data in Table IV-23 and Table IV-23 show that particularly the Ionic liquids based on C_{22}-alcohol are not soluble in rape-seed oil at room temperature. Even after heating the sample, so that the Ionic Liquid could melt. The Catanionic based on C_{22} combined with TBAH show a turbid but fluent solution after 1 week storage. The long C-chain seems to be immiscible.
It could be also concluded that the short C-chain molecules, C_1 and C_4, are not well soluble either in rape-seed oil, at room temperature. Especially, the methanol-based Ionic Liquid seems to have very low miscibility power, this might be a result of the higher polarity of this

molecule. Again, an enlargement of the cation increases the solubility, but still the maximum amount is 5 % with TBAH as counter-ion.

Generally, the Ionic Liquids based on TMAH show low miscibility with rape-seed oil, at room temperature. When the cationic part of the Catanionic is bulkier and more voluminous, the solubility properties become higher.

The good miscibility of the other Ionic Liquids can be explained by the C-chains (C_8; C_{12} and C_{18}) combined with the polypropylene oxide distribution. This combination has enhanced C-chains and these molecules have a better miscibility with rape-seed oil. This oil consists of triglycerides with mainly unsaturated C_{18} fatty acids (~ 92%).

Domańska et al. have studied the solubility of 1-butyl-, decyl-, or dodecyl-3-methylimidazolium chloride [C_4, C_8, C_{10}, C_{12} mim][Cl] in alcohols. The experimental solid-liquid equilibrium (SLE) phase diagrams investigated for [C_4 or C_8 or C_{10} or C_{12} mim][Cl] have shown that the solubility of Ionic Liquids in alcohols is mainly dependent on the C-chain of the Ionic Liquid and the alcohol, for example [C_4mim][Cl] exhibits the best solubility in butan-1-ol. This is due to same number of carbon atoms in the solvent and butyl substituent at the imidazolium ring. Comparable behaviour has been determined for [C_8 mim][Cl] in octan-1-ol, for [C_{10} mim][Cl] in decan-1-ol and [C_{12} mim][Cl] in dodecan-1-ol [244–247].

The PO-degree seems also to have a high impact on the solubility in rape-seed oil, see Table IV-23. Longer PO-degrees decrease the solubility power of the Ionic Liquid. Enlarging the amount of PO units has a direct effect on the substance polarity. The introduction of an additional oxygen atom directly decreases the solubility power of the Catanionic in the rape-seed oil at room temperature.

IV.3. Tribological properties of combinations based on alkyl ether carboxylic acids and symmetric quaternary ammonium compounds

IV.3.1 Introduction to the tribological properties of Ionic Liquids

Lubrication technology is always improving to meet new challenges or to open up new possibilities. In fact, many improvements in equipment can only occur, if the lubricant technology advances. To meet these challenges, new lubricants and improved additives must constantly be developed. A proposed solution to these challenges is the use of Ionic Liquids in the next generation of lubricants. These novel systems have been investigated since 2001, both as neat oils and as oil additives, to improve wear and friction performance.

In 2001, Lui et al. were the first to investigate the use of Ionic Liquids as lubricants, they studied alkyl-imidazolium tetrafluoroborates in steel/steel, steel/aluminium, steel/copper, steel / SiO_2, steel / Si (100), steel/sialon and Si_3N_4 / sialon ceramic contacts, showing excellent friction reduction [144,145,248,249]. Since this time, interest in these results has steadily increased the number of scientific articles to over 35 articles published each year on tribological aspects of Ionic Liquids, which reached 500 citations during the year 2009. Tribologists consider Ionic Liquids to be novel high performance lubricants in view of low volatility, high thermal and chemical stability, lack of inflammability, good solubility with many organic compounds, excellent friction and wear performance and satisfactory viscosity-temperature behaviour. Eventually, the properties can be tuned depending on the requirements enabled by the wide variability of both cation and anion so that Ionic Liquids are often truly referred to as “designer fluids”.
In the beginning, most of the research for Ionic Liquids in tribology was done by using the Ionic Liquids as neat oils. That means exchanging an existing oil combination by an Ionic Liquid. Lui et al. started it with the tests on the steel/steel combination. After that, many research groups have also checked reactive light alloys such as magnesium, aluminium and titanium [149,169,174,178,250–263].

IV.3.2 Results and discussion of the tribological properties of the prepared Catanionics

IV.3.2.1 Ionic Liquids as neat oils

Lubricants are used to control friction and wear by preventing direct contact between the surface asperities of the materials and lowering the contact temperature. Most widely used lubricants in use today are derived from petroleum.
As neat lubricants, Ionic Liquids establish a tribolayer that is physically adsorbed onto and chemically reacted with the metal surfaces to effectively reduce friction and wear under boundary lubrication
Therefore, the pure Ionic Liquids are tested as lubricants based on the circumstances described in III.3.9.

Figure IV-34 shows the Stribeck curves of the Ionic Liquids, based on different alcohols, with a constant PO-degree (PO = 6).

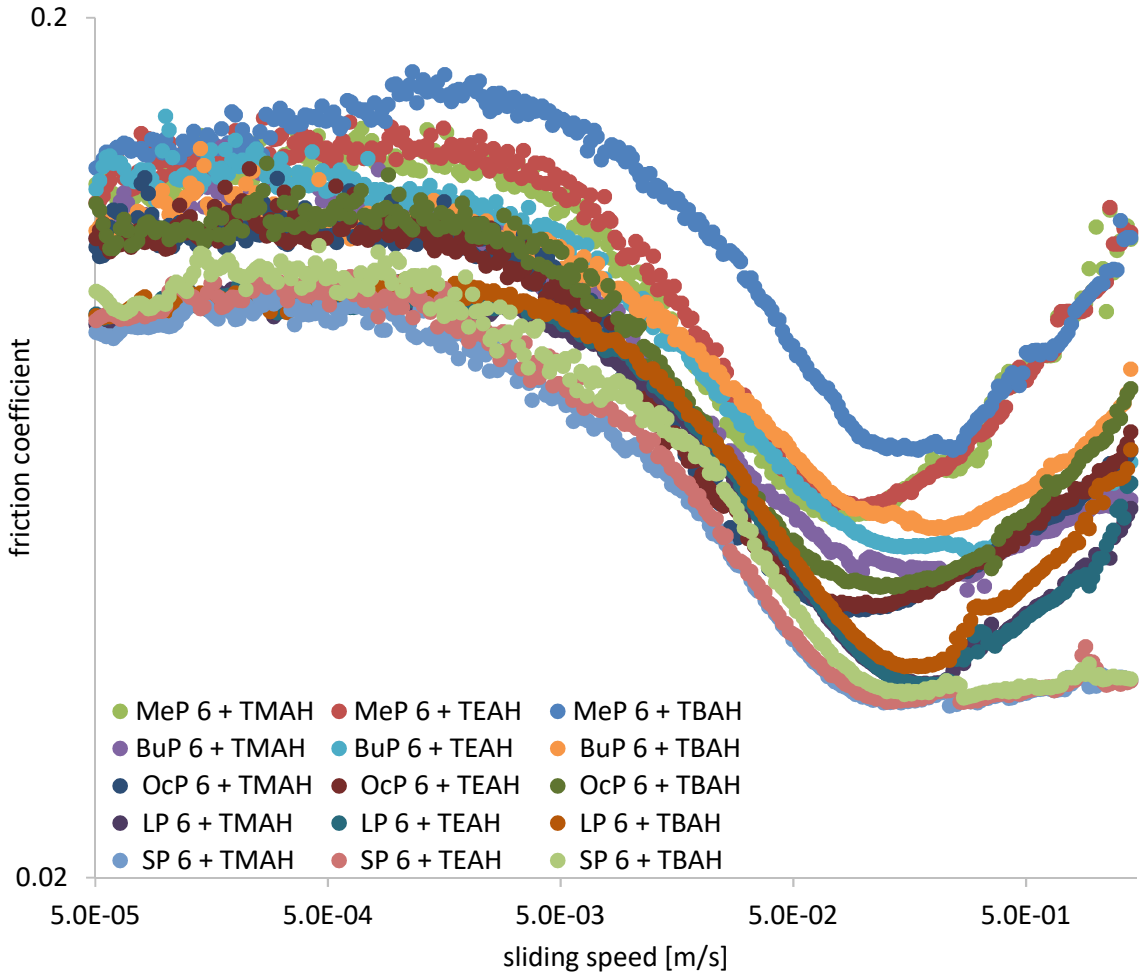

Figure IV-34: Stribeck curves of the different Ionic Liquids, based on different alcohols with constant PO-degree (PO = 6)

Figure IV-34 shows that the Ionic Liquids are capable of forming a hydrodynamic layer for a complete separation of the two specimen, ball and pin. This is depicted by the transition from

boundary lubrication, fast decrease of the friction coefficient, to the hydrodynamic area, minimum value of the friction coefficient.

The increase of the friction coefficient at high speed can be ascribed to two factors. Mainly, the viscosity of the liquid increases the shear forces, therefore the friction coefficient increases again. Second, if the laminar flow into the gap is disturbed and turbulent liquid whirls are formed, the separation of the specimen could not be completed, so higher friction coefficients were measured.
As described in III.3.9, the average friction coefficient at the beginning of the measurement and the minimum value is also determined.

The left side of Figure IV-35 shows the minimum friction coefficient values and the right side shows the average friction coefficient values of the first one hundred measuring points at the beginning of the measurement, depending on the C-chain lengths of the anionic part.

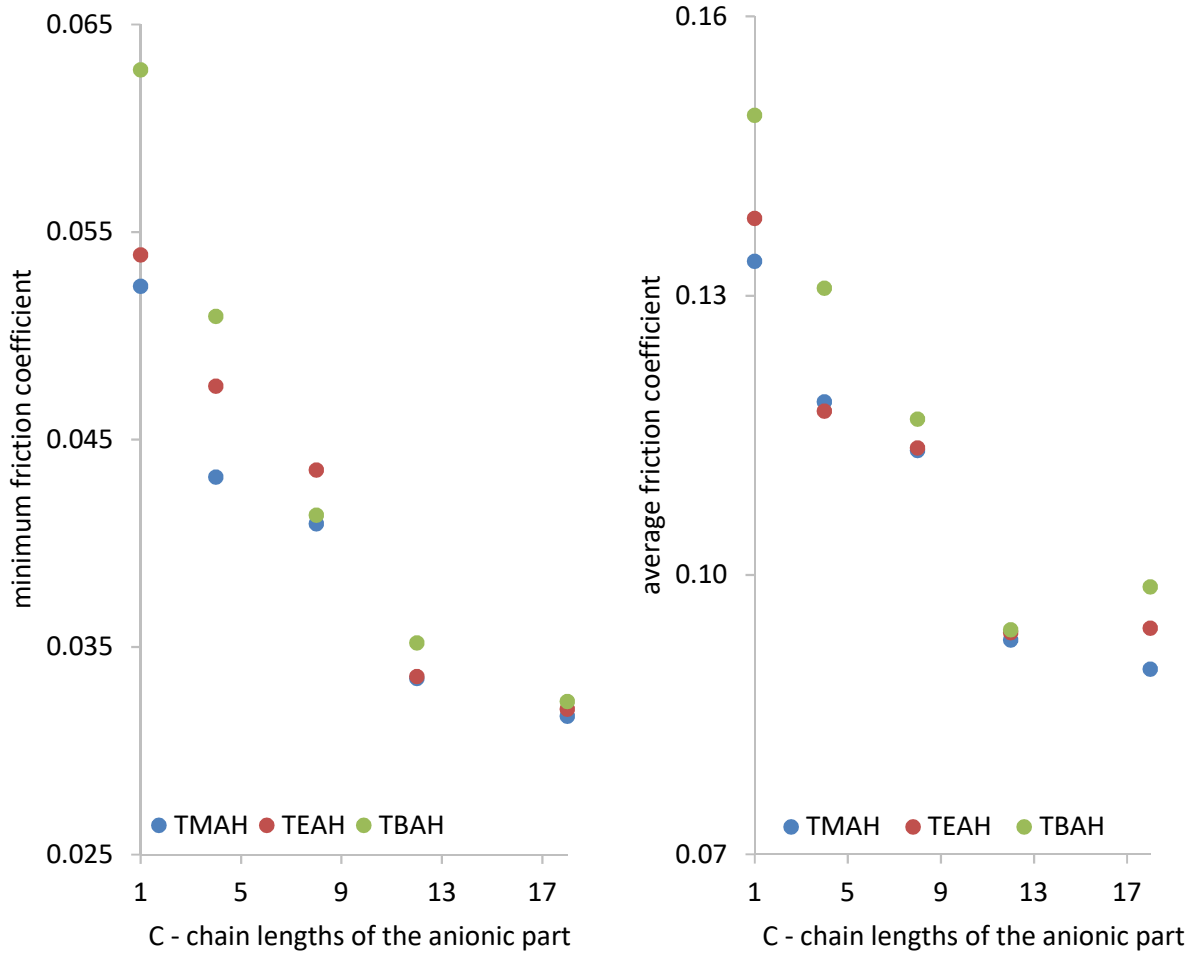

Figure IV-35: Left side shows the minimum friction coefficient values, right side shows the average value of the friction coefficient in the beginning of the measurement depending on the C-chain lengths of the different Ionic Liquids with constant PO-degree (PO = 6)

Figure IV-35 shows that with increasing C-chains, the tribological behaviour becomes better, meaning the average value in the beginning and the minimum of friction value become lower. As already described, long-chain carboxylic acids could form a uniform tribolayer, which

separates the specimen. Short chain molecules, like C_1, C_4 and C_8, do not show good lubrication behaviour. In general, following observation could be made concerning the C-chain dependence of the lubricity: $C_1 << C_4 < C_8 << C_{12} < C_{18}$.
The cationic part seems to have a significant influence on the lubricity only for short chain molecules. With longer C-chain > C_8, this dependence becomes much lower.

In Figure IV-36, the Stribeck curves of the Ionic Liquids with constant C-chain (C_{18}) and different PO-degrees are depicted.

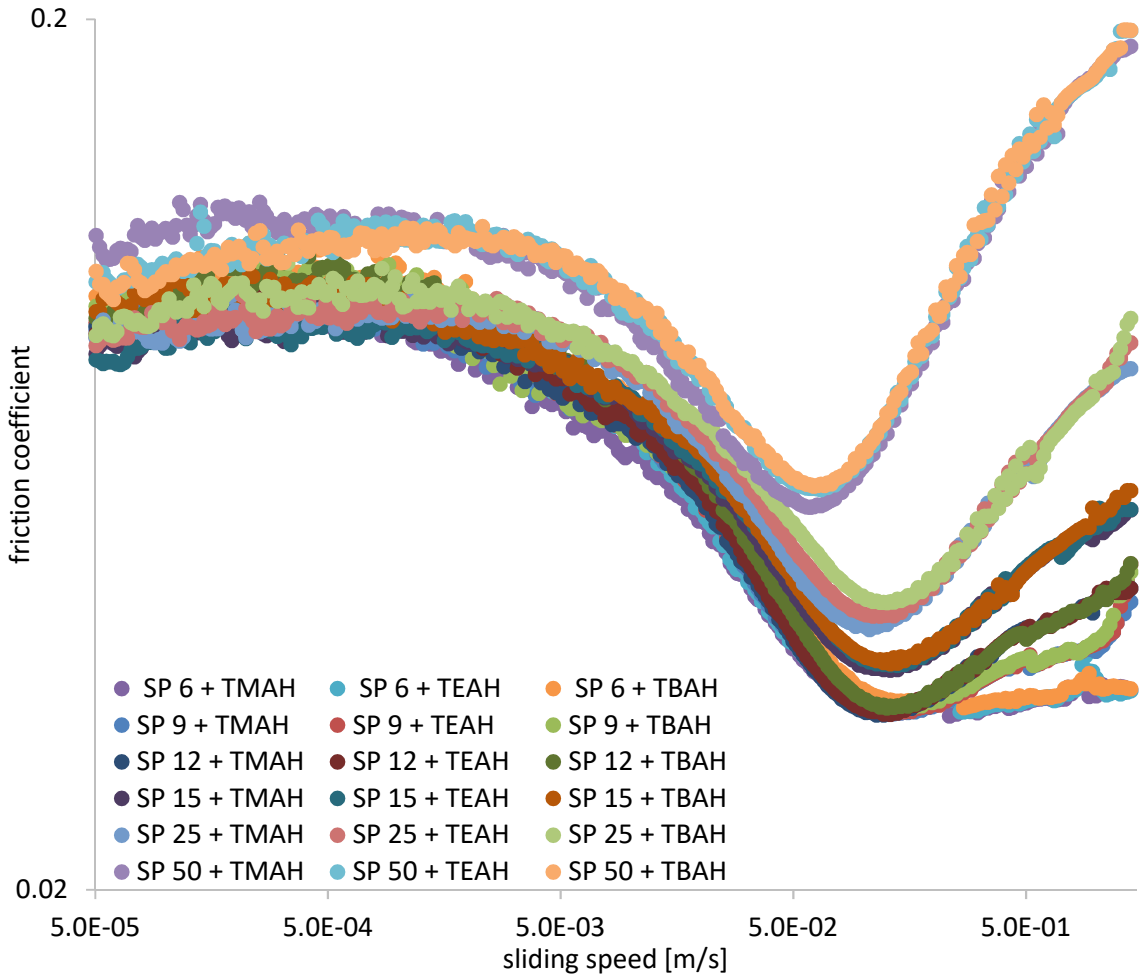

Figure IV-36: Stribeck curves of the different Ionic Liquids with constant C-chain (C_{18}) and different PO-degrees

Figure IV-36 shows a behaviour similar to Figure IV-34. The Ionic Liquids are able to separate the specimen.
In Figure IV-37, the minimum friction coefficients and the average of the first one hundred measurement points are depicted.

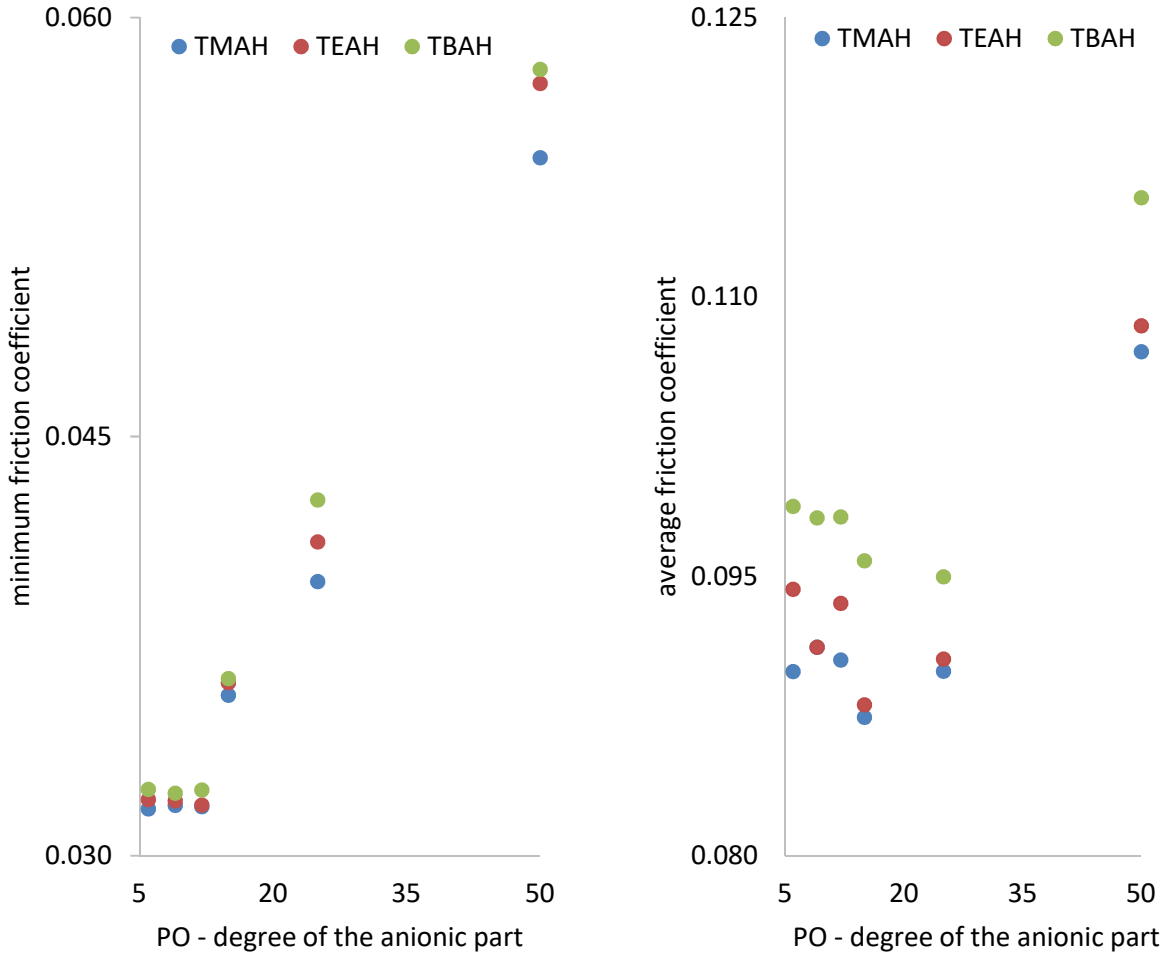

Figure IV-37: Left side shows the minimum friction coefficient values, right side shows the average value of the friction coefficient in the beginning of the measurement depending on the PO-degrees Ionic Liquids with constant C-chain length (C_{18})

The left side of Figure IV-37 shows that with increasing PO-degree of the anionic part, the lubrication power becomes lower. Especially the long PO-degrees, 25 and 50, show very bad lubrication behaviour. The minimum friction coefficient is approximately 1.5 to 2 times higher compared to the low PO-values. Particularly SP 6, C_{18} 6PO shows very good lubrication values, minimum as well as average friction coefficients. It seems that with lower PO-degrees, the lubrication properties become better, this effect could be attributed to the less intermolecular disturbance at the metal surface by the PO-chains. From Figure IV-37 it can be concluded that the lubrication power decreases in the following order, 6 PO > 9 PO > 12 PO >> 15 PO >> 25 PO >>> 50 PO.

One of the main reasons for low friction coefficients and fast development of a hydrodynamic layer, which separates the specimen, is the viscosity of the Ionic Liquid.

In Table IV-24, the achieved minimum friction coefficient, the corresponding sliding speed and the viscosity at 273.15 K for the Ionic Liquids with constant PO-degree (PO = 6) and different alkyl chains are depicted.

Anionic	Cationic	minimum friction coefficient	sliding speed [m/s]	viscosity [mPa s] at 293 K
MeP 6	TMAH	0.0524	0.0864	310.7
	TEAH	0.0539	0.0926	291.9
	TBAH	0.0628	0.1400	205.6
BuP 6	TMAH	0.0432	0.0864	550.3
	TEAH	0.0476	0.1100	499.6
	TBAH	0.0509	0.1353	381.3
OcP 6	TMAH	0.0409	0.1251	624.2
	TEAH	0.0414	0.1289	558.1
	TBAH	0.0435	0.1295	447.8
LP 6	TMAH	0.0335	0.1853	859.1
	TEAH	0.0336	0.2118	653.3
	TBAH	0.0352	0.1977	520.9
SP 6	TMAH	0.0317	0.2349	1196.2
	TEAH	0.0320	0.2605	1034.6
	TBAH	0.0324	0.2696	615.0

Table IV-24: Achieved minimum friction coefficient, corresponding sliding speed and viscosity of the Ionic Liquids, based on constant PO-degree (PO = 6) and different alkyl chains

Out of this table, the correlation between the three values can be seen. With higher viscosity, the minimum value of the friction coefficient also decreases, meaning the two moving bodies are less in contact. To achieve these states, also less speed is needed with higher viscosity. This is a result of the stronger hydrostatic pressure formed by the more viscous Ionic Liquids.

Table IV-25 shows the lubrication properties of Ionic Liquids with constant C-chain (C_{18}) and different PO-degrees.

Anionic	Cationic	minimum friction coefficient	sliding speed [m/s]	viscosity [mPa s] at 293 K
SP 6	TMAH	0.0317	0.2349	1196.2
	TEAH	0.0320	0.2605	1034.6
	TBAH	0.0324	0.2696	615.0
SP 9	TMAH	0.0318	0.1263	1035.8
	TEAH	0.0320	0.1400	876.8
	TBAH	0.0322	0.1400	734.1
SP 12	TMAH	0.0318	0.1138	711.0
	TEAH	0.0318	0.1307	650.3
	TBAH	0.0324	0.1263	556.9
SP 15	TMAH	0.0357	0.1307	642.5
	TEAH	0.0362	0.1400	575.9
	TBAH	0.0363	0.1307	473.5
SP 25	TMAH	0.0398	0.1063	509.9
	TEAH	0.0412	0.1100	394.9
	TBAH	0.0427	0.1263	312.9
SP 50	TMAH	0.0550	0.0591	351.9
	TEAH	0.0576	0.0656	287.2
	TBAH	0.0582	0.0612	221.9

Table IV-25: Achieved minimum friction coefficient, corresponding sliding speed and viscosity of the Ionic Liquids, based on constant C-chain (C_{18}) and different PO-degrees

Again, the same conclusions concerning minimum friction coefficient, corresponding sliding speed and viscosity of the Ionic Liquid can be made, as we have seen with the Ionic Liquids with different C-chains and constant PO-degree (PO = 6).

In Figure IV-38, the best lubricating Ionic Liquids based on SP 6 (C_{18} 6PO) will be compared to a natural “pure” oil without any additive, in this case rape-seed oil, and a commercially available oil, which has a high amount of additives, engine oil (10W40).

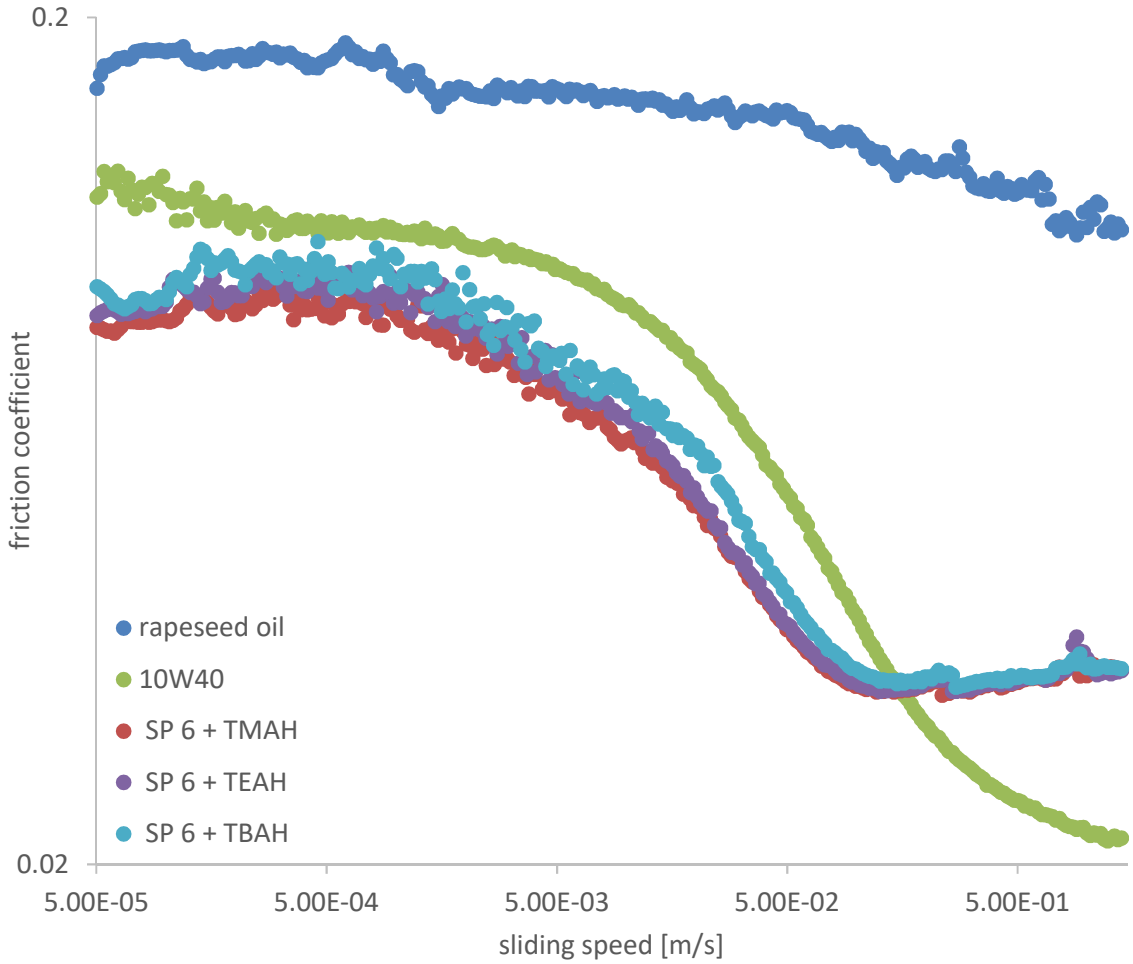

Figure IV-38: Comparison of the lubrication behaviour of rape-seed oil, 10W40 engine oil and the three different Ionic Liquids based on C_{18} 6PO

From Figure IV-38, it can be concluded that rape-seed oil shows very poor lubrication behaviour. This oil is not able to form a tribolayer, neither to separate the two specimens, ball and pin, from each other by a hydrodynamic film. The amount of wear is dramatically high and the friction coefficient stays more or less at the same value.
The engine oil starts with a higher friction coefficient compared to the Ionic Liquids. This phenomenon can be explained by the much lower viscosity of the engine oil. Nevertheless, the friction coefficient of the engine oil decreases quite fast and to low values, 1.5 times lower than the best Ionic Liquid. This can be an effect of the different additives inside the oil. In Table IV-26, the minimum friction coefficient, the corresponding sliding speed and the viscosity at 293 K are shown.

			minimum friction coefficient	sliding speed [m/s]	viscosity [mPa s] at 293 K
Rape-seed oil			0.1107	1.3264	162
10W40			0.0213	1.3733	381
Catanionic	SP 6	TMAH	0.0317	0.2349	1196.2
		TEAH	0.0320	0.2605	1034.6
		TBAH	0.0324	0.2696	615.0

Table IV-26: Achieved minimum friction coefficient, corresponding sliding speed and viscosity of rape-seed oil, engine oil (10W40) and the Ionic Liquids, based on SP 6 (C_{18} 6PO)

IV.3.2.2 Ionic Liquids as additives in a neat oil

Besides the application as neat oil, Ionic Liquids are used as additives. Already there are several publications in the literature were Ionic Liquids have been added to different oils, like mineral oil, poly-alpha olefin or ester [187,251,268–271,253–256,264–267].

In the present section, the lubrication properties of rape-seed oil in combination with the prepared Ionic Liquids are investigated. Based on the results made in Chapter Oil solubilityIV.2.1.5 Oil solubility and IV.3.2.1 Ionic Liquids as neat oils, two Ionic Liquids have been chosen, Stearyl TMAH and SP 3 TMAH (C_{18} 3PO TMAH). From the former chapter IV.3.2.1 Ionic Liquids as neat oils it can be concluded that especially long C-chain, short PO-degree and small quaternary ammonium cation based Ionic Liquids show good lubrication behaviour. Due to their bad miscibility, IV.2.1.5 Oil solubility, the maximum concentrations in rape-seed oil are 1, 2, and 5 w/w%. The molecules are solubilised and then this mixture (rape-seed oil / Ionic Liquid) is tested as lubricant based on the circumstances described in III.3.9. In Figure IV-39, the lubrication behaviors of the different Ionic Liquid mixtures are depicted.

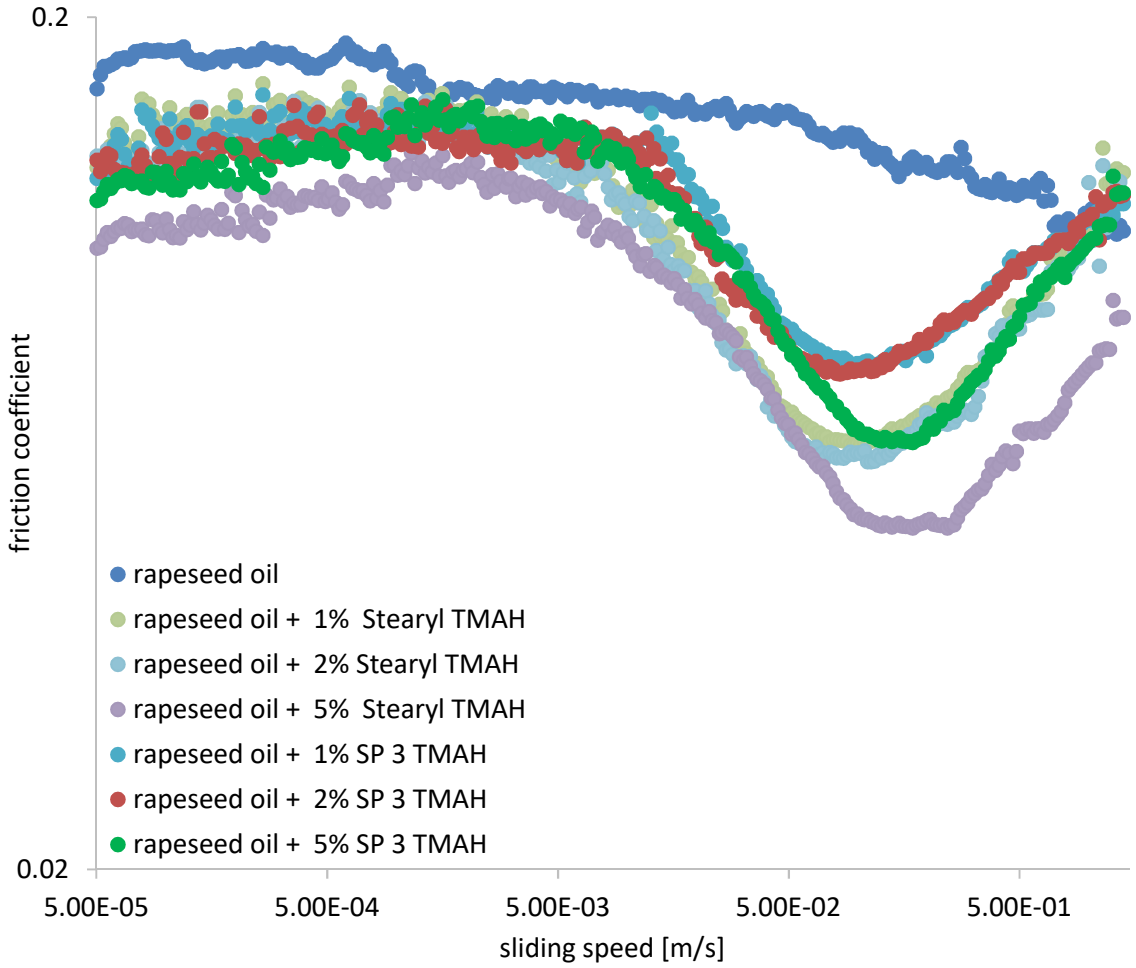

Figure IV-39: Stribeck curves of rape-seed oil and the different rape-seed oil / Ionic Liquids mixtures

It can be concluded that small amounts of the Ionic Liquids are already influencing the lubrication behaviour. As mentioned before, under the used test circumstances, rape-seed oil

is not able to form a hydrodynamic pressure. But the small amounts of the Ionic Liquid help to form a tribolayer, as well as to separate the specimen, ball and pin, from each other. But the formed film is not stable at higher sliding speeds. Nevertheless, again the influence of PO can be seen in Figure IV-39. The Ionic Liquids containing 3 moles PO exhibit a smaller lubrication power compared to the stearic acid based Ionic Liquid. In Table IV-27, the minimum friction coefficient, sliding speed and viscosity at 293 K are shown.

			minimum friction coefficient	**sliding speed [m/s]**	**viscosity [mPa s] at 293 K**
Rape-seed oil			0.1107	1.3264	162
Catanionic	Stearyl TMAH	1%	0.0630	0.1010	164
		2%	0.0602	0.9260	167
		5%	0.0503	0.0628	169
	SP 3 TMAH	1%	0.0779	0.1138	165
		2%	0.0763	0.0864	165
		5%	0.0634	0.0632	166

Table IV-27: Achieved minimum friction coefficient, corresponding sliding speed and viscosity of rape-seed oil and the different additives in rape-seed oil

To decrease the friction coefficient in industrial formulation, the addition of an organic friction modifier is possible. A typical organic friction modifier is oleic acid. So for comparison reasons, also rape-seed oil + 5 w/w% oleic acid is tested, see Figure IV-40 and Table IV-28.

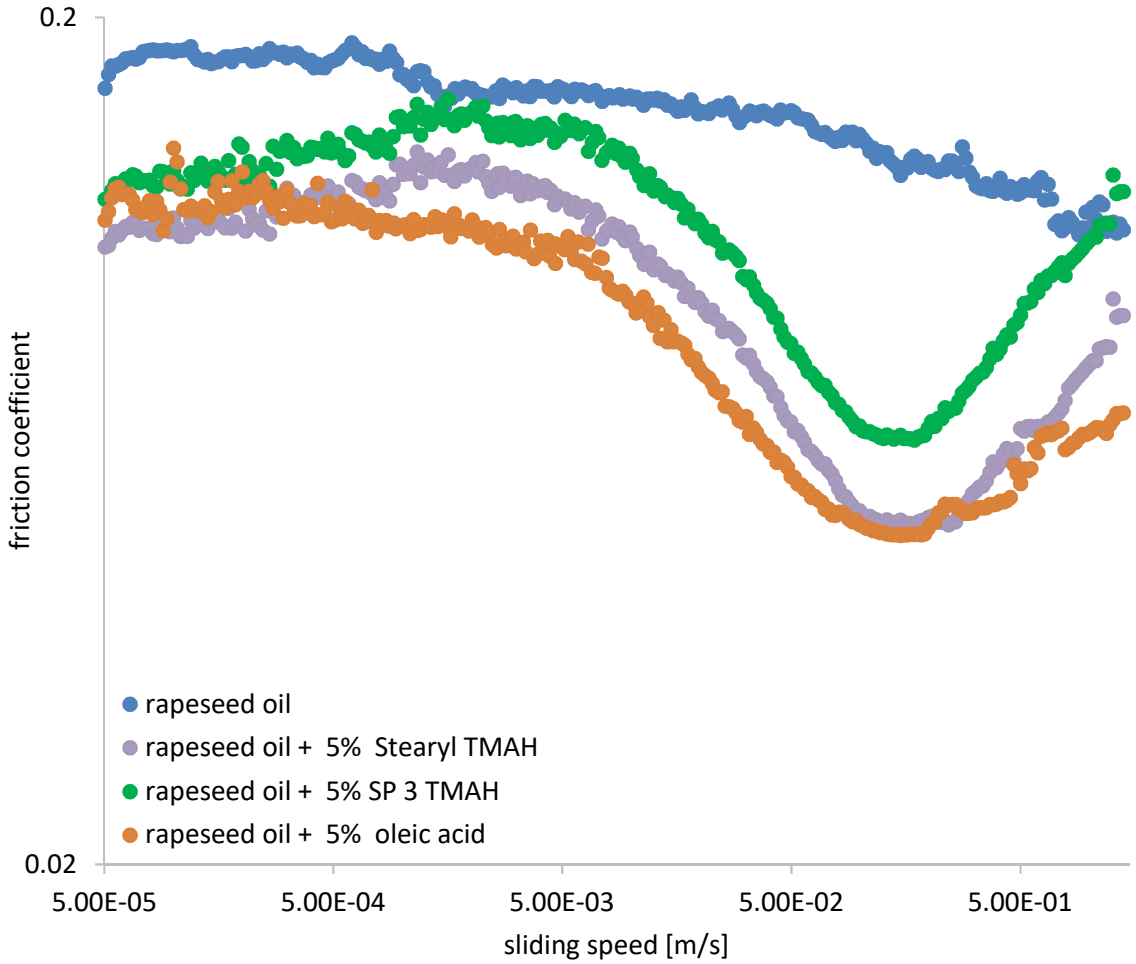

Figure IV-40: Comparison of the lubrication behaviour of rape-seed oil and the different additives in rape-seed oil

	minimum friction coefficient	sliding speed [m/s]	viscosity [mPa s] at 293 K
Rape-seed oil	0.1107	1.3264	162
Rape-seed oil + 5% oleic acid	0.0489	0.1502	161
Rape-seed oil + 5% Stearyl TMAH	0.0503	0.0628	169
Rape-seed oil + 5% SP 3 TMAH	0.0634	0.0632	166

Table IV-28: Achieved minimum friction coefficient, corresponding sliding speed and viscosity of rape-seed oil and the different additives in rape-seed oil

It can be concluded that Stearyl TMAH and oleic acid show similar tribological behaviour. The friction coefficient of the rape-seed / oleic acid mixture decreases faster than with Stearyl TMAH, but the minimum friction coefficient is almost same. The Stearyl TMAH forms already at lower sliding speed a tribolayer, which separates the specimen ball and pin from each other. The oleic acid form also this kind of layer but at much later and with higher sliding speed. There is an increase of the friction coefficient after reaching the minimum, this phenomenon explains that the tribolayer formed by oleic acid and Stearyl TMAH seems to be not very stable. Like described in chapter II.1.5.3 Boundary Lubrication described, branched molecules are disrupting the adsorbed film on the metal surface. The branching from the propoxylation causes the higher friction coefficient. Straight molecules, stearyl and oleyl, can

build up a uniform monomolecular absorbed layer on the metal surface, which results in the lower friction coefficient. the molecule distribution caused by the propoxylation also favor the weak cohesive forces of the formed tribolayer.

V Conclusion

The goal of this thesis was to gain enough data and knowledge to synthesise Ionic Liquids (Catanionics) with customized or tailor-made physico-chemical properties.
This approach has been proved to be successful. Using the conclusions from the three parts of the thesis, synthesis, physico-chemical and tribological data, a proposition for a customized sample with a defined C-chain, PO-degree, and quaternary ammonium counter-ion is possible.

In the first part, the synthesis of the Surface-Active Ionic Liquids (Catanionics) by means of the combination of alkyl ether carboxylate and quaternary ammonium compounds was studied. Following results concerning the synthesis could be obtained:

The synthesis of the alkyl ether carboxylic acid could be successfully done, using an industrial two-step pathway. After the first reaction, the addition of propylene oxide to the corresponding alcohol, an oligomer distribution of the different ethers is obtained. These distributions could be characterised as “narrow-range” distributions with a small content of free alcohol. The determined PO-degrees are very close to the proposed values, as expected. The amount of by-products, like polypropylene glycol, is also rather small.
After that, the addition of sodium monochloroacetate to the alkyl ether was performed, resulting in the corresponding alkyl ether carboxylic acids. The gained molecules could be obtained in high conversions (≥ 90%). The by-products, like glycolic acid and diglycolic acid, could be removed by an extraction step using a second phase separation step with water. The higher water content is removed via distillation and the residual by-products precipitated and could be removed by filtration.

The second part of the Ionic Liquid, the quaternary ammonium compound, is readily available with high conversion and purity on the market. The preparation of the Ionic Liquids could be easily done by mixing the alkyl ether carboxylic acid with the corresponding quaternary ammonium compound followed by removal of the formed reaction water. The gained Catanionics showed rather low contents of water and sodium chloride, i.e. ≤ 1000 ppm. These values are typical of industrial based Ionic Liquids.

The second part of this thesis deals with the determination of physico-chemical properties, like density, viscosity, conductivity, thermo stability, melting ranges, hygroscopicity and oil solubility. The properties have been correlated to the chemical structure of the corresponding Ionic Liquids.

The first figure, Figure V-1, shows that the molecular structure has a strong influence on the density. Shorter C-chains and small cations increase the density, on the contrary, longer PO-degrees decrease the density. Much smaller molecules, having a short C-chain combined with small cation are fitting to a small molar volume, which result in a rather high density, compared to long C-chain ones combined with bulky cation. The PO-chain increases the flexibility of the anionic part. This directly results in more molecules in a specific volume, resulting in higher density.

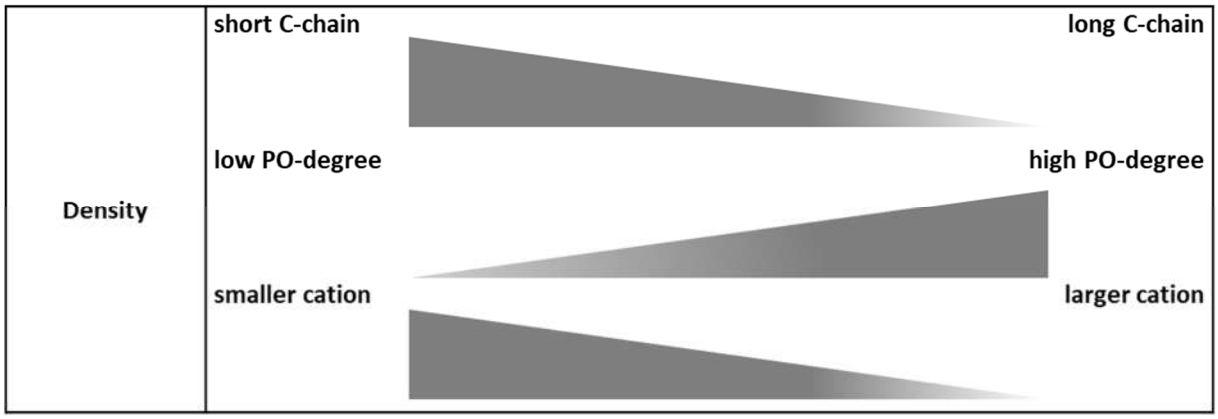

Figure V-1: Correlation between molecular structure of the different parts of the Ionic Liquid and the density

As second physico-chemical property, the viscosity has been determined. Also, here, an influence of the molecular structure has been observed, see Figure V-2. Especially short C-chain molecules with long PO-degrees combined with large cation exhibit very low viscosities. This combination results in low intermolecular lubrication, meaning low viscosity. If the molecule is enlarged by a long C-chain and the flexibility is decreased by lowering the PO-degree combined with a small cation, the intermolecular interaction become much higher, so also the viscosity increases.

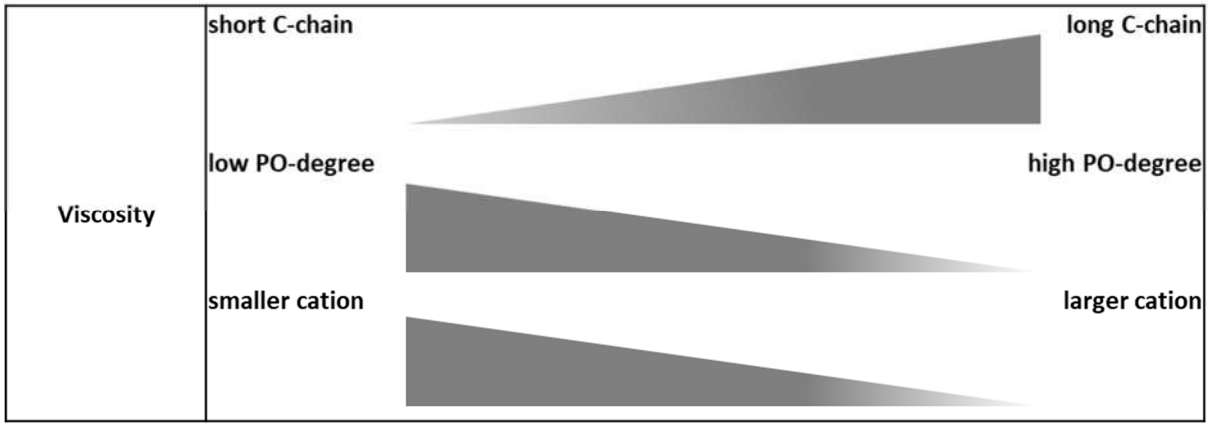

Figure V-2: Correlation between molecular structure of the different parts of the Ionic Liquid and the viscosity

The conductivity has been the third measured property of the Ionic Liquids. The determined values have been low, but also here, an influence of the molecular shape can be derived, see Figure V-3. Shorter C-chains with low PO-degrees and a small cation result in higher conductivities than Ionic Liquids with a long C-chain combined with long PO-degree and bulky cation. The mentioned combination leads to a stronger flow of the electric current. This means, larger molecules, i.e. long C-chains combined with long PO-degrees and bulky cations, decrease the flow of the electric charge in the tested Ionic Liquids.

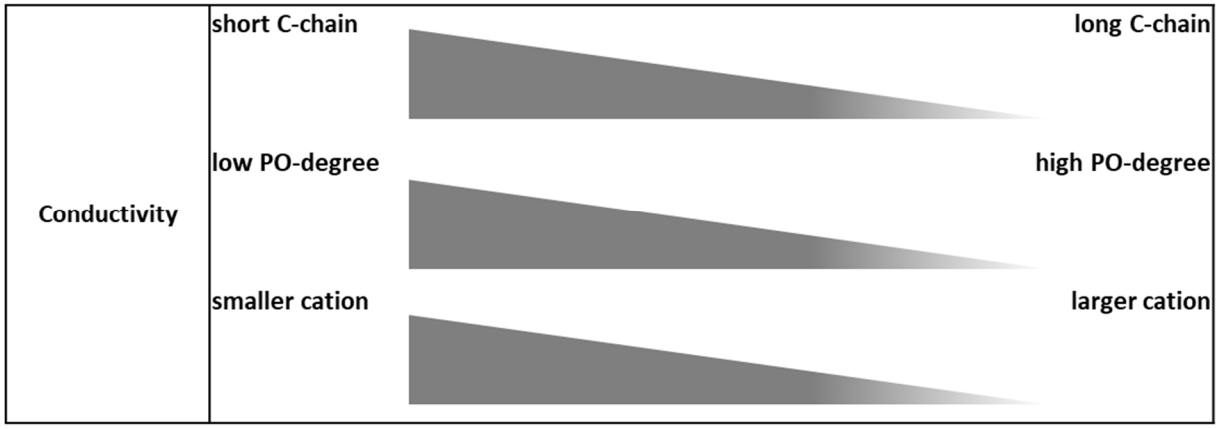

Figure V-3: Correlation between molecular structure of the different parts of the Ionic Liquid and the conductivity

The thermal stability of the tested Ionic Liquids is also related to the combination of anion and cation as well as to the molecular shape, see Figure V-4. Short C-chains and PO-degrees combined with large cations result in low thermal stability. These molecules are more easily thermally stimulated, which means they decompose at much lower temperatures. The Ionic Liquids with long C-chain, long PO-degree and small cation are thermally more stable.
All tested Ionic Liquids decompose in two steps, first always the cationic part is decomposed, followed by the anionic part.

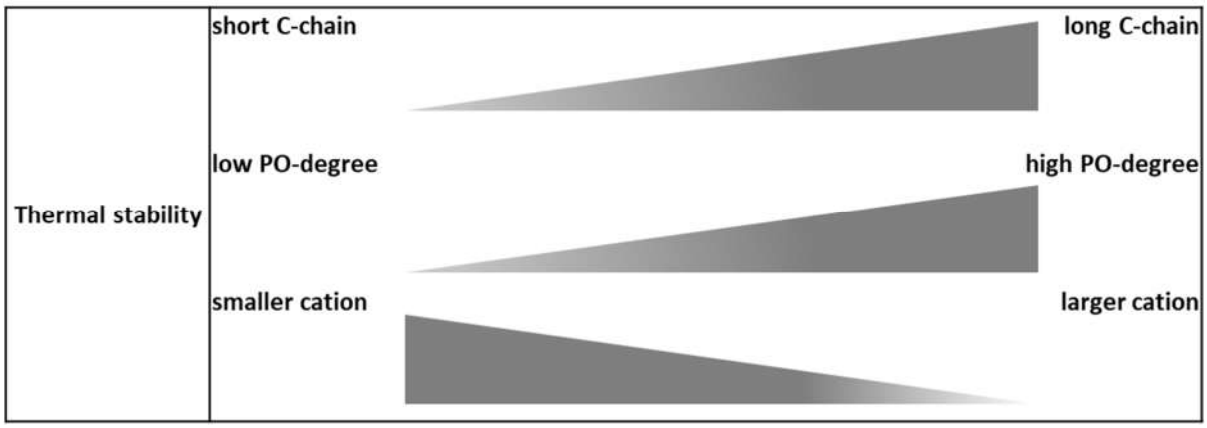

Figure V-4: Correlation between molecular structure of the different parts of the Ionic Liquid and the thermal stability

After the thermal stability, also the melting range of the Catanionics has been determined. Here, also a relation of the melting range to the tested Ionic Liquids and to their molecular structure is observable, see Figure V-5. It could be concluded that the intermolecular interactions become higher with long C-chains, short PO-degrees and small cations. This combination results in a more extended liquid region. If the Ionic Liquid consists of a short C-chain, long PO-degree and of a bulky cation, the molecules have low tendency to orientate to each other, so close packaging is disturbed.

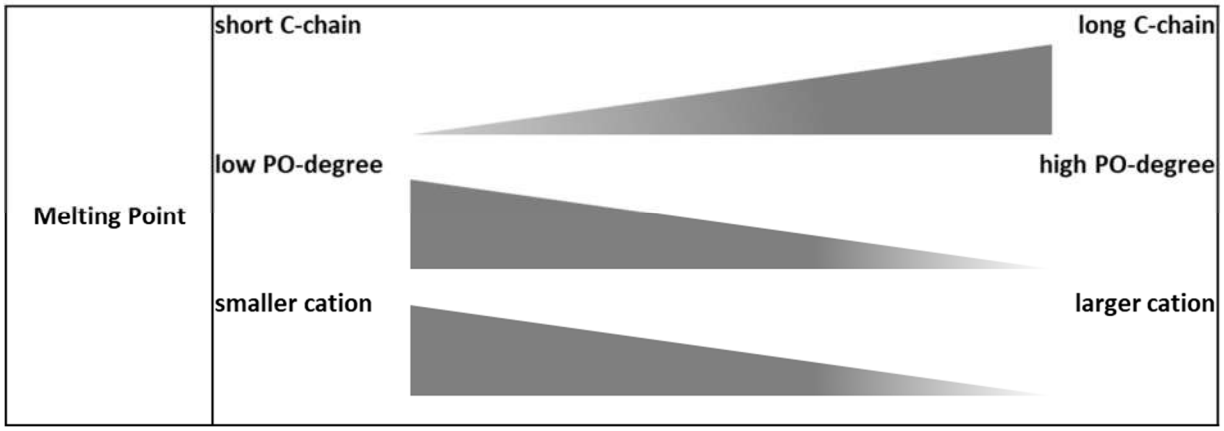

Figure V-5: Correlation between molecular structure of the different parts of the Ionic Liquid and the thermal melting point

The structure effect of the tested Ionic Liquids on the hygroscopy has been derived, see Figure V-6. Small molecules, i.e. short C-chains and PO-degrees combined with a small cation, show high hydrophilicity. In parallel, they are more hygroscopic and adsorb water from the surrounding environment. Large molecules, i.e. molecules with a long C-chain and PO-degree with a bulky cation are less hygroscopic and their affinity to water is weaker. This means the tendency to adsorb water is much lower.

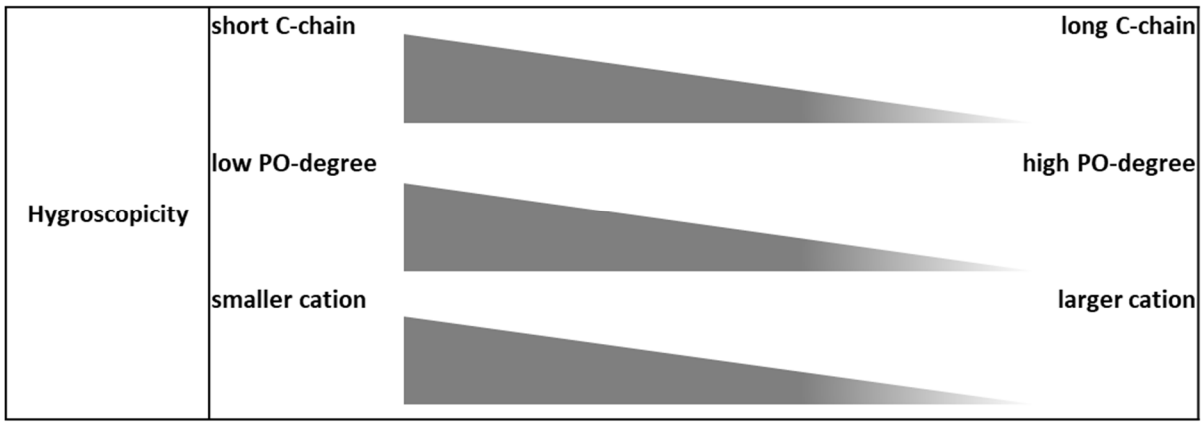

Figure V-6: Correlation between molecular structure of the different parts of the Ionic Liquid and the hygroscopicity

The consequence of the molecular shape of the tested Ionic Liquids to the oil solubility is shown in Figure V-7. Longer C-chains with shorter PO-degrees combined with bulky cations show a higher solubility in the used triglyceride.

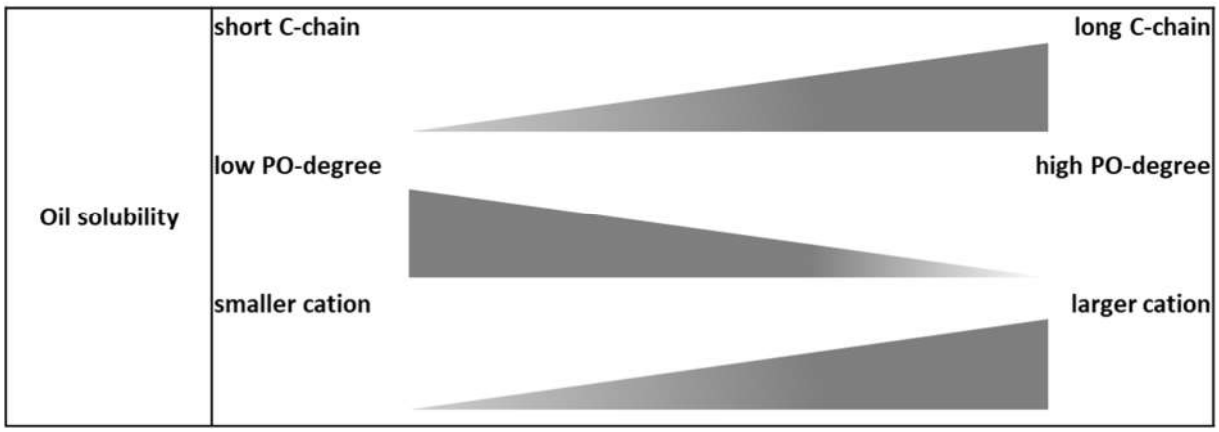

Figure V-7: Correlation between molecular structure of the different parts of the Ionic Liquid and the oil solubility

In the third part, the tribological evaluation of the different Ionic Liquids (Catanionics) has been conducted. Again, an influence of the molecular shape, in terms of C-chain lengths, PO-degree and size of the quaternary ammonium compound has been observed.

The film forming properties again are directly correlated to the molecular structure of the used Ionic Liquid. Long chain molecules, i.e molecules with C-chain longer than C_8, show good lubrication behaviour, meaning these molecules form a stable hydrodynamic film. The short-chain molecules also form a stable film, but the minimum friction coefficients are much higher, compared to the longer Ionic Liquids. Besides the molecular shape, the viscosity is the major parameter for good lubrication behaviour, meaning higher viscosity results in low minimum friction coefficients combined with stable hydrodynamic film. Long PO-degrees combined with bulky cations also result in lower viscosities. This combination directly influences the film forming properties in a negative way. A good Ionic Liquid should have a long C-chain, at least C_{18}, short PO-degree, like PO = 3 and a small cation like TMAH. Compared to natural "pure" rape-seed oil, the lubrication properties of the Ionic Liquids are much better. Rape-seed oil is even not forming a hydrodynamic film, meaning the two specimen, ball and pin, are not separated, resulting in much wear. But a commercially available engine oil (10W40) is showing much better lubrication properties. The engine oil has a much lower friction coefficient and it is forming a hydrodynamic film.
The only drawback is that with higher viscosities the sliding speed to form this hydrodynamic film is higher, this results in a longer contact time between the specimens. Longer contact times also results in higher wear. The found correlations between viscosity and tribological behaviour are similar to the performance of Poly Alpha Olefins (PAO). These polymer molecules can also be adjusted by their molecular weight, resulting in different viscosities. But in this case, the polarities and so the solubility in polar oils or the miscibility with polar additives is rather poor.
Due to the good miscibility in rape-seed oil, Stearyl TMAH and SP 3 (C_{18} 3PO) TMAH can be used as additive. It can be concluded that with increasing Ionic Liquid concentration the lubrication power also increases. Even low amounts of both Ionic Liquids can form a hydrodynamic film, and this film forming property is increased by higher Ionic Liquid concentration. Also the lowest friction coefficient is directly related to the concentration, lower values are achieved with higher concentrations. Compared to a typical organic friction modifier, i.e. oleic acid, only the Ionic Liquid without PO, Stearyl TMAH, show good lubrication

properties. The achieved minimum friction coefficient of oleic acid, is almost similar to the Stearyl TMAH based Ionic Liquid.

VI Literature

1. Jost, H. *Lubrication (tribology) education and research. A report on the present position and industry's needs*. (1966).
2. Jost, H. P. Tribology — Origin and future. *Wear* **136**, 1–17 (1990).
3. Stachowiak, G. & Batchelor, A. *Engineering Tribology*. (Elsevier, 2005).
4. Braun, O. & Naumovets, A. Nanotribology: Microscopic mechanisms of friction. *Surf. Sci. Rep.* **60**, 79–158 (2006).
5. Cooper, M. *The Inventions of Leonardo da Vinci*. (1965).
6. Amontons, G. *De la resistance causée dans les machines (About resistance and force in machines). Mémories de l'Académic Royale A*. (1699).
7. Bowden, F. & Tabor, D. *The Friction and Lubrication of Solids*. (Oxford University Press, 2001).
8. Hertz, H. Über die Berührung fester elastischer Körper. *J. für die reine und Angew. Math.* **92**, 156–171 (1881).
9. Archard, J. F. & Allibone, T. E. Elastic deformation and the laws of friction. *Proc. R. Soc. London. Ser. A. Math. Phys. Sci.* **243**, 190–205 (1957).
10. Greenwood, J. A., Williamson, J. B. P. & Bowden, F. P. Contact of nominally flat surfaces. *Proc. R. Soc. London. Ser. A. Math. Phys. Sci.* **295**, 300–319 (1966).
11. Johnson, K. L. Adhesion and friction between a smooth elastic spherical asperity and a plane surface. *Proc. R. Soc. London. Ser. A Math. Phys. Eng. Sci.* **453**, 163–179 (1997).
12. Tas, N., Sonnenberg, T., Jansen, H., Legtenberg, R. & Elwenspoek, M. Stiction in surface micromachining. *J. Micromechanics Microengineering* **6**, 385 (1996).
13. Johnson, K. L. & Johnson, K. L. *Contact mechanics*. (Cambridge university press, 1987).
14. Riedo, E., Gnecco, E., Bennewitz, R., Meyer, E. & Brune, H. Interaction Potential and Hopping Dynamics Governing Sliding Friction. *Phys. Rev. Lett.* **91**, 84502 (2003).
15. Chen, Y. L., Helm, C. A. & Israelachvili, J. N. Molecular mechanisms associated with adhesion and contact angle hysteresis of monolayer surfaces. *J. Phys. Chem.* **95**, 10736–10747 (1991).
16. OECD. *Friction, Wear and Lubrication - Tribology of Terms and Definition*. (1969).
17. Burwell, J. J. Survey of Possible Wear Mechanisms. *Wear* **1**, 119–141 (1957).
18. Suh, N. P. The delamination theory of wear. *Wear* **25**, 111–124 (1973).
19. Rabinowicz, E. *Friction and Wear of Materials*. (Wiley, 2013).
20. Kennedy, F. E., Booser, R. & Wilcock, D. F. Tribology, Lubrication, and Bearing Design. in *The CRC Handbook of Mechanical Engineering* (eds. Kreith, F. & Goswani, Y. D.) 388–429 (CRC Press, 2005).
21. Archard, J. Contact and rubbing of flat surfaces. *J. Appl. Phys.* **24**, 981–988 (1953).
22. Rabinowicz, E., Dunn, L. & Russell, P. A Study of Abrasive Wear Under Three Body Conditions. *Wear* **4**, 345–355 (1961).
23. Hamrock, B., Schmid, S. & Jacobson, B. *Fundamentals of Fluid Film Lubrication*. (Marcel Dekker, 2004).
24. Hertz, H. On the contact of solids - on the contact of rigid elastic solids and on hardness. in *Miscellanous Papers* 146–183 (Macmillan Publishers Limited, 1896).
25. Bowden, F. P. & Tabor, D. The Area of Contact between Stationary and between Moving Surfaces. *Proc. R. Soc. Lond. A. Math. Phys. Sci.* **169**, 391–413 (1939).
26. Johnson, K. L., Kendall, K. & Roberts, A. D. Surface Energy and the Contact of Elastic

Solids. *Proc. R. Soc. Lond. A. Math. Phys. Sci.* **324**, 301–313 (1971).
27. Greenwood, J. & Tripp, J. Elastic Contact of Rough Spheres. *ASME J. Appl. Mech.* **34**, 153–159 (1967).
28. Whitehouse, D. J. & Archard, J. F. The Properties of Random Surfaces of Significance in their Contact. *Proc. R. Soc. Lond. A. Math. Phys. Sci.* **316**, 97–121 (1970).
29. Nayak, P. R. Random process model of rough surfaces in plastic contact. *Wear* **26**, 305–333 (1973).
30. Polonsky, I. A. & Keer, L. M. Fast methods for solving rough contact problems: a comparative study. *J. Trib.* **122**, 36–41 (2000).
31. Greenwood, J. Problems with Surface Roughness, Fundamentals of Friction: Macroscopid and Microscopic Processes, Proc. NATO Adv. Study Inst. on Fundamentals of Frictioin, NATO ASI Series E: *Appl. Sci.* 57–76 (1992).
32. Lai, W. T. & Cheng, H. S. Computer simulation of elastic rough contacts. *ASLE Trans.* **28**, 172–180 (1985).
33. Brandt, A. & Lubrecht, A. A. Multilevel matrix multiplication and fast solution of integral equations. *J. Comput. Phys.* **90**, 348–370 (1990).
34. Nogi, T. & Kato, T. Influence of a hard surface layer on the limit of elastic contact—Part I: Analysis using a real surface model. (1997).
35. Liu, S., Wang, Q. & Liu, G. A versatile method of discrete convolution and FFT (DC-FFT) for contact analyses. *Wear* **243**, 101–111 (2000).
36. Dowson, D. *History of tribology*. (Longman, 1979).
37. Jacobson, B. The Stribeck memorial lecture. *Tribol. Int.* **36**, 781–789 (2003).
38. Bhushan, B. *Principles and applications of tribology*. (John Wiley & Sons, 1999).
39. Bhushan, B. *Modern tribology handbook, two volume set*. (CRC press, 2000).
40. Menezes, P. L., Kishore & Kailas, S. V. Study of Friction and Transfer Layer Formation in Copper-Steel Tribo-System: Role of Surface Texture and Roughness Parameters. *Tribol. Trans.* **52**, 611–622 (2009).
41. Menezes, P. L., Kishore & Kailas, S. V. On the effect of surface texture on friction and transfer layer formation—A study using Al and steel pair. *Wear* **265**, 1655–1669 (2008).
42. Hardy, W. B. & Doubleday, I. Boundary Lubrication. The Paraffin Series. *Proc. R. Soc. London. Ser. A, Contain. Pap. a Math. Phys. Character* **100**, 550–574 (1922).
43. Hardy, W. B. & Doubleday, I. Boundary Lubrication. The Temperature Coefficient. *Proc. R. Soc. London. Ser. A, Contain. Pap. a Math. Phys. Character* **101**, 487–492 (1922).
44. Bhushan, B. *Introduction to tribology*. (John Wiley & Sons, 2013).
45. Kleiman, G. G. & Landman, U. Theory of physisorption: He on metals. *Phys. Rev. B* **8**, 5484 (1973).
46. Willing, A. Lubricants based on renewable resources–an environmentally compatible alternative to mineral oil products. *Chemosphere* **43**, 89–98 (2001).
47. Fox, N. J., Tyrer, B. & Stachowiak, G. W. Boundary Lubrication Performance of Free Fatty Acids in Sunflower Oil. *Tribol. Lett.* **16**, 275–281 (2004).
48. Jahanmir, S. Chain length effects in boundary lubrication. *Wear* **102**, 331–349 (1985).
49. HIRONAKA, S. Friction properties of C18-fatty acids. *J. Japan Pet. Inst.* **31**, 216–220 (1988).
50. Hironaka, S. Boundary lubrication. in *Tribology of Mechanical Systems: A Guide to Present and Future Technologies* (eds. Vizintin, J., Kalin, K., Dohda, K. & Jahanmir, S.

(Eds)) 41–51 (ASME Press, 2004).
51. Holmberg, K. & Matthews, A. *Coatings Tribology: Properties, Mechanisms, Techniques and Applications in Surface Engineering*. (Elsevier, 2009).
52. Kumar C., P., Menezes, P. L. & Kailas, S. V. Role of Surface Texture on Friction under Boundary Lubricated Conditions. *Tribol. Online* **3**, 12–18 (2008).
53. Reynolds, O. I. On the theory of lubrication and its application to Mr. Beauchamp tower's experiments, including an experimental determination of the viscosity of olive oil. *Proc. R. Soc. London* **40**, 191–203 (1886).
54. Dowson, D. & Higginson, G. *Elastohydrodynamic lubrication*. (Pergamon Press, 1966).
55. Hamrock, B. J. & Dowson, D. *Ball bearing lubrication: the elastohydrodynamics of elliptical contacts*. (Wiley, 1981).
56. Hamrock, B. J. & Dowson, D. Isothermal elastohydrodynamic lubrication of point contacts: part III—fully flooded results. (1977).
57. Ramsey, G. *Elastohydrodynamics*. (World Scientific, 2001).
58. Mang, T. & Dresel, W. *Lubricants and lubrication*. (Wiley, 2006).
59. Blau, P. J. *Friction Science and Technology: From Concepts to Applications*. (CRC Press, 2019).
60. Plechkova, N. V & Seddon, K. R. Applications of ionic liquids in the chemical industry. *Chem. Soc. Rev.* **37**, 123–150 (2008).
61. Fraser, K. J. & MacFarlane, D. R. Phosphonium-based ionic liquids: an overview. *Aust. J. Chem.* **62**, 309–321 (2009).
62. Forsyth, S. A., Pringle, J. M. & MacFarlane, D. R. Ionic Liquids—An Overview. *Aust. J. Chem.* **57**, 113–119 (2004).
63. Keskin, S., Kayrak-Talay, D., Akman, U. & Hortaçsu, Ö. A review of ionic liquids towards supercritical fluid applications. *J. Supercrit. Fluids* **43**, 150–180 (2007).
64. Welton, T. Room-Temperature Ionic Liquids. Solvents for Synthesis and Catalysis. *Chem. Rev.* **99**, 2071–2083 (1999).
65. Walden, P. Ueber die Molekulargrösse und elektrische Leitfähigkeit einiger geschmolzener Salze. *Bull. l'Académie Impériale des Sci. St. - Pétersbg. VI série* **8**, 405–422 (1914).
66. Sugden, S. & Wilkins, H. CLXVII.—The parachor and chemical constitution. Part XII. Fused metals and salts. *J. Chem. Soc.* 1291–1298 (1929) doi:10.1039/JR9290001291.
67. Hurley, F. H. & WIer, T. P. The electrodeposition of aluminum from nonaqueous solutions at room temperature. *J. Electrochem. Soc.* **98**, 207–212 (1951).
68. Endres, F. & Zein El Abedin, S. Air and water stable ionic liquids in physical chemistry. *Phys. Chem. Chem. Phys.* **8**, 2101–2116 (2006).
69. Chum, H., Koch, V., Miller, L. & Osteryoung, R. An electrochemical scrutiny of organometallic iron complexes and hexamethylbenzene in a room temperature molten salt. *J. Am. Chem. Soc.* **97**, 3264–3265 (1975).
70. Robinson, J. & Osteryoung, R. A. An electrochemical and spectroscopic study of some aromatic hydrocarbons in the room temperature molten salt system aluminum chloride-n-butylpyridinium chloride. *J. Am. Chem. Soc.* **101**, 323–327 (1979).
71. Wilkes, J. S., Levisky, J. A., Wilson, R. A. & Hussey, C. L. Dialkylimidazolium chloroaluminate melts: a new class of room-temperature ionic liquids for electrochemistry, spectroscopy and synthesis. *Inorg. Chem.* **21**, 1263–1264 (1982).
72. Appleby, D., Hussey, C., Seddon, K. & Turp, J. Room-Temperature Ionic Liquids as Solvents for Electronic Absorption Spectroscopy of Halide Complexes. *Nature* **323**,

614–616 (1986).
73. Scheffler, T. B., Hussey, C. L., Seddon, K. R., Kear, C. M. & Armitage, P. D. Molybdenum chloro complexes in room-temperature chloroaluminate ionic liquids: stabilization of hexachloromolybdate(2-) and hexachloromolybdate(3-). *Inorg. Chem.* **22**, 2099–2100 (1983).
74. Wilkes, J. S. A short history of ionic liquids—from molten salts to neoteric solvents. *Green Chem.* **4**, 73–80 (2002).
75. Hussey, C. Room temperature molten salt systems. *Adv. molten salt Chem.* **5**, 185–230 (1983).
76. Fry, S. E. & Pienta, N. J. Effects of molten salts on reactions. Nucleophilic aromatic substitution by halide ions in molten dodecyltributylphosphonium salts. *J. Am. Chem. Soc.* **107**, 6399–6400 (1985).
77. Boon, J. A., Levisky, J. A., Pflug, J. L. & Wilkes, J. S. Friedel-Crafts reactions in ambient-temperature molten salts. *J. Org. Chem.* **51**, 480–483 (1986).
78. Dupont, J. On the solid, liquid and solution structural organization of imidazolium ionic liquids . *Journal of the Brazilian Chemical Society* vol. 15 341–350 (2004).
79. Wilkes, J. S. & Zaworotko, M. J. Air and water stable 1-ethyl-3-methylimidazolium based ionic liquids. *J. Chem. Soc. Chem. Commun.* 965–967 (1992) doi:10.1039/C39920000965.
80. Davis Jr, J. H., Forrester, K. J. & Merrigan, T. Novel organic ionic liquids (OILs) incorporating cations derived from the antifungal drug miconazole. *Tetrahedron Lett.* **39**, 8955–8958 (1998).
81. Freemantle, M. DESIGNER SOLVENTS. *Chem. Eng. News Arch.* **76**, 32–37 (1998).
82. Seddon, K. Room-Temperature Ionic Liquids: Neoteric Solvents for Clean Catalysis. *Kinet. Catal.* **37**, 693–697 (1996).
83. Seddon, K. R. Ionic Liquids for Clean Technology. *J. Chem. Technol. Biotechnol.* **68**, 351–356 (1997).
84. McFarlane, D., Sun, J., Golding, J., Meakin, P. & Forsyth, M. High conductivity molten salts based on the imide ion. *Electrochim. Acta* **45**, 1271–1278 (2000).
85. Gordon, C., Holbrey, J., Kennedy, A. & Seddon, K. Ionic liquid crystals: hexafluorophosphate salts. *J. Mater. Chem.* **8**, 2627–2636 (1998).
86. Holbrey, J. D. & Seddon, K. R. Ionic liquids. *Clean Prod. Process.* **1**, 223–236 (1999).
87. Pringle, J. M. *et al.* The effect of anion fluorination in ionic liquids—physical properties of a range of bis(methanesulfonyl)amide salts. *New J. Chem.* **27**, 1504–1510 (2003).
88. Holbrey, J. & Seddon, K. The phase behaviour of 1-alkyl-3-methylimidazolium tetrafluoroborates; ionic liquids and ionic liquid crystals. *J. Chem. Soc. Dalt. Trans.* 2133–2140 (1999) doi:10.1039/A902818H.
89. Marsh, K. N., Boxall, J. A. & Lichtenthaler, R. Room temperature ionic liquids and their mixtures—a review. *Fluid Phase Equilib.* **219**, 93–98 (2004).
90. Mantz, R. & Trulove, P. *Ionic Liquids in Synthesis*. (Wiley-VHC Verlag GmbH & CoKGaA, 2003).
91. Seddon, K. R., Stark, A. & Torres, M.-J. Viscosity and Density of 1-Alkyl-3-methylimidazolium Ionic Liquids. in *Clean Solvents* vol. 819 4–34 (American Chemical Society, 2002).
92. Del Sesto, R. E., Corley, C., Robertson, A. & Wilkes, J. S. Tetraalkylphosphonium-based ionic liquids. *J. Organomet. Chem.* **690**, 2536–2542 (2005).

93. Huddleston, J. G. *et al.* Characterization and comparison of hydrophilic and hydrophobic room temperature ionic liquids incorporating the imidazolium cation. *Green Chem.* **3**, 156–164 (2001).
94. Seddon, K. R., Stark, A. & Torres, M.-J. Influence of chloride, water, and organic solvents on the physical properties of ionic liquids . *Pure Appl. Chem.* **72**, 2275 (2000).
95. Wilkes, J. S. Properties of ionic liquid solvents for catalysis. *J. Mol. Catal. A Chem.* **214**, 11–17 (2004).
96. Tokuda, H., Hayamizu, K., Ishii, K., Susan, M. A. B. H. & Watanabe, M. Physicochemical Properties and Structures of Room Temperature Ionic Liquids. 1. Variation of Anionic Species. *J. Phys. Chem. B* **108**, 16593–16600 (2004).
97. Tokuda, H., Hayamizu, K., Ishii, K., Susan, M. A. B. H. & Watanabe, M. Physicochemical properties and structures of room temperature ionic liquids. 2. Variation of alkyl chain length in imidazolium cation. *J. Phys. Chem. B* **109**, 6103–6110 (2005).
98. Suarez, P. A. Z., Einloft, S., Dullius, J. E. L., de Souza, R. F. & Dupont, J. Synthesis and physical-chemical properties of ionic liquids based on 1-n-butyl-3-methylimidazolium cation . *J. Chim. Phys.* **95**, 1626–1639 (1998).
99. Harris, K. R., Kanakubo, M. & Woolf, L. A. Temperature and Pressure Dependence of the Viscosity of the Ionic Liquids 1-Hexyl-3-methylimidazolium Hexafluorophosphate and 1-Butyl-3-methylimidazolium Bis(trifluoromethylsulfonyl)imide. *J. Chem. Eng. Data* **52**, 1080–1085 (2007).
100. Lide, D. R. *CRC handbook of chemistry and physics*. vol. 85 (CRC press, 2004).
101. Liao, Q. & Hussey, C. L. Densities, viscosities, and conductivities of mixtures of benzene with the Lewis acidic aluminum chloride+ 1-methyl-3-ethylimidazolium chloride molten salt. *J. Chem. Eng. data* **41**, 1126–1130 (1996).
102. Ignat'ev, N. V, Welz-Biermann, U., Kucheryna, A., Bissky, G. & Willner, H. New ionic liquids with tris(perfluoroalkyl)trifluorophosphate (FAP) anions. *J. Fluor. Chem.* **126**, 1150–1159 (2005).
103. Buzzeo, M. C., Evans, R. G. & Compton, R. G. Non-haloaluminate room-temperature ionic liquids in electrochemistry—A review. *ChemPhysChem* **5**, 1106–1120 (2004).
104. MacFarlane, D. R., Meakin, P., Sun, J., Amini, N. & Forsyth, M. Pyrrolidinium Imides: A New Family of Molten Salts and Conductive Plastic Crystal Phases. *J. Phys. Chem. B* **103**, 4164–4170 (1999).
105. Vila, J. *et al.* Temperature dependence of the electrical conductivity in EMIM-based ionic liquids: evidence of Vogel–Tamman–Fulcher behavior. *Fluid Phase Equilib.* **242**, 141–146 (2006).
106. Walden, P. Über organische Lösungs- und Ionisierungsmittel. *Zeitung der Phys. Chemie* **55**, 207–246 (1906).
107. Xu, W., Cooper, E. I. & Angell, C. A. Ionic Liquids: Ion Mobilities, Glass Temperatures, and Fragilities. *J. Phys. Chem. B* **107**, 6170–6178 (2003).
108. Yoshizawa, M., Xu, W. & Angell, C. A. Ionic Liquids by Proton Transfer: Vapor Pressure, Conductivity, and the Relevance of ΔpKa from Aqueous Solutions. *J. Am. Chem. Soc.* **125**, 15411–15419 (2003).
109. Angell, C. A., Byrne, N. & Belieres, J.-P. Parallel developments in aprotic and protic ionic liquids: Physical chemistry and applications. *Acc. Chem. Res.* **40**, 1228–1236 (2007).
110. Anderson, J. L. & Armstrong, D. W. Immobilized ionic liquids as high-selectivity/high-

temperature/high-stability gas chromatography stationary phases. *Anal. Chem.* **77**, 6453–6462 (2005).
111. Han, X. & Armstrong, D. W. Using geminal dicationic ionic liquids as solvents for high-temperature organic reactions. *Org. Lett.* **7**, 4205–4208 (2005).
112. Bonhôte, P., Dias, A.-P., Papageorgiou, N., Kalyanasundaram, K. & Grätzel, M. Hydrophobic, Highly Conductive Ambient-Temperature Molten Salts. *Inorg. Chem.* **35**, 1168–1178 (1996).
113. Holbrey, J. *et al.* Efficient, halide free synthesis of new, low cost ionic liquids: 1,3-dialkylimidazolium salts containing methyl- and ethyl-sulfate anions. *Green Chem.* **4**, 407–413 (2002).
114. Awad, W. *et al.* Thermal degradation studies of alkyl-imidazolium salts and their application in nanocomposites. *Thermochim. Acta* **409**, 3–11 (2004).
115. Kroon, M. C., Buijs, W., Peters, C. J. & Witkamp, G.-J. Quantum chemical aided prediction of the thermal decomposition mechanisms and temperatures of ionic liquids. *Thermochim. Acta* **465**, 40–47 (2007).
116. Ngo, H. L., LeCompte, K., Hargens, L. & McEwen, A. B. Thermal properties of imidazolium ionic liquids. *Thermochim. Acta* **357**–**358**, 97–102 (2000).
117. Crosthwaite, J. M., Muldoon, M. J., Dixon, J. K., Anderson, J. L. & Brennecke, J. F. Phase transition and decomposition temperatures, heat capacities and viscosities of pyridinium ionic liquids. *J. Chem. Thermodyn.* **37**, 559–568 (2005).
118. MacFarlane, D. R., Forsyth, S. A., Golding, J. & Deacon, G. B. Ionic liquids based on imidazolium{,} ammonium and pyrrolidinium salts of the dicyanamide anion. *Green Chem.* **4**, 444–448 (2002).
119. Fredlake, C. P., Crosthwaite, J. M., Hert, D. G., Aki, S. N. V. K. & Brennecke, J. F. Thermophysical Properties of Imidazolium-Based Ionic Liquids. *J. Chem. Eng. Data* **49**, 954–964 (2004).
120. Fox, D. M. *et al.* Flammability, thermal stability, and phase change characteristics of several trialkylimidazolium salts. *Green Chem.* **5**, 724–727 (2003).
121. McEwen, A., Ngo, H., LeCompte, K. & Goldman, J. Electrochemical properties of imidazolium salt electrolytes for electrochemical capacitator applications. *J. Electrochem. Soc.* **146**, 1687–1695 (1999).
122. Ohtani, H., Ishimura, S. & Kumai, M. Thermal decomposition behaviors of imidazolium-type ionic liquids studied by pyrolysis-gas chromatography. *Anal. Sci.* **24**, 1335–1340 (2008).
123. Baranyai, K. J., Deacon, G. B., MacFarlane, D. R., Pringle, J. M. & Scott, J. L. Thermal Degradation of Ionic Liquids at Elevated Temperatures. *Aust. J. Chem.* **57**, 145–147 (2004).
124. Chowdhury, A. & Thynell, S. T. Confined rapid thermolysis/FTIR/ToF studies of imidazolium-based ionic liquids. *Thermochim. Acta* **443**, 159–172 (2006).
125. Valkenburg, M. E. V., Vaughn, R. L., Williams, M. & Wilkes, J. S. Thermochemistry of ionic liquid heat-transfer fluids. *Thermochim. Acta* **425**, 181–188 (2005).
126. Smiglak, M. *et al.* Combustible ionic liquids by design: is laboratory safety another ionic liquid myth? *Chem. Commun.* 2554–2556 (2006) doi:10.1039/B602086K.
127. Katritzky, A. R. *et al.* Strategies toward the design of energetic ionic liquids: nitro- and nitrile-substituted N,N'-dialkylimidazolium salts. *New J. Chem.* **30**, 349–358 (2006).
128. Xue, H., Gao, Y., Twamley, B. & Shreeve, J. M. Energetic azolium azolate salts. *Inorg. Chem.* **44**, 5068–5072 (2005).

129. Xue, H. & Shreeve, J. M. Energetic Ionic Liquids from Azido Derivatives of 1, 2, 4-Triazole. *Adv. Mater.* **17**, 2142–2146 (2005).
130. Ye, C., Xiao, J.-C., Twamley, B. & Shreeve, J. M. Energetic salts of azotetrazolate, iminobis(5-tetrazolate) and 5, 5′-bis(tetrazolate). *Chem. Commun.* 2750–2752 (2005) doi:10.1039/B502583D.
131. de Grotthuss, C. Sur la décomposition de l'eau et des corps qu'elle tient en dissolution a l'aide de l'électricité galvanique. *Ann. Chim.* **58**, 54–73 (1806).
132. Wang, S.-F. *et al.* Direct Electrochemistry and Electrocatalysis of Heme Proteins Entrapped in Agarose Hydrogel Films in Room-Temperature Ionic Liquids. *Langmuir* **21**, 9260–9266 (2005).
133. Rozniecka, E., Shul, G., Sirieix-Plenet, J., Gaillon, L. & Opallo, M. Electroactive ceramic carbon electrode modified with ionic liquid. *Electrochem. commun.* **7**, 299–304 (2005).
134. Zhou, Z., Matsumoto, H. & Tatsumi, K. Low-melting, low-viscous, hydrophobic ionic liquids: aliphatic quaternary ammonium salts with perfluoroalkyltrifluoroborates. *Chem. Eur. J.* **11**, 752–766 (2005).
135. Liu, K. *et al.* Ionic liquids based on (fluorosulfonyl)(pentafluoroethanesulfonyl)imide with various oniums. *Electrochim. Acta* **55**, 7145–7151 (2010).
136. Yu, P. *et al.* Molecular films of water-miscible ionic liquids formed on glassy carbon electrodes: characterization and electrochemical applications. *Langmuir* **21**, 9000–9006 (2005).
137. Papaiconomou, N., Salminen, J., Lee, J.-M. & Prausnitz, J. M. Physicochemical Properties of Hydrophobic Ionic Liquids Containing 1-Octylpyridinium, 1-Octyl-2-methylpyridinium, or 1-Octyl-4-methylpyridinium Cations. *J. Chem. Eng. Data* **52**, 833–840 (2007).
138. Tindale, J. J. & Ragogna, P. J. Highly fluorinated phosphonium ionic liquids: novel media for the generation of superhydrophobic coatings. *Chem. Commun.* 1831–1833 (2009).
139. Jessop, P. G. *et al.* A solvent having switchable hydrophilicity. *Green Chem.* **12**, 809–814 (2010).
140. Appetecchi, G. B., Scaccia, S., Tizzani, C., Alessandrini, F. & Passerini, S. Synthesis of Hydrophobic Ionic Liquids for Electrochemical Applications. *J. Electrochem. Soc.* **153**, A1685 (2006).
141. Zhao, D., Wu, M., Kou, Y. & Min, E. Ionic liquids: applications in catalysis. *Catal. today* **74**, 157–189 (2002).
142. Ye, C., Liu, W., Chen, Y. & Yu, L. Room-temperature ionic liquids: a novel versatile lubricant. *Chem. Commun.* 2244–2245 (2001) doi:10.1039/B106935G.
143. Minami, I. Ionic liquids in tribology. *Molecules* **14**, 2286–2305 (2009).
144. Zhou, F., Liang, Y. & Liu, W. Ionic liquid lubricants: designed chemistry for engineering applications. *Chem. Soc. Rev.* **38**, 2590–2599 (2009).
145. Palacio, M. & Bhushan, B. A review of ionic liquids for green molecular lubrication in nanotechnology. *Tribol. Lett.* **40**, 247–268 (2010).
146. Pensado, A. S., Comuñas, M. J. P. & Fernández, J. The Pressure–Viscosity Coefficient of Several Ionic Liquids. *Tribol. Lett.* **31**, 107–118 (2008).
147. Kamimura, H., Kubo, T., Minami, I. & Mori, S. Effect and mechanism of additives for ionic liquids as new lubricants. *Tribol. Int.* **40**, 620–625 (2007).
148. Jiménez, A. E., Bermúdez, M. D., Iglesias, P., Carrión, F. J. & Martínez-Nicolás, G. 1-N-

alkyl -3-methylimidazolium ionic liquids as neat lubricants and lubricant additives in steel–aluminium contacts. *Wear* **260**, 766–782 (2006).
149. Mu, Z., Zhou, F., Zhang, S., Liang, Y. & Liu, W. Effect of the functional groups in ionic liquid molecules on the friction and wear behavior of aluminum alloy in lubricated aluminum-on-steel contact. *Tribol. Int.* **38**, 725–731 (2005).
150. Cai, M., Zhao, Z., Liang, Y., Zhou, F. & Liu, W. Alkyl Imidazolium Ionic Liquids as Friction Reduction and Anti-Wear Additive in Polyurea Grease for Steel/Steel Contacts. *Tribol. Lett.* **40**, 215–224 (2010).
151. Cai, M., Liang, Y., Zhou, F. & Liu, W. Tribological Properties of Novel Imidazolium Ionic Liquids Bearing Benzotriazole Group as the Antiwear/Anticorrosion Additive in Poly(ethylene glycol) and Polyurea Grease for Steel/Steel Contacts. *ACS Appl. Mater. Interfaces* **3**, 4580–4592 (2011).
152. Cai, M. *et al.* Imidazolium Ionic Liquids As Antiwear and Antioxidant Additive in Poly(ethylene glycol) for Steel/Steel Contacts. *ACS Appl. Mater. Interfaces* **2**, 870–876 (2010).
153. Canter, N. Evaluating ionic liquids as potential lubricants. *Tribol. Lubr. Technol.* **61**, 15 (2005).
154. Minami, I., Kita, M., Kubo, T., Nanao, H. & Mori, S. The Tribological Properties of Ionic Liquids Composed of Trifluorotris(pentafluoroethyl) Phosphate as a Hydrophobic Anion. *Tribol. Lett.* **30**, 215–223 (2008).
155. Zhu, L. Y., Chen, L. G., Yang, X. & Song, H. Bin. Functionalized Ionic Liquids as Lubricants for Steel-Steel Contact. *Appl. Mech. Mater.* **138**–**139**, 630–634 (2011).
156. Canongia Lopes, J. N. A. & Pádua, A. A. H. Nanostructural Organization in Ionic Liquids. *J. Phys. Chem. B* **110**, 3330–3335 (2006).
157. Schneider, A., Brenner, J., Tomastik, C. & Franek, F. Capacity of selected ionic liquids as alternative EP/AW additive. *Lubr. Sci.* **22**, 215–223 (2010).
158. Liu, W., Ye, C., Gong, Q., Wang, H. & Wang, P. Tribological Performance of Room-Temperature Ionic Liquids as Lubricant. *Tribol. Lett.* **13**, 81–85 (2002).
159. Wang, H., Lu, Q., Ye, C., Liu, W. & Cui, Z. Friction and wear behaviors of ionic liquid of alkylimidazolium hexafluorophosphates as lubricants for steel/steel contact. *Wear* **256**, 44–48 (2004).
160. Lu, Q., Wang, H., Ye, C., Liu, W. & Xue, Q. Room temperature ionic liquid 1-ethyl-3-hexylimidazolium-bis (trifluoromethylsulfonyl)-imide as lubricant for steel–steel contact. *Tribol. Int.* **37**, 547–552 (2004).
161. Weng, L., Liu, X., Liang, Y. & Xue, Q. Effect of tetraalkylphosphonium based ionic liquids as lubricants on the tribological performance of a steel-on-steel system. *Tribol. Lett.* **26**, 11–17 (2007).
162. Minami, I., Inada, T., Sasaki, R. & Nanao, H. Tribo-chemistry of phosphonium-derived ionic liquids. *Tribol. Lett.* **40**, 225–235 (2010).
163. Zhang, L., Feng, D. & Xu, B. Tribological characteristics of alkylimidazolium diethyl phosphates ionic liquids as lubricants for steel–steel contact. *Tribol. Lett.* **34**, 95–101 (2009).
164. Qu, J., Truhan, J. J., Dai, S., Luo, H. & Blau, P. J. Ionic liquids with ammonium cations as lubricants or additives. *Tribol. Lett.* **22**, 207–214 (2006).
165. Somers, A., Howlett, P., Sun, J., MacFarlane, D. & Forsyth, M. Phosphonium Ionic Liquids as Lubricants for Aluminium-Steel. *Proc. 3rd Int. Conf. Tribol. Des. Algarve, Port. 11-13 May 2010* 273–283 (2010).

166. Somers, A., Howlett, P. C., Sun, J., MacFarlane, D. & Forsyth, M. Transition in wear performance for ionic liquid lubricants under increasing load. *Tribol. Lett.* **40**, 279–284 (2010).
167. Shah, F. U. *et al.* Novel halogen-free chelated orthoborate–phosphonium ionic liquids: synthesis and tribophysical properties. *Phys. Chem. Chem. Phys.* **13**, 12865–12873 (2011).
168. Jiménez, A. E. & Bermúdez, M. D. Ionic liquids as lubricants of titanium–steel contact. Part 2: friction, wear and surface interactions at high temperature. *Tribol. Lett.* **37**, 431–443 (2010).
169. Jiménez, A. E. & Bermúdez, M.-D. Ionic liquids as lubricants of titanium–steel contact. *Tribol. Lett.* **33**, 111–126 (2009).
170. Jiménez, A. E. & Bermúdez, M. D. Ionic liquids as lubricants of titanium–steel contact. Part 3. Ti6Al4V lubricated with imidazolium ionic liquids with different alkyl chain lengths. *Tribol. Lett.* **40**, 237–246 (2010).
171. Qu, J. *et al.* Tribological characteristics of aluminum alloys sliding against steel lubricated by ammonium and imidazolium ionic liquids. *Wear* **267**, 1226–1231 (2009).
172. Iglesias, P., Bermúdez, M. D., Carrión, F. J. & Martínez-Nicolás, G. Friction and wear of aluminium–steel contacts lubricated with ordered fluids-neutral and ionic liquid crystals as oil additives. *Wear* **256**, 386–392 (2004).
173. Chen *et al.* Tribological performance of an ionic liquid as a lubricant for steel/aluminium contacts. *J. Synth. Lubr.* **20**, 217–225 (2003).
174. Jiménez, A.-E. & Bermúdez, M.-D. Imidazolium ionic liquids as additives of the synthetic ester propylene glycol dioleate in aluminium–steel lubrication. *Wear* **265**, 787–798 (2008).
175. Mu, Z., Liu, W., Zhang, S. & Zhou, F. Functional room-temperature ionic liquids as lubricants for an aluminum-on-steel system. *Chem. Lett.* **33**, 524–525 (2004).
176. Liu, X., Zhou, F., Liang, Y. & Liu, W. Tribological performance of phosphonium based ionic liquids for an aluminum-on-steel system and opinions on lubrication mechanism. *Wear* **261**, 1174–1179 (2006).
177. Jiménez, A.-E., Bermúdez, M.-D., Jimenez, A.-E. & Bermúdez, M.-D. Ionic liquids as lubricants for steel–aluminum contacts at low and elevated temperatures. *Tribol. Lett.* **26**, 53–60 (2007).
178. Mu, Z. *et al.* Investigation of Tribological Behavior of Al–Si Alloy Against Steel Lubricated With Ionic Liquids of 1-Diethylphosphonyl-n-propyl-3- Alkylimidazolium Tetrafluoroborate. *J. Tribol.* **130**, (2008).
179. Kamimura, H. *et al.* Relationship between structure and tribological properties of ionic liquids composed of imidazolium cations. *J. Japanese Soc. Tribol.* **51**, 826–834 (2006).
180. Jiménez, A. E., Bermúdez, M. D., Carrión, F. J. & Martínez-Nicolás, G. Room temperature ionic liquids as lubricant additives in steel–aluminium contacts: Influence of sliding velocity, normal load and temperature. *Wear* **261**, 347–359 (2006).
181. Kronberger, M., Pejaković, V., Gabler, C. & Kalin, M. How anion and cation species influence the tribology of a green lubricant based on ionic liquids. *Proc. Inst. Mech. Eng. Part J J. Eng. Tribol.* **226**, 933–951 (2012).
182. Blanco, D., González, R., Hernández Battez, A., Viesca, J. L. & Fernández-González, A. Use of ethyl-dimethyl-2-methoxyethylammonium

tris(pentafluoroethyl)trifluorophosphate as base oil additive in the lubrication of TiN PVD coating. *Tribol. Int.* **44**, 645–650 (2011).
183. Pejaković, V. *et al.* Pyrrolidinium sulfate and ammonium sulfate ionic liquids as lubricant additives for steel/steel contact lubrication. *Proc. Inst. Mech. Eng. Part J J. Eng. Tribol.* **226**, 923–932 (2012).
184. Qu, J., Blau, P. J., Dai, S., Luo, H. & Meyer, H. M. Ionic Liquids as Novel Lubricants and Additives for Diesel Engine Applications. *Tribol. Lett.* **35**, 181–189 (2009).
185. Mistry, K., Fox, M. F. & Priest, M. Lubrication of an electroplated nickel matrix silicon carbide coated eutectic aluminium—silicon alloy automotive cylinder bore with an ionic liquid as a lubricant additive. *Proc. Inst. Mech. Eng. Part J J. Eng. Tribol.* **223**, 563–569 (2009).
186. Qu, J. *et al.* Antiwear Performance and Mechanism of an Oil-Miscible Ionic Liquid as a Lubricant Additive. *ACS Appl. Mater. Interfaces* **4**, 997–1002 (2012).
187. Yu, B. *et al.* Oil-miscible and non-corrosive phosphonium-based ionic liquids as candidate lubricant additives. *Wear* **289**, 58–64 (2012).
188. Battez, A. H. *et al.* Tribological behaviour of two imidazolium ionic liquids as lubricant additives for steel/steel contacts. *Wear* **266**, 1224–1228 (2009).
189. Blanco, D., Battez, A. H., Viesca, J. L., González, R. & Fernández-González, A. Lubrication of CrN Coating With Ethyl-Dimethyl-2-Methoxyethylammonium Tris(pentafluoroethyl)Trifluorophosphate Ionic Liquid as Additive to PAO 6. *Tribol. Lett.* **41**, 295–302 (2011).
190. Tadros, T. F. *Applied surfactants: principles and applications*. (John Wiley & Sons, 2006).
191. Denzer, H., Michaelson, M., Meijer, H. & Abe, H. Foam Enhancing Agent for Surfactant Mixtures. (2004).
192. Renoncourt, A. Study of supra-aggregated in catanionic surfactant systems. (University of Regensburg, 2005).
193. Aalbers, J. G. Lauryl(poly-1-oxapropene oxa ethane) carboxylic acids. (Amsterdam, 1966).
194. Britton, L. G. Thermal stability and deflagration of ethylene oxide. *Plant/Operations Prog.* **9**, 75–86 (1990).
195. Hreczuch, W., Miszkiewicz, W., Szymanowski, J., Zimoch, J. & Jerzykiewicz, A. High ethoxylated alcohols with narrow distribution of homologues. *J. Chem. Technol. Biotechnol.* **67**, 53–60 (1996).
196. Hreczuch, W. & Szymanowski, J. Synthesis of surfactants with Narrow-range distribution of the polyoxyethylene chain. *J. Am. Oil Chem. Soc.* **73**, 73–78 (1996).
197. Santacesaria, E., Di Serio, M., Garaffa, R. & Addino, G. Kinetics and mechanisms of fatty alcohol polyethoxylation. 2. Narrow-range ethoxylation obtained with barium catalysts. *Ind. Eng. Chem. Res.* **31**, 2419–2421 (1992).
198. Santacesaria, E., Di Serio, M., Garaffa, R. & Addino, G. Kinetics and mechanisms of fatty alcohol polyethoxylation. 1. The reaction catalyzed by potassium hydroxide. *Ind. Eng. Chem. Res.* **31**, 2413–2418 (1992).
199. Moloy, K. G. A Simple, Effective Boron-Halide Ethoxylation Catalyst. *Adv. Synth. Catal.* **352**, 821–826 (2010).
200. Altiokka, M. R. & Akyalçin, S. Kinetics of the Hydration of Ethylene Oxide in the Presence of Heterogeneous Catalyst. *Ind. Eng. Chem. Res.* **48**, 10840–10844 (2009).
201. Zarina Edris, N. M. and M. A. Y. Comparison Studies on Lauric Acid Ethoxylated Using

Homogenous and Heterogenous Catalysts. *Sains Malaysiana* **39**, 765–768 (2010).
202. Satkowski, W. B. & Hsu, C. G. Polyoxyethylation of Alcohol. *Ind. Eng. Chem.* **49**, 1875–1878 (1957).
203. Di Serio, M., Tesser, R., Felippone, F. & Santacesaria, E. Ethylene Oxide Solubility and Ethoxylation Kinetics in the Synthesis of Nonionic Surfactants. *Ind. Eng. Chem. Res.* **34**, 4092–4098 (1995).
204. Di Serio, M., Vairo, G., Iengo, P., Felippone, F. & Santacesaria, E. Kinetics of Ethoxylation and Propoxylation of 1- and 2-Octanol Catalyzed by KOH. *Ind. Eng. Chem. Res.* **35**, 3848–3853 (1996).
205. Zarina Edris, N. M. and M. A. Y. Comparison Studies on Lauric Acid Ethoxylated Using Homogenous and Heterogenous Catalysts. *Sains Malaysiana* (2010).
206. Rosen, M. J. *Surfactants and Interfacial Phenomena*. (John Wiley & Sons, Inc., 2004). doi:10.1002/0471670561.
207. Florence, A. T. & Attwood, D. *Physicochemical Principles of Pharmacy*. (Macmillan Education UK, 1988). doi:10.1007/978-1-349-16558-2.
208. Yeskie, M. A. & Harwell, J. H. On the structure of aggregates of adsorbed surfactants: the surface charge density at the hemimicelle/admicelle transition. *J. Phys. Chem.* **92**, 2346–2352 (1988).
209. Koopal, L. K. & Keltjens, L. Adsorption of ionic surfactants on charged solids. Adsorption models. *Colloids and surfaces* **17**, 371–388 (1986).
210. Gao, Y., Du, J. & Gu, T. Hemimicelle formation of cationic surfactants at the silica gel–water interface. *J. Chem. Soc. Faraday Trans. 1 Phys. Chem. Condens. Phases* **83**, 2671–2679 (1987).
211. Gu, T., Gao, Y. & He, L. Hemimicelle formation of cationic surfactants at the silica gel–water interface. *J. Chem. Soc. Faraday Trans. 1 Phys. Chem. Condens. Phases* **84**, 4471–4473 (1988).
212. Gu, T. & Huang, Z. Thermodynamics of hemimicellization of cetyltrimethylammonium bromide at the silica gel/water interface. *Colloids and surfaces* **40**, 71–76 (1989).
213. Gu, T. & Zhu, B.-Y. The S-type isotherm equation for adsorption of nonionic surfactants at the silica gel—water interface. *Colloids and surfaces* **44**, 81–87 (1990).
214. Koopal, L. K. & Ralston, J. Chain length effects in the adsorption of surfactants at aqueous interfaces: Comparison of existing adsorption models with a new model. *J. Colloid Interface Sci.* **112**, 362–379 (1986).
215. Rupprecht, H. Sorption von Tensiden an Festkörperoberflächen und ihre Bedeutung im Bereich der Arzneiformen BT - Lösungen und Adsorption. in (eds. Lagaly, G., Müller, F. H. & Weiss, A.) 29–44 (Steinkopff, 1978).
216. Menschutkin, N. Beiträge zur Kenntnis der Affinitätskoeffizienten der Alkylhaloide und der organischen Amine. *Zeitschrift für Phys. Chemie* **5U**, 589–600 (1890).
217. Menschutkin, N. Über die Affinitätskoeffizienten der Alkylhaloide und der Amine. *Zeitschrift für Phys. Chemie* **6U**, 41–57 (1890).
218. Hargreaves, W. R. & Deamer, D. W. Liposomes from ionic, single-chain amphiphiles. *Biochemistry* **17**, 3759–3768 (1978).
219. Kume, G., Gallotti, M. & Nunes, G. Review on Anionic/Cationic Surfactant Mixtures. *J. Surfactants Deterg.* **11**, 1–11 (2008).
220. Jurašin, D. *et al.* Lamellar to hexagonal columnar liquid crystalline phase transition in a catanionic surfactant mixture: dodecylammonium chloride–sodium bis(2-ethylhexyl) sulfosuccinate. *Soft Matter* **9**, 3349–3360 (2013).

221. Yatcilla, M. T. *et al.* Phase Behavior of Aqueous Mixtures of Cetyltrimethylammonium Bromide (CTAB) and Sodium Octyl Sulfate (SOS). *J. Phys. Chem.* **100**, 5874–5879 (1996).
222. Novak, S. *et al.* Interplay of Noncovalent Interactions in Ionic Liquid/Sodium Bis(2-ethylhexyl) Sulfosuccinate Mixtures: From Lamellar to Bicontinuous Cubic Liquid Crystalline Phase. *J. Phys. Chem. B* **120**, 12557–12567 (2016).
223. Antunes, F. E., Marques, E. F., Miguel, M. G. & Lindman, B. Polymer–vesicle association. *Adv. Colloid Interface Sci.* **147**, 18–35 (2009).
224. Holmberg, K., Jönsson, B., Kronberg, B. & Lindman, B. *Surfactants and Polymers in Aqueous Solution*. (John Wiley & Sons, Ltd, 2002). doi:10.1002/0470856424.
225. Schmölzer, S. Kinetik der Vesikelbildung in katanionischen Tensidsystemen. (University of Bayreuth, 2003).
226. Brown, P. *et al.* New catanionic surfactants with ionic liquid properties. *J. Colloid Interface Sci.* **395**, 185–189 (2013).
227. Bowers, J., Butts, C. P., Martin, P. J., Vergara-Gutierrez, M. C. & Heenan, R. K. Aggregation Behavior of Aqueous Solutions of Ionic Liquids. *Langmuir* **20**, 2191–2198 (2004).
228. Rocha, M. A. A., van den Bruinhorst, A., Schröer, W., Rathke, B. & Kroon, M. C. Physicochemical properties of fatty acid based ionic liquids. *J. Chem. Thermodyn.* **100**, 156–164 (2016).
229. Kunz, W. *et al. Onium Salts of Carboxyalkyl-terminated Polyosyalkylenes for Use as High-Polar Solvents and Electrolytes*. (2008).
230. Klein, R., Zech, O., Maurer, E., Kellermeier, M. & Kunz, W. Oligoether Carboxylates: Task-Specific Room-Temperature Ionic Liquids. *J. Phys. Chem. B* **115**, 8961–8969 (2011).
231. Müller, E. *et al.* Oligoether carboxylate counterions: An innovative way towards surfactant ionic liquids. *J. Mol. Liq.* **251**, 61–69 (2018).
232. Maurer, E. Melting and Aggregation Behaviour of Novel Bio-Compatible Anionic, Cationic and Catanionic Surfactant Systems. (Universität Regensburg, 2011).
233. Gusain, R., Dhingra, S. & Khatri, O. P. Fatty-Acid-Constituted Halogen-Free Ionic Liquids as Renewable, Environmentally Friendly, and High-Performance Lubricant Additives. *Ind. Eng. Chem. Res.* **55**, 856–865 (2016).
234. Zhang, X. & Cresswell, M. *Inorganic Controlled Release Technology Materials and Concepts for Advanced Drug Formulation*. (Butterworth-Heinemann, 2016).
235. Wasserscheid, P. & Keim, W. Ionische Flüssigkeiten - neue 'Lösungen' für die Übergangsmetallkatalyse. *Angew. Chemie* **112**, 3926 (2000).
236. Xu, W., Cooper, E. I. & Angell, C. A. Ionic Liquids: Ion Mobilities, Glass Temperatures, and Fragilities. *J. Phys. Chem. B* **107**, 6170–6178 (2003).
237. Wasserscheid, P., Welton, T., Mantz, R. & Trulove, P. *Ionic Liquids in Synthesis*. (Wiley-VHC Verlag GmbH & CoKGaA, 2003). doi:10.1021/op0340210.
238. Prasad, M. R. R., Krishnan, K., Ninan, K. N. & Krishnamurthy, V. N. Thermal decomposition of tetraalkyl ammonium tetrafluoroborates. *Thermochim. Acta* **297**, 207–210 (1997).
239. Torrecilla, J. S., Rafione, T., García, J. & Rodríguez, F. Effect of Relative Humidity of Air on Density, Apparent Molar Volume, Viscosity, Surface Tension, and Water Content of 1-Ethyl-3-methylimidazolium Ethylsulfate Ionic Liquid. *J. Chem. Eng. Data* **53**, 923–928 (2008).

240. Liu, W., Cheng, L., Zhang, Y., Wang, H. & Yu, M. The physical properties of aqueous solution of room-temperature ionic liquids based on imidazolium: Database and evaluation. *J. Mol. Liq.* **140**, 68–72 (2008).
241. Vila, J., Ginés, P., Rilo, E., Cabeza, O. & Varela, L. M. Great increase of the electrical conductivity of ionic liquids in aqueous solutions. *Fluid Phase Equilib.* **247**, 32–39 (2006).
242. Cuadrado-Prado, S. *et al.* Experimental measurement of the hygroscopic grade on eight imidazolium based ionic liquids. *Fluid Phase Equilib.* **278**, 36–40 (2009).
243. Francesco, F. Di *et al.* Water sorption by anhydrous ionic liquids. *Green Chem.* **13**, 1712–1717 (2011).
244. Domańska, U. & Bogel-Łukasik, E. Solid–liquid equilibria for systems containing 1-butyl-3-methylimidazolium chloride. *Fluid Phase Equilib.* **218**, 123–129 (2004).
245. Domańska, U. & Bogel-Łukasik, E. Measurements and Correlation of the (Solid + Liquid) Equilibria of [1-Decyl-3-methylimidazolium Chloride + Alcohols (C2−C12)]. *Ind. Eng. Chem. Res.* **42**, 6986–6992 (2003).
246. Domańska, U., Bogel-Łukasik, E. & Bogel-Łukasik, R. 1-Octanol/Water Partition Coefficients of 1Alkyl-3-methylimidazolium Chloride. *Chem. – A Eur. J.* **9**, 3033–3041 (2003).
247. Domańska, U., Bogel-Łukasik, E. & Bogel-Łukasik, R. Solubility of 1-Dodecyl-3-methylimidazolium Chloride in Alcohols (C2−C12). *J. Phys. Chem. B* **107**, 1858–1863 (2003).
248. Ye, C., Liu, W., Chen, Y. & Yu, L. Room-temperature ionic liquids: a novel versatile lubricant. *Chem. Commun.* 2244–2245 (2001) doi:10.1039/B106935G.
249. Kamimura, H. *et al.* No Title. *J. Japanese Soc. Tribol.* **51**, 826–834 (2006).
250. Shkurankov, A., Zein El Abedin, S. & Endres, F. AFM-Assisted Investigation of the Corrosion Behaviour of Magnesium and AZ91 Alloys in an Ionic Liquid with Varying Water Content. *Aust. J. Chem.* **60**, 35–42 (2007).
251. Jiménez, A. E., Bermúdez, M. D., Carrión, F. J. & Martínez-Nicolás, G. Room temperature ionic liquids as lubricant additives in steel–aluminium contacts: Influence of sliding velocity, normal load and temperature. *Wear* **261**, 347–359 (2006).
252. Jiménez, A.-E., Bermúdez, M.-D., Jimenez, A.-E. & Bermúdez, M.-D. Ionic liquids as lubricants for steel–aluminum contacts at low and elevated temperatures. *Tribol. Lett.* **26**, 53–60 (2007).
253. Jiménez, A. E., Bermúdez, M. D., Iglesias, P., Carrión, F. J. & Martínez-Nicolás, G. 1-N-alkyl -3-methylimidazolium ionic liquids as neat lubricants and lubricant additives in steel–aluminium contacts. *Wear* **260**, 766–782 (2006).
254. Qu, J., Truhan, J. J., Dai, S., Luo, H. & Blau, P. J. Ionic liquids with ammonium cations as lubricants or additives. *Tribol. Lett.* **22**, 207–214 (2006).
255. Qu, J. *et al.* Antiwear Performance and Mechanism of an Oil-Miscible Ionic Liquid as a Lubricant Additive. *ACS Appl. Mater. Interfaces* **4**, 997–1002 (2012).
256. Iglesias, P., Bermúdez, M. D., Carrión, F. J. & Martínez-Nicolás, G. Friction and wear of aluminium–steel contacts lubricated with ordered fluids-neutral and ionic liquid crystals as oil additives. *Wear* **256**, 386–392 (2004).
257. Bermúdez, M.-D., Jiménez, A.-E. & Martínez-Nicolás, G. Study of surface interactions of ionic liquids with aluminium alloys in corrosion and erosion–corrosion processes. *Appl. Surf. Sci.* **253**, 7295–7302 (2007).

258. Forsyth, M. *et al.* New Insights into the Fundamental Chemical Nature of Ionic Liquid Film Formation on Magnesium Alloy Surfaces. *ACS Appl. Mater. Interfaces* **1**, 1045–1052 (2009).
259. Caporali, S. *et al.* Interaction Between an Imidazolium Based Ionic Liquid and the AZ91D Magnesium Alloy. *Adv. Eng. Mater.* **9**, 185–190 (2007).
260. Bardi, U., Chenakin, S. P., Lavacchi, A., Pagura, C. & Tolstogouzov, A. Sputter depth profiling by secondary ion mass spectrometry coupled with sample current measurements. *Appl. Surf. Sci.* **252**, 7373–7382 (2006).
261. Birbilis, N., Howlett, P. C., MacFarlane, D. R. & Forsyth, M. Exploring corrosion protection of Mg via ionic liquid pretreatment. *Surf. Coatings Technol.* **201**, 4496–4504 (2007).
262. Forsyth, M., Howlett, P. C., Tan, S. K., MacFarlane, D. R. & Birbilis, N. An Ionic Liquid Surface Treatment for Corrosion Protection of Magnesium Alloy AZ31. *Electrochem. Solid-State Lett.* **9**, B52 (2006).
263. Howlett, P. C. *et al.* An Electrochemical Impedance Study of Ionic Liquid Film Formation and Aqueous Corrosion of Magnesium Alloy ZE41. *Isr. J. Chem.* **48**, 313–318 (2008).
264. Cai, M., Liang, Y., Zhou, F. & Liu, W. Tribological Properties of Novel Imidazolium Ionic Liquids Bearing Benzotriazole Group as the Antiwear/Anticorrosion Additive in Poly(ethylene glycol) and Polyurea Grease for Steel/Steel Contacts. *ACS Appl. Mater. Interfaces* **3**, 4580–4592 (2011).
265. Chen *et al.* Tribological performance of an ionic liquid as a lubricant for steel/aluminium contacts. *J. Synth. Lubr.* **20**, 217–225 (2003).
266. Qu, J., Blau, P. J., Dai, S., Luo, H. & Meyer, H. M. Ionic Liquids as Novel Lubricants and Additives for Diesel Engine Applications. *Tribol. Lett.* **35**, 181–189 (2009).
267. Battez, A. H. *et al.* Tribological behaviour of two imidazolium ionic liquids as lubricant additives for steel/steel contacts. *Wear* **266**, 1224–1228 (2009).
268. Blanco, D., Battez, A. H., Viesca, J. L., González, R. & Fernández-González, A. Lubrication of CrN Coating With Ethyl-Dimethyl-2-Methoxyethylammonium Tris(pentafluoroethyl)Trifluorophosphate Ionic Liquid as Additive to PAO 6. *Tribol. Lett.* **41**, 295–302 (2011).
269. Kronberger, M., Pejaković, V., Gabler, C. & Kalin, M. How anion and cation species influence the tribology of a green lubricant based on ionic liquids. *Proc. Inst. Mech. Eng. Part J J. Eng. Tribol.* **226**, 933–951 (2012).
270. Blanco, D., González, R., Hernández Battez, A., Viesca, J. L. & Fernández-González, A. Use of ethyl-dimethyl-2-methoxyethylammonium tris(pentafluoroethyl)trifluorophosphate as base oil additive in the lubrication of TiN PVD coating. *Tribol. Int.* **44**, 645–650 (2011).
271. Pejaković, V. *et al.* Pyrrolidinium sulfate and ammonium sulfate ionic liquids as lubricant additives for steel/steel contact lubrication. *Proc. Inst. Mech. Eng. Part J J. Eng. Tribol.* **226**, 923–932 (2012).

VII Appendix

VII.1. List of Figures

VII.2. List of Tables

VII.3. Data of Analysis

VII.3.1 NMR-data

MeP 6 + TMAH:
^{1}H NMR (300 MHz, $CDCl_3$, 25°C, TMS): δ = 0.8 (s, 3H; C**H$_3$**), 3.2-3.8 (m, 34H)
^{13}C NMR (300 MHz, $CDCl_3$, 25°C, TMS): δ = 17.33 (CH2CH**C**H3O), 23.22 (**C**H_3), 77.06 (t, $N(CH_3)_4^+$)
MeP 6 + TEAH:
^{1}H NMR (300 MHz, $CDCl_3$, 25°C, TMS): δ = 0.8 (s, 3H; C**H$_3$**), 1.3 (t, 3H; $N(CH_2C\mathbf{H}_3)_4^+$), 3.2-3.8 (m, 34H)
^{13}C NMR (300 MHz, $CDCl_3$, 25°C, TMS): δ = 17.35 ($CH_2CH\mathbf{C}H_3O$), 23.12 (**C**H_3), 77.22 (t, $N(\mathbf{C}H_2CH_3)_4^+$)
MeP 6 + TBAH:
^{1}H NMR (300 MHz, $CDCl_3$, 25°C, TMS): δ = 0.8 (s, 3H; C**H$_3$**), 1.0 (t, 3H; $N(CH_2CH_2CH_2C\mathbf{H}_3)_4^+$), 1.4 (d, 2H; $N(CH_2CH_2C\mathbf{H}_2CH_3)_4^+$), 3.2-3.8 (m, 34H)
^{13}C NMR (300 MHz, $CDCl_3$, 25°C, TMS): δ = 17.23 ($CH_2CH\mathbf{C}H_3O$), 23.35 (**C**H_3), 77.16 (t, $N(\mathbf{C}H_2CH_2CH_2CH_3)_4^+$)

BuP 6 + TMAH:
^{1}H NMR (300 MHz, $CDCl_3$, 25°C, TMS): δ = 0.8 (t, 3H; $CH_2C\mathbf{H}_3$), 1.1 (d, 6H; C**H**$_2CH_3$), 3.2-3.8 (m, 34H)
^{13}C NMR (300 MHz, $CDCl_3$, 25°C, TMS): δ = 17.41 ($CH_2CH\mathbf{C}H_3O$), 23.33 (**C**H_3), 77.06 (t, $N(CH_3)_4^+$)
BuP 6 + TEAH:
^{1}H NMR (300 MHz, $CDCl_3$, 25°C, TMS): δ = 0.8 (s, 3H; C**H$_3$**), 1.1 (d, 6H; C**H**$_2CH_3$), 1.3 (t, 3H; $N(CH_2C\mathbf{H}_3)_4^+$), 3.2-3.8 (m, 34H)
^{13}C NMR (300 MHz, $CDCl_3$, 25°C, TMS): δ = 17.33 ($CH_2CH\mathbf{C}H_3O$), 77.08 (t, $N(\mathbf{C}H_2CH_3)_4^+$)
BuP 6 + TBAH:
^{1}H NMR (300 MHz, $CDCl_3$, 25°C, TMS): δ = 0.8 (s, 3H; C**H$_3$**), 1.0 (t, 3H; $N(CH_2CH_2CH_2C\mathbf{H}_3)_4^+$), 1.1 (d, 6H; C**H**$_2CH_3$), 1.4 (d, 2H; $N(CH_2CH_2C\mathbf{H}_2CH_3)_4^+$), 3.2-3.8 (m, 34H)
^{13}C NMR (300 MHz, $CDCl_3$, 25°C, TMS): δ = 17.30 ($CH_2CH\mathbf{C}H_3O$), 23.12 (**C**H_3), 77.09 (t, $N(\mathbf{C}H_2CH_2CH_2CH_3)_4^+$)

OcP 6 + TMAH:
^{1}H NMR (300 MHz, $CDCl_3$, 25°C, TMS): δ = 0.8 (t, 3H; $CH_2C\mathbf{H}_3$), 1.0 (d, 8H; C**H**$_2CH_3$), 3.2-3.8 (m, 34H)
^{13}C NMR (300 MHz, $CDCl_3$, 25°C, TMS): δ = 17.03 ($CH_2CH\mathbf{C}H_3O$), 23.25 (**C**H_3), 77.56 (t, $N(CH_3)_4^+$)
OcP 6 + TEAH:
^{1}H NMR (300 MHz, $CDCl_3$, 25°C, TMS): δ = 0.8 (s, 3H; C**H$_3$**), 1.1 (d, 8H; C**H**$_2CH_3$), 1.4 (t, 3H; $N(CH_2C\mathbf{H}_3)_4^+$), 3.2-3.8 (m, 34H)
^{13}C NMR (300 MHz, $CDCl_3$, 25°C, TMS): δ = 17.63 ($CH_2CH\mathbf{C}H_3O$), 75.26 (t, $N(\mathbf{C}H_2CH_3)_4^+$)
OcP 6 + TBAH:
^{1}H NMR (300 MHz, $CDCl_3$, 25°C, TMS): δ = 0.8 (s, 3H; C**H$_3$**), 1.0 (t, 3H; $N(CH_2CH_2CH_2C\mathbf{H}_3)_4^+$), 1.1 (d, 8H; C**H**$_2CH_3$),1.4 (d, 2H; $N(CH_2CH_2C\mathbf{H}_2CH_3)_4^+$), 3.2-3.8 (m, 34H)

^{13}C NMR (300 MHz, $CDCl_3$, 25°C, TMS): δ = 16.93 ($CH_2CH\mathbf{C}H_3O$), 22.92 ($\mathbf{C}H_3$), 76.06 (t, $N(\mathbf{C}H_2CH_2CH_2CH_3)_4^+$)

LP 6 + TMAH:

^{1}H NMR (300 MHz, $CDCl_3$, 25°C, TMS): δ = 0.8 (t, 3H; $CH_2C\mathbf{H_3}$), 1.1 (d, 12H; $C\mathbf{H}_2CH_3$), 3.2-3.8 (m, 34H)

^{13}C NMR (300 MHz, $CDCl_3$, 25°C, TMS): δ = 16.94 ($CH_2CH\mathbf{C}H_3O$), 24.02 ($\mathbf{C}H_3$), 76.86 (t, $N(CH_3)_4^+$)

LP 6 + TEAH:

^{1}H NMR (300 MHz, $CDCl_3$, 25°C, TMS): δ = 0.8 (s, 3H; $C\mathbf{H_3}$), 1.1 (d, 12H; $C\mathbf{H}_2CH_3$), 1.3 (t, 3H; $N(CH_2C\mathbf{H}_3)_4^+$), 3.2-3.8 (m, 34H)

^{13}C NMR (300 MHz, $CDCl_3$, 25°C, TMS): δ = 17.13 ($CH_2CH\mathbf{C}H_3O$), 75.26 (t, $N(\mathbf{C}H_2CH_3)_4^+$)

LP 6 + TBAH:

^{1}H NMR (300 MHz, $CDCl_3$, 25°C, TMS): δ = 0.8 (s, 3H; $C\mathbf{H_3}$), 1.0 (t, 3H; $N(CH_2CH_2CH_2C\mathbf{H}_3)_4^+$), 1.1 (d, 12H; $C\mathbf{H}_2CH_3$),1.4 (d, 2H; $N(CH_2CH_2C\mathbf{H}_2CH_3)_4^+$), 3.2-3.8 (m, 34H)

^{13}C NMR (300 MHz, $CDCl_3$, 25°C, TMS): δ = 16.93 ($CH_2CH\mathbf{C}H_3O$), 22.22 ($\mathbf{C}H_3$), 77.06 (t, $N(\mathbf{C}H_2CH_2CH_2CH_3)_4^+$)

SP 6 + TMAH:

^{1}H NMR (300 MHz, $CDCl_3$, 25°C, TMS): δ = 0.8 (t, 3H; $CH_2C\mathbf{H_3}$), 1.1 (d, 18H; $C\mathbf{H}_2CH_3$), 3.2-3.8 (m, 34H)

^{13}C NMR (300 MHz, $CDCl_3$, 25°C, TMS): δ = 17.33 ($CH_2CH\mathbf{C}H_3O$), 23.22 ($\mathbf{C}H_3$), 77.06 (t, $N(CH_3)_4^+$)

SP 6 + TEAH:

^{1}H NMR (300 MHz, $CDCl_3$, 25°C, TMS): δ = 0.8 (s, 3H; $C\mathbf{H_3}$), 1.1 (d, 18H; $C\mathbf{H}_2CH_3$), 1.3 (t, 3H; $N(CH_2C\mathbf{H}_3)_4^+$), 3.2-3.8 (m, 34H)

^{13}C NMR (300 MHz, $CDCl_3$, 25°C, TMS): δ = 17.13 ($CH_2CH\mathbf{C}H_3O$), 76.16 (t, $N(\mathbf{C}H_2CH_3)_4^+$)

SP 6 + TBAH:

^{1}H NMR (300 MHz, $CDCl_3$, 25°C, TMS): δ = 0.8 (s, 3H; $C\mathbf{H_3}$), 1.0 (t, 3H; $N(CH_2CH_2CH_2C\mathbf{H}_3)_4^+$), 1.1 (d, 18H; $C\mathbf{H}_2CH_3$),1.4 (d, 2H; $N(CH_2CH_2C\mathbf{H}_2CH_3)_4^+$), 3.2-3.8 (m, 34H)

^{13}C NMR (300 MHz, $CDCl_3$, 25°C, TMS): δ = 19.33 ($CH_2CH\mathbf{C}H_3O$), 22.82 ($\mathbf{C}H_3$), 77.06 (t, $N(\mathbf{C}H_2CH_2CH_2CH_3)_4^+$)

BP 6 + TMAH:

^{1}H NMR (300 MHz, $CDCl_3$, 25°C, TMS): δ = 0.8 (t, 3H; $CH_2C\mathbf{H_3}$), 1.1 (d, 22H; $C\mathbf{H}_2CH_3$), 3.2-3.8 (m, 34H)

^{13}C NMR (300 MHz, $CDCl_3$, 25°C, TMS): δ = 19.23 ($CH_2CH\mathbf{C}H_3O$), 22.92 ($\mathbf{C}H_3$), 77.06 (t, $N(CH_3)_4^+$)

BP 6 + TEAH:

^{1}H NMR (300 MHz, $CDCl_3$, 25°C, TMS): δ = 0.8 (s, 3H; $C\mathbf{H_3}$), 1.1 (d, 22H; $C\mathbf{H}_2CH_3$), 1.3 (t, 3H; $N(CH_2C\mathbf{H}_3)_4^+$), 3.2-3.8 (m, 34H)

^{13}C NMR (300 MHz, $CDCl_3$, 25°C, TMS): δ = 16.33 ($CH_2CH\mathbf{C}H_3O$), 75.17 (t, $N(\mathbf{C}H_2CH_3)_4^+$)

BP 6 + TBAH:

^{1}H NMR (300 MHz, $CDCl_3$, 25°C, TMS): δ = 0.8 (s, 3H; $C\mathbf{H_3}$), 1.0 (t, 3H; $N(CH_2CH_2CH_2C\mathbf{H}_3)_4^+$), 1.1 (d, 22H; $C\mathbf{H}_2CH_3$),1.4 (d, 2H; $N(CH_2CH_2C\mathbf{H}_2CH_3)_4^+$), 3.2-3.8 (m, 34H)

^{13}C NMR (300 MHz, $CDCl_3$, 25°C, TMS): δ = 16.87 ($CH_2CH\mathbf{C}H_3O$), 22.88 ($\mathbf{C}H_3$), 77.17 (t, $N(\mathbf{C}H_2CH_2CH_2CH_3)_4^+$)

Stearyl + TMAH:

^{1}H NMR (300 MHz, $CDCl_3$, 25°C, TMS): δ = 0.8 (t, 3H; $CH_2C\mathbf{H_3}$), 1.1 (d, 18H; $C\mathbf{H}_2CH_3$), 1.45 (m, 2H; $C\mathbf{H}_2CH_2COO^-$), 2.10 (t, 2H; $C\mathbf{H}_2COO^-$)

^{13}C NMR (300 MHz, $CDCl_3$, 25°C, TMS): δ = 17.33 ($CH_2CH\mathbf{C}H_3O$), 23.22 ($\mathbf{C}H_3$), 31.15 ($\mathbf{C}H_2CH_2COO^-$), 37.44 ($\mathbf{C}H_2COO^-$), 77.06 (t, $N(CH_3)_4^+$)

Stearyl + TEAH:

^{1}H NMR (300 MHz, $CDCl_3$, 25°C, TMS): δ = 0.8 (s, 3H; $C\mathbf{H_3}$), 1.1 (d, 18H; $C\mathbf{H}_2CH_3$), 1.3 (t, 3H; $N(CH_2C\mathbf{H}_3)_4^+$), 1.45 (m, 2H; $C\mathbf{H}_2CH_2COO^-$), 2.10 (t, 2H; $C\mathbf{H}_2COO^-$)

^{13}C NMR (300 MHz, $CDCl_3$, 25°C, TMS): δ = 17.33 ($CH_2CH\mathbf{C}H_3O$), 31.15 ($\mathbf{C}H_2CH_2COO^-$), 37.44 ($\mathbf{C}H_2COO^-$), 75.26 (t, $N(\mathbf{C}H_2CH_3)_4^+$)

Stearyl + TBAH:

^{1}H NMR (300 MHz, $CDCl_3$, 25°C, TMS): δ = 0.8 (s, 3H; $C\mathbf{H_3}$), 1.0 (t, 3H; $N(CH_2CH_2CH_2C\mathbf{H}_3)_4^+$), 1.1 (d, 18H; $C\mathbf{H}_2CH_3$),1.4 (d, 2H; $N(CH_2CH_2C\mathbf{H}_2CH_3)_4^+$), 1.45 (m, 2H; $C\mathbf{H}_2CH_2COO^-$), 2.10 (t, 2H; $C\mathbf{H}_2COO^-$)

^{13}C NMR (300 MHz, $CDCl_3$, 25°C, TMS): δ = 17.33 ($CH_2CH\mathbf{C}H_3O$), 23.22 ($\mathbf{C}H_3$), 31.15 ($\mathbf{C}H_2CH_2COO^-$), 37.44 ($\mathbf{C}H_2COO^-$), 77.06 (t, $N(\mathbf{C}H_2CH_2CH_2CH_3)_4^+$)

SP 3 + TMAH:

^{1}H NMR (300 MHz, $CDCl_3$, 25°C, TMS): δ = 0.8 (t, 3H; $CH_2C\mathbf{H_3}$), 1.1 (d, 18H; $C\mathbf{H}_2CH_3$), 3.2-3.8 (m, 19H)

^{13}C NMR (300 MHz, $CDCl_3$, 25°C, TMS): δ = 17.33 ($CH_2CH\mathbf{C}H_3O$), 23.22 ($\mathbf{C}H_3$), 77.06 (t, $N(CH_3)_4^+$)

SP 3 + TEAH:

^{1}H NMR (300 MHz, $CDCl_3$, 25°C, TMS): δ = 0.8 (s, 3H; $C\mathbf{H_3}$), 1.1 (d, 18H; $C\mathbf{H}_2CH_3$), 1.3 (t, 3H; $N(CH_2C\mathbf{H}_3)_4^+$), 3.2-3.8 (m, 19H)

^{13}C NMR (300 MHz, $CDCl_3$, 25°C, TMS): δ = 17.33 ($CH_2CH\mathbf{C}H_3O$), 75.26 (t, $N(\mathbf{C}H_2CH_3)_4^+$)

SP 3 + TBAH:

^{1}H NMR (300 MHz, $CDCl_3$, 25°C, TMS): δ = 0.8 (s, 3H; $C\mathbf{H_3}$), 1.0 (t, 3H; $N(CH_2CH_2CH_2C\mathbf{H}_3)_4^+$), 1.1 (d, 18H; $C\mathbf{H}_2CH_3$),1.4 (d, 2H; $N(CH_2CH_2C\mathbf{H}_2CH_3)_4^+$), 3.2-3.8 (m, 19H)

^{13}C NMR (300 MHz, $CDCl_3$, 25°C, TMS): δ = 17.33 ($CH_2CH\mathbf{C}H_3O$), 23.22 ($\mathbf{C}H_3$), 77.06 (t, $N(\mathbf{C}H_2CH_2CH_2CH_3)_4^+$)

SP 9 + TMAH:

^{1}H NMR (300 MHz, $CDCl_3$, 25°C, TMS): δ = 0.8 (t, 3H; $CH_2C\mathbf{H_3}$), 1.1 (d, 18H; $C\mathbf{H}_2CH_3$), 3.2-3.8 (m, 54H)

^{13}C NMR (300 MHz, $CDCl_3$, 25°C, TMS): δ = 17.33 ($CH_2CH\mathbf{C}H_3O$), 23.22 ($\mathbf{C}H_3$), 77.06 (t, $N(CH_3)_4^+$)

SP 9 + TEAH:

^{1}H NMR (300 MHz, $CDCl_3$, 25°C, TMS): δ = 0.8 (s, 3H; $C\mathbf{H_3}$), 1.1 (d, 18H; $C\mathbf{H}_2CH_3$), 1.3 (t, 3H; $N(CH_2C\mathbf{H}_3)_4^+$), 3.2-3.8 (m, 54H)

^{13}C NMR (300 MHz, $CDCl_3$, 25°C, TMS): δ = 17.33 ($CH_2CH\mathbf{C}H_3O$), 75.26 (t, $N(\mathbf{C}H_2CH_3)_4^+$)

SP 9 + TBAH:

^{1}H NMR (300 MHz, $CDCl_3$, 25°C, TMS): δ = 0.8 (s, 3H; $C\mathbf{H_3}$), 1.0 (t, 3H; $N(CH_2CH_2CH_2C\mathbf{H}_3)_4^+$), 1.1 (d, 18H; $C\mathbf{H}_2CH_3$),1.4 (d, 2H; $N(CH_2CH_2C\mathbf{H}_2CH_3)_4^+$), 3.2-3.8 (m, 54H)

^{13}C NMR (300 MHz, $CDCl_3$, 25°C, TMS): δ = 17.33 ($CH_2CH\mathbf{C}H_3O$), 23.22 ($\mathbf{C}H_3$), 77.06 (t, $N(\mathbf{C}H_2CH_2CH_2CH_3)_4^+$)

SP 12 + TMAH:

^{1}H NMR (300 MHz, $CDCl_3$, 25°C, TMS): δ = 0.8 (t, 3H; $CH_2C\mathbf{H_3}$), 1.1 (d, 18H; $C\mathbf{H}_2CH_3$), 3.2-3.8 (m, 74H)

^{13}C NMR (300 MHz, $CDCl_3$, 25°C, TMS): δ = 17.33 ($CH_2CH\mathbf{C}H_3O$), 23.22 ($\mathbf{C}H_3$), 77.06 (t, $N(CH_3)_4^+$)

SP 12 + TEAH:

^{1}H NMR (300 MHz, $CDCl_3$, 25°C, TMS): δ = 0.8 (s, 3H; $C\mathbf{H_3}$), 1.1 (d, 18H; $C\mathbf{H}_2CH_3$), 1.3 (t, 3H; $N(CH_2C\mathbf{H}_3)_4^+$), 3.2-3.8 (m, 74H)

^{13}C NMR (300 MHz, $CDCl_3$, 25°C, TMS): δ = 17.33 ($CH_2CH\mathbf{C}H_3O$), 75.26 (t, $N(\mathbf{C}H_2CH_3)_4^+$)

SP 12 + TBAH:

^{1}H NMR (300 MHz, $CDCl_3$, 25°C, TMS): δ = 0.8 (s, 3H; $C\mathbf{H_3}$), 1.0 (t, 3H; $N(CH_2CH_2CH_2C\mathbf{H}_3)_4^+$), 1.1 (d, 18H; $C\mathbf{H}_2CH_3$),1.4 (d, 2H; $N(CH_2CH_2C\mathbf{H}_2CH_3)_4^+$), 3.2-3.8 (m, 74H)

^{13}C NMR (300 MHz, $CDCl_3$, 25°C, TMS): δ = 17.33 ($CH_2CH\mathbf{C}H_3O$), 23.22 ($\mathbf{C}H_3$), 77.06 (t, $N(\mathbf{C}H_2CH_2CH_2CH_3)_4^+$)

SP 15 + TMAH:

^{1}H NMR (300 MHz, $CDCl_3$, 25°C, TMS): δ = 0.8 (t, 3H; $CH_2C\mathbf{H_3}$), 1.1 (d, 18H; $C\mathbf{H}_2CH_3$), 3.2-3.8 (m, 89H)

^{13}C NMR (300 MHz, $CDCl_3$, 25°C, TMS): δ = 17.33 ($CH_2CH\mathbf{C}H_3O$), 23.22 ($\mathbf{C}H_3$), 77.06 (t, $N(CH_3)_4^+$)

SP 15 + TEAH:

^{1}H NMR (300 MHz, $CDCl_3$, 25°C, TMS): δ = 0.8 (s, 3H; $C\mathbf{H_3}$), 1.1 (d, 18H; $C\mathbf{H}_2CH_3$), 1.3 (t, 3H; $N(CH_2C\mathbf{H}_3)_4^+$), 3.2-3.8 (m, 89H)

^{13}C NMR (300 MHz, $CDCl_3$, 25°C, TMS): δ = 17.33 ($CH_2CH\mathbf{C}H_3O$), 75.26 (t, $N(\mathbf{C}H_2CH_3)_4^+$)

SP 15 + TBAH:

^{1}H NMR (300 MHz, $CDCl_3$, 25°C, TMS): δ = 0.8 (s, 3H; $C\mathbf{H_3}$), 1.0 (t, 3H; $N(CH_2CH_2CH_2C\mathbf{H}_3)_4^+$), 1.1 (d, 18H; $C\mathbf{H}_2CH_3$),1.4 (, 2H; $N(CH_2CH_2C\mathbf{H}_2CH_3)_4^+$), 3.2-3.8 (m, 89H)

^{13}C NMR (300 MHz, $CDCl_3$, 25°C, TMS): δ = 17.33 ($CH_2CH\mathbf{C}H_3O$), 23.22 ($\mathbf{C}H_3$), 77.06 (t, $N(\mathbf{C}H_2CH_2CH_2CH_3)_4^+$)

SP 25 + TMAH:

^{1}H NMR (300 MHz, $CDCl_3$, 25°C, TMS): δ = 0.8 (t, 3H; $CH_2C\mathbf{H_3}$), 1.1 (d, 18H; $C\mathbf{H}_2CH_3$), 3.2-3.8 (m, 148H)

^{13}C NMR (300 MHz, $CDCl_3$, 25°C, TMS): δ = 17.33 ($CH_2CH\mathbf{C}H_3O$), 23.22 ($\mathbf{C}H_3$), 77.06 (t, $N(CH_3)_4^+$)

SP 25 + TEAH:

^{1}H NMR (300 MHz, $CDCl_3$, 25°C, TMS): δ = 0.8 (s, 3H; $C\mathbf{H_3}$), 1.1 (d, 18H; $C\mathbf{H}_2CH_3$), 1.3 (t, 3H; $N(CH_2C\mathbf{H}_3)_4^+$), 3.2-3.8 (m, 148H)

^{13}C NMR (300 MHz, $CDCl_3$, 25°C, TMS): δ = 17.33 ($CH_2CH\mathbf{C}H_3O$), 75.26 (t, $N(\mathbf{C}H_2CH_3)_4^+$)

SP 25 + TBAH:

^{1}H NMR (300 MHz, $CDCl_3$, 25°C, TMS): δ = 0.8 (s, 3H; $C\mathbf{H_3}$), 1.0 (t, 3H; $N(CH_2CH_2CH_2C\mathbf{H}_3)_4^+$), 1.1 (d, 18H; $C\mathbf{H}_2CH_3$),1.4 (4, 2H; $N(CH_2CH_2C\mathbf{H}_2CH_3)_4^+$), 3.2-3.8 (m, 148H)

^{13}C NMR (300 MHz, $CDCl_3$, 25°C, TMS): δ = 17.33 ($CH_2CH\mathbf{C}H_3O$), 23.22 ($\mathbf{C}H_3$), 77.06 (t, $N(\mathbf{C}H_2CH_2CH_2CH_3)_4^+$)

SP 50 + TMAH:

^{1}H NMR (300 MHz, $CDCl_3$, 25°C, TMS): δ = 0.8 (t, 3H; $CH_2C\mathbf{H_3}$), 1.1 (d, 18H; $C\mathbf{H}_2CH_3$), 3.2-3.8 (m, 304H)

^{13}C NMR (300 MHz, $CDCl_3$, 25°C, TMS): δ = 17.33 ($CH_2CH\mathbf{C}H_3O$), 23.22 ($\mathbf{C}H_3$), 77.06 (t, $N(CH_3)_4^+$)

SP 50 + TEAH:

^{1}H NMR (300 MHz, $CDCl_3$, 25°C, TMS): δ = 0.8 (s, 3H; $C\mathbf{H_3}$), 1.1 (d, 18H; $C\mathbf{H}_2CH_3$), 1.3 (t, 3H; $N(CH_2C\mathbf{H}_3)_4^+$), 3.2-3.8 (m, 304H)

^{13}C NMR (300 MHz, $CDCl_3$, 25°C, TMS): δ = 17.33 ($CH_2CH\mathbf{C}H_3O$), 75.26 (t, $N(\mathbf{C}H_2CH_3)_4^+$)

SP 50 + TBAH:

^{1}H NMR (300 MHz, $CDCl_3$, 25°C, TMS): δ = 0.8 (s, 3H; $C\mathbf{H_3}$), 1.0 (t, 3H; $N(CH_2CH_2CH_2C\mathbf{H}_3)_4^+$), 1.1 (d, 18H; $C\mathbf{H}_2CH_3$),1.4 (4, 2H; $N(CH_2CH_2C\mathbf{H}_2CH_3)_4^+$), 3.2-3.8 (m, 304H)

^{13}C NMR (300 MHz, $CDCl_3$, 25°C, TMS): δ = 17.33 ($CH_2CH\mathbf{C}H_3O$), 23.22 ($\mathbf{C}H_3$), 77.06 (t, $N(\mathbf{C}H_2CH_2CH_2CH_3)_4^+$)

VII.3.2 Density data

	Density [g/cm³] at							
Catanionic	**298.15 K**	**308.15 K**	**318.15 K**	**328.15 K**	**338.15 K**	**348.15 K**	**358.15 K**	**368.15K**
MeP 6 + TMAH	1.002	0.9939	0.9871	0.9814	0.9747	0.9678	0.9617	0.9541
BuP 6 + TMAH	0.9869	0.9802	0.9735	0.9674	0.9598	0.9531	0.9462	0.9397
OcP 6 + TMAH	0.9763	0.9691	0.9634	0.9562	0.9503	0.9433	0.9369	0.9301
LP6 + TMAH	0.9655	0.9586	0.9528	0.9456	0.9388	0.9329	0.9261	0.9198
BP 6 + TMAH	-	-	-	0.9231	0.9168	0.9097	0.9039	0.8976
Stearyl + TMAH	-	-	0.8856	0.8809	0.8742	0.8692	0.8636	0.8571
SP 3 + TMAH	0.9419	0.9369	0.9302	0.9238	0.9171	0.9102	0.9043	0.8981
SP 6 + TMAH	0.9546	0.9479	0.9413	0.9345	0.9281	0.9223	0.9162	0.9092
SP 9 + TMAH	0.9626	0.9562	0.9489	0.9429	0.9356	0.9301	0.9236	0.9165
SP 12 + TMAH	0.9674	0.9609	0.9545	0.9481	0.94091	0.9343	0.9272	0.9209
SP 15 + TMAH	0.9763	0.9691	0.9621	0.9549	0.9491	0.9424	0.9349	0.9289
SP 25 + TMAH	0.9845	0.9773	0.9719	0.9647	0.9581	0.9509	0.9439	0.9374
SP 50 + TMAH	1.0013	0.9938	0.9850	0.9786	0.9720	0.9654	0.9586	0.9515
MeP 6 + TEAH	0.9883	0.9816	0.9749	0.9681	0.9614	0.9547	0.9481	0.9413
BuP 6 + TEAH	0.9737	0.9672	0.9604	0.9536	0.9468	0.9401	0.9333	0.9267
OcP 6 + TEAH	0.9630	0.9564	0.9499	0.9433	0.9368	0.9301	0.9236	0.9170
LP6 + TEAH	0.9520	0.9457	0.9391	0.9326	0.9260	0.9194	0.9129	0.9063
BP 6 + TEAH	-	-	0.9166	0.9101	0.9036	0.8971	0.8906	0.8842
Stearyl + TEAH	-	-	0.8728	0.8674	0.8615	0.8558	0.8501	0.8436
SP 3 + TEAH	0.9282	0.9230	0.9166	0.9103	0.9040	0.8976	0.8913	0.8850
SP 6 + TEAH	0.9409	0.9347	0.9282	0.9217	0.9152	0.9088	0.9023	0.8960
SP 9 + TEAH	0.9496	0.9431	0.9364	0.9298	0.9231	0.9165	0.9098	0.9032
SP 12 + TEAH	0.9544	0.948	0.9413	0.9345	0.9278	0.9211	0.9144	0.9075
SP 15 + TEAH	0.9624	0.9559	0.9491	0.9423	0.9355	0.9288	0.9220	0.9153
SP 25 + TEAH	0.9716	0.9654	0.9585	0.9516	0.9446	0.9377	0.9308	0.9239
SP 50 + TEAH	0.9884	0.982	0.9746	0.9672	0.9599	0.9525	0.9459	0.9385
MeP 6 + TBAH	0.9802	0.9733	0.9669	0.9604	0.9539	0.9461	0.9399	0.9328
BuP 6 + TBAH	0.9655	0.9596	0.9522	0.9466	0.9387	0.9328	0.9251	0.9184
OcP 6 + TBAH	0.9542	0.9489	0.9416	0.9354	0.9292	0.9222	0.9151	0.9092
LP6 + TBAH	0.9441	0.9371	0.9312	0.9247	0.9182	0.9111	0.9052	0.8981
BP 6 + TBAH	-	-	0.9080	0.9022	0.8950	0.8892	0.8823	0.8768
Stearyl + TBAH	-	-	0.8641	0.8593	0.8532	0.8487	0.8420	0.8359
SP 3 + TBAH	0.9201	0.9144	0.9079	0.9014	0.8955	0.8891	0.8832	0.8767
SP 6 + TBAH	0.9322	0.9264	0.9201	0.9138	0.9072	0.9001	0.8937	0.8874
SP 9 + TBAH	0.9413	0.9342	0.9283	0.9213	0.9142	0.9081	0.9014	0.8954
SP 12 + TBAH	0.9465	0.9409	0.9331	0.9261	0.9191	0.9135	0.9061	0.8992
SP 15 + TBAH	0.9544	0.9481	0.941	0.9344	0.9273	0.9201	0.9142	0.9073
SP 25 + TBAH	0.9626	0.9563	0.9505	0.9427	0.9354	0.9296	0.9224	0.9147
SP 50 + TBAH	0.9803	0.9736	0.9663	0.9591	0.9518	0.9448	0.9376	0.9305

VII.3.3 Molar Volume data

	Molar Volume [cm³/mol] at							
Catanionic	**298.15 K**	**308.15 K**	**318.15 K**	**328.15 K**	**338.15 K**	**348.15 K**	**358.15 K**	**368.15K**
MeP 6 + TMAH	513.32	517.51	521.07	524.10	527.70	531.46	534.83	539.09
BuP 6 + TMAH	561.82	565.66	569.55	573.14	577.68	581.74	585.99	590.04
OcP 6 + TMAH	627.43	632.09	635.83	640.62	644.60	649.38	653.82	658.60
LP6 + TMAH	690.07	695.03	699.27	704.59	709.69	714.18	719.43	724.35
BP 6 + TMAH	-	-	-	877.81	883.85	890.74	896.46	902.75
Stearyl + TMAH	-	-	403.62	405.78	408.89	411.24	413.91	417.05
SP 3 + TMAH	614.31	617.59	622.04	626.35	630.92	635.71	639.85	644.27
SP 6 + TMAH	783.80	789.34	794.88	800.66	806.18	811.25	816.66	822.94
SP 9 + TMAH	966.83	973.30	980.79	987.03	994.73	1000.61	1007.65	1015.46
SP 12 + TMAH	1132.62	1140.29	1147.93	1155.68	1164.51	1172.75	1181.73	1189.81
SP 15 + TMAH	1299.33	1308.99	1318.51	1328.45	1336.57	1346.07	1356.87	1365.64
SP 25 + TMAH	1882.03	1895.90	1906.43	1920.66	1933.89	1948.53	1962.98	1976.59
SP 50 + TMAH	3298.50	3323.40	3353.09	3375.02	3397.93	3421.16	3445.43	3471.14
MeP 6 + TEAH	577.20	581.14	585.14	589.25	593.35	597.52	601.68	606.02
BuP 6 + TEAH	627.05	631.27	635.74	640.27	644.87	649.46	654.19	658.85
OcP 6 + TEAH	694.35	699.14	703.93	708.85	713.77	718.91	723.97	729.18
LP6 + TEAH	758.78	763.84	769.20	774.57	780.09	785.69	791.28	797.04
BP 6 + TEAH	-	-	945.24	951.99	958.84	965.79	972.84	979.88
Stearyl + TEAH	-	-	473.82	476.77	480.03	483.23	486.47	490.22
SP 3 + TEAH	683.82	687.67	692.47	697.26	702.12	707.13	712.13	717.20
SP 6 + TEAH	854.84	860.51	866.54	872.65	878.85	885.04	891.41	897.68
SP 9 + TEAH	1039.14	1046.30	1053.79	1061.27	1068.97	1076.67	1084.60	1092.53
SP 12 + TEAH	1206.83	1214.98	1223.63	1232.53	1241.43	1250.46	1259.62	1269.20
SP 15 + TEAH	1376.39	1385.75	1395.68	1405.75	1415.97	1426.18	1436.70	1447.22
SP 25 + TEAH	1964.76	1977.38	1991.61	2006.05	2020.92	2035.79	2050.88	2066.20
SP 50 + TEAH	3398.31	3420.46	3446.43	3472.80	3499.21	3526.39	3551.00	3579.00
MeP 6 + TBAH	686.09	690.96	695.53	700.24	705.01	710.82	715.51	720.96
BuP 6 + TBAH	738.08	742.62	748.39	752.82	759.16	763.96	770.32	775.94
OcP 6 + TBAH	807.71	812.22	818.52	823.95	829.44	835.74	842.22	847.69
LP6 + TBAH	873.23	879.76	885.33	891.55	897.87	904.86	910.76	917.96
BP 6 + TBAH	-	-	1066.60	1073.45	1082.09	1089.15	1097.67	1104.55
Stearyl + TBAH	-	-	596.70	600.03	604.32	607.53	612.36	616.83
SP 3 + TBAH	800.76	805.75	811.52	817.37	822.76	828.68	834.22	840.40
SP 6 + TBAH	972.30	978.39	985.09	991.88	999.10	1006.98	1014.19	1021.39
SP 9 + TBAH	1156.68	1165.52	1172.93	1181.76	1191.02	1199.02	1207.93	1216.03
SP 12 + TBAH	1324.73	1332.62	1343.76	1353.91	1364.23	1372.59	1383.80	1394.42
SP 15 + TBAH	1494.87	1504.80	1516.15	1526.86	1538.55	1550.59	1560.60	1572.47
SP 25 + TBAH	2089.06	2102.92	2115.75	2133.26	2149.90	2163.32	2180.20	2198.56
SP 50 + TBAH	3530.15	3554.92	3581.51	3608.49	3635.89	3662.94	3691.17	3719.45

VII.3.4 Viscosity data

	Viscosity [mPas] at										
	273.15 K	**283.15 K**	**293.15 K**	**303.15 K**	**313.15 K**	**323.15 K**	**333.15 K**	**343.15 K**	**353.15 K**	**363.15 K**	**373.15 K**
MeP 6 + TMAH	1198.9	586.5	310.7	176.3	105.9	66.4	43.6	29.6	21.2	15.9	11.3
BuP 6 + TMAH	2900.8	1176.9	550.3	288.6	165.3	100.3	65.9	45.2	32.3	23.5	18.3
OcP 6 + TMAH	3400.2	1349.8	624.2	330.2	186.2	115.3	72.6	49.9	35.2	25.9	19.0
LP 6 + TMAH	5007.3	1912.5	859.1	433.9	241.1	144.6	91.9	60.9	44.1	32.0	24.1
SP 6 + TMAH	-	-	1196.2	587.8	317.8	196.7	116.8	77.2	53.4	38.4	28.2
BP 60 + TMAH	-	-	-	-	-	550.3	306.9	190.2	120.3	79.9	56.3
Stearyl + TMAH	-	-	-	-	-	417.9	235.0	144.1	93.6	64.2	45.9
SP 3 + TMAH	-	-	-	670.2	359.2	209.0	130.1	85.5	59.0	42.3	31.3
SP 9 + TMAH	6420.1	2377.2	1035.8	511.9	280.0	165.0	103.9	69.1	48.2	34.7	26.0
SP 12 + TMAH	4027.2	1565.9	711.0	362.3	203.1	122.7	80.0	53.4	37.8	27.6	20.9
SP 15 + TMAH	3542.3	1399.9	642.5	330.9	185.9	114.1	73.6	51.1	35.6	26.6	19.9
SP 25 + TMAH	2735.6	1102.3	509.9	265.9	151.8	92.3	53.9	41.4	29.6	21.9	16.7
SP 50 + TMAH	1790.6	738.9	351.9	188.5	109.9	67.9	44.9	31.1	22.5	15.7	12.9
MeP 6 + TEAH	1199.3	566.7	291.9	161.6	95.1	58.9	38.2	25.9	17.8	12.6	9.5
BuP 6 + TEAH	2639.3	1062.3	499.6	261.9	149.6	93.3	60.5	40.2	28.7	21.4	16.2
OcP 6 + TEAH	2567.2	1186.3	558.1	286.1	162.4	103.8	66.3	44.1	30.1	22.2	17.0
LP 6 + TEAH	3615.9	1425.9	653.3	335.6	190.2	113.3	74.2	49.9	35.6	26.6	19.1
SP 6 + TEAH	-	2374.9	1034.6	510.9	278.8	164.6	103.8	69.0	48.1	34.8	25.9
BP 60 + TEAH	-	-	-	-	942.2	487.1	274.4	165.4	105.3	73.6	51.9
Stearyl + TEAH	-	-	-	-	709.1	353.6	198.1	120.0	77.4	52.8	38.0
SP 3 + TEAH	-	-	1311.1	632.3	338.2	196.5	122.2	80.3	55.4	39.6	29.3
SP 9 + TEAH	5566.0	1995.6	876.8	436.5	239.9	142.2	90.2	60.4	42.1	30.6	22.8
SP 12 + TEAH	3727.1	1441.6	650.3	331.3	185.6	112.1	71.9	48.9	34.6	25.2	19.1
SP 15 + TEAH	3352.6	1276.9	575.9	290.1	161.5	98.1	63.6	42.6	30.1	22.3	16.7
SP 25 + TEAH	2360.3	931.9	394.9	222.9	126.6	77.9	47.6	32.6	24.4	18.5	14.0
SP 50 + TEAH	1483.1	606.2	287.2	152.6	88.6	55.3	36.6	25.5	18.4	13.8	10.7
MeP 6 + TBAH	939.6	418.5	205.6	109.6	62.5	37.8	24.1	15.9	10.9	7.7	5.6
BuP 6 + TBAH	2083.6	825.7	381.3	198.1	112.9	69.4	45.3	31.1	22.2	16.4	12.6
OcP 6 + TBAH	2512.4	981.3	447.8	230.2	130.1	79.3	51.5	35.1	25.0	18.4	14.0
LP 6 + TBAH	3002.6	1156.3	520.9	266.3	149.1	90.3	58.0	40.3	28.1	21.0	15.3
SP 6 + TBAH	-	2000.2	615.0	407.8	219.1	127.9	80.0	52.8	36.7	26.4	19.8
BP 60 + TBAH	-	-	-	1666.9	781.1	409.1	235.1	143.5	93.6	63.2	44.6
Stearyl + TBAH	-	-	-	-	600.9	295.0	162.6	97.9	63.3	43.1	31.1
SP 3 + TBAH	-	-	1048.1	496.4	262.3	151.2	93.5	61.3	42.1	30.2	22.3
SP 9 + TBAH	4857.3	1728.9	734.1	356.6	192.4	112.9	71.0	47.2	32.8	23.7	17.7
SP 12 + TBAH	3423.9	1269.8	556.9	277.7	153.3	91.5	58.4	39.4	27.9	20.3	15.6
SP 15 + TBAH	2875.9	1073.9	473.5	237.4	133.5	85.4	79.8	34.5	25.8	18.0	13.6
SP 25 + TBAH	1760.8	685.5	312.9	161.9	91.9	56.9	36.5	25.2	18.1	13.4	10.3
SP 50 + TBAH	1254.2	485.6	221.9	115.0	65.6	40.6	26.5	18.4	13.4	10.0	7.6

VII.3.5 Conductivity data

	Conductivity [µS/cm-1] at							
	293.15 K	**303.15 K**	**313.15 K**	**323.15 K**	**333.15 K**	**343.15 K**	**353.15 K**	**363.15 K**
MeP 6 + TMAH	211.2	452.1	692.5	1110.4	1718.2	2434.6	3274.1	4662.3
BuP 6 + TMAH	102.2	200.2	321.5	555.3	844.6	1201.2	1559.7	2200.1
OcP 6 + TMAH	55.6	102.3	189.6	289.0	436.1	649.2	962.4	1400.3
LP 6 + TMAH	32.3	71.1	124.9	179.6	278.9	403.6	641.1	800.3
SP 6 + TMAH	16.3	34.6	60.7	106.5	152.3	211.3	366.3	500.2
BP 60 + TMAH	-	-	-	18.1	37.4	55.3	100.2	122.2
Stearyl + TMAH	-	-	-	109.2	186.3	327.2	518.5	751.2
SP 3 + TMAH	-	41.6	76.3	136.5	211.8	310.3	512.3	625.2
SP 9 + TMAH	9.3	20.5	36.3	62.2	103.8	166.8	203.6	360.0
SP 12 + TMAH	9.1	19.3	35.5	62.5	98.7	155.2	187.4	255.3
SP 15 + TMAH	8.3	18.2	34.5	62.7	95.8	154.2	189.9	196.8
SP 25 + TMAH	4.7	7.2	14.1	19.3	28.5	36.3	65.3	88.9
SP 50 + TMAH	1.9	3.6	5.3	12.3	16.5	22.2	29.5	40.0
MeP 6 + TEAH	171.2	323.7	562.3	942.2	1427.1	2133.3	2973.7	4367.3
BuP 6 + TEAH	75.7	133.3	245.6	444.6	655.9	883.7	1265.5	1625.9
OcP 6 + TEAH	52.4	85.3	166.3	291.2	500.3	665.3	932.7	1200.3
LP 6 + TEAH	27.4	56.2	95.7	155.7	243.5	379.7	522.6	729.4
SP 6 + TEAH	12.5	23.5	53.3	83.2	125.6	189.0	307.9	355.3
BP 60 + TEAH	-	-	9.2	13.6	29.6	50.3	72.6	94.3
Stearyl + TEAH	-	-	51.1	121.3	175.5	316.3	509.0	732.4
SP 3 + TEAH	17.8	35.3	73.9	123.5	192.3	302.3	416.3	576.5
SP 9 + TEAH	8.2	18.3	32.7	55.5	105.5	174.1	302.3	347.0
SP 12 + TEAH	8.5	18.9	32.7	51.3	99.6	170.9	292.2	332.0
SP 15 + TEAH	7.9	20.2	35.6	50.2	92.3	152.3	165.4	265.8
SP 25 + TEAH	3.1	6.3	15.2	17.3	29.5	32.9	61.6	86.2
SP 50 + TEAH	1.6	3.2	5.4	12.2	17.2	19.6	22.6	33.4
MeP 6 + TBAH	138.2	271.4	422.2	705.1	1323.3	1982.1	2702.3	3284.6
BuP 6 + TBAH	54.0	101.7	195.4	361.3	456.4	705.6	950.1	1258.9
OcP 6 + TBAH	24.2	50.2	91.3	157.0	247.9	375.3	533.7	735.4
LP 6 + TBAH	17.8	38.3	77.5	106.0	149.5	279.7	403.2	559.8
SP 6 + TBAH	11.0	17.9	33.2	60.3	97.8	122.6	155.9	256.4
BP 60 + TBAH	-	2.2	6.0	8.6	13.0	25.7	39.6	55.6
Stearyl + TBAH	-	-	35.6	74.9	132.2	210.5	326.5	402.3
SP 3 + TBAH	9.6	19.8	45.8	83.3	121.3	160.2	234.2	332.9
SP 9 + TBAH	10.4	13.3	27.1	56.6	92.0	117.2	148.6	278.0
SP 12 + TBAH	9.5	13.7	21.9	61.3	98.8	115.5	167.6	252.6
SP 15 + TBAH	9.3	13.1	18.6	56.0	94.8	118.9	169.8	242.5
SP 25 + TBAH	1.9	4.5	11.4	18.3	23.2	30.2	56.2	73.3
SP 50 + TBAH	0.9	2.8	4.3	7.3	11.3	16.4	21.2	25.3

VII.3.6 Hygroscopy data

	absorbed water [%]						
	2 hrs.	**3 hrs.**	**4 hrs.**	**8 hrs.**	**12 hrs.**	**24 hrs.**	**120 hrs.**
MeP 6 + TMAH	2.26	3.43	4.60	5.70	6.74	7.28	10.00
BuP 6 + TMAH	1.44	2.28	3.67	4.22	4.70	4.85	7.95
OcP 6 + TMAH	1.22	1.69	3.18	3.54	3.91	4.06	7.23
LP 6 + TMAH	1.02	1.25	2.49	2.96	3.26	3.47	6.60
SP 6 + TMAH	0.92	1.34	1.78	2.22	2.70	2.93	6.10
BP 6 + TMAH	0.76	0.94	1.40	1.74	2.10	2.47	5.62
Stearyl + TMAH	1.15	1.44	1.80	2.60	2.90	2.93	6.34
SP 3 + TMAH	1.17	1.39	1.74	2.46	2.68	2.85	6.20
SP 6 + TMAH	0.92	1.21	1.65	2.32	2.57	2.70	6.10
SP 9 + TMAH	0.89	1.20	1.50	2.19	2.27	2.41	5.99
SP 12 + TMAH	0.92	1.11	1.22	1.99	2.13	2.23	5.84
SP 15 + TMAH	0.93	1.01	1.16	1.90	2.08	2.19	5.80
SP 25 + TMAH	0.89	0.98	1.07	1.89	1.93	2.10	5.70
SP 50 + TMAH	0.86	0.97	1.04	1.75	1.83	1.98	5.62
MeP 6 + TEAH	1.62	2.25	3.92	4.97	6.32	6.62	9.72
BuP 6 + TEAH	1.52	1.94	2.86	3.49	4.11	4.48	7.59
LP 6 + TEAH	1.21	1.06	1.86	2.30	2.85	3.31	6.33
SP 6 + TEAH	0.98	1.14	1.57	1.93	2.35	2.62	5.82
BP 6 + TEAH	0.84	0.99	1.23	1.58	2.16	2.44	5.52
Stearyl + TEAH	1.07	1.36	1.72	2.54	2.73	2.83	5.92
SP 3 + TEAH	0.95	1.19	1.63	2.40	2.55	2.77	5.90
SP 6 + TEAH	0.98	1.33	1.57	2.20	2.35	2.62	5.82
SP 9 + TEAH	1.00	1.32	1.42	2.00	2.11	2.50	5.76
SP 12 + TEAH	0.98	0.94	1.18	1.88	2.07	2.33	5.63
SP 15 + TEAH	0.96	0.93	1.13	1.87	2.05	2.16	5.52
SP 25 + TEAH	0.94	0.91	1.05	1.76	1.91	2.04	5.49
SP 50 + TEAH	0.84	0.91	1.02	1.70	1.81	1.91	5.36
MeP 6 + TBAH	1.35	2.18	3.66	4.32	5.75	6.02	9.24
BuP 6 + TBAH	1.14	1.91	2.31	2.92	3.23	3.66	6.80
OcP 6 + TBAH	1.12	1.28	2.14	2.76	2.84	2.91	6.07
LP 6 + TBAH	1.05	1.24	1.76	1.87	2.51	2.80	5.88
SP 6 + TBAH	0.94	0.95	1.54	2.13	2.18	2.58	5.63
BP 6 + TBAH	0.79	0.88	1.19	1.36	1.80	2.38	5.44
Stearyl + TBAH	1.02	1.24	1.65	2.40	2.67	2.77	5.83
SP 3 + TBAH	0.91	1.17	1.58	2.24	2.44	2.65	5.70
SP 6 + TBAH	0.94	0.95	1.54	2.13	2.18	2.58	5.63
SP 9 + TBAH	0.92	0.94	1.38	1.97	2.02	2.41	5.53
SP 12 + TBAH	0.90	0.93	1.28	1.88	1.93	2.33	5.43
SP 15 + TBAH	0.84	0.91	1.11	1.75	1.85	2.13	5.22
SP 25 + TBAH	0.81	0.91	1.05	1.70	1.80	1.94	5.00
SP 50 + TBAH	0.84	0.90	0.97	1.52	1.76	1.85	4.89

	H_2O content at the beginning [ppm]	H_2O content after 24 hrs. [ppm]	H_2O content after 120 hrs. [ppm]
MeP 6 + TMAH	985	1057	1083
BuP 6 + TMAH	972	1019	1049
OcP 6 + TMAH	868	903	931
LP 6 + TMAH	855	885	911
SP 6 + TMAH	860	885	912
BP 6 + TMAH	845	866	893
Stearyl + TMAH	560	576	595
SP 3 + TMAH	721	742	766
SP 6 + TMAH	860	883	912
SP 9 + TMAH	851	871	902
SP 12 + TMAH	836	855	885
SP 15 + TMAH	799	816	845
SP 25 + TMAH	803	820	849
SP 50 + TMAH	775	790	819
MeP 6 + TEAH	955	1018	1048
BuP 6 + TEAH	921	962	991
OcP 6 + TEAH	869	903	929
LP 6 + TEAH	841	869	894
SP 6 + TEAH	851	873	901
BP 6 + TEAH	832	852	878
Stearyl + TEAH	621	639	658
SP 3 + TEAH	714	734	756
SP 6 + TEAH	851	873	901
SP 9 + TEAH	826	847	874
SP 12 + TEAH	814	833	860
SP 15 + TEAH	784	801	827
SP 25 + TEAH	771	787	813
SP 50 + TEAH	749	763	789
MeP 6 + TBAH	941	998	1028
BuP 6 + TBAH	900	933	961
OcP 6 + TBAH	888	914	942
LP 6 + TBAH	891	916	943
SP 6 + TBAH	799	820	941
SP 6 + TBAH	803	822	847
BP 6 + TBAH	941	998	1028
Stearyl + TBAH	452	465	478
SP 3 + TBAH	700	719	740
SP 6 + TBAH	799	820	844
SP 9 + TBAH	786	805	829
SP 12 + TBAH	741	758	781
SP 15 + TBAH	752	768	791
SP 25 + TBAH	711	725	747
SP 50 + TBAH	699	712	733

VIII Declaration

Hiermit erkläre ich, dass ich die vorliegende Dissertation ohne unzulässige Hilfe Dritter und ohne Benutzung anderer als der angegebenen Hilfsmittel angefertigt habe.

Die aus anderen Quellen direkt oder indirekt übernommenen Daten und Konzepte sind unter Angabe des Literaturzitats gekennzeichnet.

Die Arbeit wurde bisher weder im In- noch Ausland in gleicher oder ähnlicher Form einer anderen Prüfungsbehörde vorgelegt.

Regensburg, _____

_____

Thomas Myrdek